Alexandre Morin

Mathematical modelling and numerical simulation of two-phase multi-component flows of CO_2 mixtures in pipes

Thesis for the degree of Philosophiae Doctor

Trondheim, October 2012

Norwegian University of Science and Technology
Faculty of Engineering Science and Technology
Department of Energy and Process Engineering

NTNU – Trondheim
Norwegian University of
Science and Technology

NTNU
Norwegian University of Science and Technology

Thesis for the degree of Philosophiae Doctor

Faculty of Engineering Science and Technology
Department of Energy and Process Engineering

© Alexandre Morin

ISBN 978-82-471-3907-3 (printed ver.)
ISBN 978-82-471-3908-0 (electronic ver.)
ISSN 1503-8181

Doctoral theses at NTNU, 2012:296

Printed by NTNU-trykk

Abstract

In this thesis, the modelling of one-dimensional two-phase flows is studied, as well as the associated numerical methods. The background for this study is the need for numerical tools to simulate fast transients in pressurised carbon dioxide pipelines, amongst other things the crack arrest problem. This is a coupled mechanical and fluid-dynamical problem, where the pressurised gas causes a crack to propagate along the pipe, while being depressurised to the atmosphere. The crack stops when the pressure at the crack tip cannot drive it any longer.

Two-phase flow models were derived from the fundamental local conservation laws for mass, momentum and total energy. Through averaging of these relations, a system of one-dimensional transport equations was obtained, that must be closed by physical models and assumptions. The underlying assumptions made in some of the classical models of the literature are made clear. The numerical methods to solve hyperbolic conservation laws, based on the Finite Volume Method, are subsequently presented.

A partially-analytical Roe scheme for the N-phase drift-flux model has been derived. The wave structure of the model is presented. It is mostly analytical, except for some thermodynamical parameters. This makes the scheme very flexible with respect to the thermodynamical relations. An algorithm to resolve the thermodynamical state of a mixture of N phases following the stiffened gas equation of state is derived.

A Roe scheme for the six-equation two-fluid model has been derived. This model needs to be regularised to be hyperbolic. A tool to verify the physical relevance of a regularisation term is provided.

The instantaneous chemical relaxation is performed on a five-equation two-fluid model to derive a four-equation model, where the phases are in full mechanical, thermal and chemical equilibrium at all times.

An application example of numerical methods to solve the crack arrest problem is presented. A method is developed to evaluate the flow through a crack, and compared in the single-phase case to an analytical method.

Preface

The present work was financed through the academic part of the BIGCCS Centre, established within the Centres for Environment-friendly Energy Research (CEER) scheme and coordinated by SINTEF Energy Research. The BIGCCS Centre aims at enabling sustainable power generation from fossil fuels based on cost-effective CO_2 capture, safe transport, and underground storage of CO_2. I gratefully acknowledge the following partners for their contributions: Aker Solutions, ConocoPhillips, Det Norske Veritas, Gassco, Hydro, Shell, Statoil, TOTAL, GDF SUEZ and the Research Council of Norway (193816/S60).

I would like to thank my supervisor, Professor Inge R. Gran, and my co-supervisor Dr Svend Tollak Munkejord. Svend Tollak provided me guidance while giving me autonomy, in the right amount so that I could make this work my own, while keeping the deadlines. His knowledge of the domain was of great help in defining an interesting and rewarding project.

I owe a great thanks to Dr. Tore Flåtten, employed at SINTEF Energy Research. Our conversations helped me understand the field of systems of conservation laws, and find interesting challenges to work on. This collaboration resulted in a series of paper published together. I also thank my colleagues Morten Hammer and Peder Kristian Aursand from SINTEF Energy Research for interesting discussions.

Finally, I would like to thank all my colleagues from the Department of Energy and Process Engineering at NTNU, and at SINTEF Energy Research, and particularly Maxime Mussard for helping me rest my mind in coffee breaks.

Trondheim, August 2012,
Alexandre Morin.

Contents

Abstract iii

Preface v

Nomenclature xi

1. Introduction 1

2. Physical modelling 5
2.1. The local conservation equations 5
2.2. Equivalence of energy and entropy equations 7
2.3. Interface relations 11
2.3.1. Mass relation 12
2.3.2. Momentum relation 13
2.3.3. Energy relation 16
2.3.4. Energy relation expressed as an enthalpy relation . 17
2.3.5. Internal energy relation 19
2.3.6. Entropy relation 20
2.4. Averaging 21
2.4.1. Ensemble averaging 22
2.4.2. Ensemble averaged balance equations 22
2.4.3. Average variables 23
2.4.4. Manipulations on the averaged equations 25
2.4.5. Averaging of the interfacial relations 28
2.4.6. Relations between the average balance equations . 32
2.4.7. Summary of the transport equations 34
2.5. Two-phase flow models 36
2.5.1. The seven-equation two-pressure model 38
2.5.2. The six-equation model 45
2.5.3. Hyperbolicity of the two-fluid model 47
2.5.4. Variations of the two-fluid model 51

2.5.5. The drift-flux models 52
2.6. Summary 53

3. Numerical methods **55**
3.1. Structure of systems of conservation laws 56
3.1.1. Scalar conservation laws 56
3.1.2. System of linear conservation laws 57
3.1.3. Riemann problem for systems of non-linear conservation laws 59
3.2. Finite-volume methods 60
3.2.1. Central vs. upwind scheme 62
3.2.2. Lax-Friedrichs, Richtmyer and FORCE fluxes . . . 62
3.2.3. The MUSTA method 63
3.2.4. Upwind schemes 64
3.2.5. Second order accuracy 70
3.3. Systems of non-conservative transport equations 72
3.3.1. Resolution of non-conservative terms 72
3.3.2. Non-conservative terms treated with fractional-step methods 75
3.4. Summary 77

4. Summary of the contributions **79**
4.1. Paper A 79
4.2. Paper B 81
4.3. Paper C 82
4.4. Paper D 84
4.5. Paper E 85
4.6. Paper F 87
4.7. Paper G 89
4.8. Paper H 90

5. Conclusions and continuation **95**

Bibliography **99**

A. Numerical Resolution of CO2 Transport Dynamics **109**

B. On Solutions to Equilibrium Problems for Systems of Stiffened Gases 123

C. Wave Propagation in Multicomponent Flow Models 153

D. Towards a formally path-consistent Roe scheme for the six-equation two-fluid model 177

E. A Roe Scheme for a Compressible Six-Equation Two-Fluid Model 183

F. On interface transfer terms in two-fluid models 211

G. A Two-Fluid Four-Equation Model with Instantaneous Thermodynamical Equilibrium 219

H. Pipeline flow modelling with source terms due to leakage: The straw method 243

Nomenclature

Latin Letters

a	Advection velocity (Chap. 3)	m/s
a	Interfacial area density (Chap. 2)	m^2/m^3
A	Cross-section area in (2.4)	m^2
$\boldsymbol{A}$	Jacobian matrix of the fluxes	–
$\mathcal{A}^{\pm}\Delta Q_{i-1/2}$	Fluctuations	–
$\boldsymbol{b}$	External body force	m/s^2
$\boldsymbol{B}$	Matrix of non-conservative factors	–
c	Speed of sound	m/s
C_v	Specific heat at constant volume	J/(K.kg)
e	Specific internal energy (Chap. 2)	J/kg
e	Specific total energy in Sec. 3.3	J/kg
E	Ensemble (Sec. 2.4)	–
E	Interfacial heat exchange (Chap. 2)	$J/(m^3.s)$
E	Total energy (Sec. 3.1.3)	J/m^3
$\mathcal{E}$	Averaging operator	–
f	Scalar flux	–
$\boldsymbol{F}$	Vector of fluxes	–
$\boldsymbol{F}_{st}$	Surface tension normal stress	N/m^2
h	Specific enthalpy	J/kg
H	Heaviside function (Chap. 3)	–
$H_{s,k}$	Mean curvature	1/m
$\mathcal{H}$	Temperature relaxation constant	$J/(m^3.s.K)$
I	Mechanical interaction term	1/s
$\boldsymbol{J}$	General flux	–
$\mathcal{J}$	Mechanical relaxation constant	1/(Pa.s)
$\mathcal{K}$	Phase relaxation constant	mol.s/m
L	Contour line, see equation (2.45)	m
m	Elementary ensemble of realisations (Sec. 2.4)	–
m	Number of equations in the system (Chap. 3)	–
$\boldsymbol{M}$	Jacobian of the non-conservative fluxes (Chap. 3)	–

$\boldsymbol{M}$	Interfacial momentum exchange (Chap. 2)	N/m^3
n	Specific amount of matter (Sec. 2.2)	mol/kg
$\boldsymbol{n}$	Normal vector	–
p	Pressure	Pa
$\boldsymbol{q}$	Internal heat flux	W/m^2
r	Specific external heat source	W/kg
r_{chem}	Heat production from a chemical reaction (Sec. 2.2)	W/kg
$\boldsymbol{R}$	Matrix of the right eigenvectors	–
$\boldsymbol{R}^p$	Columns of $\boldsymbol{R}$	–
s	Shock speed (Chap. 3)	–
s	Specific entropy (Chap. 2)	J/(kg.K)
s_{irr}	Specific entropy creation from irreversible processes	W/(K.kg)
$\boldsymbol{s}$	General source (Sec. 2.4)	–
$S^{\pm}$	Velocities of the slowest and fastest waves	–
$\boldsymbol{S}$	Vector of sources	–
t	Time	s
T	Temperature	K
$\boldsymbol{T}$	Stress tensor	Pa
u	Scalar conserved variable	–
$\boldsymbol{U}$	Vector of conserved variables	–
v	Velocity	m/s
v_τ	Interfacial velocity, see equation (2.210)	m/s
$\boldsymbol{v}$	Velocity vector	m/s
V	Control volume	m^3
w^p	Components of $\boldsymbol{W}$	–
W	Interfacial work	$N/(m^2.s)$
$\boldsymbol{W}$	Vector of the characteristic variables	–
$\mathcal{W}$	Wave	–
x	Length coordinate	m
z	Path	–
$\boldsymbol{Z}$	Vector of non-conservative fluxes	–
$\boldsymbol{Z}$	Extremities of the Roe integration path in Sec. 3.2.4	–

Greek Letters

α	Amplitude of a wave (Chap. 3)	–
α	Volume fraction (Chap. 2)	–
γ	Heat capacity ratio	–

Γ	First Grüneisen parameter	–
δ	Interfacial delta function, see equation (2.91)	–
Δp	Pressure difference, see equation (2.207)	Pa
ε	Specific internal energy in	J/kg
θ	Smoothness measure	–
λ	Eigenvalue	–
Λ	Interfacial mass exchange	$kg/(m^3.s)$
$\mathbf{\Lambda}$	Diagonal matrix containing the eigenvalues	–
μ	Chemical potential (Sec. 2.2)	J/mol
μ	Realisation (Sec. 2.4)	–
ν	Specific volume in Sec. 3.3	m^3/kg
ν	Volume element (Chap. 2)	m^3
ξ	Parameterisation of an integration path	–
ρ	Density	kg/m^3
σ	Slope of a segment (Chap. 3)	–
σ	Surface tension, see equation (2.39)	N/m
ς	Surface element	m^2
Σ	Control surface	m^2
$\boldsymbol{\tau}$	Viscous stress tensor	Pa
$\boldsymbol{\tau}_{st}$	Surface tension tangential stress	N/m^2
χ	Characteristic function (phase indicator), see equation (2.60)	–
φ	Slope limiter function	–
Φ	Flux limiter function (Chap. 3)	–
Φ	Slip relation, see equation (2.224)	m/s
Ψ	General function	–

Subscripts

c	Conservative part
g	Gas phase
i	Component or interface (context dependent in Chap. 2)
i	Spatial index (Chap. 3)
k	Phase k
ℓ	Liquid phase
l	Left state
nc	Non-conservative part
p	Wave or eigenvalue index
r	Right state

s	Surface quantity
σ	Designates a control surface

Superscripts

$'$	Fluctuation, see equation (2.76)
$*$	Value at $x = 0$ in the Riemann problem solution
0	Initial state
$\sim$	Approximate value of $*$-state.
n	Time step

Other symbols

$\bar{\Psi}$	Ensemble average of Ψ
$\hat{\Psi}$	Average of Ψ in the context of the linearised system (3.44)
$\tilde{\Psi}$	Limited version of Ψ, see equation (3.62)

Abbreviations

FL	FLIC
FO	FORCE
HLL	Harten, Lax and van Leer
LF	Lax-Friedrichs
LHS	Left-hand side
RHS	Right-hand side
Ri	Richtmyer

1 Introduction

In the framework of carbon capture and storage (CCS), pipelines are an option to transport carbon dioxide (CO_2) over large distances, between the point of capture and the storage site. According to the International Energy Agency's BLUE Map scenario, CCS will contribute to reducing the global CO_2 emissions by about 8 gigatonnes in 2050 [36]. In addition to allow cost optimisation, simulation tools are required to ensure the operation safety of the pipelines, both in normal and accidental situations. One of the main risks is the occurrence of a crack propagation (cf. Figure 1.1). Driven by the internal pressure of the pipe, an initial crack may propagate due to the concentration of tension at the crack tip. Besides, the depressurisation of the gas through a crack may cool the pipe material, possibly leading to transition in the material mechanical behaviour, and reducing its strength. A depressurisation of the pipeline may occur both in normal operation, for example for maintenance, and in accidental

Figure 1.1: A pipe after a crack has propagated.
Credit: SINTEF Material and Chemistry.

circumstances, for example an excavator puncturing the pipe.

In a simplified explanation, the crack arrest problem can be seen as a race between the propagating crack and the pressure wave inside the pipe. A crack in an initially pressurised pipe will cause a depressurisation. The depressurisation wave will propagate away from the initial crack, releasing the stress on the walls. However, if the stress at the crack tip is strong enough, the crack will propagate at a given speed. If the crack is faster than the pressure wave, the pressure at the crack tip will always remain high, and the crack will continue to run. Otherwise it will stop. In practice, the problem is dependent on many thermodynamical, fluid-dynamical and mechanical parameters, like the pressure, the temperature, the number of phases and the flow regime, the steel quality, *etc.* Hence, tools are required to simulate this coupled mechanical and fluid-dynamical problem in order to be able to avoid crack propagation.

These issues are already known from natural gas transport. Tools have been developed, however, they are empirical and suited for material and pressures used 30–40 years ago [68]. They have to be recalibrated for each pipe material of interest, making parameter studies difficult. Besides, the thermodynamical behaviour of the fluid is an important parameter, and natural gas and CO_2 are very different on this point. Therefore, there is an interest in developing numerical tools helping to design CO_2 transport pipelines. These tools will naturally be applicable to transport of other gases.

Under transport conditions, CO_2 will normally be supercritical or in liquid state (critical point: 73.8 bar, 31.1°C [67]). During a depressurisation, multiphase mixtures will occur, for example liquid-gas, but supercritical CO_2 and dry ice may also be present. Thus, the numerical tool must involve multiphase flow models. In the present work, the mixtures are limited to liquid and gas.

Numerical simulation tools for multiphase flows already exist. The nuclear industry uses them in safety analysis, and many codes have been developed (CATHARE [8], RELAP5/MOD3 [75], WAHA3 [42]). The main interest in nuclear safety analysis is in heat transfer and transport to ensure that the nuclear core is always cooled. The petroleum industry also uses multiphase flow simulation tools to design pipelines for oil and gas transport (OLGA [6], LedaFlow [15]). However, these tools do not include the crack arrest problem, they are more designed for normal operation, for

example evaluating the pumping energy requirement and the occurrence of slug flows. Numerical simulation tools for the crack arrest problem should on the contrary focus on very fast transients, since the pressure waves are important. These regimes are not covered by the existing tools from the nuclear or the petroleum industry.

The present thesis treats both the fluid-dynamical models and the numerical methods for the crack arrest problem. Chapter 2 shows the complete derivation of a multiphase flow model and all the assumptions that are made in the process. Chapter 3 presents the numerical methods for conservation laws. Then, in Chapter 4, brief summaries of the papers are presented, and my personal contributions in each of them are made clear. Chapter 5 gives some concluding remarks.

2 Physical modelling

In this chapter, we derive one-dimensional two-phase flow models. In the first part, we start from the fundamental conservation laws for mass, momentum and energy, and mostly follow the derivation presented in the book of Drew and Passman [17]. We first present the local conservation laws, before we derive the interface relations. Then these relations are averaged to produce one-dimensional transport equations. In the second part (Section 2.5), we introduce modelling assumptions which will lead to a closed model, ready to be solved by numerical methods for transport equations. This derivation mostly contains already known elements, but is presented here in a way that makes visible the underlying modelling assumptions in well-known and widely-used two-phase flow models.

2.1. The local conservation equations

Inside each phase, the behaviour of the material is governed by local conservation equations [17, Sec. 8.1]. First, mass is conserved. For a fluid phase k, we have

$$\frac{\partial \rho_k}{\partial t} + \nabla \cdot (\rho_k \boldsymbol{v}_k) = 0, \tag{2.1}$$

where ρ_k is the density of phase k and $\boldsymbol{v}_k$ its velocity. Then, momentum is transported, but not locally conserved since it can be exchanged with the environment through external forces. Its transport equation is

$$\frac{\partial}{\partial t}(\rho_k \boldsymbol{v}_k) + \nabla \cdot (\rho_k \boldsymbol{v}_k \otimes \boldsymbol{v}_k) = -\nabla p_k + \nabla \cdot \boldsymbol{\tau}_k + \rho_k \boldsymbol{b}_k, \tag{2.2}$$

where p is the pressure, $\boldsymbol{\tau}$ is the stress tensor and $\boldsymbol{b}$ the external body force. The symbol $\otimes$ represents the outer product. Finally, we can derive a transport equation for total energy or entropy. It will be proved in the

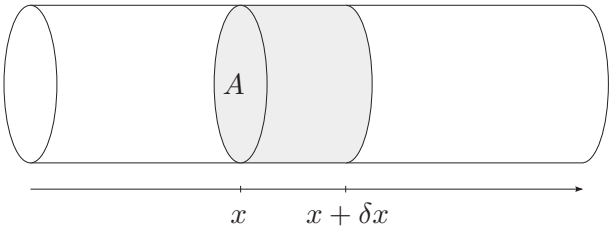

Figure 2.1: One-dimensional control volume in a pipe.

following that both are physically equivalent (in the absence of shocks). The total energy transport equation is

$$\frac{\partial}{\partial t}\left(\rho_k\left(e_k+\tfrac{1}{2}v_k^2\right)\right)+\nabla\cdot\left(\rho_k\boldsymbol{v}_k\left(e_k+\tfrac{1}{2}v_k^2\right)\right) \\ =\nabla\cdot\left((\boldsymbol{\tau}_k-p_k\boldsymbol{I})\cdot\boldsymbol{v}_k-\boldsymbol{q}_k\right)+\rho_k(r_k+\boldsymbol{b}_k\cdot\boldsymbol{v}_k), \quad (2.3)$$

where e is the internal energy, $\boldsymbol{q}$ is the internal heat flux and r is the external heat source.

When it comes to the entropy transport equation, Drew and Passman [17, Sec. 8.1] give an inequality. In the present derivation, we make it an equality, and specify the missing terms. To this end, we write the entropy balance in a motionless fluid, in a one-dimensional control volume $[x, x+\delta x]$ of cross-section area A, as shown in Figure 2.1. All the quantities are considered uniform to first order in the control volume. In a time interval $[t, t+\delta t]$, the extensive entropy $S(x,t)=\rho(x,t)s(x,t)A\delta x$ in the control volume will vary due to the internal heat flux q through both ends of the control volume. Note that the entropy flux due to the heat flux involves the temperature $T(x,t)$ inside the control volume. The external heat source r also affects the entropy in the control volume. The remaining entropy sources are gathered in s'_{irr}.

$$(\rho(x,t+\delta t)s(x,t+\delta t)-\rho(x,t)s(x,t))A\delta x=\frac{q(x,t)A\delta t}{T(x,t)} \\ -\frac{q(x+\delta x,t)A\delta t}{T(x,t)}+(\rho A\delta x)\frac{r\delta t}{T(x,t)}+(\rho A\delta x)s'_{irr}\delta t, \quad (2.4)$$

This corresponds – to first order after having simplified $A\delta t\delta x$ – to the

equation

$$\frac{\partial(\rho s)}{\partial t} = -\frac{1}{T}\frac{\partial q}{\partial x} + \frac{\rho r}{T} + \rho s'_{irr}. \tag{2.5}$$

By adding a term for convective transport of entropy to the latter equation, we obtain the entropy transport equation for phase k

$$\frac{\partial}{\partial t}(\rho_k s_k) + \nabla \cdot (\rho_k \boldsymbol{v}_k s_k) = -\frac{1}{T_k}\nabla \cdot \boldsymbol{q}_k + \frac{\rho_k r_k}{T_k} + \rho_k s'_{k,irr}. \tag{2.6}$$

2.2. Equivalence of energy and entropy equations

Starting from the entropy equation (2.6), we are able to recover the internal energy part of the energy equation (2.3). We first expand the gradient and the divergence in equation (2.6), where we drop the phase index k for clarity

$$\frac{\partial(\rho s)}{\partial t} + \sum_j \frac{\partial(\rho v_j s)}{\partial x_j} = \sum_j \left(-\frac{1}{T}\frac{\partial q_j}{\partial x_j}\right) + \frac{\rho r}{T} + \rho s'_{irr}. \tag{2.7}$$

Expanding the derivatives in the two first terms and using the mass equation (2.1), we obtain

$$\rho\frac{\partial s}{\partial t} + \sum_j \rho v_j \frac{\partial s}{\partial x_j} = \sum_j \left(-\frac{1}{T}\frac{\partial q_j}{\partial x_j}\right) + \frac{\rho r}{T} + \rho s'_{irr}. \tag{2.8}$$

Now, the fundamental thermodynamic relation states, in a version which is also valid out of equilibrium,

$$T\,\mathrm{d}s = \mathrm{d}e - \frac{p}{\rho^2}\,\mathrm{d}\rho - \sum_i \mu_i\,\mathrm{d}n_i, \tag{2.9}$$

where μ_i is the thermodynamic potential of component i in phase k, and n_i the specific amount of matter of component i in phase k.

The latter differential is substituted into the entropy equation (2.6),

$$\frac{\rho}{T}\left(\frac{\partial e}{\partial t}-\frac{p}{\rho^2}\frac{\partial \rho}{\partial t}-\sum_i \mu_i \frac{\partial n_i}{\partial t}\right) + \sum_j \frac{\rho v_j}{T}\left(\frac{\partial e}{\partial x_j}-\frac{p}{\rho^2}\frac{\partial \rho}{\partial x_j}-\sum_i \mu_i \frac{\partial n_i}{\partial x_j}\right) = \sum_j \left(-\frac{1}{T}\frac{\partial q_j}{\partial x_j}\right)+\frac{\rho r}{T}+\rho s'_{irr}, \quad (2.10)$$

which is simplified into, using the mass equation (2.1)

$$\frac{\partial \rho e}{\partial t}+\sum_j \frac{\partial \rho v_j e}{\partial x_j}+\sum_j p\frac{\partial v_j}{\partial x_j} = \sum_j \left(-\frac{\partial q_j}{\partial x_j}\right)+\rho r + \rho \sum_i \left(\mu_i \frac{\partial n_i}{\partial t}+\sum_j \left(v_j \mu_i \frac{\partial n_i}{\partial x_j}\right)\right)+T\rho s'_{irr}. \quad (2.11)$$

We have now demonstrated that the entropy equation (2.6) leads, through the thermodynamic relation (2.9), to an internal energy transport equation

$$\frac{\partial \rho e}{\partial t}+\nabla\cdot(\rho \boldsymbol{v} e)+p\nabla\cdot\boldsymbol{v} = -\nabla\cdot\boldsymbol{q}+\rho r+\rho\sum_i \mu_i\left(\frac{\partial n_i}{\partial t}+\boldsymbol{v}\cdot\nabla n_i\right)+T\rho s'_{irr}. \quad (2.12)$$

In this equation, the term

$$\rho\sum_i \mu_i\left(\frac{\partial n_i}{\partial t}+\boldsymbol{v}\cdot\nabla n_i\right) \quad (2.13)$$

can be written with a material derivative as

$$\rho\sum_i \mu_i \frac{Dn_i}{Dt}. \quad (2.14)$$

It is the internal energy consumption rate due to the evolution of chemical reactions. It can be summarised in the term

$$\rho \sum_i \mu_i \frac{Dn_i}{Dt} = -\rho r_{chem}. \tag{2.15}$$

Remark that this concerns bulk chemical reactions. It does not include phase change or other reactions at the interface. After substitution in (2.12), the internal energy transport equation becomes

$$\frac{\partial \rho e}{\partial t} + \nabla \cdot (\rho \boldsymbol{v} e) + p \nabla \cdot \boldsymbol{v} = -\nabla \cdot \boldsymbol{q} + \rho r - \rho r_{chem} + T \rho s'_{irr}. \tag{2.16}$$

The kinetic part of the energy equation (2.3) comes from the momentum equation (2.2), which is multiplied by $\boldsymbol{v}$

$$\underbrace{\boldsymbol{v} \cdot \frac{\partial}{\partial t}(\rho \boldsymbol{v}) + \boldsymbol{v} \cdot \nabla \cdot (\rho \boldsymbol{v} \otimes \boldsymbol{v})}_{\text{LHS}} = -\boldsymbol{v} \cdot \nabla p + \boldsymbol{v} \cdot \nabla \cdot \boldsymbol{\tau} + \boldsymbol{v} \cdot \rho \boldsymbol{b}. \tag{2.17}$$

The vector operators of the left-hand side are expanded

$$\text{LHS} = \sum_i v_i \frac{\partial (\rho v_i)}{\partial t} + \sum_i \left(v_i \sum_j \frac{\partial \left(\rho v_i v_j \right)}{\partial x_j} \right), \tag{2.18}$$

and the derivatives expanded such that the left-hand side of the mass equation (2.1) appears multiplied by a factor v_i^2

$$\begin{aligned} \text{LHS} = & \sum_i \left(\rho v_i \frac{\partial v_i}{\partial t} \right) \\ & + \sum_i \left(\rho v_i v_j \sum_j \frac{\partial v_i}{\partial x_j} \right) + \sum_i v_i^2 \left(\frac{\partial \rho}{\partial t} + \sum_j \frac{\partial (\rho v_j)}{\partial x_j} \right). \end{aligned} \tag{2.19}$$

Therefore, the left-hand side becomes

$$\text{LHS} = \sum_i \left(\frac{1}{2} \rho \frac{\partial v_i^2}{\partial t} \right) + \sum_i \left(\frac{1}{2} \rho v_j \sum_j \frac{\partial v_i^2}{\partial x_j} \right), \tag{2.20}$$

and we can use the mass equation (2.1) again to move everything inside the derivatives

$$\text{LHS} = \sum_i \left(\frac{1}{2} \frac{\partial \rho v_i^2}{\partial t} \right) + \sum_i \left(\frac{1}{2} \sum_j \frac{\partial \rho v_i^2 v_j}{\partial x_j} \right). \tag{2.21}$$

This is equivalent to

$$\text{LHS} = \frac{1}{2} \frac{\partial \rho v^2}{\partial t} + \frac{1}{2} \nabla \cdot \left(\rho v^2 \boldsymbol{v} \right). \tag{2.22}$$

Therefore the kinetic part of the energy equation is

$$\frac{\partial}{\partial t} \left(\frac{1}{2} \rho v^2 \right) + \nabla \cdot \left(\frac{1}{2} \rho v^2 \boldsymbol{v} \right) = \boldsymbol{v} \cdot (-\nabla p + \nabla \cdot \boldsymbol{\tau}) + \rho \boldsymbol{v} \cdot \boldsymbol{b}. \tag{2.23}$$

We obtain the total energy equation by adding (2.16) and (2.23)

$$\begin{aligned} \frac{\partial}{\partial t} \left(\rho \left(e + \frac{1}{2} v^2 \right) \right) + \nabla \cdot \left(\rho \boldsymbol{v} \left(e + \frac{1}{2} v^2 \right) \right) = \boldsymbol{v} \cdot (-\nabla p + \nabla \cdot \boldsymbol{\tau}) \\ - p \nabla \cdot \boldsymbol{v} - \nabla \cdot \boldsymbol{q} + \rho \left(r + \boldsymbol{v} \cdot \boldsymbol{b} \right) - \rho r_{chem} + T \rho s'_{irr}. \end{aligned} \tag{2.24}$$

Comparing the latter equation with the energy equation (2.3), we are able to be more specific about the term s'_{irr}. First, the evolution of a chemical reaction comes with entropy creation. However, it does not have any effect on the system's total energy, because it is an internal energy transformation from chemical potential energy to heat. Therefore it seems reasonable to cancel the term ρr_{chem} in the energy equation (2.24) by integrating it in s'_{irr}. It will thus appear in the entropy equation (2.6). Second, there should be an entropy production term related to the viscous dissipation of kinetic energy in the velocity gradients. Since the total energy is conserved, unless there is an exchange with the environment, the terms accounting for internal phenomena should be in conservative form. For a Newtonian fluid, $\boldsymbol{\tau}$ is symmetrical and we can write

$$\boldsymbol{\tau} : \nabla \boldsymbol{v} + \boldsymbol{v} \cdot \nabla \cdot \boldsymbol{\tau} = \nabla \cdot (\boldsymbol{\tau} \cdot \boldsymbol{v}), \tag{2.25}$$

where the operator : represents the double-dot product between to matrices of the same dimensions. $\boldsymbol{v} \cdot \nabla \cdot \boldsymbol{\tau}$ appears in the kinetic energy

equation (2.23). Therefore, to form the conservative term $\nabla \cdot (\boldsymbol{\tau} \cdot \boldsymbol{v})$ in the total energy equation (2.3), the viscous dissipation of kinetic energy must take the form

$$\rho s_{visc} = \frac{\boldsymbol{\tau} : \nabla \boldsymbol{v}}{T}. \tag{2.26}$$

Thus, the entropy production term can be rewritten

$$\rho s'_{irr} = \frac{\boldsymbol{\tau} : \nabla \boldsymbol{v}}{T} + \frac{\rho r_{chem}}{T} + \rho s_{irr}. \tag{2.27}$$

Remark also that

$$\boldsymbol{v} \cdot \nabla p + p \nabla \cdot \boldsymbol{v} = \nabla \cdot (p \boldsymbol{v}). \tag{2.28}$$

Consequently, the right-hand side of the energy equation (2.24) derived from the entropy and momentum equations is equivalent to the right-hand side of (2.3) if we assume that we already account for all entropy sources, so that $s_{irr} = 0$. The entropy equation (2.6) is rewritten as

$$\frac{\partial}{\partial t}(\rho s) + \nabla \cdot (\rho \boldsymbol{v} s) = -\frac{1}{T} \nabla \cdot \boldsymbol{q} + \frac{\rho r}{T} + \frac{\boldsymbol{\tau} : \nabla \boldsymbol{v}}{T} + \frac{\rho r_{chem}}{T} + \rho s_{irr}. \tag{2.29}$$

2.3. Interface relations

The equations presented above are bulk equations for one phase. In multiphase flows, several phases share the physical domain and interact at their interfaces. In the present section, we derive the interface relations that relate the bulk quantities of two adjacent phases. A control surface Σ_S is defined across the interface (cf. Figure 2.2), of infinitesimal thickness 2ε. In addition, one control surface for each phase is defined such that one of its faces is on the interface, and the other faces are superimposed with Σ_S in the bulk of the phase. They are called Σ_{g} and Σ_ℓ. These three control surfaces are attached to the interface, so that their velocities are that of the interface. They define three control volumes, called V_S, V_{g} and V_ℓ respectively, that we consider as open sets. This means that the interface is contained in V_S, but not in V_{g} and V_ℓ. The interface is denoted by Σ_i. In the following, the fluxes through the short sides of thickness ε are always neglected, since ε can be taken as small as one wants with respect to the length of the long sides.

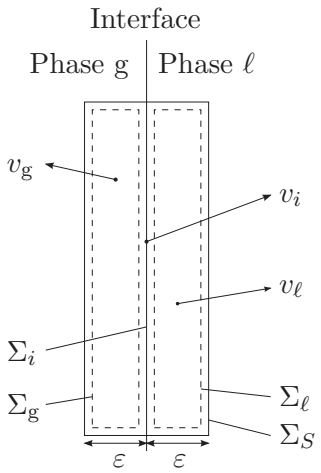

Figure 2.2: Control volumes on the interface

2.3.1. Mass relation

We start with the differential form of the mass equation for phase k (2.1)

$$\frac{\partial \rho_k}{\partial t} + \nabla \cdot (\rho_k \boldsymbol{v}_k) = 0. \tag{2.30}$$

We first integrate it over a control volume V_σ, and use the divergence theorem to transform the volume integral of the divergence to a surface integral over the control surface Σ_σ delimiting V_σ. This gives

$$\int_{V_\sigma} \frac{\partial \rho_k}{\partial t} \,\mathrm{d}\nu + \oint_{\Sigma_\sigma} \rho_k \boldsymbol{v}_k \cdot \boldsymbol{n}_\sigma \,\mathrm{d}\varsigma = 0, \tag{2.31}$$

where $\boldsymbol{n}_\sigma$ is the unit vector normal to surface Σ_σ and pointing outwards. k denotes the relevant phase $k = \mathrm{g}$ or $k = \ell$. Then we add and subtract the interface velocity $\boldsymbol{v}_i$ from $\boldsymbol{v}_k$, to obtain

$$\int_{V_\sigma} \frac{\partial \rho_k}{\partial t} \,\mathrm{d}\nu + \oint_{\Sigma_\sigma} \rho_k \boldsymbol{v}_i \cdot \boldsymbol{n}_\sigma \,\mathrm{d}\varsigma + \oint_{\Sigma_\sigma} \rho_k (\boldsymbol{v}_k - \boldsymbol{v}_i) \cdot \boldsymbol{n}_\sigma \,\mathrm{d}\varsigma = 0. \tag{2.32}$$

This can be rewritten as

$$\frac{D_i}{Dt} \left(\int_{V_\sigma} \rho_k \,\mathrm{d}\nu \right) + \oint_{\Sigma_\sigma} \rho_k (\boldsymbol{v}_k - \boldsymbol{v}_i) \cdot \boldsymbol{n}_\sigma \,\mathrm{d}\varsigma = 0, \tag{2.33}$$

where

$$\frac{D_i}{Dt} = \frac{\partial}{\partial t} + \boldsymbol{v}_i \cdot \nabla \tag{2.34}$$

is the material derivative with respect to a fluid particle attached to the interface, therefore having a velocity $\boldsymbol{v}_i$. We can write this because $\boldsymbol{v}_i$ is the velocity of the control surface, it is not a function of x in the bulk. Therefore, it can be taken out of the integral and the gradient.

Now, we write equation (2.33) for the control volume V_S, from which we subtract (2.33) written for V_g and for V_ℓ. Since the interface does not contain mass, the volume integrals in domains V_g and V_ℓ cancel with that in domain V_S. On the other hand, though all the contributions on the control surface Σ_S are cancelled by contributions on the control surfaces Σ_g and Σ_ℓ, those on the interface Σ_i remain. We obtain

$$0 = -\int_{\Sigma_i} \rho_\mathrm{g}(\boldsymbol{v}_\mathrm{g} - \boldsymbol{v}_i) \cdot \boldsymbol{n}_\mathrm{g} \,\mathrm{d}\varsigma - \int_{\Sigma_i} \rho_\ell(\boldsymbol{v}_\ell - \boldsymbol{v}_i) \cdot \boldsymbol{n}_\ell \,\mathrm{d}\varsigma, \tag{2.35}$$

where $\boldsymbol{n}_\mathrm{g}$ and $\boldsymbol{n}_\ell$ are the unit vectors normal to the interface, pointing outwards from the phases g and ℓ respectively. Since the latter equation is valid for any surface element of the interface, the sum of the integrands is uniformly zero. We obtain the mass interface relation

$$0 = \rho_\mathrm{g}(\boldsymbol{v}_\mathrm{g} - \boldsymbol{v}_i) \cdot \boldsymbol{n}_\mathrm{g} + \rho_\ell(\boldsymbol{v}_\ell - \boldsymbol{v}_i) \cdot \boldsymbol{n}_\ell. \tag{2.36}$$

2.3.2. Momentum relation

We follow the same principle as for the mass relation above, from the momentum equation (2.2). The momentum conservation law in integral form for the control volumes V_σ where $\sigma = S, \mathrm{g}, \ell$ is

$$\begin{aligned}\frac{D_i}{Dt}\left(\int_{V_\sigma} \rho_k \boldsymbol{v}_k \,\mathrm{d}\nu\right) = &-\oint_{\Sigma_\sigma} \rho_k \boldsymbol{v}_k \otimes (\boldsymbol{v}_k - \boldsymbol{v}_i) \cdot \boldsymbol{n}_\sigma \,\mathrm{d}\varsigma \\ &+ \oint_{\Sigma_\sigma} (\boldsymbol{\tau}_k - p_k \boldsymbol{I})\boldsymbol{n}_\sigma \,\mathrm{d}\varsigma + \int_{V_\sigma} \rho_k \boldsymbol{b}_k \,\mathrm{d}\nu. \end{aligned} \tag{2.37}$$

The latter equation is then written for the control surfaces Σ_g and Σ_ℓ and subtracted from the one written for Σ_S. Now, the volume integrals have to be treated carefully. They indeed do not necessarily cancel. Since we

are working with open sets, the interface Σ_i remains after the subtraction of the control volumes V_g and V_ℓ from the control volume V_S. Therefore surface terms can remain. Since the interface has no mass, it does not have momentum, so that no surface term can remain on the left-hand side. However, as to the body force term $\int_{V_\sigma} \rho_k \boldsymbol{b}_k \,\mathrm{d}\nu$, it may reduce to a non-zero surface term. For example, surface tension acts as an external force on the phases and is a surface force term.

Surface tension is composed of two forces. The first is normal to the interface and is caused by the curvature of the interface (cf. Figure 2.3a). We first need to define the mean curvature of a surface. The principal curvatures κ_1 and κ_2 of a surface at a given point are the minimum and maximum curvatures of the surface at that point. They are algebraic values, positive if the curve bends in the same direction as the chosen normal vector, negative otherwise. They are the inverse of the curvature radii R_1 and R_2. The mean curvature is defined as

$$H_{s,k} = \frac{1}{2}\left(\frac{1}{R_1} + \frac{1}{R_2}\right). \tag{2.38}$$

Remark that this is an algebraic value, dependent on the choice of normal vector. Here the index k means that the normal vector used is $\boldsymbol{n}_k$, pointing outwards from phase k. For example, on Figure 2.3a where the interface is convex seen from phase g, $H_{s,\ell}$ is defined with respect to $\boldsymbol{n}_\ell$ and is therefore negative. The mean curvature with respect to phase g is $H_{s,\mathrm{g}} = -H_{s,\ell}$. Then, the normal component of the surface tension force can be expressed invariably with respect to both phases and is equal to

$$\boldsymbol{F}_{st} = 2\sigma H_{s,\mathrm{g}} \boldsymbol{n}_\mathrm{g} = 2\sigma H_{s,\ell} \boldsymbol{n}_\ell, \tag{2.39}$$

where σ is the surface tension. It tends to flatten the interface.

The second component of the surface tension is tangential, and is caused by a gradient of surface tension on the interface (cf. Figure 2.3b). A gradient in surface tension can be caused by chemicals, like surfactants, or a temperature gradient in the fluid for example. This causes the interface to be more strongly curved where the surface tension is higher. This also causes a jump in tangential stress across the interface, which means that the phases exert a tangential force on each other. The tangential stress is given by

$$\boldsymbol{\tau}_{st} = \nabla_s \sigma, \tag{2.40}$$

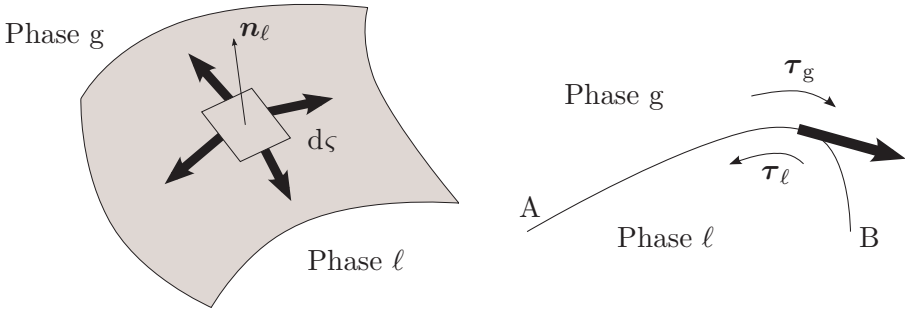

(a) Normal component

(b) Tangential component ($\sigma_A < \sigma_B$)

Figure 2.3: Surface tension

where $\nabla_s \sigma$ is the surface gradient of the surface tension.

The surface integrals are treated as in the previous subsection, only the contributions on the interface remain. We have consequently

$$\begin{aligned} 0 = &- \oint_{\Sigma_i} [\rho_\mathrm{g} \boldsymbol{v}_\mathrm{g} \otimes (\boldsymbol{v}_\mathrm{g} - \boldsymbol{v}_i) \cdot \boldsymbol{n}_\mathrm{g} + \rho_\ell \boldsymbol{v}_\ell \otimes (\boldsymbol{v}_\ell - \boldsymbol{v}_i) \cdot \boldsymbol{n}_\ell] \cdot \mathrm{d}\varsigma \\ &+ \oint_{\Sigma_i} [(\boldsymbol{\tau}_\mathrm{g} - p_\mathrm{g} \boldsymbol{I}) \cdot \boldsymbol{n}_\mathrm{g} + (\boldsymbol{\tau}_\ell - p_\ell \boldsymbol{I}) \cdot \boldsymbol{n}_\ell] \cdot \mathrm{d}\varsigma \\ &+ \int_{\Sigma_i} (2\sigma H_{s,\mathrm{g}} \boldsymbol{n}_\mathrm{g} + \nabla_s \sigma) \cdot \mathrm{d}\varsigma. \end{aligned} \tag{2.41}$$

Since the latter equation is valid for any surface element of the interface, the sum of the integrands is uniformly zero. We obtain the momentum interface relation

$$\begin{aligned} 0 = &\rho_\mathrm{g} \boldsymbol{v}_\mathrm{g} \otimes (\boldsymbol{v}_\mathrm{g} - \boldsymbol{v}_i) \cdot \boldsymbol{n}_\mathrm{g} + \rho_\ell \boldsymbol{v}_\ell \otimes (\boldsymbol{v}_\ell - \boldsymbol{v}_i) \cdot \boldsymbol{n}_\ell \\ &- (\boldsymbol{\tau}_\mathrm{g} - p_\mathrm{g} \boldsymbol{I}) \cdot \boldsymbol{n}_\mathrm{g} - (\boldsymbol{\tau}_\ell - p_\ell \boldsymbol{I}) \cdot \boldsymbol{n}_\ell - \nabla_s \sigma - 2\sigma H_{s,\mathrm{g}} \boldsymbol{n}_\mathrm{g}. \end{aligned} \tag{2.42}$$

2.3.3. Energy relation

We now apply the energy conservation law in integral form coming from (2.3) to the three control volumes V_σ where $\sigma = S, \mathrm{g}, \ell$, which gives

$$\begin{aligned}
&\underbrace{\frac{D_i}{Dt}\left(\int_{V_\sigma} \rho_k \left(e_k + \tfrac{1}{2}v_k^2\right) \mathrm{d}\nu\right)}_{i} = \\
&\quad \underbrace{-\oint_{\Sigma_\sigma} \rho_k \left(e_k + \tfrac{1}{2}v_k^2\right)(\boldsymbol{v}_k - \boldsymbol{v}_i)\cdot\boldsymbol{n}_\sigma \,\mathrm{d}\varsigma}_{ii} + \underbrace{\oint_{\Sigma_\sigma} ((\boldsymbol{\tau}_k - p_k\boldsymbol{I})\boldsymbol{v}_k)\cdot\boldsymbol{n}_\sigma \,\mathrm{d}\varsigma}_{iii} \\
&\qquad + \underbrace{\oint_{\Sigma_\sigma} \boldsymbol{q}_k\cdot(-\boldsymbol{n}_\sigma)\,\mathrm{d}\varsigma}_{iv} + \underbrace{\int_{V_\sigma} \rho_k r_k \,\mathrm{d}\nu}_{v} + \underbrace{\int_{V_\sigma} \rho_k \boldsymbol{b}_k\cdot\boldsymbol{v}_k \,\mathrm{d}\nu}_{vi},
\end{aligned} \tag{2.43}$$

and apply the same process of subtracting the contributions of the relations for g and ℓ from the contributions of the relation for S. The resulting relation is

$$\begin{aligned}
&\underbrace{\frac{D_i}{Dt}\left(\int_{\Sigma_i} e_{s,i}\,\mathrm{d}\varsigma\right)}_{\mathrm{I}} = \\
&\quad \underbrace{-\oint_{\Sigma_i} \left(\rho_\mathrm{g}\left(e_\mathrm{g} + \tfrac{1}{2}v_\mathrm{g}^2\right)(\boldsymbol{v}_\mathrm{g} - \boldsymbol{v}_i)\cdot\boldsymbol{n}_\mathrm{g} + \rho_\ell\left(e_\mathrm{g} + \tfrac{1}{2}v_\ell^2\right)(\boldsymbol{v}_\ell - \boldsymbol{v}_i)\cdot\boldsymbol{n}_\ell\right)\mathrm{d}\varsigma}_{\mathrm{II}} \\
&\qquad + \underbrace{\oint_{\Sigma_i} \left[((\boldsymbol{\tau}_\mathrm{g} - p_\mathrm{g}\boldsymbol{I})\boldsymbol{v}_\mathrm{g})\cdot\boldsymbol{n}_\mathrm{g} + ((\boldsymbol{\tau}_\ell - p_\ell\boldsymbol{I})\boldsymbol{v}_\ell)\cdot\boldsymbol{n}_\ell\right]\mathrm{d}\varsigma}_{\mathrm{III}} \\
&\underbrace{-\oint_{\Sigma_i} \left[\boldsymbol{q}_\mathrm{g}\cdot\boldsymbol{n}_\mathrm{g} + \boldsymbol{q}_\ell\cdot\boldsymbol{n}_\ell\right]\mathrm{d}\varsigma}_{\mathrm{IV}} + \underbrace{\int_{\Sigma_i} r_{s,i}\,\mathrm{d}\varsigma}_{\mathrm{V}} + \underbrace{\int_{\Sigma_i} (2\sigma H_{s,\mathrm{g}}\boldsymbol{n}_\mathrm{g} + \nabla_s\sigma)\cdot\boldsymbol{v}_i\,\mathrm{d}\varsigma}_{\mathrm{VI}},
\end{aligned} \tag{2.44}$$

where the index s, i designates a surface quantity on the interface. In the subtraction, the terms have been treated as follows. Since the interface has no mass, it has no kinetic energy. However, it has internal energy

for example in the form of surface tension. Therefore, from the term i in (2.43) an interface contribution will remain, which is the term I. Term II is a surface integral and follows from term ii, as term III follows from term iii, and term IV from term iv. Then, the subtraction of the volume energy source terms – term v – leaves the surface energy source term V, acting along the interface. Note that it is an external source: it is not for example the heat production due to phase change. It could be radiation warming up a dark fluid at the interface with a transparent phase. Finally, the subtraction of the terms accounting for the work of the body forces – term vi – leaves the surface force work term VI. It can be for example the work of the force due to interfacial tension.

Now, term I is a material derivative on the interface. We can expand it and write it as

$$\frac{D_i}{Dt}\left(\int_{\Sigma_i} e_{s,i}\,\mathrm{d}\varsigma\right) = \int_{\Sigma_i} \frac{\partial e_{s,i}}{\partial t}\,\mathrm{d}\varsigma + \int_{L_i} e_{s,i}\boldsymbol{v}_i\cdot\boldsymbol{n}_{L_i}\,\mathrm{d}l, \tag{2.45}$$

where L_i is the contour line of the surface element on the interface Σ_i, and $\boldsymbol{n}_{L_i}$ a vector normal to the contour line pointing outwards. Using the divergence theorem, we obtain

$$\frac{D_i}{Dt}\left(\int_{\Sigma_i} e_{s,i}\,\mathrm{d}\varsigma\right) = \int_{\Sigma_i} \frac{\partial e_{s,i}}{\partial t}\,\mathrm{d}\varsigma + \int_{\Sigma_i} \nabla_s\cdot(e_{s,i}\boldsymbol{v}_i)\,\mathrm{d}\varsigma. \tag{2.46}$$

Now, since (2.44) is valid for any surface element of the interface, the sum of the integrands on each sides of the equal sign are uniformly equal to each other. We obtain the energy interface relation

$$\begin{aligned}\frac{\partial e_{s,i}}{\partial t} + \nabla_s\cdot(\boldsymbol{v}_i e_{s,i}) = \\ -\rho_\mathrm{g}\left(e_\mathrm{g}+\tfrac{1}{2}v_\mathrm{g}^2\right)(\boldsymbol{v}_\mathrm{g}-\boldsymbol{v}_i)\cdot\boldsymbol{n}_\mathrm{g} - \rho_\ell\left(e_\mathrm{g}+\tfrac{1}{2}v_\ell^2\right)(\boldsymbol{v}_\ell-\boldsymbol{v}_i)\cdot\boldsymbol{n}_\ell \\ +(\boldsymbol{\tau}_\mathrm{g}-p_\mathrm{g}\boldsymbol{I})\boldsymbol{v}_\mathrm{g}\cdot\boldsymbol{n}_\mathrm{g} + (\boldsymbol{\tau}_\ell - p_\ell\boldsymbol{I})\boldsymbol{v}_\ell\cdot\boldsymbol{n}_\ell \\ -\boldsymbol{q}_\mathrm{g}\cdot\boldsymbol{n}_\mathrm{g} - \boldsymbol{q}_\ell\cdot\boldsymbol{n}_\ell + r_{s,i} + 2\sigma H_{s,\mathrm{g}}\boldsymbol{n}_\mathrm{g}\cdot\boldsymbol{v}_i + \boldsymbol{v}_i\cdot\nabla_s\sigma.\end{aligned} \tag{2.47}$$

2.3.4. Energy relation expressed as an enthalpy relation

Using the definition of the enthalpy

$$h = e + \frac{p}{\rho}, \tag{2.48}$$

the mass transfer and stress terms in (2.47) can be transformed as

$$\begin{aligned}
&-\rho_k \left(e_k + \tfrac{1}{2}v_k^2\right)(\boldsymbol{v}_k - \boldsymbol{v}_i)\cdot\boldsymbol{n}_k + (\boldsymbol{\tau}_k - p_k\boldsymbol{I})\boldsymbol{v}_k\cdot\boldsymbol{n}_k \\
&\quad = -\rho_k\left(e_k + \frac{p_k}{\rho_k} + \tfrac{1}{2}v_k^2\right)(\boldsymbol{v}_k - \boldsymbol{v}_i)\cdot\boldsymbol{n}_k - p_k\boldsymbol{v}_i\cdot\boldsymbol{n}_k + \boldsymbol{\tau}_k\boldsymbol{v}_k\cdot\boldsymbol{n}_k \\
&\quad = -\rho_k\left(h_k + \tfrac{1}{2}v_k^2\right)(\boldsymbol{v}_k - \boldsymbol{v}_i)\cdot\boldsymbol{n}_k - p_k\boldsymbol{v}_i\cdot\boldsymbol{n}_k + \boldsymbol{\tau}_k\boldsymbol{v}_k\cdot\boldsymbol{n}_k.
\end{aligned} \tag{2.49}$$

Substituting this for $k = \mathrm{g}$ and $k = \ell$ in (2.47), we obtain

$$\begin{aligned}
&\frac{\partial e_{s,i}}{\partial t} + \nabla_s\cdot(\boldsymbol{v}_i e_{s,i}) = \\
&\quad -\rho_{\mathrm{g}}\left(h_{\mathrm{g}} + \tfrac{1}{2}v_{\mathrm{g}}^2\right)(\boldsymbol{v}_{\mathrm{g}} - \boldsymbol{v}_i)\cdot\boldsymbol{n}_{\mathrm{g}} - \rho_\ell\left(h_\ell + \tfrac{1}{2}v_\ell^2\right)(\boldsymbol{v}_\ell - \boldsymbol{v}_i)\cdot\boldsymbol{n}_\ell \\
&\qquad + \boldsymbol{\tau}_{\mathrm{g}}\boldsymbol{v}_{\mathrm{g}}\cdot\boldsymbol{n}_{\mathrm{g}} + \boldsymbol{\tau}_\ell\boldsymbol{v}_\ell\cdot\boldsymbol{n}_\ell - p_{\mathrm{g}}\boldsymbol{v}_i\cdot\boldsymbol{n}_{\mathrm{g}} - p_\ell\boldsymbol{v}_i\cdot\boldsymbol{n}_\ell \\
&\qquad - \boldsymbol{q}_{\mathrm{g}}\cdot\boldsymbol{n}_{\mathrm{g}} - \boldsymbol{q}_\ell\cdot\boldsymbol{n}_\ell + r_{s,i} + 2\sigma H_{s,\mathrm{g}}\boldsymbol{n}_{\mathrm{g}}\cdot\boldsymbol{v}_i + \boldsymbol{v}_i\cdot\nabla_s\sigma.
\end{aligned} \tag{2.50}$$

Now, we know that the pressure difference between the two phases is due to the normal component of the surface tension force. Therefore the work of the former is equal to the work of the latter. We then have

$$p_{\mathrm{g}}\boldsymbol{v}_i\cdot\boldsymbol{n}_{\mathrm{g}} + p_\ell\boldsymbol{v}_i\cdot\boldsymbol{n}_\ell = 2\sigma H_{s,\mathrm{g}}\boldsymbol{n}_{\mathrm{g}}\cdot\boldsymbol{v}_i. \tag{2.51}$$

Substituting this into (2.50) gives

$$\begin{aligned}
&\frac{\partial e_{s,i}}{\partial t} + \nabla_s\cdot(\boldsymbol{v}_i e_{s,i}) = \\
&\quad -\rho_{\mathrm{g}}\left(h_{\mathrm{g}} + \tfrac{1}{2}v_{\mathrm{g}}^2\right)(\boldsymbol{v}_{\mathrm{g}} - \boldsymbol{v}_i)\cdot\boldsymbol{n}_{\mathrm{g}} - \rho_\ell\left(h_\ell + \tfrac{1}{2}v_\ell^2\right)(\boldsymbol{v}_\ell - \boldsymbol{v}_i)\cdot\boldsymbol{n}_\ell \\
&\quad + \boldsymbol{\tau}_{\mathrm{g}}\boldsymbol{v}_{\mathrm{g}}\cdot\boldsymbol{n}_{\mathrm{g}} + \boldsymbol{\tau}_\ell\boldsymbol{v}_\ell\cdot\boldsymbol{n}_\ell - \boldsymbol{q}_{\mathrm{g}}\cdot\boldsymbol{n}_{\mathrm{g}} - \boldsymbol{q}_\ell\cdot\boldsymbol{n}_\ell + r_{s,i} + \boldsymbol{v}_i\cdot\nabla_s\sigma.
\end{aligned} \tag{2.52}$$

2.3.5. Internal energy relation

The internal energy equation in integral form, derived from (2.16), for the three control volumes V_σ, where $\sigma = S, \mathrm{g}, \ell$ is

$$\underbrace{\frac{D_i}{Dt}\left(\int_{V_\sigma} \rho_k e_k \,\mathrm{d}\nu\right)}_{i} + \underbrace{\oint_{\Sigma_\sigma} \rho_k e_k (v_k - v_\mathrm{i}) \cdot \boldsymbol{n}_\sigma \,\mathrm{d}\varsigma}_{ii}$$
$$= \underbrace{-\oint_{\Sigma_\sigma} p_k \boldsymbol{v}_k \cdot \boldsymbol{n}_\sigma \,\mathrm{d}\varsigma}_{iii} \underbrace{-\oint_{\Sigma_\sigma} \boldsymbol{q}_k \cdot \boldsymbol{n}_\sigma \,\mathrm{d}\varsigma}_{iv} + \underbrace{\int_{V_\sigma} \rho_k r_k \,\mathrm{d}\nu}_{v} + \underbrace{\int_{V_\sigma} \boldsymbol{\tau}_k : \nabla \boldsymbol{v}_k \,\mathrm{d}\nu}_{vi}. \tag{2.53}$$

We apply the subtraction process and obtain

$$\underbrace{\frac{D_i}{Dt}\left(\int_{\Sigma_i} e_{s,i} \,\mathrm{d}\varsigma\right)}_{\mathrm{I}} = \underbrace{-\oint_{\Sigma_i} \rho_\mathrm{g} e_\mathrm{g} (v_\mathrm{g} - v_\mathrm{i}) \cdot \boldsymbol{n}_\mathrm{g} \,\mathrm{d}\varsigma - \oint_{\Sigma_i} \rho_\ell e_\mathrm{g} (v_\ell - v_\mathrm{i}) \cdot \boldsymbol{n}_\ell \,\mathrm{d}\varsigma}_{\mathrm{II}}$$
$$\underbrace{-\oint_{\Sigma_i} p_\mathrm{g} \boldsymbol{v}_\mathrm{g} \cdot \boldsymbol{n}_\mathrm{g} \,\mathrm{d}\varsigma - \oint_{\Sigma_i} p_\ell \boldsymbol{v}_\ell \cdot \boldsymbol{n}_\ell \,\mathrm{d}\varsigma}_{\mathrm{III}}$$
$$\underbrace{-\oint_{\Sigma_i} \boldsymbol{q}_\mathrm{g} \cdot \boldsymbol{n}_\mathrm{g} \,\mathrm{d}\varsigma - \oint_{\Sigma_i} \boldsymbol{q}_\ell \cdot \boldsymbol{n}_\ell \,\mathrm{d}\varsigma}_{\mathrm{IV}} + \underbrace{\int_{\Sigma_i} r_{s,i} \,\mathrm{d}\varsigma}_{\mathrm{V}}. \tag{2.54}$$

As for the energy equation, an interfacial energy may remain from term i in (2.53). This is term I in (2.54). The terms ii, iii and iv are surface integrals and their treatment is straightforward. The next term (v) is the external heat source r_k, which may leave an interfacial contribution (term V). Finally, the viscous dissipation term vi disappears since there is a no-slip condition at the interface. Due to phase change for example, the velocity may be discontinuous across the interface, however, this would be due to mass changing phase and not to slip of the phases.

We then have, since the relation is valid for any surface element of the

interface,

$$\frac{\partial e_{s,i}}{\partial t} + \nabla_s \cdot (e_{s,i} v_\mathrm{i}) = -\rho_\mathrm{g} e_\mathrm{g} (v_\mathrm{g} - v_\mathrm{i}) \cdot \boldsymbol{n}_\mathrm{g} - \rho_\ell e_\mathrm{g} (v_\ell - v_\mathrm{i}) \cdot \boldsymbol{n}_\ell - p_\mathrm{g} \boldsymbol{v}_\mathrm{g} \cdot \boldsymbol{n}_\mathrm{g} - p_\ell \boldsymbol{v}_\ell \cdot \boldsymbol{n}_\ell - \boldsymbol{q}_\mathrm{g} \cdot \boldsymbol{n}_\mathrm{g} - \boldsymbol{q}_\ell \cdot \boldsymbol{n}_\ell + r_{s,i}. \quad (2.55)$$

2.3.6. Entropy relation

Finally, we can apply the same method to the entropy balance (2.6) across the interface. However, some concepts appear, which are difficult to define. For the three control volumes V_σ where $\sigma = S, \mathrm{g}, \ell$, we have

$$\underbrace{\frac{D_i}{Dt}\left(\int_{V_\sigma} \rho_k s_k \,\mathrm{d}\nu\right)}_{i} = \underbrace{-\oint_{\Sigma_\sigma} \rho_k s_k (\boldsymbol{v}_k - \boldsymbol{v}_i) \cdot \boldsymbol{n}_\sigma \,\mathrm{d}\varsigma}_{ii} + \underbrace{\oint_{\Sigma_\sigma} \frac{\boldsymbol{q}_k}{T_k} \cdot (-\boldsymbol{n}_\sigma) \,\mathrm{d}\varsigma}_{iii} + \underbrace{\int_{V_\sigma} \frac{\rho_k r_k}{T_k} \,\mathrm{d}\nu}_{iv} + \underbrace{\int_{V_\sigma} \frac{\boldsymbol{\tau}_k : \nabla \boldsymbol{v}_k}{T_k} \,\mathrm{d}\nu}_{v} + \underbrace{\int_{V_\sigma} \frac{\rho_k r_{chem,k}}{T_k} \,\mathrm{d}\nu}_{vi} + \underbrace{\int_{V_\sigma} \rho_k s_{irr,k} \,\mathrm{d}\nu}_{vii}. \quad (2.56)$$

The subtraction of the volume integrals is then performed, and gives the relation

$$\underbrace{\frac{\partial s_{s,i}}{\partial t} + \nabla_s \cdot (s_{s,i} \boldsymbol{v}_i)}_{\mathrm{I}} = \underbrace{-\rho_\mathrm{g} s_\mathrm{g} (\boldsymbol{v}_\mathrm{g} - \boldsymbol{v}_i) \cdot \boldsymbol{n}_\mathrm{g} - \rho_\ell s_\ell (\boldsymbol{v}_\ell - \boldsymbol{v}_i) \cdot \boldsymbol{n}_\ell}_{\mathrm{II}} \underbrace{-\frac{\boldsymbol{q}_\mathrm{g}}{T_\mathrm{g}} \cdot \boldsymbol{n}_\mathrm{g} - \frac{\boldsymbol{q}_\ell}{T_\ell} \cdot \boldsymbol{n}_\ell}_{\mathrm{III}} \underbrace{+\frac{r_{s,i,\mathrm{g}}}{T_\mathrm{g}} + \frac{r_{s,i,\ell}}{T_\ell}}_{\mathrm{IV}} \underbrace{+\frac{r_{s,chem,i,\mathrm{g}}}{T_\mathrm{g}} + \frac{r_{s,chem,i,\ell}}{T_\ell}}_{\mathrm{VI}} \underbrace{+ s_{irr,s,i}}_{\mathrm{VII}} \cdot \quad (2.57)$$

For the term i in (2.56), a surface entropy term $s_{s,i}$ may remain, which is term I in (2.57). The terms ii and iii are surface integrals and have straightforward treatment. The next volume integral term is iv, and represents the external heat sources. An interfacial term (IV) can remain.

Next, the viscous dissipation term v does not leave any surface terms, as explained in the section above. The term vi represents the entropy creation due to chemical reaction. An interfacial term (VI) may remain in case of phase change or other interfacial chemical reactions. Finally, for the last term vii, there may be an interfacial entropy creation due to irreversible phenomena. This is term VII.

Note that the terms $r_{s,i}$ and $r_{s,chem,i}$ had to be split into phasic contributions, because the entropy production involves phase temperatures. An interface temperature does not exist. It is not necessarily straightforward how to split those terms, especially the chemical reaction heat production, because it involves knowing on which side of the interface the heat is produced.

2.4. Averaging

The balance equations describe the behaviour of the bulk in a phase, while the interface relations describe the interactions between the phases. To obtain fluid-dynamical equations for multiphase flow, we can use averaging techniques. There are different averaging methods, with respect to time, space or ensemble [17]. Spatial averaging consists in averaging the thermodynamical and fluid-dynamical quantities over a given domain at a given time. Typically, one can perform averaging over the cross-section of a pipe flow [4]. The drawback of this method is that it can lose relevance when the characteristic dimensions of the flow – for example bubble size – are larger than the dimensions of the averaging domain. Time averaging [38, 95] consists in looking at a given point, and average the quantities over time. The same drawback can be noticed, when the flow characteristic time scales are larger than the averaging time scale.

These drawbacks can be conceptually avoided by using ensemble averaging. It consists in averaging the quantities – at a given time and a given location – over all the possible realisations of a flow. The ensemble of the realisations of a flow is the ensemble of all the possible micro- and mesoscopic configurations that give the observed macroscopic flow. For example, the flow of a bubbly liquid is characterised by its velocity, the gas fraction, the size of the bubbles, *etc.*, but the actual precise position of the bubbles is not relevant to the study of the flow. It will vary over time and space even if the macroscopic flow remains the same. The draw-

back of ensemble averaging compared to spatial averaging is that it does not take into account the cross-sectional structure of the flow. It is then common to combine ensemble averaging with spatial averaging [4].

In the present work, we perform the ensemble averaging of the equations derived above.

2.4.1. Ensemble averaging

The definition of the ensemble average of a quantity Ψ in a flow at point $\boldsymbol{x}$ and time t is

$$\mathcal{E}(\Psi(\boldsymbol{x},t)) = \int_E \Psi(\boldsymbol{x},t;\mu)\,\mathrm{d}m(\mu), \tag{2.58}$$

where μ is a micro- and mesoscopic realisation of the flow, $\mathrm{d}m(\mu)$ is the "occurrence weight" of the realisation μ, and E is the ensemble of all the realisations μ that give the observed macroscopic flow.

2.4.2. Ensemble averaged balance equations

The generic balance equation for a quantity Ψ can be written [17, Sec. 11]

$$\frac{\partial}{\partial t}(\rho\boldsymbol{\Psi}) + \nabla\cdot(\rho\boldsymbol{\Psi}\otimes\boldsymbol{v}) = \nabla\cdot\boldsymbol{J} + \rho\boldsymbol{s}, \tag{2.59}$$

where $\boldsymbol{J}$ is the flux of the transported quantity and $\boldsymbol{s}$ its source. This generic balance equation becomes after averaging

$$\begin{aligned}\frac{\partial}{\partial t}\mathcal{E}(\chi_k\rho\boldsymbol{\Psi}) + \nabla\cdot\mathcal{E}(\chi_k\rho\boldsymbol{\Psi}\otimes\boldsymbol{v}) - \nabla\cdot\mathcal{E}(\chi_k\boldsymbol{J})& \\ - \mathcal{E}(\chi_k\rho\boldsymbol{s}) = \mathcal{E}([\rho\boldsymbol{\Psi}\otimes(\boldsymbol{v}-\boldsymbol{v}_i) - \boldsymbol{J}]\cdot\nabla\chi_k)&\end{aligned} \tag{2.60}$$

where χ_k is the characteristic function or phase indicator function defined by

$$\chi_k(\boldsymbol{x},t;\mu) = \begin{cases} 1 & \text{if phase } k \text{ is present at } (\boldsymbol{x},t) \text{ in realisation } \mu, \\ 0 & \text{otherwise.}\end{cases} \tag{2.61}$$

The Gauss and Leibniz rules [17, p. 103] have been used. They give relations between the average of a derivative and the derivative of an average. They are, respectively,

$$\mathcal{E}(\chi_k\nabla f) = \nabla\mathcal{E}(\chi_k f) - \mathcal{E}(f_{k,i}\nabla\chi_k) \tag{2.62}$$

and

$$\mathcal{E}\left(\chi_k \frac{\partial f}{\partial t}\right) = \frac{\partial \mathcal{E}(\chi_k f)}{\partial t} - \mathcal{E}\left(f_{k,i} \frac{\partial \chi_k}{\partial t}\right), \tag{2.63}$$

where $f_{k,i}$ is the surface average of f_k at the interface. Note that all the quantities are defined over the whole domain. For example, $\rho(\boldsymbol{x}, t)$ jumps between the liquid density and the gas density across the domain, depending on which phase is present at point $\boldsymbol{x}$ and at time t in the realisation μ. The characteristic function for phase k designates which is the phase present at this point.

Now, the mass equation (2.1) is recovered from (2.59) by setting $\Psi = 1$, $\boldsymbol{J} = 0$ and $\boldsymbol{s} = 0$. Its averaged expression is therefore

$$\frac{\partial}{\partial t}\mathcal{E}(\chi_k \rho) + \nabla \cdot \mathcal{E}(\chi_k \rho \boldsymbol{v}) = \mathcal{E}(\rho(\boldsymbol{v} - \boldsymbol{v}_i) \cdot \nabla \chi_k). \tag{2.64}$$

The momentum equation (2.2) follows from (2.59) by setting $\boldsymbol{\Psi} = \boldsymbol{v}$, $\boldsymbol{J} = \boldsymbol{T} = \boldsymbol{\tau} - p\boldsymbol{I}$ and $\boldsymbol{s} = \boldsymbol{b}$. Its average expression is

$$\begin{aligned}\frac{\partial}{\partial t}\mathcal{E}(\chi_k \rho \boldsymbol{v}) + \nabla \cdot \mathcal{E}(\chi_k \rho \boldsymbol{v} \otimes \boldsymbol{v}) = \nabla \cdot \mathcal{E}(\chi_k(\boldsymbol{\tau} - p\boldsymbol{I})) \\ + \mathcal{E}(\chi_k \rho \boldsymbol{b}) + \mathcal{E}([\rho \boldsymbol{v}(\boldsymbol{v} - \boldsymbol{v}_i) - (\boldsymbol{\tau} - p\boldsymbol{I})] \cdot \nabla \chi_k).\end{aligned} \tag{2.65}$$

Finally, the energy equation (2.3) is found from (2.59) by setting $\Psi = e + \frac{1}{2}v^2$, $\boldsymbol{J} = \boldsymbol{T}\boldsymbol{v} - \boldsymbol{q} = (\boldsymbol{\tau} - p\boldsymbol{I})\boldsymbol{v} - \boldsymbol{q}$ and $\boldsymbol{s} = r + \boldsymbol{b} \cdot \boldsymbol{v}$. Its average expression is

$$\begin{aligned}\frac{\partial}{\partial t}\mathcal{E}\left(\chi_k \rho \left(e + \tfrac{1}{2}v^2\right)\right) + \nabla \cdot \mathcal{E}\left(\chi_k \rho \left(e + \tfrac{1}{2}v^2\right) \boldsymbol{v}\right) \\ = \nabla \cdot \mathcal{E}(\chi_k((\boldsymbol{\tau} - p\boldsymbol{I})\boldsymbol{v} - \boldsymbol{q})) + \mathcal{E}(\chi_k \rho(r + \boldsymbol{b} \cdot \boldsymbol{v})) \\ + \mathcal{E}\left(\left[\rho \left(e + \tfrac{1}{2}v^2\right)(\boldsymbol{v} - \boldsymbol{v}_i) - ((\boldsymbol{\tau} - p\boldsymbol{I})\boldsymbol{v} - \boldsymbol{q})\right] \cdot \nabla \chi_k\right).\end{aligned} \tag{2.66}$$

2.4.3. Average variables

In the above section, we have derived the average of the balance equations. To be able to use the equations, we have to define average variables, such that we obtain balance equations that describe the behaviour of average quantities. First, the ensemble average of the characteristic function is [17]

$$\alpha_k = \mathcal{E}(\chi_k), \tag{2.67}$$

where the averaging operator $\mathcal{E}$ was defined in (2.58). α_k is usually called the volume fraction of phase k in the mixture, though it is not strictly one since it is not a spatial average. However, it is closely related as it can be seen as the expected value of the volume fraction [17, p. 122]. The average of the density is weighted by α_k

$$\bar{\rho}_k = \frac{\mathcal{E}(\chi_k \rho)}{\alpha_k}. \tag{2.68}$$

All the other average variables are averages weighted either by α_k or $\alpha_k \bar{\rho}_k$. They are

- Velocity average
$$\bar{\boldsymbol{v}}_k = \frac{\mathcal{E}(\chi_k \rho \boldsymbol{v})}{\alpha_k \bar{\rho}_k}. \tag{2.69}$$
- Stress tensor average
$$\bar{\boldsymbol{\tau}}_k - \bar{p}_k \boldsymbol{I} = \frac{\mathcal{E}(\chi_k \boldsymbol{\tau})}{\alpha_k} - \frac{\mathcal{E}(\chi_k p)\boldsymbol{I}}{\alpha_k}. \tag{2.70}$$
- Body force average
$$\bar{\boldsymbol{b}}_k = \frac{\mathcal{E}(\chi_k \rho \boldsymbol{b})}{\alpha_k \bar{\rho}_k}. \tag{2.71}$$
- Internal energy average
$$\bar{e}_k = \frac{\mathcal{E}(\chi_k \rho e)}{\alpha_k \bar{\rho}_k}. \tag{2.72}$$
- Heat flux average
$$\bar{\boldsymbol{q}}_k = \frac{\mathcal{E}(\chi_k \boldsymbol{q})}{\alpha_k}. \tag{2.73}$$
- Heat source average
$$\bar{r}_k = \frac{\mathcal{E}(\chi_k \rho r)}{\alpha_k \bar{\rho}_k}. \tag{2.74}$$

Note that these are only definitions. No modelling assumptions are made.

2.4.4. Manipulations on the averaged equations

We can now use the average variables in the balance equations.

Mass equation

The mass equation (2.64) can be written

$$\frac{\partial}{\partial t}(\alpha_k \bar{\rho}_k) + \nabla \cdot (\alpha_k \bar{\rho}_k \bar{\boldsymbol{v}}_k) = \mathcal{E}(\rho(\boldsymbol{v} - \boldsymbol{v}_i) \cdot \nabla \chi_k). \tag{2.75}$$

It is now a balance equation for the quantity $\alpha_k \bar{\rho}_k$. The term on the right-hand side is the average of the mass transfer to phase k from the other phases. It will be discussed in Section 2.4.6.

Momentum equation

When it comes to the momentum equation (2.65), the definitions of the average variables are not enough. The average of the product $\boldsymbol{v} \otimes \boldsymbol{v}$ cannot simply be written as the product of two averages. We define the fluctuation of the velocity with respect to its average as [17, p. 124]

$$\boldsymbol{v}'_k = \boldsymbol{v} - \bar{\boldsymbol{v}}_k. \tag{2.76}$$

Remark that this definition applies at any point, regardless of which phase is present at this point. However, it is only relevant at points where phase k is present. The use of the characteristic function χ_k assures us that we always use the relevant definition of the fluctuation. Being aware that $\mathcal{E}(\bar{\Psi}) = \bar{\Psi}$ and that the average of the fluctuation is zero, we can write

$$\begin{aligned}
\mathcal{E}(\chi_k \rho \boldsymbol{v} \otimes \boldsymbol{v}) &= \mathcal{E}(\chi_k \rho (\bar{\boldsymbol{v}}_k + \boldsymbol{v}'_k) \otimes (\bar{\boldsymbol{v}}_k + \boldsymbol{v}'_k)) \\
&= \mathcal{E}(\chi_k \rho \bar{\boldsymbol{v}}_k \otimes \bar{\boldsymbol{v}}_k) + \mathcal{E}(\chi_k \rho \boldsymbol{v}'_k \otimes \boldsymbol{v}'_k) \\
&= \mathcal{E}(\chi_k \rho) \bar{\boldsymbol{v}}_k \otimes \bar{\boldsymbol{v}}_k + \mathcal{E}(\chi_k \rho \boldsymbol{v}'_k \otimes \boldsymbol{v}'_k) \\
&= \alpha_k \bar{\rho}_k \bar{\boldsymbol{v}}_k \otimes \bar{\boldsymbol{v}}_k - \alpha_k \boldsymbol{T}^t_k,
\end{aligned} \tag{2.77}$$

where we have introduced the Reynolds-stress tensor $\boldsymbol{T}^t_k$. Its concept is similar to the Reynolds-stress tensor in turbulence, but the definition of the velocity fluctuation is different. It accounts for an apparent stress

caused by the fluctuation of the fluid velocity, that disappears from the product of the averages. The definition of $\boldsymbol{T}_k^t$ is

$$\boldsymbol{T}_k^t = -\frac{\mathcal{E}(\chi_k \rho \boldsymbol{v}_k' \otimes \boldsymbol{v}_k')}{\alpha_k}. \tag{2.78}$$

We can now rewrite the averaged momentum equation

$$\begin{aligned}\frac{\partial}{\partial t}(\alpha_k \bar{\rho}_k \bar{\boldsymbol{v}}_k) + \nabla \cdot (\alpha_k \bar{\rho}_k \bar{\boldsymbol{v}}_k \otimes \bar{\boldsymbol{v}}_k) = \nabla \cdot (\alpha_k \bar{\boldsymbol{\tau}}_k - \alpha_k \bar{p}_k \boldsymbol{I}) \\ + \nabla \cdot (\alpha_k \boldsymbol{T}_k^t) + \alpha_k \bar{\rho}_k \bar{\boldsymbol{b}}_k + \mathcal{E}([\rho \boldsymbol{v} \otimes (\boldsymbol{v} - \boldsymbol{v}_i) - (\boldsymbol{\tau} - p\boldsymbol{I})] \cdot \nabla \chi_k).\end{aligned} \tag{2.79}$$

The term

$$\mathcal{E}([\rho \boldsymbol{v} \otimes (\boldsymbol{v} - \boldsymbol{v}_i) - (\boldsymbol{\tau} - p\boldsymbol{I})] \cdot \nabla \chi_k)$$

on the right-hand side represents the momentum exchange between the phases, which is caused by mass transfer and mechanical work at their interfaces. It will be discussed in Section 2.4.6.

Energy equation

Now, we turn to the averaged energy equation (2.66). Similarly to the momentum equation, we have to take into account the fluctuation velocity. By the same principle as used in (2.77), we can write the average of the kinetic energy

$$\mathcal{E}\left(\chi_k \rho \tfrac{1}{2} v^2\right) = \frac{1}{2} \alpha_k \bar{\rho}_k \bar{v}_k^2 + \frac{1}{2} \alpha_k \bar{\rho}_k \bar{e}_k^{kin}, \tag{2.80}$$

where

$$\bar{e}_k^{kin} = \frac{\mathcal{E}\left(\chi_k \rho \boldsymbol{v}_k' \cdot \boldsymbol{v}_k'\right)}{\alpha_k \bar{\rho}_k} \tag{2.81}$$

is the average of the fluctuation kinetic energy. Further, we can write the average of the kinetic energy flux

$$\mathcal{E}\left(\chi_k \rho \tfrac{1}{2} v^2 \boldsymbol{v}\right) = \frac{1}{2} \alpha_k \bar{\rho}_k \left(\bar{v}_k^2 + \bar{e}_k^{kin}\right) \bar{\boldsymbol{v}}_k - \bar{\boldsymbol{v}}_k \cdot \alpha_k \boldsymbol{T}_k^t + \frac{1}{2} \alpha_k \bar{\rho}_k \overline{\boldsymbol{v} e_k^{kin}}, \tag{2.82}$$

where

$$\overline{\boldsymbol{v} e_k^{kin}} = \frac{\mathcal{E}\left(\chi_k \rho \boldsymbol{v}_k' \cdot \boldsymbol{v}_k' \otimes \boldsymbol{v}_k'\right)}{\alpha_k \bar{\rho}_k} \tag{2.83}$$

is the average of the fluctuating flux of fluctuation kinetic energy. We also have to do the same for various terms containing the velocity. The internal energy

$$\mathcal{E}\left(\chi_k \rho e \boldsymbol{v}\right) = \alpha_k \bar{\rho}_k \bar{e}_k \bar{\boldsymbol{v}}_k + \alpha_k \bar{\rho}_k \overline{\boldsymbol{v} e_k^f}, \tag{2.84}$$

where

$$\overline{\boldsymbol{v} e_k^f} = \frac{\mathcal{E}\left(\chi_k \rho e \boldsymbol{v}_k'\right)}{\alpha_k \bar{\rho}_k} \tag{2.85}$$

is the average of the fluctuating flux of internal energy, the stress tensor

$$\mathcal{E}(\chi_k(\boldsymbol{\tau} - p\boldsymbol{I})\boldsymbol{v}) = \alpha_k(\bar{\boldsymbol{\tau}}_k - \bar{p}_k \boldsymbol{I})\bar{\boldsymbol{v}}_k + \alpha_k \overline{\boldsymbol{v}\boldsymbol{T}_k^f}, \tag{2.86}$$

where

$$\overline{\boldsymbol{v}\boldsymbol{T}_k^f} = \frac{\mathcal{E}(\chi_k((\boldsymbol{\tau} - p\boldsymbol{I})\boldsymbol{v}_k'))}{\alpha_k} \tag{2.87}$$

is the average of the fluctuating work of the stress tensor, and the external forces

$$\mathcal{E}(\chi_k \rho \boldsymbol{b} \cdot \boldsymbol{v}) = \alpha_k \bar{\rho}_k \bar{\boldsymbol{b}}_k \cdot \bar{\boldsymbol{v}}_k + \alpha_k \bar{\rho}_k \overline{\boldsymbol{v}\boldsymbol{b}_k^f}, \tag{2.88}$$

where

$$\overline{\boldsymbol{v}\boldsymbol{b}_k^f} = \frac{\mathcal{E}(\chi_k \rho \boldsymbol{b} \cdot \boldsymbol{v}_k')}{\alpha_k \bar{\rho}_k} \tag{2.89}$$

is the average of the fluctuating work of the external forces.

After inserting the various average variables and rearranging, we obtain the average energy equation

$$\begin{aligned}
&\frac{\partial}{\partial t}\left(\alpha_k \bar{\rho}_k \left(\bar{e}_k + \frac{1}{2}\bar{v}_k^2 + \frac{1}{2}\bar{e}_k^{kin}\right)\right) + \nabla \cdot \left(\alpha_k \bar{\rho}_k \left(\bar{e}_k + \frac{1}{2}\bar{v}_k^2 + \frac{1}{2}\bar{e}_k^{kin}\right)\bar{\boldsymbol{v}}_k\right) \\
&\quad = \nabla \cdot \left(\alpha_k \left(\bar{\boldsymbol{\tau}}_k - \bar{p}_k \boldsymbol{I} + \boldsymbol{T}_k^t\right)\bar{\boldsymbol{v}}_k\right) - \nabla \cdot (\alpha_k \bar{\boldsymbol{q}}_k) + \alpha_k \bar{\rho}_k (\bar{r}_k + \bar{\boldsymbol{b}}_k \cdot \bar{\boldsymbol{v}}_k) \\
&\qquad + \nabla \cdot \left(\alpha_k \left(\overline{\boldsymbol{v}\boldsymbol{T}_k^f} - \bar{\rho}_k \overline{\boldsymbol{v} e_k^f} - \frac{1}{2}\bar{\rho}_k \overline{\boldsymbol{v} e_k^{kin}}\right)\right) + \alpha_k \bar{\rho}_k \overline{\boldsymbol{v}\boldsymbol{b}_k^f} \\
&\qquad + \mathcal{E}\left(\left[\rho\left(e + \tfrac{1}{2}v^2\right)(\boldsymbol{v} - \boldsymbol{v}_i) - ((\boldsymbol{\tau} - p\boldsymbol{I})\boldsymbol{v} - \boldsymbol{q})\right] \cdot \nabla \chi_k\right).
\end{aligned} \tag{2.90}$$

Note that $\boldsymbol{T}_k^t$ is symmetrical, therefore the multiplication by $\bar{\boldsymbol{v}}_k$ is commutative. This is a transport equation for the averaged total energy. The kinetic energy is split between the contribution due to the average

velocity, and the component due to the fluctuation of the velocity. The fluctuation of the velocity also caused the appearance of terms accounting for the fluctuation of other quantities, like the body forces. Again, the term

$$\mathcal{E}\left(\left[\rho\left(e+\tfrac{1}{2}v^2\right)(\boldsymbol{v}-\boldsymbol{v}_i)-((\boldsymbol{\tau}-p\boldsymbol{I})\boldsymbol{v}-\boldsymbol{q})\right]\cdot\nabla\chi_k\right)$$

represents the energy exchange between the phases, and is discussed in Section 2.4.6.

2.4.5. Averaging of the interfacial relations

We have performed the averaging process on the bulk equations. These equations contain interaction terms between the phases. By averaging the interfacial relations (2.36), (2.42) and (2.47), we can relate the interaction terms for the different phases with each other. We first introduce the interfacial delta function [17, p. 101]

$$\delta(\boldsymbol{x}-\boldsymbol{x}_i)=\begin{cases}\infty & \text{if } \boldsymbol{x} \text{ is on the interface,}\\ 0 & \text{if } \boldsymbol{x} \text{ is not on the interface,}\end{cases} \tag{2.91}$$

such that, in the context of volume averaging,

$$\int_V \delta(\boldsymbol{x}-\boldsymbol{x}_i)\,\mathrm{d}\nu = S, \tag{2.92}$$

where V is any control volume, and S the interface area contained in V. Explained in words, this function designates the interface and gives it a non-zero weight in volume integrals. In the context of ensemble averaging, the principle is similar. We have

$$\int_E \delta(\boldsymbol{x}-\boldsymbol{x}_i)\,\mathrm{d}m(\mu) = m_i, \tag{2.93}$$

where E is an ensemble of realisations μ, which are weighted by their occurence weight $m(\mu)$. The integral is equal to the probability m_i that the point $\boldsymbol{x}$ is on the interface in the ensemble E. Equipped with this tool, we can give a non-zero weight to the interface in the ensemble averaging process. To derive the average of the interfacial relations, they are multiplied by the delta function, before averaging is performed. To this end, we can remark that we have [17, p. 101]

$$\delta(\boldsymbol{x}-\boldsymbol{x}_i)\boldsymbol{n}_k = -\nabla\chi_k. \tag{2.94}$$

Mass relation

For the mass relation (2.36), this gives

$$\mathcal{E}\Big[\Big(\rho_{\mathrm{g}}\left(\boldsymbol{v}_{\mathrm{g}}-\boldsymbol{v}_i\right)\cdot\boldsymbol{n}_{\mathrm{g}}+\rho_\ell\left(\boldsymbol{v}_\ell-\boldsymbol{v}_i\right)\cdot\boldsymbol{n}_\ell\Big)\cdot\delta\left(\boldsymbol{x}-\boldsymbol{x}_i\right)\Big]=0. \tag{2.95}$$

With the relation (2.94), this becomes

$$\mathcal{E}(\rho_{\mathrm{g}}(\boldsymbol{v}_{\mathrm{g}}-\boldsymbol{v}_i)\cdot\nabla\chi_{\mathrm{g}})+\mathcal{E}(\rho_\ell(\boldsymbol{v}_\ell-\boldsymbol{v}_i)\cdot\nabla\chi_\ell)=0, \tag{2.96}$$

which can be written synthetically

$$\Lambda_{\mathrm{g}}+\Lambda_\ell=0, \tag{2.97}$$

where

$$\Lambda_k=\mathcal{E}(\rho_k(\boldsymbol{v}_k-\boldsymbol{v}_i)\cdot\nabla\chi_k). \tag{2.98}$$

Momentum relation

Applying the averaging process to the momentum relation (2.42), we obtain

$$\begin{aligned}\mathcal{E}(\rho_{\mathrm{g}}\boldsymbol{v}_{\mathrm{g}}\otimes(\boldsymbol{v}_{\mathrm{g}}-\boldsymbol{v}_i)\cdot\delta(\boldsymbol{x}-\boldsymbol{x}_i)\boldsymbol{n}_{\mathrm{g}})+\mathcal{E}(\rho_\ell\boldsymbol{v}_\ell\otimes(\boldsymbol{v}_\ell-\boldsymbol{v}_i)\cdot\delta(\boldsymbol{x}-\boldsymbol{x}_i)\boldsymbol{n}_\ell)\\ -\mathcal{E}((\boldsymbol{\tau}_{\mathrm{g}}-p_{\mathrm{g}}\boldsymbol{I})\,\delta(\boldsymbol{x}-\boldsymbol{x}_i)\boldsymbol{n}_{\mathrm{g}})-\mathcal{E}((\boldsymbol{\tau}_\ell-p_\ell\boldsymbol{I})\,\delta(\boldsymbol{x}-\boldsymbol{x}_i)\boldsymbol{n}_\ell)\\ -\mathcal{E}(\delta(\boldsymbol{x}-\boldsymbol{x}_i)\nabla_s\sigma)-\mathcal{E}(2\sigma H_{s,g}\delta(\boldsymbol{x}-\boldsymbol{x}_i)\boldsymbol{n}_{\mathrm{g}})=0.\end{aligned} \tag{2.99}$$

By the use of the relation (2.94), as well as of the definitions

$$\overline{\nabla_s\sigma}=\mathcal{E}(\delta(\boldsymbol{x}-\boldsymbol{x}_i)\nabla_s\sigma) \tag{2.100}$$

and

$$\overline{2\sigma H_{s,g}\boldsymbol{n}_{\mathrm{g}}}=\mathcal{E}(2\sigma H_{s,g}\delta(\boldsymbol{x}-\boldsymbol{x}_i)\boldsymbol{n}_{\mathrm{g}}), \tag{2.101}$$

it becomes

$$\begin{aligned}-\mathcal{E}(\rho_{\mathrm{g}}\boldsymbol{v}_{\mathrm{g}}\otimes(\boldsymbol{v}_{\mathrm{g}}-\boldsymbol{v}_i)\cdot\nabla\chi_{\mathrm{g}})-\mathcal{E}(\rho_\ell\boldsymbol{v}_\ell\otimes(\boldsymbol{v}_\ell-\boldsymbol{v}_i)\cdot\nabla\chi_\ell)\\ +\mathcal{E}((\boldsymbol{\tau}_{\mathrm{g}}-p_{\mathrm{g}}\boldsymbol{I})\,\nabla\chi_{\mathrm{g}})+\mathcal{E}((\boldsymbol{\tau}_\ell-p_\ell\boldsymbol{I})\,\nabla\chi_\ell)-\overline{\nabla_s\sigma}-\overline{2\sigma H_{s,g}\boldsymbol{n}_{\mathrm{g}}}=0.\end{aligned} \tag{2.102}$$

This can be written synthetically

$$\bar{\boldsymbol{v}}^m_{\mathrm{g},i}\Lambda_\mathrm{g} + \bar{\boldsymbol{v}}^m_{\ell,i}\Lambda_\ell + \boldsymbol{M}_\mathrm{g} + \boldsymbol{M}_\ell = -\overline{\nabla_s \sigma} - \overline{2\sigma H_{s,\mathrm{g}} \boldsymbol{n}_\mathrm{g}}, \tag{2.103}$$

where the average interface velocity $\bar{\boldsymbol{v}}^m_{k,i}$ is defined as

$$\bar{\boldsymbol{v}}^m_{k,i} = \frac{\mathcal{E}(\rho_k \boldsymbol{v}_k \otimes (\boldsymbol{v}_k - \boldsymbol{v}_i)\cdot\nabla\chi_k)}{\mathcal{E}(\rho_k(\boldsymbol{v}_k - \boldsymbol{v}_i)\cdot\nabla\chi_k)}, \tag{2.104}$$

and the interfacial stress is defined by

$$\boldsymbol{M}_k = -\mathcal{E}((\boldsymbol{\tau}_k - p_k\boldsymbol{I})\,\nabla\chi_k) \tag{2.105}$$

Energy relation

Finally, we average the energy interfacial relation (2.47). By multiplying it by the interface delta function and averaging, we obtain

$$\begin{aligned}
&\underbrace{\mathcal{E}\left(\frac{\partial e_{s,i}}{\partial t}\delta(\boldsymbol{x}-\boldsymbol{x}_i)\right)}_{\mathrm{I}} + \underbrace{\mathcal{E}(\nabla_s\cdot(\boldsymbol{v}_i e_{s,i})\,\delta(\boldsymbol{x}-\boldsymbol{x}_i))}_{\mathrm{II}} = \\
&\qquad - \underbrace{\mathcal{E}\left(\rho_\mathrm{g}\left(e_\mathrm{g}+\tfrac{1}{2}v_\mathrm{g}^2\right)(\boldsymbol{v}_\mathrm{g}-\boldsymbol{v}_i)\cdot\delta(\boldsymbol{x}-\boldsymbol{x}_i)\boldsymbol{n}_\mathrm{g}\right)}_{\mathrm{III_g}} \\
&\qquad - \underbrace{\mathcal{E}\left(\rho_\ell\left(e_\mathrm{g}+\tfrac{1}{2}v_\ell^2\right)(\boldsymbol{v}_\ell-\boldsymbol{v}_i)\cdot\delta(\boldsymbol{x}-\boldsymbol{x}_i)\boldsymbol{n}_\ell\right)}_{\mathrm{III}_\ell} \\
&+ \underbrace{\mathcal{E}(((\boldsymbol{\tau}_\mathrm{g}-p_\mathrm{g}\boldsymbol{I})\,\boldsymbol{v}_\mathrm{g})\cdot\delta(\boldsymbol{x}-\boldsymbol{x}_i)\boldsymbol{n}_\mathrm{g})}_{\mathrm{IV_g}} + \underbrace{\mathcal{E}(((\boldsymbol{\tau}_\ell-p_\ell\boldsymbol{I})\,\boldsymbol{v}_\ell)\cdot\delta(\boldsymbol{x}-\boldsymbol{x}_i)\boldsymbol{n}_\ell)}_{\mathrm{IV}_\ell} \\
&\qquad - \underbrace{\mathcal{E}(\boldsymbol{q}_\mathrm{g}\cdot\delta(\boldsymbol{x}-\boldsymbol{x}_i)\boldsymbol{n}_\mathrm{g})}_{\mathrm{V_g}} - \underbrace{\mathcal{E}(\boldsymbol{q}_\ell\cdot\delta(\boldsymbol{x}-\boldsymbol{x}_i)\boldsymbol{n}_\ell)}_{\mathrm{V}_\ell} \\
&+ \underbrace{\mathcal{E}(r_{s,i}\delta(\boldsymbol{x}-\boldsymbol{x}_i))}_{\mathrm{VI}} + \underbrace{\mathcal{E}(2\sigma H_{s,\mathrm{g}}\delta(\boldsymbol{x}-\boldsymbol{x}_i)\boldsymbol{n}_\mathrm{g}\cdot\boldsymbol{v}_i)}_{\mathrm{VII}} + \underbrace{\mathcal{E}(\delta(\boldsymbol{x}-\boldsymbol{x}_i)\boldsymbol{v}_i\cdot\nabla_s\sigma)}_{\mathrm{VIII}}.
\end{aligned} \tag{2.106}$$

We first need to define a quantity that represents the probability that the point $\boldsymbol{x}$ is on the interface. It can be interpreted as a measure of the amount of interface area in the flow. It is the average of the delta function

$$a_k = \mathcal{E}(\delta(\boldsymbol{x} - \boldsymbol{x}_i)). \tag{2.107}$$

For the term I, we write the average as

$$\begin{aligned} \mathcal{E}\left(\frac{\partial e_{s,i}}{\partial t}\delta(\boldsymbol{x} - \boldsymbol{x}_i)\right) &= \mathcal{E}\left(\frac{\partial e_{s,i}}{\partial t}\delta(\boldsymbol{x} - \boldsymbol{x}_i)\right)\frac{\mathcal{E}(\delta(\boldsymbol{x} - \boldsymbol{x}_i))}{\mathcal{E}(\delta(\boldsymbol{x} - \boldsymbol{x}_i))} \\ &= a_k\overline{\frac{\partial e_{s,i}}{\partial t}}, \end{aligned} \tag{2.108}$$

where the average variation of interface energy is defined by

$$\overline{\frac{\partial e_{s,i}}{\partial t}} = \frac{\mathcal{E}\left(\frac{\partial e_{s,i}}{\partial t}\delta(\boldsymbol{x} - \boldsymbol{x}_i)\right)}{\mathcal{E}(\delta(\boldsymbol{x} - \boldsymbol{x}_i))}, \tag{2.109}$$

and for the term II

$$\begin{aligned} \mathcal{E}(\nabla_s \cdot (\boldsymbol{v}_i e_{s,i})\,\delta(\boldsymbol{x} - \boldsymbol{x}_i)) &= \mathcal{E}(\nabla_s \cdot (\boldsymbol{v}_i e_{s,i})\,\delta(\boldsymbol{x} - \boldsymbol{x}_i))\frac{\mathcal{E}(\delta(\boldsymbol{x} - \boldsymbol{x}_i))}{\mathcal{E}(\delta(\boldsymbol{x} - \boldsymbol{x}_i))} \\ &= a_k\overline{\nabla_s \cdot (\boldsymbol{v}_i e_{s,i})}. \end{aligned} \tag{2.110}$$

where the average gradient of interface energy is defined by

$$\overline{\nabla_s \cdot (\boldsymbol{v}_i e_{s,i})} = \frac{\mathcal{E}(\nabla_s \cdot (\boldsymbol{v}_i e_{s,i})\,\delta(\boldsymbol{x} - \boldsymbol{x}_i))}{\mathcal{E}(\delta(\boldsymbol{x} - \boldsymbol{x}_i))}. \tag{2.111}$$

On the right-hand side of (2.106), the terms III_g and III_ℓ are rewritten as

$$\mathcal{E}\left(\rho_k\left(e_k + \tfrac{1}{2}v_k^2\right)(\boldsymbol{v}_k - \boldsymbol{v}_i)\cdot\nabla\chi_k\right) = \left(\bar{e}_{k,i} + \tfrac{1}{2}\bar{v}^{e^2}_{k,i}\right)\Lambda_k, \tag{2.112}$$

where the interfacial averages are defined as

$$\bar{e}_{k,i} = \frac{\mathcal{E}(\rho_k e_k(\boldsymbol{v}_k - \boldsymbol{v}_i)\cdot\nabla\chi_k)}{\mathcal{E}(\rho_k(\boldsymbol{v}_k - \boldsymbol{v}_i)\cdot\nabla\chi_k)}, \tag{2.113}$$

and

$$\bar{v}^{e^2}_{k,i} = \frac{\mathcal{E}(\rho_k v_k^2(\boldsymbol{v}_k - \boldsymbol{v}_i)\cdot\nabla\chi_k)}{\mathcal{E}(\rho_k(\boldsymbol{v}_k - \boldsymbol{v}_i)\cdot\nabla\chi_k)}. \tag{2.114}$$

Next, the terms $\mathrm{IV_g}$ and IV_ℓ are the interfacial work

$$W_k = -\mathcal{E}(((\boldsymbol{\tau}_k - p_k\boldsymbol{I})\boldsymbol{v}_k)\cdot\nabla\chi_k), \tag{2.115}$$

$\mathrm{V_g}$ and V_ℓ are the interfacial heat transfer

$$E_k = \mathcal{E}(\boldsymbol{q}_k\cdot\nabla\chi_k), \tag{2.116}$$

and VI is the interfacial external energy source

$$\begin{aligned}\mathcal{E}(r_{s,i}\delta(\boldsymbol{x}-\boldsymbol{x}_i)) &= \mathcal{E}(r_{s,i}\delta(\boldsymbol{x}-\boldsymbol{x}_i))\frac{\mathcal{E}(\delta(\boldsymbol{x}-\boldsymbol{x}_i))}{\mathcal{E}(\delta(\boldsymbol{x}-\boldsymbol{x}_i))}\\ &= a_k\bar{r}_{s,i},\end{aligned} \tag{2.117}$$

where the average interface external energy source is defined by

$$\bar{r}_{s,i} = \frac{\mathcal{E}(r_{s,i}\delta(\boldsymbol{x}-\boldsymbol{x}_i))}{\mathcal{E}(\delta(\boldsymbol{x}-\boldsymbol{x}_i))}. \tag{2.118}$$

The terms VII and VIII represent the work from the interfacial tension

$$\mathcal{E}(2\sigma H_{s,\mathrm{g}}\delta(\boldsymbol{x}-\boldsymbol{x}_i)\boldsymbol{n}_\mathrm{g}\cdot\boldsymbol{v}_i) = \overline{2\sigma H_{s,\mathrm{g}}\boldsymbol{n}_\mathrm{g}\cdot\boldsymbol{v}_i} \tag{2.119}$$

and

$$\mathcal{E}(\delta(\boldsymbol{x}-\boldsymbol{x}_i)\boldsymbol{v}_i\cdot\nabla_s\sigma) = \overline{\boldsymbol{v}_i\cdot\nabla_s\sigma}. \tag{2.120}$$

Using the definitions above, we can write the averaged energy relation

$$\begin{aligned}&\left(\bar{e}_{\mathrm{g},i} + \tfrac{1}{2}\bar{v}^{e^2}_{\mathrm{g},i}\right)\Lambda_\mathrm{g} + \left(\bar{e}_{\ell,i} + \tfrac{1}{2}\bar{v}^{e^2}_{\ell,i}\right)\Lambda_\ell + W_\mathrm{g} + W_\ell + E_\mathrm{g} + E_\ell\\ &= a_k\overline{\frac{\partial e_{s,i}}{\partial t}} + a_k\overline{\nabla_s\cdot(\boldsymbol{v}_i e_{s,i})} - a_k\bar{r}_{s,i} - \overline{2\sigma H_{s,\mathrm{g}}\boldsymbol{n}_\mathrm{g}\cdot\boldsymbol{v}_i} - \overline{\boldsymbol{v}_i\cdot\nabla_s\sigma}.\end{aligned} \tag{2.121}$$

2.4.6. Relations between the average balance equations

In the average mass balance equation (2.75), we can recognise the term

$$\Lambda_k = \mathcal{E}(\rho(\boldsymbol{v}-\boldsymbol{v}_i)\cdot\nabla\chi_k) \tag{2.122}$$

from the interfacial relation (2.97). Thus, the average mass balance equation can be written

$$\frac{\partial}{\partial t}(\alpha_k\bar{\rho}_k) + \nabla\cdot(\alpha_k\bar{\rho}_k\bar{\boldsymbol{v}}_k) = \Lambda_k, \tag{2.123}$$

where the terms Λ_k for the different phases are related through (2.97).

Similarly, we had an exchange term in the momentum balance equation (2.79), which is also present in the average interfacial momentum relation (2.103)

$$\mathcal{E}([\rho \boldsymbol{v} \otimes (\boldsymbol{v} - \boldsymbol{v}_i) - (\boldsymbol{\tau} - p\boldsymbol{I})] \cdot \nabla \chi_k) = \bar{\boldsymbol{v}}^m_{k,i} \Lambda_k + \boldsymbol{M}_k. \tag{2.124}$$

Thus we can write the average momentum equation as

$$\begin{aligned} \frac{\partial}{\partial t}(\alpha_k \bar{\rho}_k \bar{\boldsymbol{v}}_k) + \nabla \cdot (\alpha_k \bar{\rho}_k \bar{\boldsymbol{v}}_k \otimes \bar{\boldsymbol{v}}_k) = \\ \nabla \cdot (\alpha_k (\bar{\boldsymbol{\tau}}_k - \bar{p}_k \boldsymbol{I} + \boldsymbol{T}^t_k)) + \alpha_k \bar{\rho}_k \bar{\boldsymbol{b}}_k + \bar{\boldsymbol{v}}^m_{k,i} \Lambda_k + \boldsymbol{M}_k. \end{aligned} \tag{2.125}$$

However, some formulations of the multiphase flow models require the definition of an interfacial pressure, which is defined as [17, p. 128]

$$p_{i,k} = \frac{\mathcal{E}(p\delta(\boldsymbol{x} - \boldsymbol{x}_i))}{\mathcal{E}(\delta(\boldsymbol{x} - \boldsymbol{x}_i))}. \tag{2.126}$$

Note that the interfacial pressure is not necessarily the same for all the phases. It arises from the fact that the pressure just next to the interface may be different from the average bulk pressure. Now, remark that

$$\begin{aligned} \mathcal{E}(p_{i,k} \nabla \chi_k) &= \frac{\mathcal{E}(p\delta(\boldsymbol{x} - \boldsymbol{x}_i))}{\mathcal{E}(\delta(\boldsymbol{x} - \boldsymbol{x}_i))} \mathcal{E}(\nabla \chi_k) \\ &= p_{i,k} \nabla \mathcal{E}(\chi_k) \\ &= p_{i,k} \nabla \alpha_k. \end{aligned} \tag{2.127}$$

Then a new interfacial force density is defined as

$$\boldsymbol{M}_{i,k} = -\mathcal{E}(\boldsymbol{\tau}_k \nabla \chi_k) + \mathcal{E}((p_k - p_{i,k}) \nabla \chi_k), \tag{2.128}$$

such that, in (2.124),

$$\begin{aligned} \boldsymbol{M}_k &= -\mathcal{E}(\boldsymbol{\tau}_k \nabla \chi_k) + \mathcal{E}(p_k \nabla \chi_k) \\ &= \boldsymbol{M}_{i,k} + p_{i,k} \nabla \alpha_k. \end{aligned} \tag{2.129}$$

An alternative to the momentum equation (2.125) is then

$$\begin{aligned} \frac{\partial}{\partial t}(\alpha_k \bar{\rho}_k \bar{\boldsymbol{v}}_k) + \nabla \cdot (\alpha_k \bar{\rho}_k \bar{\boldsymbol{v}}_k \otimes \bar{\boldsymbol{v}}_k) = \\ -\alpha_k \nabla \bar{p}_k - (\bar{p}_k - p_{i,k}) \nabla \alpha_k + \nabla \cdot (\alpha_k (\bar{\boldsymbol{\tau}}_k + \boldsymbol{T}^t_k)) + \alpha_k \bar{\rho}_k \bar{\boldsymbol{b}}_k + \bar{\boldsymbol{v}}^m_{k,i} \Lambda_k + \boldsymbol{M}_{i,k}. \end{aligned} \tag{2.130}$$

The exchange term in the energy balance equation (2.90) also appears in the energy interfacial relation (2.121). It is

$$\mathcal{E}\left(\left[\rho\left(e+\tfrac{1}{2}v^2\right)(\boldsymbol{v}-\boldsymbol{v}_i)-((\boldsymbol{\tau}-p\boldsymbol{I})\boldsymbol{v}-\boldsymbol{q})\right]\cdot\nabla\chi_k\right) = \left(\bar{e}_{k,i}+\tfrac{1}{2}\bar{v}_{k,i}^{e^2}\right)\Lambda_k+W_k+E_k. \quad (2.131)$$

The average energy equation then becomes

$$\begin{aligned}\frac{\partial}{\partial t}\left(\alpha_k\bar{\rho}_k\left(\bar{e}_k+\frac{1}{2}\bar{v}_k^2+\frac{1}{2}\bar{e}_k^{kin}\right)\right)+\nabla\cdot\left(\alpha_k\bar{\rho}_k\left(\bar{e}_k+\frac{1}{2}\bar{v}_k^2+\frac{1}{2}\bar{e}_k^{kin}\right)\bar{\boldsymbol{v}}_k\right)\\ =\nabla\cdot\left(\alpha_k\left(\bar{\boldsymbol{\tau}}_k-\bar{p}_k\boldsymbol{I}+\boldsymbol{T}_k^t\right)\bar{\boldsymbol{v}}_k\right)-\nabla\cdot(\alpha_k\bar{\boldsymbol{q}}_k)+\alpha_k\bar{\rho}_k(\bar{r}_k+\bar{\boldsymbol{b}}_k\cdot\bar{\boldsymbol{v}}_k)\\ +\nabla\cdot\left(\alpha_k\left(\overline{\boldsymbol{v}\boldsymbol{T}_k^f}-\bar{\rho}_k\overline{\boldsymbol{v}e_k^f}-\frac{1}{2}\bar{\rho}_k\overline{\boldsymbol{v}e_k^{kin}}\right)\right)+\alpha_k\bar{\rho}_k\overline{\boldsymbol{v}\boldsymbol{b}_k^f}\\ +\left(\bar{e}_{k,i}+\tfrac{1}{2}\bar{v}_{k,i}^{e^2}\right)\Lambda_k+W_k+E_k. \quad (2.132)\end{aligned}$$

Remark that the friction between the phases is contained in W_k. It is not the friction at the interface, but includes the shear stress in the whole boundary layer.

We also need an equation describing the behaviour of the interface. This is called the topological equation in [17, p. 101] and describes the movement of the characteristic function χ_k

$$\frac{\partial\chi_k}{\partial t}+\boldsymbol{v}_i\cdot\nabla\chi_k=0, \quad (2.133)$$

where $\boldsymbol{v}_i$ is the velocity of the interface.

2.4.7. Summary of the transport equations

We summarise the results of the sections above. The mass transport equation for phase $k=\mathrm{g},\ell$ is given by (2.123)

$$\frac{\partial}{\partial t}(\alpha_k\bar{\rho}_k)+\nabla\cdot(\alpha_k\bar{\rho}_k\bar{\boldsymbol{v}}_k)=\Lambda_k, \quad (2.134)$$

where the interfacial interaction terms are related by (2.97)

$$\Lambda_{\mathrm{g}}+\Lambda_\ell=0. \quad (2.135)$$

The momentum transport equation for phase $k = \mathrm{g}, \ell$ in its original form is given by (2.125)

$$\frac{\partial}{\partial t}(\alpha_k \bar{\rho}_k \bar{\boldsymbol{v}}_k) + \nabla \cdot (\alpha_k \bar{\rho}_k \bar{\boldsymbol{v}}_k \otimes \bar{\boldsymbol{v}}_k) = \nabla \cdot (\alpha_k (\bar{\boldsymbol{\tau}}_k - \bar{p}_k \boldsymbol{I} + \boldsymbol{T}_k^t)) + \alpha_k \bar{\rho}_k \bar{\boldsymbol{b}}_k + \bar{\boldsymbol{v}}_{k,i}^m \Lambda_k + \boldsymbol{M}_k, \quad (2.136)$$

where the interfacial interaction terms are related by (2.103)

$$\bar{\boldsymbol{v}}_{\mathrm{g},i}^m \Lambda_\mathrm{g} + \bar{\boldsymbol{v}}_{\ell,i}^m \Lambda_\ell + \boldsymbol{M}_\mathrm{g} + \boldsymbol{M}_\ell = -\overline{\nabla_s \sigma} - \overline{2\sigma H_{s,\mathrm{g}} \boldsymbol{n}_\mathrm{g}}. \quad (2.137)$$

To define the alternative form, we first introduce the definition (2.129)

$$\boldsymbol{M}_k = \boldsymbol{M}_{i,k} + p_{i,k} \nabla \alpha_k, \quad (2.138)$$

and the momentum equation becomes (2.130)

$$\frac{\partial}{\partial t}(\alpha_k \bar{\rho}_k \bar{\boldsymbol{v}}_k) + \nabla \cdot (\alpha_k \bar{\rho}_k \bar{\boldsymbol{v}}_k \otimes \bar{\boldsymbol{v}}_k) = -\alpha_k \nabla \bar{p}_k - (\bar{p}_k - p_{i,k}) \nabla \alpha_k + \nabla \cdot (\alpha_k (\bar{\boldsymbol{\tau}}_k + \boldsymbol{T}_k^t)) + \alpha_k \bar{\rho}_k \bar{\boldsymbol{b}}_k + \bar{\boldsymbol{v}}_{k,i}^m \Lambda_k + \boldsymbol{M}_{i,k}. \quad (2.139)$$

The total energy transport equation for phase $k = \mathrm{g}, \ell$ is given by (2.132)

$$\begin{aligned} \frac{\partial}{\partial t}\left(\alpha_k \bar{\rho}_k \left(\bar{e}_k + \frac{1}{2}\bar{v}_k^2 + \frac{1}{2}\bar{e}_k^{kin}\right)\right) + \nabla \cdot \left(\alpha_k \bar{\rho}_k \left(\bar{e}_k + \frac{1}{2}\bar{v}_k^2 + \frac{1}{2}\bar{e}_k^{kin}\right) \bar{\boldsymbol{v}}_k\right) \\ = \nabla \cdot \left(\alpha_k \left(\bar{\boldsymbol{\tau}}_k - \bar{p}_k \boldsymbol{I} + \boldsymbol{T}_k^t\right) \bar{\boldsymbol{v}}_k\right) - \nabla \cdot (\alpha_k \bar{\boldsymbol{q}}_k) + \alpha_k \bar{\rho}_k (\bar{r}_k + \bar{\boldsymbol{b}}_k \cdot \bar{\boldsymbol{v}}_k) \\ + \nabla \cdot \left(\alpha_k \left(\overline{\boldsymbol{v}\boldsymbol{T}_k^f} - \bar{\rho}_k \overline{\boldsymbol{v} e_k^f} - \frac{1}{2}\bar{\rho}_k \overline{\boldsymbol{v} e_k^{kin}}\right)\right) + \alpha_k \bar{\rho}_k \overline{\boldsymbol{v}\boldsymbol{b}_k^f} \\ + \left(\bar{e}_{k,i} + \tfrac{1}{2}\bar{v}_{k,i}^{e^2}\right) \Lambda_k + W_k + E_k, \end{aligned} \quad (2.140)$$

where the interfacial interaction terms are related by (2.121)

$$\begin{aligned} &\left(\bar{e}_{\mathrm{g},i} + \tfrac{1}{2}\bar{v}_{\mathrm{g},i}^{e^2}\right) \Lambda_\mathrm{g} + \left(\bar{e}_{\ell,i} + \tfrac{1}{2}\bar{v}_{\ell,i}^{e^2}\right) \Lambda_\ell + W_\mathrm{g} + W_\ell + E_\mathrm{g} + E_\ell \\ &= a_k \overline{\frac{\partial e_{s,i}}{\partial t}} + a_k \overline{\nabla_s \cdot (\boldsymbol{v}_i e_{s,i})} - a_k \bar{r}_{s,i} - \overline{2\sigma H_{s,\mathrm{g}} \boldsymbol{n}_\mathrm{g} \cdot \boldsymbol{v}_i} - \overline{\boldsymbol{v}_i \cdot \nabla_s \sigma}. \end{aligned} \quad (2.141)$$

2.5. Two-phase flow models

The averaged transport equations (2.123), (2.125) and (2.132) involve many more unknowns than there are equations. Thus we need closure laws to make the system solvable. But first, to define one-dimensional two-phase flow models, the transport equations should be averaged over the cross-section. This process is very similar to the ensemble averaging described above. Here we do it implicitly, and write the one-dimensional equations directly. In the following, we will drop the bar for the average variables.

Mass equation

The mass transport equation (2.123) becomes

$$\frac{\partial}{\partial t}(\alpha_k \rho_k) + \frac{\partial}{\partial x}(\alpha_k \rho_k v_k) = \Lambda_k, \tag{2.142}$$

where $\Lambda_k = 0$ if we assume that there is no mass exchange between the phases. To model phase change, one possibility is to define Λ_k as a relaxation term [53, 22, 64, 79, 94]. It may take the following form, for example for the gas phase in a liquid-gas mixture

$$\Lambda_{\mathrm{g}} = \mathcal{K}(\mu_\ell - \mu_{\mathrm{g}}), \tag{2.143}$$

where $\mathcal{K}$ is some positive relaxation constant and μ_k is the chemical potential in phase k. This term will force the chemical potentials towards each other through phase change.

Momentum equation

The momentum equation (2.125) becomes

$$\begin{aligned}\frac{\partial}{\partial t}(\alpha_k \rho_k v_k) + \frac{\partial}{\partial x}\left(\alpha_k \rho_k v_k^2\right) + \frac{\partial}{\partial x}(\alpha_k p_k) = \\ \frac{\partial \alpha_k (\tau_{k,xx} + T^t_{k,xx})}{\partial x} + m_{\tau,k} + \alpha_k \rho_k b_k + v^m_{k,i}\Lambda_k + M_k,\end{aligned} \tag{2.144}$$

where $\tau_{k,xx}$ and $T^t_{k,xx}$ are the longitudinal components of the stress tensors $\bar{\boldsymbol{\tau}}_k$ and $\boldsymbol{T}^t_k$. $m_{\tau,k}$ is a cross-sectional average of the other components of

the stress tensors and represents the transversal momentum dissipation due to shear stress and to the fluctuation of velocity. The contributions from the fluctuations are often neglected. In the case of inviscid flow, we can write $\tau_{k,xx} = 0$ and $m_{\tau,k} = 0$. Otherwise, the term $m_{\tau,k}$ represents friction on the walls. The next term, $\alpha_k \rho_k b_k$, represents the projection of the body forces on the flow direction, for example gravity. The term $v^m_{k,i}\Lambda_k$ represents the momentum transfer associated with phase change. It requires the definition of an interfacial velocity $v^m_{k,i}$ (See for example v_i in Paper G [55], Section 4.7). Finally, the term M_k is the momentum exchange between the phases due to the interfacial stress. The alternative form of the momentum equation (2.130) becomes

$$\frac{\partial}{\partial t}(\alpha_k \rho_k v_k) + \frac{\partial}{\partial x}\left(\alpha_k \rho_k v_k^2\right) + \alpha_k \frac{\partial p_k}{\partial x} + (p_k - p_{i,k})\frac{\partial \alpha_k}{\partial x} = \\ + \frac{\partial \alpha_k (\tau_{k,xx} + T^t_{k,xx})}{\partial x} + m_{\tau,k} + \alpha_k \rho_k b_k + v^m_{k,i}\Lambda_k + M_{i,k}. \quad (2.145)$$

Energy equation

For the one-dimensional energy equation, we neglect in (2.132) the fluctuation quantities $\bar{e}^{kin}_k$, $\overline{\boldsymbol{v}\boldsymbol{T}^f_k}$, $\overline{\boldsymbol{v}e^f_k}$, $\overline{\boldsymbol{v}e^{kin}_k}$ and $\overline{\boldsymbol{v}\boldsymbol{b}^f_k}$

$$\frac{\partial}{\partial t}\left(\alpha_k \rho_k \left(e_k + \frac{1}{2}v_k^2\right)\right) + \frac{\partial}{\partial x}\left(\alpha_k \rho_k \left(e_k + \frac{1}{2}v_k^2\right) v_k\right) + \frac{\partial}{\partial x}(\alpha_k p_k v_k) \\ = \frac{\partial}{\partial x}(\alpha_k(\tau_{k,xx} + T^t_{k,xx})v_k) - \frac{\partial}{\partial x}(\alpha_k q_k) + \alpha_k \rho_k (r_k + b_k v_k) \\ + \left(e_{k,i} + \tfrac{1}{2}v^{e^2}_{k,i}\right)\Lambda_k + W_k + E_k. \quad (2.146)$$

Similarly to the momentum equation, the longitudinal effects of the stress tensors $\tau_{k,xx}$ and $T^t_{k,xx}$ are present. Concerning their transversal contributions, we can argue that they should disappear in the cross-sectional averaging, since they represent fluid friction on the wall. Friction is a diffusive effect that transforms kinetic energy into thermal energy. Since the equation describes the evolution of total energy, friction should not have any effect in this equation. It is only an internal energy exchange over the cross-section. The second term on the right-hand side, $\partial_x(\alpha_k q_k)$, accounts for the longitudinal heat transfer by conduction. It is often

neglected, when the conductive fluxes are negligible compared to the convective fluxes. The term $\alpha_k\rho_k(r_k+b_kv_k)$ represents the energy brought by external heat sources and by the work of the body forces. Then comes the energy exchange term $(e_{k,i}+1/2v_{k,i}^{e^2})\Lambda_k$, related to mass exchange. This term involves an interfacial internal energy $e_{k,i}$ and another interfacial velocity $v_{k,i}^e$. W_k and E_k are the averaged interfacial work and heat transfer, respectively. The interfacial heat transfer is sometimes neglected. It may also be modelled by a relaxation term

$$E_{\mathrm{g}} = \mathcal{H}(T_\ell - T_{\mathrm{g}}), \tag{2.147}$$

where $\mathcal{H}$ is a positive constant.

Finally, the one-dimensional average of the topological equation (2.133) is [17, p. 101]

$$\frac{\partial\alpha_k}{\partial t} + v_{\mathrm{i}}\frac{\partial\alpha_k}{\partial x} = 0. \tag{2.148}$$

2.5.1. The seven-equation two-pressure model

We now have two phases in presence, g and ℓ. We write the one-dimensional conservation equations, for which we have made the assumptions of inviscid flow, no mass exchange, no heat transfer, no heat source and no body forces. In addition, we neglect surface tension and all other interface phenomena. However, we keep the terms for interfacial momentum and energy exchange. The equations are

$$\frac{\partial\alpha_{\mathrm{g}}}{\partial t} + v_{\mathrm{i}}\frac{\partial\alpha_{\mathrm{g}}}{\partial x} = I_{\mathrm{g}\ell}, \tag{2.149}$$

$$\frac{\partial\alpha_{\mathrm{g}}\rho_{\mathrm{g}}}{\partial t} + \frac{\partial\alpha_{\mathrm{g}}\rho_{\mathrm{g}}v_{\mathrm{g}}}{\partial x} = 0, \tag{2.150}$$

$$\frac{\partial\alpha_\ell\rho_\ell}{\partial t} + \frac{\partial\alpha_\ell\rho_\ell v_\ell}{\partial x} = 0, \tag{2.151}$$

$$\frac{\partial\alpha_{\mathrm{g}}\rho_{\mathrm{g}}v_{\mathrm{g}}}{\partial t} + \frac{\partial}{\partial x}\left(\alpha_{\mathrm{g}}\rho_{\mathrm{g}}v_{\mathrm{g}}^2 + \alpha_{\mathrm{g}}p_{\mathrm{g}}\right) = M_{\mathrm{g}\ell}, \tag{2.152}$$

$$\frac{\partial\alpha_\ell\rho_\ell v_\ell}{\partial t} + \frac{\partial}{\partial x}\left(\alpha_\ell\rho_\ell v_\ell^2 + \alpha_\ell p_\ell\right) = M_{\ell\mathrm{g}} = -M_{\mathrm{g}\ell}, \tag{2.153}$$

$$\frac{\partial}{\partial t}\left(\alpha_{\mathrm{g}}\rho_{\mathrm{g}}\left(e_{\mathrm{g}}+\frac{v_{\mathrm{g}}^2}{2}\right)\right)+\frac{\partial}{\partial x}\left(\alpha_{\mathrm{g}}\rho_{\mathrm{g}}\left(e_{\mathrm{g}}+\frac{v_{\mathrm{g}}^2}{2}\right)v_{\mathrm{g}}+\alpha_{\mathrm{g}}v_{\mathrm{g}}p_{\mathrm{g}}\right) = E_{\mathrm{g}}+v_{\mathrm{g}}M_{\mathrm{g}\ell}, \tag{2.154}$$

$$\frac{\partial}{\partial t}\left(\alpha_{\ell}\rho_{\ell}\left(e_{\mathrm{g}}+\frac{v_{\ell}^2}{2}\right)\right)+\frac{\partial}{\partial x}\left(\alpha_{\ell}\rho_{\ell}\left(e_{\mathrm{g}}+\frac{v_{\ell}^2}{2}\right)v_{\ell}+\alpha_{\ell}v_{\ell}p_{\ell}\right) = E_{\ell}+v_{\ell}M_{\ell\mathrm{g}}. \tag{2.155}$$

The interaction term $I_{\mathrm{g}\ell}$ in the topological equation (2.149) allows for a transversal movement of the interface – *via* the volume fraction – due to mechanical action of the phases on each other. The interaction terms for the momentum exchange between the phases by mechanical work $M_{\mathrm{g}\ell}$ and $M_{\ell\mathrm{g}}$ correspond to M_k in (2.144). The interfacial momentum relation (2.103) with the assumptions given above then implies that $M_{\ell\mathrm{g}} = -M_{\mathrm{g}\ell}$. In the energy equation, the interaction terms E_{g} and E_{ℓ} correspond to E_k, and $v_{\mathrm{g}}M_{\mathrm{g}\ell}$ and $v_{\ell}M_{\ell\mathrm{g}}$ correspond to W_k in (2.146). The energy interfacial relation (2.121) with the assumptions mentioned above implies that

$$E_{\mathrm{g}}+v_{\mathrm{g}}M_{\mathrm{g}\ell} = -(E_{\ell}-v_{\ell}M_{\mathrm{g}\ell}). \tag{2.156}$$

The interaction terms for the energy equations were defined in this way, because, by multiplying the momentum equations by their respective velocities v_{g} and v_{ℓ} and subtracting them from their respective energy equations, we obtain the internal energy equations

$$\frac{\partial}{\partial t}(\alpha_{\mathrm{g}}\rho_{\mathrm{g}}e_{\mathrm{g}})+\frac{\partial}{\partial x}(\alpha_{\mathrm{g}}\rho_{\mathrm{g}}e_{\mathrm{g}}v_{\mathrm{g}})+\alpha_{\mathrm{g}}p_{\mathrm{g}}\frac{\partial v_{\mathrm{g}}}{\partial x} = E_{\mathrm{g}}, \tag{2.157}$$

$$\frac{\partial}{\partial t}(\alpha_{\ell}\rho_{\ell}e_{\mathrm{g}})+\frac{\partial}{\partial x}(\alpha_{\ell}\rho_{\ell}e_{\mathrm{g}}v_{\ell})+\alpha_{\ell}p_{\ell}\frac{\partial v_{\ell}}{\partial x} = E_{\ell}. \tag{2.158}$$

Expression of the interaction terms E_{g} and E_{ℓ}

The model (2.149)–(2.155) contains the undefined interaction terms $I_{\mathrm{g}\ell}$, E_{g}, E_{ℓ} and $M_{\mathrm{g}\ell}$. Using thermodynamical relations, we are able to specify E_{g} and E_{ℓ}. We first derive entropy transport equations from the internal energy equations (2.157)–(2.158). The fundamental thermodynamical

relation reads

$$\mathrm{d}e_k = T_k \,\mathrm{d}s_k + \frac{p_k}{\rho_k^2}\,\mathrm{d}\rho_k. \tag{2.159}$$

The internal energy equations (2.157)–(2.158) can be rewritten through the mass equations (2.150)–(2.151), for a phase k,

$$\alpha_k\rho_k\frac{\partial e_k}{\partial t} + \alpha_k\rho_k v_k\frac{\partial e_k}{\partial x} + \alpha_k p_k\frac{\partial v_k}{\partial x} = E_k. \tag{2.160}$$

Substituting the thermodynamical relation (2.159), we obtain a first entropy equation

$$\alpha_k\rho_k\left(T_k\frac{\partial s_k}{\partial t} + \frac{p_k}{\rho_k^2}\frac{\partial \rho_k}{\partial t}\right) + \alpha_k\rho_k v_k\left(T_k\frac{\partial s_k}{\partial x} + \frac{p_k}{\rho_k^2}\frac{\partial \rho_k}{\partial x}\right) + \alpha_k p_k\frac{\partial v_k}{\partial x} = E_k. \tag{2.161}$$

Now, the mass equations (2.150)–(2.151) give an expression for the density derivative

$$\alpha_k\left(\frac{\partial \rho_k}{\partial t} + v_k\frac{\partial \rho_k}{\partial x}\right) = -\rho_k\frac{\partial \alpha_k}{\partial t} - \rho_k\frac{\partial \alpha_k v_k}{\partial x}, \tag{2.162}$$

so that the entropy equation (2.161) finally becomes

$$\frac{\partial \alpha_k\rho_k s_k}{\partial t} + \frac{\partial \alpha_k\rho_k s_k v_k}{\partial x} = \frac{p_k}{T_k}\frac{\partial \alpha_k}{\partial t} + \frac{p_k v_k}{T_k}\frac{\partial \alpha_k}{\partial x} + \frac{E_k}{T_k}. \tag{2.163}$$

Another thermodynamical differential for the function $p_k(\rho_k, e_k)$ is [62]

$$\mathrm{d}p_k = \left(c_k^2 - \Gamma_k\frac{p_k}{\rho_k}\right)\mathrm{d}\rho_k + \Gamma_k\rho_k\,\mathrm{d}e_k, \tag{2.164}$$

where Γ_k is the first Grüneisen parameter for phase k, defined by

$$\Gamma = \frac{1}{\rho C_v}\left(\frac{\partial p}{\partial T}\right)_\rho, \tag{2.165}$$

and C_v is the specific heat capacity at constant volume. The differential (2.164) gives, by the fundamental thermodynamical relation (2.159),

$$\mathrm{d}s_k = \frac{1}{\Gamma_k\rho_k T_k}\,\mathrm{d}p_k - \frac{c_k^2}{\Gamma_k\rho_k T_k}\,\mathrm{d}\rho_k. \tag{2.166}$$

Now, we can substitute the differential (2.166) in the entropy equation (2.163)

$$\frac{\alpha_k}{\Gamma_k T_k}\frac{\partial p_k}{\partial t} - \frac{\alpha_k c_k^2}{\Gamma_k T_k}\frac{\partial \rho_k}{\partial t} + v_k\frac{\alpha_k}{\Gamma_k T_k}\frac{\partial p_k}{\partial x} - v_k\frac{\alpha_k c_k^2}{\Gamma_k T_k}\frac{\partial \rho_k}{\partial x} = \frac{p_k}{T_k}\frac{\partial \alpha_k}{\partial t} + \frac{p_k v_k}{T_k}\frac{\partial \alpha_k}{\partial x} + \frac{E_k}{T_k}. \quad (2.167)$$

The mass equations (2.150)–(2.151), multiplied by the factor $\frac{c_k^2}{\Gamma_k T_k}$, are added to the latter equation, and after simplification, we obtain

$$E_k = \left(\frac{\rho_k c_k^2}{\Gamma_k} - p_k\right)\left(\frac{\partial \alpha_k}{\partial t} + v_k\frac{\partial \alpha_k}{\partial x}\right) + \frac{\alpha_k}{\Gamma_k}\left(\frac{\partial p_k}{\partial t} + v_k\frac{\partial p_k}{\partial x}\right) + \frac{\alpha_k \rho_k c_k^2}{\Gamma_k}\frac{\partial v_k}{\partial x}. \quad (2.168)$$

Expression of the interaction term $M_{g\ell}$

Using the relation (2.156), we are also able to specify $M_{g\ell}$. Substituting (2.168) for phases g and ℓ, we find

$$\begin{aligned}(v_g - v_\ell)M_{g\ell} = &-\left(\frac{\rho_g c_g^2}{\Gamma_g} - p_g\right)\left(\frac{\partial \alpha_g}{\partial t} + v_g\frac{\partial \alpha_g}{\partial x}\right) \\ &-\left(\frac{\rho_\ell c_\ell^2}{\Gamma_\ell} - p_\ell\right)\left(\frac{\partial \alpha_\ell}{\partial t} + v_\ell\frac{\partial \alpha_\ell}{\partial x}\right) - \frac{\alpha_g}{\Gamma_g}\left(\frac{\partial p_g}{\partial t} + v_g\frac{\partial p_g}{\partial x}\right) \\ &-\frac{\alpha_\ell}{\Gamma_\ell}\left(\frac{\partial p_\ell}{\partial t} + v_\ell\frac{\partial p_\ell}{\partial x}\right) - \frac{\alpha_g \rho_g c_g^2}{\Gamma_g}\frac{\partial v_g}{\partial x} - \frac{\alpha_\ell \rho_\ell c_\ell^2}{\Gamma_\ell}\frac{\partial v_\ell}{\partial x}. \quad (2.169)\end{aligned}$$

Expression of the interaction term $I_{g\ell}$

The remaining interaction term $I_{g\ell}$ in (2.149) says something on how the phases reach mechanical equilibrium. Contrarily to the terms E_g, E_ℓ and $M_{g\ell}$, it cannot be defined through the thermodynamical relations. It requires an assumption. If $I_{g\ell} = 0$, the phases are insensitive to each other's pressure, and behave as if the interface were a wall that moves at velocity v_i. Otherwise, it may follow a relaxation law, for example

$$I_{g\ell} = \mathcal{J}(p_g - p_\ell), \quad (2.170)$$

with $\mathcal{J}$ some positive constant. Thus, if $p_\mathrm{g} > p_\ell$, the interaction term will tend to increase the g-phase volume fraction α_g, thus decreasing p_g. The term disappears at mechanical equilibrium $p_\mathrm{g} = p_\ell$.

Additional assumptions

The system contains seven transport equations. In addition, there are two independent thermodynamical parameters per phase, therefore thermodynamics brings two additional independent relations per phase. Finally, we have the relation $\alpha_\mathrm{g} + \alpha_\ell = 0$. This amounts to 12 relations. On the other hand, each phase is described by its volume fraction α, its five thermodynamical variables ρ, p, T, s and e, and its velocity v. This amounts to 14 variables. We have left aside the interfacial velocity v_i as it requires its own modelling assumption. Therefore the system requires two additional relations in order to be closed. We have derived the phasic entropy transport equation (2.163)

$$\frac{\partial \alpha_k \rho_k s_k}{\partial t} + \frac{\partial \alpha_k \rho_k s_k v_k}{\partial x} = \frac{p_k}{T_k}\frac{\partial \alpha_k}{\partial t} + \frac{p_k v_k}{T_k}\frac{\partial \alpha_k}{\partial x} + \frac{E_k}{T_k}, \tag{2.171}$$

where the interaction term E_k is given by (2.168)

$$E_k = \left(\frac{\rho_k c_k^2}{\Gamma_k} - p_k\right)\left(\frac{\partial \alpha_k}{\partial t} + v_k \frac{\partial \alpha_k}{\partial x}\right) + \frac{\alpha_k}{\Gamma_k}\left(\frac{\partial p_k}{\partial t} + v_k \frac{\partial p_k}{\partial x}\right) + \frac{\alpha_k \rho_k c_k^2}{\Gamma_k}\frac{\partial v_k}{\partial x}. \tag{2.172}$$

The two additional relations are found by making an assumption on the phasic entropy sources

$$\frac{\partial \alpha_\mathrm{g} \rho_\mathrm{g} s_\mathrm{g}}{\partial t} + \frac{\partial \alpha_\mathrm{g} \rho_\mathrm{g} s_\mathrm{g} v_\mathrm{g}}{\partial x} = \frac{(p_\mathrm{g} - p_\ell)\Gamma_\mathrm{g}}{2T_\mathrm{g}} I_{\mathrm{g}\ell}, \tag{2.173}$$

$$\frac{\partial \alpha_\ell \rho_\ell s_\ell}{\partial t} + \frac{\partial \alpha_\ell \rho_\ell s_\ell v_\ell}{\partial x} = \frac{(p_\mathrm{g} - p_\ell)\Gamma_\ell}{2T_\ell} I_{\mathrm{g}\ell}. \tag{2.174}$$

Note that $I_{\mathrm{g}\ell}$ has the same sign as $(p_\mathrm{g} - p_\ell)$, so that $(p_\mathrm{g} - p_\ell) I_{\mathrm{g}\ell}$ is always positive. These source terms create entropy when the system evolves towards mechanical equilibrium. They are necessary in order for the final system not to be singular when $v_\mathrm{g} = v_\ell$. By summing the two phasic equations (2.173) and (2.174), we can verify that the entropy of

the mixture always increases. Then, due to the entropy equation (2.163), we have, for phase g,

$$\frac{p_\mathrm{g}}{T_\mathrm{g}}\frac{\partial \alpha_\mathrm{g}}{\partial t} + \frac{p_\mathrm{g} v_\mathrm{g}}{T_\mathrm{g}}\frac{\partial \alpha_\mathrm{g}}{\partial x} + \frac{E_\mathrm{g}}{T_\mathrm{g}} = \frac{(p_\mathrm{g} - p_\ell)\Gamma_\mathrm{g}}{2T_\mathrm{g}} I_{\mathrm{g}\ell}. \tag{2.175}$$

Substituting E_g and simplifying, we obtain a relation giving the time derivative of the pressures

$$\alpha_\mathrm{g}\frac{\partial p_\mathrm{g}}{\partial t} = -\alpha_\mathrm{g} v_\mathrm{g}\frac{\partial p_\mathrm{g}}{\partial x} - \rho_\mathrm{g} c_\mathrm{g}^2\left(\frac{\partial \alpha_\mathrm{g}}{\partial t} + \frac{\partial \alpha_\mathrm{g} v_\mathrm{g}}{\partial x}\right) + \frac{1}{2}(p_\mathrm{g} - p_\ell)\Gamma_\mathrm{g} I_{\mathrm{g}\ell}, \tag{2.176}$$

$$\alpha_\ell\frac{\partial p_\ell}{\partial t} = -\alpha_\ell v_\ell\frac{\partial p_\ell}{\partial x} - \rho_\ell c_\ell^2\left(\frac{\partial \alpha_\ell}{\partial t} + \frac{\partial \alpha_\ell v_\ell}{\partial x}\right) + \frac{1}{2}(p_\mathrm{g} - p_\ell)\Gamma_\ell I_{\mathrm{g}\ell}, \tag{2.177}$$

The topological equation (2.149) gives an expression for the time derivative of the volume fraction

$$\frac{\partial \alpha_\mathrm{g}}{\partial t} = -v_\mathrm{i}\frac{\partial \alpha_\mathrm{g}}{\partial x} + I_{\mathrm{g}\ell}. \tag{2.178}$$

We can now remove all the time derivatives in the interaction terms. Substituting them in E_g and simplifying, we obtain

$$E_\mathrm{g} = -p_\mathrm{g}(v_\mathrm{g} - v_\mathrm{i})\frac{\partial \alpha_\mathrm{g}}{\partial x} - p_\mathrm{g} I_{\mathrm{g}\ell} + \frac{1}{2}(p_\mathrm{g} - p_\ell) I_{\mathrm{g}\ell}, \tag{2.179}$$

and by symmetry

$$E_\ell = -p_\ell(v_\ell - v_\mathrm{i})\frac{\partial \alpha_\ell}{\partial x} + p_\ell I_{\mathrm{g}\ell} + \frac{1}{2}(p_\mathrm{g} - p_\ell) I_{\mathrm{g}\ell}. \tag{2.180}$$

For the momentum exchange term $M_{\mathrm{g}\ell}$, we start from (2.156) that we rewrite as

$$M_{\mathrm{g}\ell} = -\frac{E_\mathrm{g}}{v_\mathrm{g} - v_\ell} - \frac{E_\ell}{v_\mathrm{g} - v_\ell}, \tag{2.181}$$

After substitution, it becomes

$$M_{\mathrm{g}\ell} = \frac{p_\mathrm{g}(v_\mathrm{g} - v_\mathrm{i}) - p_\ell(v_\ell - v_\mathrm{i})}{v_\mathrm{g} - v_\ell}\frac{\partial \alpha_\mathrm{g}}{\partial x}. \tag{2.182}$$

The total energy exchange term becomes

$$E_\mathrm{g} + v_\mathrm{g} M_{\mathrm{g}\ell} = \frac{p_\mathrm{g} v_\ell(v_\mathrm{g} - v_\mathrm{i}) - p_\ell v_\mathrm{g}(v_\ell - v_\mathrm{i})}{v_\mathrm{g} - v_\ell}\frac{\partial \alpha_\mathrm{g}}{\partial x} - \frac{1}{2}(p_\mathrm{g} + p_\ell) I_{\mathrm{g}\ell}. \tag{2.183}$$

Remark that these interaction terms are not singular when $v_\mathrm{g} = v_\ell$, as long as $v_\mathrm{i} \to v$ when $(v_\mathrm{g}, v_\ell) \to (v, v)$. In this case, the numerator and denominator of $M_{\mathrm{g}\ell}$ and of the first term in $E_\mathrm{g} + v_\mathrm{g} M_{\mathrm{g}\ell}$ go to zero at the same order of $(v_\mathrm{g} - v_\ell)$, thus the terms do not diverge. For example, if $v_\mathrm{i} = (v_\mathrm{g} + v_\ell)/2$, we have

$$M_{\mathrm{g}\ell} = \frac{p_\mathrm{g} + p_\ell}{2} \frac{\partial \alpha_\mathrm{g}}{\partial x}, \tag{2.184}$$

and

$$E_\mathrm{g} + v_\mathrm{g} M_{\mathrm{g}\ell} = \frac{p_\mathrm{g} v_\ell + p_\ell v_\mathrm{g}}{2} \frac{\partial \alpha_\mathrm{g}}{\partial x} - \frac{1}{2}(p_\mathrm{g} + p_\ell) I_{\mathrm{g}\ell}. \tag{2.185}$$

The seven-equation model

To summarise, the seven-equation model derived above is

$$\frac{\partial \alpha_\mathrm{g}}{\partial t} + v_\mathrm{i} \frac{\partial \alpha_\mathrm{g}}{\partial x} = \mathcal{J}(p_\mathrm{g} - p_\ell), \tag{2.186}$$

$$\frac{\partial \alpha_\mathrm{g} \rho_\mathrm{g}}{\partial t} + \frac{\partial \alpha_\mathrm{g} \rho_\mathrm{g} v_\mathrm{g}}{\partial x} = 0 \tag{2.187}$$

$$\frac{\partial \alpha_\ell \rho_\ell}{\partial t} + \frac{\partial \alpha_\ell \rho_\ell v_\ell}{\partial x} = 0 \tag{2.188}$$

$$\frac{\partial \alpha_\mathrm{g} \rho_\mathrm{g} v_\mathrm{g}}{\partial t} + \frac{\partial}{\partial x}\left(\alpha_\mathrm{g} \rho_\mathrm{g} v_\mathrm{g}^2 + \alpha_\mathrm{g} p_\mathrm{g}\right) = \frac{p_\mathrm{g}(v_\mathrm{g} - v_\mathrm{i}) - p_\ell(v_\ell - v_\mathrm{i})}{v_\mathrm{g} - v_\ell} \frac{\partial \alpha_\mathrm{g}}{\partial x} \tag{2.189}$$

$$\frac{\partial \alpha_\ell \rho_\ell v_\ell}{\partial t} + \frac{\partial}{\partial x}\left(\alpha_\ell \rho_\ell v_\ell^2 + \alpha_\ell p_\ell\right) = -\frac{p_\mathrm{g}(v_\mathrm{g} - v_\mathrm{i}) - p_\ell(v_\ell - v_\mathrm{i})}{v_\mathrm{g} - v_\ell} \frac{\partial \alpha_\mathrm{g}}{\partial x} \tag{2.190}$$

$$\frac{\partial}{\partial t}\left(\alpha_{\mathrm{g}}\rho_{\mathrm{g}}\left(e_{\mathrm{g}}+\frac{v_{\mathrm{g}}^2}{2}\right)\right)+\frac{\partial}{\partial x}\left(\alpha_{\mathrm{g}}\rho_{\mathrm{g}}\left(e_{\mathrm{g}}+\frac{v_{\mathrm{g}}^2}{2}\right)v_{\mathrm{g}}+\alpha_{\mathrm{g}}v_{\mathrm{g}}p_{\mathrm{g}}\right)= \frac{p_{\mathrm{g}}v_\ell(v_{\mathrm{g}}-v_{\mathrm{i}})-p_\ell v_{\mathrm{g}}(v_\ell-v_{\mathrm{i}})}{v_{\mathrm{g}}-v_\ell}\frac{\partial\alpha_{\mathrm{g}}}{\partial x}-\frac{1}{2}(p_{\mathrm{g}}+p_\ell)\mathcal{J}(p_{\mathrm{g}}-p_\ell), \tag{2.191}$$

$$\frac{\partial}{\partial t}\left(\alpha_\ell\rho_\ell\left(e_{\mathrm{g}}+\frac{v_\ell^2}{2}\right)\right)+\frac{\partial}{\partial x}\left(\alpha_\ell\rho_\ell\left(e_{\mathrm{g}}+\frac{v_\ell^2}{2}\right)v_\ell+\alpha_\ell v_\ell p_\ell\right)= -\frac{p_{\mathrm{g}}v_\ell(v_{\mathrm{g}}-v_{\mathrm{i}})-p_\ell v_{\mathrm{g}}(v_\ell-v_{\mathrm{i}})}{v_{\mathrm{g}}-v_\ell}\frac{\partial\alpha_{\mathrm{g}}}{\partial x}+\frac{1}{2}(p_{\mathrm{g}}+p_\ell)\mathcal{J}(p_{\mathrm{g}}-p_\ell). \tag{2.192}$$

Seven-equation models have been used for example in [3, 74, 79, 80], with different closure laws. A closure for the interfacial velocity which respects both the conservation requirements and the second law of thermodynamics was proposed in [39, 40], though in a slightly different framework. In their formulation of the model, the interfacial pressure and momentum also have to be explicitly closed. Note also that the exact closures proposed involve derivatives, therefore the system loses its hyperbolic character since products of derivatives appear. These terms can be linearised to keep a hyperbolic system.

2.5.2. The six-equation model

The six-equation model is derived from the seven-equation two-pressure model by letting the mechanical relaxation be instantaneous. This means that $\mathcal{J}\to\infty$ in (2.170), and that $p_{\mathrm{g}}=p_\ell$ at all times. Thus, $\mathcal{J}(p_{\mathrm{g}}-p_\ell)$ is an undefined form, and the volume-fraction advection equation (2.186) loses significance. We replace it by the relation $p_{\mathrm{g}}=p_\ell$. In practice, this means that we can replace p_{g} and p_ℓ by p in the other equations (2.187)–(2.192), and replace $\mathcal{J}(p_{\mathrm{g}}-p_\ell)$ by derivatives of α_{g} using the volume-fraction advection equation (2.186). The model becomes, after simplification,

$$\frac{\partial\alpha_{\mathrm{g}}\rho_{\mathrm{g}}}{\partial t}+\frac{\partial\alpha_{\mathrm{g}}\rho_{\mathrm{g}}v_{\mathrm{g}}}{\partial x}=0, \tag{2.193}$$

$$\frac{\partial\alpha_\ell\rho_\ell}{\partial t}+\frac{\partial\alpha_\ell\rho_\ell v_\ell}{\partial x}=0, \tag{2.194}$$

$$\frac{\partial \alpha_{\mathrm{g}} \rho_{\mathrm{g}} v_{\mathrm{g}}}{\partial t} + \frac{\partial}{\partial x}\left(\alpha_{\mathrm{g}} \rho_{\mathrm{g}} v_{\mathrm{g}}^2 + \alpha_{\mathrm{g}} p\right) = p \frac{\partial \alpha_{\mathrm{g}}}{\partial x}, \tag{2.195}$$

$$\frac{\partial \alpha_\ell \rho_\ell v_\ell}{\partial t} + \frac{\partial}{\partial x}\left(\alpha_\ell \rho_\ell v_\ell^2 + \alpha_\ell p\right) = -p \frac{\partial \alpha_{\mathrm{g}}}{\partial x}, \tag{2.196}$$

$$\begin{aligned} \frac{\partial}{\partial t}\left(\alpha_{\mathrm{g}} \rho_{\mathrm{g}}\left(e_{\mathrm{g}} + \frac{v_{\mathrm{g}}^2}{2}\right)\right) + \frac{\partial}{\partial x}\left(\alpha_{\mathrm{g}} \rho_{\mathrm{g}}\left(e_{\mathrm{g}} + \frac{v_{\mathrm{g}}^2}{2}\right) v_{\mathrm{g}} + \alpha_{\mathrm{g}} v_{\mathrm{g}} p\right) \\ = -p \frac{\partial \alpha_{\mathrm{g}}}{\partial t}, \end{aligned} \tag{2.197}$$

$$\begin{aligned} \frac{\partial}{\partial t}\left(\alpha_\ell \rho_\ell\left(e_{\mathrm{g}} + \frac{v_\ell^2}{2}\right)\right) + \frac{\partial}{\partial x}\left(\alpha_\ell \rho_\ell\left(e_{\mathrm{g}} + \frac{v_\ell^2}{2}\right) v_\ell + \alpha_\ell v_\ell p\right) \\ = p \frac{\partial \alpha_{\mathrm{g}}}{\partial t}. \end{aligned} \tag{2.198}$$

This is the basic six-equation two-fluid model [37, 62, 69, 85, 93] for inviscid fluids, without phase change or heat exchange. Note that the source terms in the entropy equations (2.173) and (2.174) are not undefined forms. Since $(p_{\mathrm{g}} - p_\ell)$ appears squared in

$$\frac{\partial \alpha_{\mathrm{g}} \rho_{\mathrm{g}} s_{\mathrm{g}}}{\partial t} + \frac{\partial \alpha_{\mathrm{g}} \rho_{\mathrm{g}} s_{\mathrm{g}} v_{\mathrm{g}}}{\partial x} = \frac{(p_{\mathrm{g}} - p_\ell)\Gamma_{\mathrm{g}}}{2T_{\mathrm{g}}} \mathcal{J}(p_{\mathrm{g}} - p_\ell), \tag{2.199}$$

$$\frac{\partial \alpha_\ell \rho_\ell s_\ell}{\partial t} + \frac{\partial \alpha_\ell \rho_\ell s_\ell v_\ell}{\partial x} = \frac{(p_{\mathrm{g}} - p_\ell)\Gamma_\ell}{2T_\ell} \mathcal{J}(p_{\mathrm{g}} - p_\ell), \tag{2.200}$$

the source terms vanish when $\mathcal{J} \to \infty$ and $(p_{\mathrm{g}} - p_\ell) \to (p, p)$. Thus the entropy equations in the six-equation two-fluid model are

$$\frac{\partial \alpha_{\mathrm{g}} \rho_{\mathrm{g}} s_{\mathrm{g}}}{\partial t} + \frac{\partial \alpha_{\mathrm{g}} \rho_{\mathrm{g}} s_{\mathrm{g}} v_{\mathrm{g}}}{\partial x} = 0, \tag{2.201}$$

$$\frac{\partial \alpha_\ell \rho_\ell s_\ell}{\partial t} + \frac{\partial \alpha_\ell \rho_\ell s_\ell v_\ell}{\partial x} = 0. \tag{2.202}$$

This can be seen as an underlying assumption in the six-equation model, which may not be the only possible choice. It directly follows from the assumption that entropy follows the equations (2.173)–(2.174) (cf. also Paper F [23], Section 4.6).

The model (2.193)–(2.198) contains time derivatives. They can be replaced by spatial derivatives. The equations (2.176) and (2.177) now give

$$\alpha_{\mathrm{g}} \frac{\partial p}{\partial t} = -\alpha_{\mathrm{g}} v_{\mathrm{g}} \frac{\partial p}{\partial x} - \rho_{\mathrm{g}} c_{\mathrm{g}}^2 \left(\frac{\partial \alpha_{\mathrm{g}}}{\partial t} + \frac{\partial \alpha_{\mathrm{g}} v_{\mathrm{g}}}{\partial x}\right), \tag{2.203}$$

$$\alpha_\ell \frac{\partial p}{\partial t} = -\alpha_\ell v_\ell \frac{\partial p}{\partial x} - \rho_\ell c_\ell^2 \left(\frac{\partial \alpha_\ell}{\partial t} + \frac{\partial \alpha_\ell v_\ell}{\partial x} \right). \tag{2.204}$$

and allow determining $\partial_t p$ and $\partial_t \alpha_\mathrm{g}$. We first combine the relations to eliminate $\partial_t p$, which gives

$$\begin{aligned}(\alpha_\ell \rho_\mathrm{g} c_\mathrm{g}^2 + \alpha_\mathrm{g} \rho_\ell c_\ell^2) \frac{\partial \alpha_\mathrm{g}}{\partial t} = -\alpha_\mathrm{g} \alpha_\ell (v_\mathrm{g} - v_\ell) \frac{\partial p}{\partial x} \\ - \alpha_\ell \rho_\mathrm{g} c_\mathrm{g}^2 \frac{\partial \alpha_\mathrm{g} v_\mathrm{g}}{\partial x} + \alpha_\mathrm{g} \rho_\ell c_\ell^2 \frac{\partial \alpha_\ell v_\ell}{\partial x},\end{aligned} \tag{2.205}$$

and then to eliminate $\partial_t \alpha_\mathrm{g}$, which gives

$$\begin{aligned}(\alpha_\mathrm{g} \rho_\ell c_\ell^2 + \alpha_\ell \rho_\mathrm{g} c_\mathrm{g}^2) \frac{\partial p}{\partial t} = -(\alpha_\mathrm{g} \rho_\ell c_\ell^2 v_\mathrm{g} + \alpha_\ell \rho_\mathrm{g} c_\mathrm{g}^2 v_\ell) \frac{\partial p}{\partial x} \\ - \rho_\mathrm{g} c_\mathrm{g}^2 \rho_\ell c_\ell^2 \frac{\partial \alpha_\mathrm{g} v_\mathrm{g}}{\partial x} - \rho_\mathrm{g} c_\mathrm{g}^2 \rho_\ell c_\ell^2 \frac{\partial \alpha_\ell v_\ell}{\partial x}.\end{aligned} \tag{2.206}$$

The six-equation model is used in various codes (CATHARE [8], RELAP5/MOD3 [75], WAHA3 [42]). This model can be completed with various interaction terms, like phase change [4, 38], drag force [4, 38, 95], [17, p.226], lift [17, p.227], Basset force [38], [17, p.229], virtual mass force [4, 16, 38, 48, 99, 95], [17, p.227].

2.5.3. Hyperbolicity of the two-fluid model

Inviscid two-phase flow models should be hyperbolic, which means that the Jacobian matrix of the fluxes should be diagonalisable with real eigenvalues. The eigenvalues of a model are the propagation velocities of the transported quantities. The six-equation two-fluid model in its basic form has complex eigenvalues when $v_\mathrm{g} \neq v_\ell$ [29, 85, 86, 41].

Regularisation of the model

The regularisation of this model is debated in the literature. Pokharna *et al.* [72] argue that the lack of hyperbolicity is caused by the instabilities inherent to two-phase flows (Rayleigh-Taylor, Kelvin-Helmholtz). They write that the phenomena that should dampen the shorter wavelengths are lost in the averaging process, for example the surface tension. Therefore, the instabilities remain and the model loses its hyperbolicity. A

regularisation should then act on shorter wavelengths, while leaving the longer wavelengths unaffected. Prosperetti and Jones [73] studied the stability of two-phase flow models and showed that, when they only include first order derivatives, the stability criteria are independent from the wave number of the perturbation. If higher-order derivatives are included, the stability criteria become dependent on the wave number. This complies with the idea of Pokharna *et al.* [72], that the model should differentiate short and long wavelengths.

Song and Ishii [83] derive equations including the *momentum flux parameter* [4, 38, 82, 83], which accounts for the flow structure over a cross-section of the flow. This structure was lost in the averaging process. They assert that this stabilises the two-fluid model. This *momentum flux parameter* takes different forms depending on the flow structure, each form giving a restricted stability domain to the equation system. If the flow enters an unstable regime, its structure will evolve to recover stability. In other words, the governing equations can be temporarily unstable, but the *momentum flux parameter* will evolve to make the model hyperbolic again.

Regularisation using interfacial pressure

Often, though, the model is simply regularised by adding terms that make the eigenvalues real. One possibility is to introduce a virtual mass force term, however it is not enough to obtain hyperbolicity for low phase slip velocities [65]. Städtke [84, Sec. 5.1.1] proposed to add to the virtual mass force term, the effect of the interfacial pressure and of the compressibility, making the model hyperbolic. Another option is take advantage of the alternative form of the momentum equation (2.145), where the interfacial pressure p_i appears [4, 8, 13, 14, 20, 62, 69, 86, 93]. Neglecting the same terms as above (cf. Section 2.5.1), we obtain for the gas phase

$$\frac{\partial}{\partial t}(\alpha_{\mathrm{g}}\rho_{\mathrm{g}}v_{\mathrm{g}}) + \frac{\partial}{\partial x}\left(\alpha_{\mathrm{g}}\rho_{\mathrm{g}}v_{\mathrm{g}}^2\right) + \alpha_{\mathrm{g}}\frac{\partial p}{\partial x} + \Delta p\frac{\partial \alpha_{\mathrm{g}}}{\partial x} = M_{i,\mathrm{g}\ell}, \tag{2.207}$$

where

$$\Delta p = p - p_i. \tag{2.208}$$

Then we drop the assumption of irreversibility (2.173)–(2.174), and instead, make an assumption on the interaction term $M_{i,\mathrm{g}\ell}$. It may be

zero if friction between the phases is neglected. Otherwise it may be a relaxation term on the velocities

$$M_{i,\mathrm{g}\ell} = \mathcal{U}(v_\ell - v_\mathrm{g}). \tag{2.209}$$

The second necessary assumption is made on the energy exchange term. It involves a velocity v_τ that must be modelled. The exchange term becomes

$$E_\mathrm{g} + v_\mathrm{g} M_{\mathrm{g}\ell} = -p\frac{\partial \alpha_\mathrm{g}}{\partial t} - v_\tau \Delta p \frac{\partial \alpha_\mathrm{g}}{\partial x}, \tag{2.210}$$

or equivalently

$$E_\ell - v_\ell M_{\mathrm{g}\ell} = p\frac{\partial \alpha_\mathrm{g}}{\partial t} + v_\tau \Delta p \frac{\partial \alpha_\mathrm{g}}{\partial x}. \tag{2.211}$$

Now, from (2.129), we have

$$M_{\mathrm{g}\ell} = M_{i,\mathrm{g}\ell} + p_i \frac{\partial \alpha_\mathrm{g}}{\partial x} \tag{2.212}$$

so that we can evaluate

$$E_\mathrm{g} = -v_\mathrm{g} M_{i,\mathrm{g}\ell} - v_\mathrm{g} p_i \frac{\partial \alpha_\mathrm{g}}{\partial x} - p\frac{\partial \alpha_\mathrm{g}}{\partial t} - v_\tau \Delta p \frac{\partial \alpha_\mathrm{g}}{\partial x} \tag{2.213}$$

and

$$E_\ell = v_\ell M_{i,\mathrm{g}\ell} + v_\ell p_i \frac{\partial \alpha_\mathrm{g}}{\partial x} + p\frac{\partial \alpha_\mathrm{g}}{\partial t} + v_\tau \Delta p \frac{\partial \alpha_\mathrm{g}}{\partial x}. \tag{2.214}$$

The entropy equation for the gas phase can be found from (2.163), where E_g is substituted

$$\frac{\partial \alpha_\mathrm{g}\rho_\mathrm{g} s_\mathrm{g}}{\partial t} + \frac{\partial \alpha_\mathrm{g}\rho_\mathrm{g} s_\mathrm{g} v_\mathrm{g}}{\partial x} = \Delta p \frac{v_\mathrm{g} - v_\tau}{T_\mathrm{g}} \frac{\partial \alpha_\mathrm{g}}{\partial x} - \frac{v_\mathrm{g}}{T_\mathrm{g}} M_{i,\mathrm{g}\ell}. \tag{2.215}$$

For the second law of thermodynamics to be respected, the right-hand side of the entropy equation must be positive. If $M_{i,\mathrm{g}\ell}$ is an algebraic term, the factor

$$\Delta p \frac{v_\mathrm{g} - v_\tau}{T_\mathrm{g}} \tag{2.216}$$

in the first term should be sensitive to the sign of $\partial_x \alpha_\mathrm{g}$, so that this term would always be positive. The resulting model would then change nature, and it would not be possible to write it in quasilinear form (cf. Chapter 3).

Thus, the specific numerical solvers for transport equations could not be used. Otherwise, if the factor is not sensitive to the sign, the positivity of the entropy production cannot be enforced. This is the main drawback of this approach. However, Δp is generally small compared to the pressure, and it is expected that the entropy production or destruction due to this term will remain small. As to $M_{i,\mathrm{g}\ell}$, depending on the interphase friction model adopted, it may also be negative and violate the second law of thermodynamics. The relation between regularisation terms and the second law of thermodynamics is further discussed in Paper F ([23], Section 4.6).

The pressure difference Δp can model different physical phenomena, for example hydrostatic pressure in a stratified flow [4], but also surface tension in a dispersed flow. For the purpose of numerical testing, we can use a term without particular physical significance, which has been derived from mathematical considerations [10, 20, 60, 62, 65, 69, 86, 93](See also Paper E [57], Section 4.5, and Paper G [55], Section 4.7)

$$\Delta p = \delta \frac{\alpha_\mathrm{g}\alpha_\ell\rho_\mathrm{g}\rho_\ell(v_\mathrm{g}-v_\ell)^2}{\alpha_\ell\rho_\mathrm{g}+\alpha_\mathrm{g}\rho_\ell}. \tag{2.217}$$

When the parameter δ is equal to one, this is the minimum pressure difference between the phases necessary to make the model hyperbolic at the first order of $(v_\mathrm{g}-v_\ell)$. It has first been shown for some particular cases of the two-fluid six-equation model [86, 93], then for the two-fluid four-equation model without energy equations [20], and for the general two-fluid six-equation model [46]. With δ larger than one, the model is hyperbolic in an interval $|v_\mathrm{g}-v_\ell|<\Omega$, where Ω is dependent on δ. In [47], the authors study the hyperbolicity domain of the multifield model, which the six-equation two-fluid model is a particular case of, for regularisation terms that are very similar to (2.217). If the velocity v_τ is defined by

$$v_\tau = \frac{\alpha_\mathrm{g}\Gamma_\mathrm{g}v_\mathrm{g}+\alpha_\ell\Gamma_\ell v_\ell}{\alpha_\mathrm{g}\Gamma_\mathrm{g}+\alpha_\ell\Gamma_\ell}, \tag{2.218}$$

the interface friction only produces heat, and is not associated with deformation [62].

2.5.4. Variations of the two-fluid model

The six-equation two-fluid model contains the assumption that the mechanical equilibrium between the phases is instantaneous. There are in addition two other quantities which should evolve towards an equilibrium, the temperature and the chemical potential. In the derivation of the multiphase flow equations (Section 2.5), exchange terms between the phases appear. As mentioned previously, Λ_k in (2.142) models phase change and can be an algebraic relaxation term as in (2.143). This would attract the system towards chemical equilibrium. Relaxation has been studied for example in [22, 43, 53, 64, 71, 79, 94]. A very stiff relaxation source term may approach the equilibrium model [2], in which the chemical equilibrium would be instantaneous. We can also assume this equilibrium to be instantaneous and derive the corresponding model. Then, only the mixture mass equation makes sense instead of the phasic mass equations (2.193)–(2.194), and the model contains five transport equations. The equality of the chemical potentials replaces one transport equation to close the model.

When it comes to the thermal equilibrium, it can be modelled using the exchange term E_k in the energy equation (2.145). The algebraic relaxation term (2.147) will attract the model towards thermal equilibrium at a finite rate. Otherwise, similarly to the case of the chemical equilibrium, this equilibrium can be assumed to be instantaneous. Then only the mixture energy equation makes sense, thus reducing the number of transport equations by one. The missing relation is the equality of the temperatures. This is for example used in OLGA [6]. These two assumptions of instantaneous equilibrium can be used at the same time, thus giving a system of four equations, describing a two-phase flow in full thermal, mechanical and thermodynamical equilibrium at all times (cf. Paper G [55], Section 4.7).

An interesting result about instantaneous relaxation and equilibrium model is the subcharacteristic condition [12, 22, 51, 53, 64] (cf. also Paper G [55], Section 4.7). It states that for the relaxation process to be stable, thus producing a stable equilibrium model, the eigenvalues of the equilibrium model must be interlaced in the eigenvalues of the relaxation model. A direct consequence of this is for example that the speed of sound in an equilibrium model must be lower than the speed of sound in the

relaxation model. A stable relaxation process cannot make information travel faster. As a matter of fact, this suggests that there is something wrong in the relaxation process leading from the seven-equation two-fluid model to the six-equation two-fluid model. Chen *et. al.* [11, 12] showed that a relaxation process that creates entropy leads to a hyperbolic model. Since the six-equation two-fluid model is not hyperbolic, this suggests that there may be something wrong in the entropy of the mechanical relaxation process.

2.5.5. The drift-flux models

Another category of two-phase flow models involves the mixture momentum instead of the phasic momenta, which are recovered through an algebraic relation. These models are called drift-flux models [24, 63, 81, 85, 100], and contain only one mixture momentum equation. The main advantages of these models is that they are in conservation form, and that they are hyperbolic – though only conditionally [7] – thus well-posed. However, the phasic velocities are then less independent of each other, which makes the model more suitable for flows where the phase movements are highly correlated, for example bubbly and slug flows [5, 27, 33],[59, p. 173]. They may be less suited for flows like stratified flows, where the phases interact less [83]. As with the two-fluid models, they can have varying number of transport equations, depending on the assumptions on the equilibria [52, 22] (cf. Paper G [55], Section 4.7).

Drift-flux models are derived by summing the momentum equations in their corresponding two-fluid models. The five-equation drift-flux model derived from (2.193)–(2.198) reads, for example,

$$\frac{\partial \alpha_{\mathrm{g}} \rho_{\mathrm{g}}}{\partial t} + \frac{\partial \alpha_{\mathrm{g}} \rho_{\mathrm{g}} v_{\mathrm{g}}}{\partial x} = 0, \tag{2.219}$$

$$\frac{\partial \alpha_{\ell} \rho_{\ell}}{\partial t} + \frac{\partial \alpha_{\ell} \rho_{\ell} v_{\ell}}{\partial x} = 0, \tag{2.220}$$

$$\frac{\partial}{\partial t}(\alpha_{\mathrm{g}} \rho_{\mathrm{g}} v_{\mathrm{g}} + \alpha_{\ell} \rho_{\ell} v_{\ell}) + \frac{\partial}{\partial x}\left(\alpha_{\mathrm{g}} \rho_{\mathrm{g}} v_{\mathrm{g}}^2 + \alpha_{\ell} \rho_{\ell} v_{\ell}^2 + p\right) = 0, \tag{2.221}$$

$$\frac{\partial}{\partial t}\left(\alpha_{\mathrm{g}}\rho_{\mathrm{g}}\left(e_{\mathrm{g}}+\frac{v_{\mathrm{g}}^2}{2}\right)\right)+\frac{\partial}{\partial x}\left(\alpha_{\mathrm{g}}\rho_{\mathrm{g}}\left(e_{\mathrm{g}}+\frac{v_{\mathrm{g}}^2}{2}\right)v_{\mathrm{g}}+\alpha_{\mathrm{g}}v_{\mathrm{g}}p\right) = -p\frac{\partial\alpha_{\mathrm{g}}}{\partial t}, \tag{2.222}$$

$$\frac{\partial}{\partial t}\left(\alpha_{\ell}\rho_{\ell}\left(e_{\mathrm{g}}+\frac{v_{\ell}^2}{2}\right)\right)+\frac{\partial}{\partial x}\left(\alpha_{\ell}\rho_{\ell}\left(e_{\mathrm{g}}+\frac{v_{\ell}^2}{2}\right)v_{\ell}+\alpha_{\ell}v_{\ell}p\right) = -p\frac{\partial\alpha_{\ell}}{\partial t}. \tag{2.223}$$

The phasic velocities are then recovered through an algebraic relation in the form

$$v_{\mathrm{g}}-v_{\ell}=\Phi(\boldsymbol{U}). \tag{2.224}$$

2.6. Summary

In this chapter, we have derived the classical forms of the six-equation two-fluid model and of the drift-flux model. We started from the fundamental local conservation laws and ensemble averaged them in a multiphase mixture. Then, cross-sectional average gave one-dimensional transport equations. The relations between the interaction terms were made clear, and we saw that an additional assumption was needed to close the model. This freedom can be used to derive a model that is both hyperbolic and physically consistent.

The classical systems of transport equations for multiphase flows derived in the present chapter are non-linear and hyperbolic, or they are made hyperbolic by regularisation terms. The adapted numerical solvers for these systems are the subject of the next chapter.

3 Numerical methods

A system of one-dimensional conservation laws can be written in the general form

$$\frac{\partial \boldsymbol{U}}{\partial t} + \frac{\partial \boldsymbol{F}(\boldsymbol{U})}{\partial x} = 0, \tag{3.1}$$

where $\boldsymbol{U}$ is a vector of conserved variables and $\boldsymbol{F}(\boldsymbol{U})$ is the flux vector of the conserved quantities. It governs the behaviour of the quantities that are the components of $\boldsymbol{U}$. Specifically, $\boldsymbol{U}$ is transported in the domain and its total amount is conserved (except at the boundaries). With the Jacobian matrix of the flux vector

$$\boldsymbol{A}(\boldsymbol{U}) = \frac{\partial \boldsymbol{F}(\boldsymbol{U})}{\partial \boldsymbol{U}}, \tag{3.2}$$

this system can be rewritten in the quasilinear form

$$\frac{\partial \boldsymbol{U}}{\partial t} + \boldsymbol{A}(\boldsymbol{U})\frac{\partial \boldsymbol{U}}{\partial x} = 0. \tag{3.3}$$

This form is useful for some of the numerical methods for conservation laws. We can also analyse the structure of the system from this form.

There exist systems that contain terms which cannot be written in the form (3.1). One example is non-conservative terms, which will create or destroy $\boldsymbol{U}$. The system then takes the form

$$\frac{\partial \boldsymbol{U}}{\partial t} + \frac{\partial \boldsymbol{F}(\boldsymbol{U})}{\partial x} + \boldsymbol{B}(\boldsymbol{U})\frac{\partial \boldsymbol{Z}(\boldsymbol{U})}{\partial x} = 0, \tag{3.4}$$

where the vector $\boldsymbol{Z}(\boldsymbol{U})$ contains non-conserved variables, while the factors of the derivatives of $\boldsymbol{Z}(\boldsymbol{U})$ are in the matrix $\boldsymbol{B}(\boldsymbol{U})$. Algebraic source terms may also appear, in the form

$$\frac{\partial \boldsymbol{U}}{\partial t} + \frac{\partial \boldsymbol{F}(\boldsymbol{U})}{\partial x} + \boldsymbol{B}(\boldsymbol{U})\frac{\partial \boldsymbol{Z}(\boldsymbol{U})}{\partial x} = \boldsymbol{S}(\boldsymbol{U}). \tag{3.5}$$

In this chapter, we will discuss how to include non-conservative terms in the numerical solvers for conservation laws. On the other hand, algebraic terms have to be solved separately from the conservative fluxes and the non-conservative terms. This will not be further discussed here.

3.1. Structure of systems of conservation laws

3.1.1. Scalar conservation laws

The advection of a quantity u at constant velocity a is governed by the linear advection equation

$$\frac{\partial u}{\partial t} + a\frac{\partial u}{\partial x} = 0. \tag{3.6}$$

It will simply translate the function $u(x,t)$ at velocity a. Now, if the velocity is not constant anymore, but a function of u, the equation is said to be non-linear. For example, the inviscid Burgers' equation reads

$$\frac{\partial u}{\partial t} + u\frac{\partial u}{\partial x} = 0. \tag{3.7}$$

The quantity u is advected at velocity u. Non-linear transport equations may produce shocks – discontinuities – from initially smooth functions. So does Burgers' equation (cf. Figure 3.1). The velocity s of a shock is a function of u_l and u_r, the values of the variable u at the left and

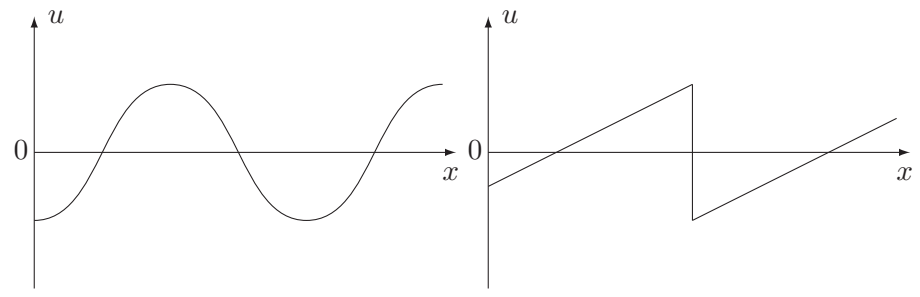

(a) Initial state (b) After shock formation

Figure 3.1: Formation of a shock with the Burgers' equation.

the right of the shock, respectively. It is given by the Rankine-Hugoniot condition [50, p. 213]

$$s(u_r - u_l) = f(u_r) - f(u_l), \tag{3.8}$$

where

$$f(u) = \frac{u^2}{2} \tag{3.9}$$

is the flux function of the Burgers' equation expressed in conservative form

$$\frac{\partial u}{\partial t} + \frac{\partial f(u)}{\partial x} = 0. \tag{3.10}$$

3.1.2. System of linear conservation laws

Systems of linear conservation laws can be written

$$\frac{\partial \boldsymbol{U}}{\partial t} + \boldsymbol{A}\frac{\partial \boldsymbol{U}}{\partial x} = 0, \tag{3.11}$$

where $\boldsymbol{A}$ is a square matrix with constant coefficients of dimension m. We assume that the system is hyperbolic, which means that $\boldsymbol{A}$ can be diagonalised with real eigenvalues. Then we can write

$$\boldsymbol{R}^{-1}\boldsymbol{A}\boldsymbol{R} = \boldsymbol{\Lambda}, \tag{3.12}$$

where $\boldsymbol{R}$ is the matrix of the right eigenvectors of $\boldsymbol{A}$, and $\boldsymbol{\Lambda}$ is the diagonal matrix of the eigenvalues of $\boldsymbol{A}$. Then we can rewrite (3.11) as [50, p. 32]

$$\boldsymbol{R}^{-1}\frac{\partial \boldsymbol{U}}{\partial t} + \boldsymbol{R}^{-1}\boldsymbol{A}\boldsymbol{R}\boldsymbol{R}^{-1}\frac{\partial \boldsymbol{U}}{\partial x} = 0, \tag{3.13}$$

and defining the vector of the characteristic variables $\boldsymbol{W} = \boldsymbol{R}^{-1}\boldsymbol{U}$, we obtain

$$\frac{\partial \boldsymbol{W}}{\partial t} + \boldsymbol{\Lambda}\frac{\partial \boldsymbol{W}}{\partial x} = 0. \tag{3.14}$$

The system (3.14) is a system of decoupled scalar linear advection equations, where the propagation velocities are the eigenvalues of $\boldsymbol{A}$. The advected quantities are defined by the right eigenvectors of $\boldsymbol{A}$ contained in the matrix $\boldsymbol{R}$. According to the definition of $\boldsymbol{W}$, we have

$$\boldsymbol{U} = \boldsymbol{R}\boldsymbol{W}. \tag{3.15}$$

It can also be written [50, p. 48]

$$\boldsymbol{U} = \sum_{p=1}^{m} w^p \boldsymbol{R}^p, \tag{3.16}$$

where w^p are the components of $\boldsymbol{W}$ and $\boldsymbol{R}^p$ are the columns of $\boldsymbol{R}$. This is a decomposition of the state $\boldsymbol{U}$ in the eigenvectors of $\boldsymbol{A}$, with weights w^p. Thus, $\boldsymbol{U}$ is a combination of waves $w^p \boldsymbol{R}^p$ travelling at different velocities determined by the eigenvalues of $\boldsymbol{A}$.

Riemann problem

Now, we consider a Riemann problem, defined by a system of hyperbolic conservation laws and an initial condition composed of two constant states separated by a single discontinuity [50, p. 52]

$$\boldsymbol{U}^0(x) = \begin{cases} \boldsymbol{U}_l & \text{if } x < 0, \\ \boldsymbol{U}_r & \text{if } x > 0. \end{cases} \tag{3.17}$$

The jump $\Delta \boldsymbol{U}^0 = \boldsymbol{U}_r - \boldsymbol{U}_l$ initially situated at $x = 0$ will break down into m propagating waves, having as velocities the eigenvalues of $\boldsymbol{A}$. The discontinuities $\Delta \boldsymbol{U}_{p,p+1} = \boldsymbol{U}_{p+1} - \boldsymbol{U}_p$, $p \in [0, m-1]$ will be eigenvectors of $\boldsymbol{A}$, such that

$$\boldsymbol{U}_0 = \boldsymbol{U}_l, \tag{3.18}$$

$$\boldsymbol{U}_p = \boldsymbol{U}_r, \tag{3.19}$$

$$\sum_{p=0}^{m-1} \Delta \boldsymbol{U}_{p,p+1} = \Delta \boldsymbol{U}^0. \tag{3.20}$$

To solve the Riemann problem means to break down $\Delta \boldsymbol{U}^0$ into propagating waves. The waves can be either rarefaction waves or discontinuities. Rarefaction waves are continuous curves, whose profile is determined by the shape of the flux function derivative. In the case of a discontinuity, its velocity is given by the Rankine-Hugoniot condition (3.8) extended for systems. For a system of linear conservation laws (3.11), the flux function can be written

$$\boldsymbol{F}(\boldsymbol{U}) = \boldsymbol{A}\boldsymbol{U}. \tag{3.21}$$

Thus the Rankine-Hugoniot condition (3.8) can be simplified as

$$s(\boldsymbol{U}_r - \boldsymbol{U}_l) = \boldsymbol{A}(\boldsymbol{U}_r - \boldsymbol{U}_l). \tag{3.22}$$

This is an eigenvalue problem: the only acceptable discontinuities are those for which $\Delta\boldsymbol{U} = \boldsymbol{U}_r - \boldsymbol{U}_l$ is an eigenvector of $\boldsymbol{A}$. They will propagate with a velocity equal to the associated eigenvalue.

The initial discontinuity $\Delta\boldsymbol{U}^0$ has then first to be decomposed into waves satisfying the Rankine-Hugoniot condition [50, p. 54]

$$\mathcal{W}^p = \alpha^p \boldsymbol{R}^p, \tag{3.23}$$

where α^p gives the amplitude of the wave of family p in the initial jump, and is the component p of the vector

$$\boldsymbol{\alpha} = \boldsymbol{R}^{-1}\Delta\boldsymbol{U}^0. \tag{3.24}$$

Then, the solution of the Riemann problem is given by [50, p. 55]

$$\boldsymbol{U}(x,t) = \boldsymbol{U}_l + \sum_{p=1}^{m} H(x - \lambda^p t)\mathcal{W}^p, \tag{3.25}$$

where λ^p is the eigenvalue of $\boldsymbol{A}$ associated to the wave of family p, and $H(x)$ is the Heaviside function

$$H(x) = \begin{cases} 0 & \text{if } x < 0, \\ 1 & \text{if } x > 0. \end{cases} \tag{3.26}$$

3.1.3. Riemann problem for systems of non-linear conservation laws

Systems of non-linear conservation laws cannot be decoupled as in the section above. However, we can extend the definition of hyperbolicity by saying that a non-linear system (3.1) is hyperbolic if the Jacobian matrix $\boldsymbol{A}(\boldsymbol{U}(x,t))$ in the quasilinear form (3.3) is hyperbolic for any $\boldsymbol{U}$. Then, at a given point and time (x,t), the eigenvalues of the matrix $\boldsymbol{A}(\boldsymbol{U}(x,t))$ are the local propagation velocities of the waves $\mathcal{W}^p(x,t) = \alpha^p(x,t)\boldsymbol{R}^p(x,t)$. The propagation velocities in the smooth regions for systems of non-linear

conservation laws are therefore functions of the state $\boldsymbol{U}(x,t)$. For the discontinuities, as was mentioned in Section 3.1.1, their velocities are functions of the left and right states $\boldsymbol{U}_l$ and $\boldsymbol{U}_r$. The Rankine-Hugoniot condition (3.8)

$$s(\boldsymbol{U}_r - \boldsymbol{U}_l) = \boldsymbol{F}(\boldsymbol{U}_r) - \boldsymbol{F}(\boldsymbol{U}_l) \tag{3.27}$$

is still valid. However, it cannot be simplified to (3.22) as for linear systems. Nevertheless, it still defines families of acceptable discontinuities, either shocks or contact discontinuities, which are eigenvectors of some average matrix $\boldsymbol{A}(\boldsymbol{U}_l, \boldsymbol{U}_r)$. In addition, if $\boldsymbol{U}_r - \boldsymbol{U}_l$ is an acceptable discontinuity for the wave family p, the relation (3.27) defines the propagation speed s^p for this wave.

Figure 3.2 illustrates the Riemann problem and its solution with an example for the compressible Euler equations

$$\begin{pmatrix} \rho \\ \rho v \\ E \end{pmatrix}_t + \begin{pmatrix} \rho v \\ \rho v^2 + p \\ (E+p)v \end{pmatrix}_x = 0, \tag{3.28}$$

where ρ is the density, v the velocity, p the pressure, and

$$E = \rho \left(e + \frac{1}{2} u^2 \right), \tag{3.29}$$

where e is the internal energy. Subfigure (a) shows the initial condition. Subfigure (b) shows the characteristics emanating from the initial discontinuity, and having as slope, at each point, the eigenvalues of the system. Subfigure (c) shows the solution at time t_1. There are one shock and one contact discontinuity propagating to the right. To the left, a rarefaction wave propagates.

3.2. Finite-volume methods

Finite-volume methods are numerical methods suitable to solve approximately systems of hyperbolic conservation laws. They are derived from the integral form of the transport equations (3.1), which is discretised in space and time. With a forward Euler time step, this gives for the cell i in Figure 3.3

$$\frac{\boldsymbol{U}_i^{n+1} - \boldsymbol{U}_i^n}{\Delta t} + \frac{\boldsymbol{F}_{i+1/2}^n - \boldsymbol{F}_{i-1/2}^n}{\Delta x} = 0, \tag{3.30}$$

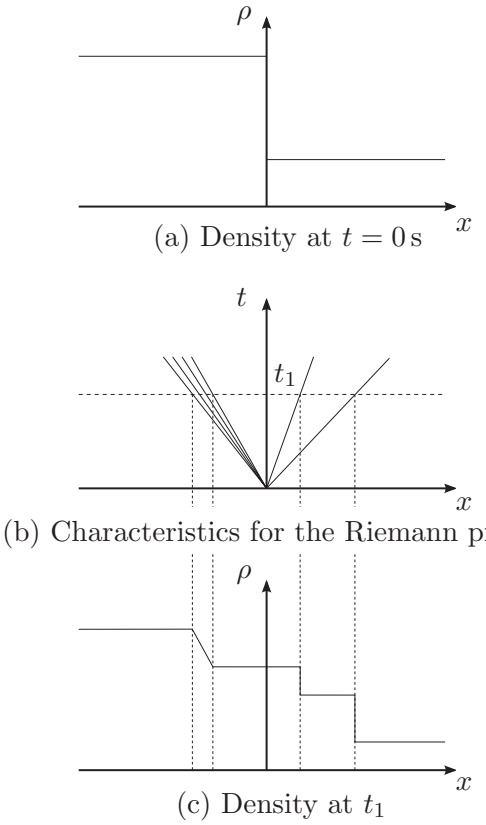

(a) Density at $t = 0\,\mathrm{s}$

(b) Characteristics for the Riemann problem

(c) Density at t_1

Figure 3.2: Riemann problem for the compressible Euler equations.

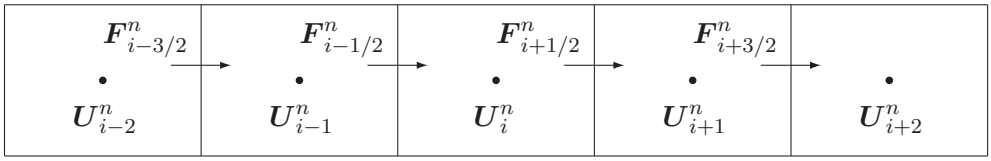

Figure 3.3: Cells and fluxes in the finite-volume method.

where i is the cell index, and n indicates the time step. This is enough to determine $\boldsymbol{U}_i^{n+1}$ at the next time step. One of the advantages of this method is that it is by essence conservative, whatever the definition of

a consistent numerical flux function $\boldsymbol{F}^n_{i-1/2}$. The flux entering a cell is leaving from its adjacent cell, therefore the sum of $\boldsymbol{U}^n_i$ over the domain is conserved, excluding the contributions at the boundaries. Now, defining a numerical scheme comes down to defining the numerical flux function.

3.2.1. Central vs. upwind scheme

Numerical methods for systems of partial differential equations try to evaluate the fluxes at the cell interfaces to predict the solution at the next time step. Central schemes use the information from the cells on both sides symmetrically. However, as discussed in Section 3.1, hyperbolic systems govern the propagation of waves. The upwind schemes take into account the waves' propagation direction to determine which side – the upwind side – is relevant to evaluate the flux related to a given family of waves. Therefore, these schemes are generally more accurate than the central schemes, in that they are less subject to numerical dissipation. In particular, discontinuities are resolved more sharply by upwind schemes.

3.2.2. Lax-Friedrichs, Richtmyer and FORCE fluxes

One simple method to define the numerical flux function is the Lax-Friedrichs method. The intercell flux is defined by [90, Sec. 14.5.1]

$$\boldsymbol{F}^{LF}_{i-1/2} = \frac{1}{2}\left(\boldsymbol{F}\left(\boldsymbol{U}_{i-1}\right) + \boldsymbol{F}\left(\boldsymbol{U}_i\right) - a\left(\boldsymbol{U}_i - \boldsymbol{U}_{i-1}\right)\right), \tag{3.31}$$

where $a = \Delta x/\Delta t$ plays the role of extra numerical viscosity. This scheme is first order and very diffusive. Another flux is the Richtmyer flux, defined in two steps [90, Sec. 14.5.1]. First, an intermediate state is predicted as

$$\boldsymbol{U}^{Ri}_{i-1/2} = \frac{1}{2}\left(\boldsymbol{U}_{i-1} + \boldsymbol{U}_i\right) - \frac{1}{2}\frac{\Delta t}{\Delta x}\left(\boldsymbol{F}\left(\boldsymbol{U}_i\right) - \boldsymbol{F}\left(\boldsymbol{U}_{i-1}\right)\right), \tag{3.32}$$

before the intercell flux is evaluated as

$$\boldsymbol{F}^{Ri}_{i-1/2} = \boldsymbol{F}\left(\boldsymbol{U}^{Ri}_{i-1/2}\right). \tag{3.33}$$

The Richtmyer flux is second-order accurate for the smooth regions of the solution, but will oscillate at discontinuities.

The FORCE scheme combines the two previous ones and defines the intercell flux as [90, Sec. 14.5.1]

$$\boldsymbol{F}_{i-1/2}^{FO} = \frac{1}{2}\left(\boldsymbol{F}_{i-1/2}^{LF} + \boldsymbol{F}_{i-1/2}^{Ri}\right), \tag{3.34}$$

where $\boldsymbol{F}_{i-1/2}^{LF}$ is given by (3.31) and $\boldsymbol{F}_{i-1/2}^{Ri}$ by (3.33).

3.2.3. The MUSTA method

Solving systems of conservation laws using finite-volume methods can be seen as discretising the solution and solving a Riemann problem at each interface. As seen in Section 3.1.3 and illustrated by Figure 3.2, in a Riemann problem, waves propagate to the left and to the right. The state at $x = 0$ – called $\boldsymbol{U}^*$ – remains constant at any time after the waves have departed from the initial discontinuity. Therefore the initial discontinuity $\boldsymbol{U}^* - \boldsymbol{U}_l$ would only produce left-travelling waves, as $\boldsymbol{U}_r - \boldsymbol{U}^*$ would produce right-travelling waves. Knowing the state $\boldsymbol{U}^*$ would therefore allow building an upwind scheme. In the MUSTA method [89, 91], this state is approached by numerically solving each Riemann problem in a virtual domain. The intercell flux in the original domain is subsequently set to be the FORCE flux at the interface in the middle of the virtual domain

$$\boldsymbol{F}_{i-1/2}^{MUSTA} = \boldsymbol{F}^{FO}\left(\boldsymbol{U}_N^{\text{virt}}, \boldsymbol{U}_{N+1}^{\text{virt}}\right), \tag{3.35}$$

for a virtual domain with cell values $\boldsymbol{U}_i^{\text{virt}}, i = 1, .., 2N$. When N increases, the MUSTA flux (3.35) tends to

$$\boldsymbol{F}_{i-1/2}^{MUSTA} = \boldsymbol{F}\left(\boldsymbol{U}_{i-1/2}^{\sim}\right), \tag{3.36}$$

where $\boldsymbol{U}_{i-1/2}^{\sim}$ is the MUSTA approximation of $\boldsymbol{U}^*$ between the states $\boldsymbol{U}_{i-1}$ and $\boldsymbol{U}_i$. In [61], the virtual domain was tested with 2 to 8 cells, while the number of time steps in the virtual domain is set to half of the cell number. It was found that 4 cells make a good compromise with respect to accuracy and computational cost. The MUSTA method was applied to the two-fluid six-equation model in [62]. This method was used as a comparison with the Roe scheme (cf. next section) derived in Paper E [57] (Section 4.5).

3.2.4. Upwind schemes

Godunov's method

The principle of Godunov's method is to solve exactly the Riemann problems at each cell interface, before averaging the solution in each cell. Then, the solution is reconstructed, for example as a piecewise constant function, and the sequence is iterated [50, p. 76]. This is not efficient in practice. However, noticing that the state $\boldsymbol{U}^*$ mentioned in Section 3.2.3 is constant over a time step, we can design an equivalent scheme based on the formulation (3.30), instead of averaging the evolved reconstructed function after each time step. The state $\boldsymbol{U}^*$ is found by solving the Riemann problem at each cell interface, and the intercell fluxes in (3.30) are evaluated by

$$\boldsymbol{F}_{i-1/2}^{Godunov} = \boldsymbol{F}\left(\boldsymbol{U}_{i-1/2}^*\left(\boldsymbol{U}_{i-1}, \boldsymbol{U}_i\right)\right). \tag{3.37}$$

The main drawback of the Godunov scheme is that the Riemann problem must be solved exactly.

A slight reorganisation of (3.30) gives a formulation that can be useful in defining approximate Riemann solvers. We know that the intercell flux $\boldsymbol{F}_{i-1/2}$ is equal to $\boldsymbol{F}\left(\boldsymbol{U}_{i-1/2}^*\right)$. Now, the cell-flux $\boldsymbol{F}(\boldsymbol{U}_i)$ is introduced in (3.30) to give

$$\boldsymbol{U}_i^{n+1} = \boldsymbol{U}_i^n + \frac{\Delta t}{\Delta x}\left(\boldsymbol{F}\left(\boldsymbol{U}_{i+1/2}^*\right) - \boldsymbol{F}(\boldsymbol{U}_i) - \boldsymbol{F}\left(\boldsymbol{U}_{i-1/2}^*\right) + \boldsymbol{F}(\boldsymbol{U}_i)\right), \tag{3.38}$$

where the exponents n have been dropped on the fluxes. This can be rewritten as [50, p. 313]

$$\boldsymbol{U}_i^{n+1} = \boldsymbol{U}_i^n - \frac{\Delta t}{\Delta x}\left(\mathcal{A}^-\Delta Q_{i+1/2} + \mathcal{A}^+\Delta Q_{i-1/2}\right), \tag{3.39}$$

where we have defined the fluctuations by

$$\mathcal{A}^-\Delta Q_{i-1/2} = \boldsymbol{F}\left(\boldsymbol{U}_{i-1/2}^*\right) - \boldsymbol{F}(\boldsymbol{U}_{i-1}), \tag{3.40}$$

$$\mathcal{A}^+\Delta Q_{i-1/2} = \boldsymbol{F}(\boldsymbol{U}_i) - \boldsymbol{F}\left(\boldsymbol{U}_{i-1/2}^*\right). \tag{3.41}$$

In the wave propagation form, we have [50, p. 315]

$$\mathcal{A}^- \Delta Q_{i-1/2} = \sum_{p=1}^{m} \left(s^p_{i-1/2}\right)^- \mathcal{W}^p_{i-1/2} \tag{3.42}$$

$$\mathcal{A}^+ \Delta Q_{i-1/2} = \sum_{p=1}^{m} \left(s^p_{i-1/2}\right)^+ \mathcal{W}^p_{i-1/2}, \tag{3.43}$$

with the notations used in Sections 3.1.2–3.1.3. The notation $(s)^-$ stands for $\min(0, s)$, while $(s)^+$ stands for $\max(0, s)$. They select, respectively, the left-travelling and right-travelling waves.

Approximate Riemann solvers

There exist non-linear systems for which the solution of the Riemann problem in not known, for example the two-fluid six-equation model. For these systems, it is simpler to solve at each interface a linearised problem instead. The linearisation of (3.3) at the interface of cells $i-1$ and i can be written [50, p. 315]

$$\frac{\partial \boldsymbol{U}}{\partial t} + \hat{\boldsymbol{A}}(\boldsymbol{U}_{i-1}, \boldsymbol{U}_i) \frac{\partial \boldsymbol{U}}{\partial x} = 0, \tag{3.44}$$

where $\hat{\boldsymbol{A}}$ is an approximation of the Jacobian of the flux function $\boldsymbol{A}$ in (3.3), valid in a neighbourhood of $\boldsymbol{U}_{i-1}$ and $\boldsymbol{U}_i$. To ensure that the linearised problem is hyperbolic and consistent with the original conservation law, two conditions should be fulfilled:

R1: The matrix $\hat{\boldsymbol{A}}(\boldsymbol{U}_{i-1}, \boldsymbol{U}_i)$ should be diagonalisable with real eigenvalues,

R2: The matrix $\hat{\boldsymbol{A}}(\boldsymbol{U}_{i-1}, \boldsymbol{U}_i)$ should converge smoothly towards $\boldsymbol{A}(\boldsymbol{U})$ when $(\boldsymbol{U}_{i-1}, \boldsymbol{U}_i) \to (\boldsymbol{U}, \boldsymbol{U})$ for any state $\boldsymbol{U}$.

The VFRoe scheme

The VFRoe scheme is based on solving a linearised Riemann problem (3.44). The approximate Jacobian is defined as [28]

$$\hat{\boldsymbol{A}}(\boldsymbol{U}_{i-1}, \boldsymbol{U}_i) = \boldsymbol{A}(\bar{\boldsymbol{U}}), \tag{3.45}$$

where $\bar{\boldsymbol{U}}(\boldsymbol{U}_{i-1}, \boldsymbol{U}_i)$ is some average of $\boldsymbol{U}_{i-1}$ and $\boldsymbol{U}_i$. Then, the approximation $\boldsymbol{U}^{\sim}_{i-1/2}$ of the $\boldsymbol{U}^{*}_{i-1/2}$-state in (3.37) is found by constructing the solution of the linearised Riemann problem, as in (3.25). Its expression is [28]

$$\boldsymbol{U}^{\sim}_{i-1/2} = \boldsymbol{U}_{i-1} + \sum_{p/\hat{\lambda}^p<0} \hat{\alpha}^p_{i-1/2} \hat{\boldsymbol{R}}^p_{i-1/2}, \tag{3.46}$$

where $\hat{\lambda}^p_{i-1/2}$ is the p^{th} eigenvalue of the approximate Jacobian $\hat{\boldsymbol{A}}_{i-1/2}$, $\hat{\boldsymbol{R}}^p_{i-1/2}$ its p^{th} right eigenvector, and the wave strengths are defined as

$$\hat{\alpha}^p_{i-1/2} = \hat{\boldsymbol{L}}^p_{i-1/2} \cdot (\boldsymbol{U}_i - \boldsymbol{U}_{i-1}), \tag{3.47}$$

where $\hat{\boldsymbol{L}}^p_{i-1/2}$ is the p^{th} left eigenvector of $\hat{\boldsymbol{A}}_{i-1/2}$. The numerical flux is given by (3.37) where $\boldsymbol{U}^{*}_{i-1/2}$ is replaced by $\boldsymbol{U}^{\sim}_{i-1/2}$. The method is intrinsically conservative.

The Roe scheme

In addition to the conditions R1 and R2, a third condition on the linearised matrix $\hat{\boldsymbol{A}}(\boldsymbol{U}_{i-1}, \boldsymbol{U}_i)$ gives nice properties to the scheme. It is the requirement that [50, p. 318]

R3: If $\boldsymbol{U}_{i-1}$ and $\boldsymbol{U}$ are connected by a single wave $\mathcal{W} = \boldsymbol{U}_i - \boldsymbol{U}_{i-1}$ in the true Riemann solution, then $\mathcal{W}$ should also be an eigenvector of $\hat{\boldsymbol{A}}_{i-1/2}$.

This means that if a single discontinuity is travelling in an otherwise smooth flow, the approximate solution will agree with the exact solution. The condition can be rewritten as

$$\hat{\boldsymbol{A}}_{i-1/2}(\boldsymbol{U}_i - \boldsymbol{U}_{i-1}) = \boldsymbol{F}(\boldsymbol{U}_i) - \boldsymbol{F}(\boldsymbol{U}_{i-1}). \tag{3.48}$$

This also has the consequence that

$$\mathcal{A}^{-}\Delta Q_{i-1/2} + \mathcal{A}^{+}\Delta Q_{i-1/2} = \boldsymbol{F}(\boldsymbol{U}_i) - \boldsymbol{F}(\boldsymbol{U}_{i-1}) \tag{3.49}$$

is satisfied, which guarantees that the scheme (3.39) is conservative.

Roe [77] introduced a method to derive a linearised matrix satisfying the three conditions. The principle is to define $\hat{\boldsymbol{A}}_{i-1/2}$ as the average of

the matrix $\boldsymbol{A}$ along a path $\boldsymbol{U}(\xi), \xi \in [0,1]$ between $\boldsymbol{U}_{i-1}$ and $\boldsymbol{U}_i$, which gives

$$\hat{\boldsymbol{A}}_{i-1/2} = \int_0^1 \frac{\mathrm{d}\boldsymbol{F}(\boldsymbol{U}(\xi))}{\mathrm{d}\boldsymbol{U}}\,\mathrm{d}\xi. \tag{3.50}$$

However, instead of evaluating this integral, an invertible *parameter vector* $z(\boldsymbol{U})$ is used as a change of variable [50, p. 319]. The path becomes $z(\xi) = \boldsymbol{Z}_{i-1} + (\boldsymbol{Z}_i - \boldsymbol{Z}_{i-1})\xi$. This gives

$$\boldsymbol{F}(\boldsymbol{U}_i) - \boldsymbol{F}(\boldsymbol{U}_{i-1}) = \underbrace{\left[\int_0^1 \frac{\mathrm{d}\boldsymbol{F}(z(\xi))}{\mathrm{d}z}\,\mathrm{d}\xi\right]}_{\hat{\boldsymbol{C}}_{i-1/2}}(\boldsymbol{Z}_i - \boldsymbol{Z}_{i-1}) \tag{3.51}$$

and

$$\boldsymbol{U}_i - \boldsymbol{U}_{i-1} = \underbrace{\left[\int_0^1 \frac{\mathrm{d}\boldsymbol{U}(z(\xi))}{\mathrm{d}z}\,\mathrm{d}\xi\right]}_{\hat{\boldsymbol{B}}_{i-1/2}}(\boldsymbol{Z}_i - \boldsymbol{Z}_{i-1}). \tag{3.52}$$

The average matrix, called Roe matrix, is now simply

$$\hat{\boldsymbol{A}}_{i-1/2} = \hat{\boldsymbol{C}}_{i-1/2}\hat{\boldsymbol{B}}^{-1}_{i-1/2}. \tag{3.53}$$

The matrix such defined is actually the matrix $\boldsymbol{A}$ evaluated for a particular state, called Roe averaged state. This ensures that if the original problem was hyperbolic, the linearised problem will also be. In addition, the convergence of $\hat{\boldsymbol{A}}_{i-1/2}$ towards $\boldsymbol{A}(\boldsymbol{U})$ when the left and right states converge towards $\boldsymbol{U}$ is ensured. The Roe scheme consists in diagonalising the matrix $\hat{\boldsymbol{A}}_{i-1/2}$ to evaluate the fluctuations (3.42)–(3.43), which are then used in the update formula (3.39).

A weakness of the Roe scheme is that the solution may violate the second law of thermodynamics. If an eigenvalue changes sign in the middle of a rarefaction wave, the Roe scheme will predict an unphysical shock. This problem can be solved with an entropy fix, for example the Harten entropy fix [31].

The Roe scheme may be very computationally efficient if the eigenstructure of the matrix $\hat{\boldsymbol{A}}$ is known analytically. However, it is not always possible to know it. Then the matrix must be diagonalised numerically. This is computationally expensive, and poses problems around resonant

states (cf. Paper E [57], Section 4.5). In [66], the authors propose an iterative method to avoid numerical diagonalisation, thus avoiding the problems near resonance. However, it involves numerous matrix-matrix multiplications, and the question of the overall computational efficiency compared to the MUSTA scheme arises. The MUSTA scheme is indeed more diffusive than the Roe scheme [61, 62], but it does not require matrix diagonalisations. This is an advantage when the dimension of the system is large, because matrix operation are computationally expensive. Therefore, no general conclusion can be drawn here from the comparison of the Roe and MUSTA schemes in term of accuracy-over-computational-time rate.

Roe schemes have been derived for different models. Roe [77] applied his method to the Euler equations. For the three-equation drift-flux model without any energy equation, Roe schemes were presented in [26, 76, 78]. Roe schemes have also been derived for the four and five-equation two-fluid models, without energy equation and with or without pressure relaxation [60], for the seven-equation two-fluid model with pressure relaxation [45], for the six-equation two-fluid model (cf. Paper E [57], Section 4.5).

Positively conservative schemes

The Roe scheme suffers from a downside. In some situation, the Roe averaging may lead to a non-physical average state, for example having a negative pressure or density for the Euler equations [50, p.327]. This is caused by the linearisation of the intercell matrix. Schemes which do not have this drawback are called positively conservative. This is the case of the exact Godunov solver.

The scheme of Harten, Lax and van Leer (HLL) is an approximate Godunov solver which is positively conservative. In this scheme, instead of looking for the exact $\boldsymbol{U}^*$ state and use (3.37), an approximate value $\boldsymbol{U}^{HLL}$ is constructed such that $\boldsymbol{U}^{HLL}$ is the average value of $\boldsymbol{U}$ in the domain between the slowest wave and the fastest wave. This average value can be evaluated exactly without solving the Riemann problem, as long as the velocities of the slowest and the fastest waves are known,

through [32],[90, p. 319]

$$\boldsymbol{U}_{i-1/2}^{HLL} = \frac{S^+\boldsymbol{U}_i - S^-\boldsymbol{U}_{i-1} + \boldsymbol{F}_{i-1} - \boldsymbol{F}_i}{S^+ - S^-}, \tag{3.54}$$

where S^- is the velocity of the slowest wave, S^+ the velocity of the fastest wave, $\boldsymbol{U}_{i-1}$ and $\boldsymbol{U}_i$ the states on the left and right sides, respectively, and $\boldsymbol{F}_{i-1}$ and $\boldsymbol{F}_i$ the fluxes on the left and right sides, respectively. Then the numerical intercell flux is defined by

$$\boldsymbol{F}_{i-1/2}^{HLL} = \boldsymbol{F}_{i-1} + S^- \left(\boldsymbol{U}_{i-1/2}^{HLL} - \boldsymbol{U}_{i-1}\right). \tag{3.55}$$

In the HLL scheme, the minimum and maximum wave speeds S^- and S^+ are taken as the absolute lower and upper bounds of the wave velocities that might arise. In [19], the HLLE scheme was proposed, where the velocities are defined using the Roe average state as

$$S_{i-1/2}^- = \min_p \left(\min\left(\lambda_{i-1}^p, \hat{\lambda}_{i-1/2}^p\right)\right), \tag{3.56}$$

$$S_{i-1/2}^+ = \max_p \left(\max\left(\lambda_i^p, \hat{\lambda}_{i-1/2}^p\right)\right), \tag{3.57}$$

where λ_i^p is the p^{th} eigenvalue of the Jacobian $\boldsymbol{A}(\boldsymbol{U}_i)$, and $\hat{\lambda}_{i-1/2}^p$ is the p^{th} eigenvalue of the Roe matrix $\hat{\boldsymbol{A}}_{i-1/2}$. The HLLE method resolves shocks more sharply than the HLL method. Besides, as for the Roe scheme, the HLLE method will give the exact solution for two states connected by a single shock [50, p.329]. The main drawback of this method is that it only resolves the slowest and the fastest waves, and is very diffusive for the middle ones. In [92], Toro *et. al.* derived the HLLC method, where a contact discontinuity is restored for the Euler equations. This also works fine for the drift-flux models, which have two fast pressure waves, while all the middle waves travel at the mixture velocity. Thus, there is only one wave to restore. When it comes to the the six-equation two-fluid model, the HLL scheme was applied in [97, 98]. However, the authors did not reconstruct the missing waves. In [46], the author built a HLLC-similar scheme for the six-equation two-fluid model. They assert that, in addition to the two fast pressure waves, they only need to take into account the eigenvalue of the fastest of the slow waves. This is valid as long as the

four slow waves have similar velocities. The resulting SEDES scheme is more diffusive than the Roe scheme, however it has better properties close to a single-phase state [46].

3.2.5. Second order accuracy

Second-order accurate schemes perform better than first-order accurate schemes on smooth regions of the solution. However, they oscillate at discontinuities [50, p. 103]. One says that the total variation (TV) of the solution increases. A method which only decreases the TV (called TV diminishing – TVD) will not be subject to this phenomenon [90, Sec. 13.6]. An idea to reach second-order accuracy for the smooth regions while keeping the TVD property is to use second-order accurate fluxes in smooth regions, while relying on first-order accurate fluxes near discontinuities. This can be achieved for example by the FLIC scheme [90, Sec. 14.5.2], using the FORCE flux as low-order flux, and the Richtmyer flux as high-order flux. A flux limiter $\Phi_{i-1/2}$ then chooses which combination of flux is to be used. The intercell flux takes the form

$$\boldsymbol{F}^{FL}_{i-1/2} = (1 - \Phi_{i-1/2})\boldsymbol{F}^{FO}_{i-1/2} + \Phi_{i-1/2}\boldsymbol{F}^{Ri}_{i-1/2}. \tag{3.58}$$

Now, the method comes down to choosing the limiter function $\Phi_{i-1/2}$. It should be close to 0 in smooth regions, and close to 1 in the neighbourhood of discontinuities. It is a function $\Phi(\theta) \in [0, 1]$, where θ measures the slope variation between to adjacent cells, defined by

$$\theta_{i-1/2} = \frac{u^j_{i-2} - u^j_{i-1}}{u^j_{i-1} - u^j_i} \tag{3.59}$$

for some component u^j of the vector $\boldsymbol{U}$. No ideal limiter function exists, but many can be found in the literature. See for example [50, p. 115]. However, Munkejord reported, in [59, p. 104], difficulties to apply this method to the isentropic two-fluid model.

Another strategy to obtain higher order TVD schemes is to reconstruct the solution as a piecewise polynomial function of a given order, instead of keeping a piecewise constant function. For example, in the MUSCL reconstruction [96], the solution is a piecewise linear function. The slope σ_i of each segment is evaluated using a slope-limiter function, that takes as

argument the variation rate of some component u^j of $\boldsymbol{U}$ on each side of the cell. For a cell i and the component j of $\boldsymbol{U}$, it reads

$$\sigma_i = \varphi\left(\frac{u_i^j - u_{i-1}^j}{\Delta x}, \frac{u_{i+1}^j - u_i^j}{\Delta x}\right), \tag{3.60}$$

where $\varphi(a, b)$ generally returns a value in $[a, b]$, see for example [50, p. 111]. Other methods use higher order polynomial reconstruction, like ENO and WENO [50, p. 197].

A specific second-order extension exists for the Roe scheme, called wave limiter. The principle is similar to the previous methods, but uses the wave structure of the model. Now, the numerical scheme (3.39) is augmented as [50, Sec. 6.13]

$$\begin{aligned}\boldsymbol{U}_i^{n+1} = \boldsymbol{U}_i^n - \frac{\Delta t}{\Delta x}\left(\mathcal{A}^- \Delta Q_{i+1/2} + \mathcal{A}^+ \Delta Q_{i-1/2}\right) \\ - \frac{\Delta t}{\Delta x}\left(\tilde{\boldsymbol{F}}_{i+1/2} - \tilde{\boldsymbol{F}}_{i-1/2}\right),\end{aligned} \tag{3.61}$$

where the limited flux $\tilde{\boldsymbol{F}}_{i-1/2}$ is defined using a limited wave $\tilde{\mathcal{W}}^p$

$$\tilde{\boldsymbol{F}}_{i-1/2} = \frac{1}{2}\sum_{p=1}^{m} |\hat{\lambda}_{i-1/2}^p| \left(1 - \frac{\Delta t}{\Delta x}|\hat{\lambda}_{i-1/2}^p|\right) \tilde{\mathcal{W}}^p, \tag{3.62}$$

where $\hat{\lambda}_{i-1/2}^p$ is the p^{th} eigenvalue of the Roe matrix $\hat{\boldsymbol{A}}_{i-1/2}$. The limiter function $\Phi(\theta^p)$ – similar to the flux limiter in the FLIC method and to the slope limiter in the MUSCL approach – appears in the definition of the limited wave $\tilde{\mathcal{W}}^p$, but now, θ^p compares the jump of family p with the jump of the same family at the upwind interface

$$\theta_{i-1/2}^p = \frac{\alpha_{I-1/2}^p}{\alpha_{i-1/2}^p} \qquad \text{with } I = \begin{cases} i-1 & \text{if } \hat{\lambda}_{i-1/2}^p > 0, \\ i+1 & \text{if } \hat{\lambda}_{i-1/2}^p < 0. \end{cases} \tag{3.63}$$

$\alpha_{i-1/2}^p$ was defined in (3.24). The limited version of $\alpha_{i-1/2}^p$ can then be defined as

$$\tilde{\alpha}_{i-1/2}^p = \alpha_{i-1/2}^p \Phi\left(\theta_{i-1/2}^p\right), \tag{3.64}$$

which is the limited scalar coefficient used in the definition of the limited wave

$$\tilde{\mathcal{W}}^p = \tilde{\alpha}^p_{i-1/2}\hat{\boldsymbol{R}}^p_{i-1/2}, \tag{3.65}$$

where $\hat{\boldsymbol{R}}^p_{i-1/2}$ is the p^{th} eigenvector of the Roe matrix at the interface $i-1/2$. Various limiter functions $\Phi(\theta^p)$ can be used [50, p. 115].

3.3. Systems of non-conservative transport equations

We have now discussed numerical methods for conservation laws. However, some models of interest, containing non-conservative differential terms, cannot be written in conservation form (3.1). The non-conservative terms can only be written in the form $\boldsymbol{B}(\boldsymbol{U})\partial_x\boldsymbol{Z}(\boldsymbol{U})$ as in (3.4) that we recall here,

$$\frac{\partial \boldsymbol{U}}{\partial t} + \frac{\partial \boldsymbol{F}(\boldsymbol{U})}{\partial x} + \boldsymbol{B}(\boldsymbol{U})\frac{\partial \boldsymbol{Z}(\boldsymbol{U})}{\partial x} = 0, \tag{3.66}$$

where the matrix $\boldsymbol{B}(\boldsymbol{U})$ is different from the identity matrix. In addition, the integral

$$\int_{\boldsymbol{U}_l}^{\boldsymbol{U}_r} \boldsymbol{B}(\boldsymbol{U})\frac{\partial \boldsymbol{Z}(\boldsymbol{U})}{\partial \boldsymbol{U}}\,\mathrm{d}\boldsymbol{U} \tag{3.67}$$

is not independent of the integration path from $\boldsymbol{U}_l$ to $\boldsymbol{U}_r$. If this integral is independent of the path, it is possible to evaluate the integral

$$\breve{\boldsymbol{F}}(\boldsymbol{U}) = \int_{\boldsymbol{U}_0}^{\boldsymbol{U}} \boldsymbol{B}(\tilde{\boldsymbol{U}})\frac{\partial \boldsymbol{Z}(\tilde{\boldsymbol{U}})}{\partial \tilde{\boldsymbol{U}}}\,\mathrm{d}\tilde{\boldsymbol{U}} \tag{3.68}$$

for any convenient path and reference state $\boldsymbol{U}_0$, such that the term $\boldsymbol{B}(\boldsymbol{U})\partial_x\boldsymbol{Z}(\boldsymbol{U})$ can be rewritten using the conservative flux function $\breve{\boldsymbol{F}}(\boldsymbol{U})$ as

$$\boldsymbol{B}(\boldsymbol{U})\frac{\partial \boldsymbol{Z}(\boldsymbol{U})}{\partial x} = \frac{\partial \breve{\boldsymbol{F}}(\boldsymbol{U})}{\partial x}. \tag{3.69}$$

In this case, the system actually conserves $\boldsymbol{U}$.

3.3.1. Resolution of non-conservative terms

Systems of non-conservative transport equations are known to be challenging to solve. For conservative systems, the Lax-Wendroff Theorem [49]

guarantees that if the numerical scheme converges, it converges to the right weak solution. For non-conservative systems, the theorem does not apply. Parés [70] proposed a theoretical framework – the *formally path-consistent* framework – to treat the non conservative terms $\boldsymbol{B}(\boldsymbol{U})\partial_x \boldsymbol{Z}(\boldsymbol{U})$ in (3.66). The principle is to average the non-conservative factor matrix $\boldsymbol{B}(\boldsymbol{U})$ over a given path between the left and right states $\boldsymbol{U}_{i-1}$ and $\boldsymbol{U}_i$. This was done for the two-fluid six-equation model for example in [62] and in Paper E [57] (Section 4.5). However, Castro *et al.* [9] showed that schemes following the *formally path-consistent* framework do not necessarily yield the right shock speeds. Abgrall and Karni [1] made the same observation, but in addition showed that the scheme does not even satisfy the Rankine-Hugoniot condition prescribed by the chosen path.

Hou and Le Floch [35] studied, for scalar conservation laws, the convergence of numerical schemes in non-conservative form. They concluded that schemes in non-conservative form could not converge to the right weak solution in the presence of discontinuities. They proved that this problem cannot be solved by an entropy correction of the scheme. Even with schemes in non-conservative form corrected to respect the viscous form of a conservative scheme, the wave velocities are not properly resolved. Hou and Le Floch mention, however, that this problem could be solved by switching to a conservative scheme in the regions where discontinuities are present. This is nevertheless not possible when the model itself does not exist in conservative form, like the two-fluid six-equation model.

In [21], Fjordholm and Mishra derived entropy corrections for finite-difference schemes for two systems of transport equations in non-conservative formulation. The method is based on entropy-conservative schemes [87, 88]. It consists in suppressing the numerical viscosity from the numerical scheme, before reintroducing a viscosity term to stabilise it. Consequently, one has control over the viscosity of the scheme. The authors applied the method to two example models, the equations of compressible inviscid gas dynamics in Lagrangian coordinates studied in [1], and the isothermal Euler equations studied in [44]. The two models have one thing in common, which is that they are two systems of conservation laws which can be formulated, through a change of variables, in non-conservative form. First, to find the entropy-conservative schemes for the non-conservative models, the authors apply the change of variables

to the entropy-conservative scheme derived for the conservative model. Then, to find the right viscosity term, they apply again the change of variables to the conservative model, augmented with entropy correction. The scheme for the non-conservative model, augmented with the viscosity terms, then seems to converge to the expected right solution. The authors mention that there is no general theory to derive an entropy-conservative scheme for a non-conservative system. Additionally, they needed to know the entropy correction of the conservative scheme to be able to derive the entropy correction of the non-conservative scheme. It seems that the method actually corrects the non-conservative formulation of the model by retrieving the underlying conservative properties of the equivalent conservative model. It is not clear how this method could be applied to models for which there is no equivalent conservation formulation, like the six-equation two-fluid model.

The *formally path-consistent* framework has nevertheless good properties for some non-conservative systems [18]. When the non-conservative products are only active across linear degenerate fields, the method behaves well. This is the case for the Baer-Nunziato model [3], which is a seven-equation two-fluid model. This is not the case for the six-equation two-fluid model, since the volume fraction jumps across a pressure wave. Therefore the term $p\partial_x\alpha_\mathrm{g}$ in the momentum equations (2.195)–(2.196) and $p\partial_t\alpha_\mathrm{g}$ in the energy equations (2.197)–(2.198) are active. Note that the Baer-Nunziato model with mechanical relaxation (cf. Section 2.5.2) treated as an algebraic source term – which approaches the six-equation two-fluid model – may nevertheless be incorrectly solved, as will be shown in Section 3.3.2. It is also mentioned in [18] that the inaccuracy of the wave propagation for non-conservative systems is expected to be small for real-life physical models, for which the solutions are often rather smooth due to physical viscosity terms. In the crack arrest problem, strong pressure variations are expected during depressurisation. However, they will propagate as rarefaction waves, therefore the may not be concerned by the wrong propagation velocity. To conclude, as written in [18], *path-conservative schemes must not be used as general-purpose black-box tools to solve any kind of general nonlinear non-conservative hyperbolic system.*

Finally, as mentioned in [35], as well as in [9, 18] in the context of *formally path-consistent* schemes, diffusion-free schemes like the Glimm scheme [30] correctly handle the non-conservative terms. Front tracking

for hyperbolic conservation laws [34] is also little subject to numerical diffusion (and diffusion-free for scalar conservation laws) and could be an option.

3.3.2. Non-conservative terms treated with fractional-step methods

Another approach exists to treat non-conservative terms, the fractional-step method [50, p. 380] or time-splitting strategies [13, 69], in which the non-conservative terms are treated similarly to algebraic source terms.

Example case

We will use as example case the Euler equations of fluid dynamics in Lagrangian coordinates studied by Abgrall and Karni in [1]. In conservative formulation, they are

$$\begin{aligned} \nu_t - u_x &= 0 \\ u_t + p_x &= 0 \\ e_t + (pu)_x &= 0, \end{aligned} \tag{3.70}$$

where $\nu = 1/\rho$ is the specific volume, u is the velocity, p is the pressure and e is the specific total energy. The perfect gas equation of state is used. Its expression is

$$\varepsilon = \frac{p\nu}{\gamma - 1}. \tag{3.71}$$

Through a change of variables, it can be expressed in non-conservative formulation

$$\begin{aligned} \nu_t - u_x &= 0 \\ u_t + p_x &= 0 \\ \varepsilon_t + p(u)_x &= 0, \end{aligned} \tag{3.72}$$

where ε is the specific internal energy, such that $e = \varepsilon + u^2/2$. The Jacobian matrix of the conservative formulation (3.70) is

$$\boldsymbol{A}_{\mathrm{c}} = \begin{pmatrix} 0 & -1 & 0 \\ -\frac{p}{\nu} & -\frac{(\gamma-1)u}{\nu} & \frac{\gamma-1}{\nu} \\ -\frac{up}{\nu} & p - \frac{(\gamma-1)u^2}{\nu} & \frac{(\gamma-1)u}{\nu} \end{pmatrix}, \tag{3.73}$$

while for the non-conservative formulation, we first write the matrices according to (3.66)

$$\boldsymbol{B} = \begin{pmatrix} 0 & -1 & 0 \\ 0 & 0 & 1 \\ 0 & p & 0 \end{pmatrix} \text{ and } \boldsymbol{M} = \frac{\partial \boldsymbol{Z}(\boldsymbol{U})}{\partial \boldsymbol{U}} = \begin{pmatrix} 1 & 0 & 0 \\ 0 & 1 & 0 \\ -\frac{p}{\nu} & 0 & \frac{\gamma-1}{\nu} \end{pmatrix}, \tag{3.74}$$

and the Jacobian is

$$\boldsymbol{A}_{\text{nc}} = \boldsymbol{B}\boldsymbol{M}. \tag{3.75}$$

These systems are equivalent to each other for smooth solutions. In addition, if a linear path is chosen to evaluate the average of $\boldsymbol{B}$, they have the same shock relations, which means that they admit the same acceptable discontinuities [1]. The authors solved both systems with a Roe scheme, using the *formally path-consistent* approach with a linear path for the non-conservative terms. The Roe averages, used in $\boldsymbol{A}_c$ and in $\boldsymbol{M}$, are in both cases

$$\hat{\nu} = \frac{\nu_l + \nu_r}{2}, \tag{3.76}$$

$$\hat{u} = \frac{u_l + u_r}{2}, \tag{3.77}$$

$$\hat{p} = \frac{p_l + p_r}{2}. \tag{3.78}$$

The path-conservative average of the pressure, used in $\boldsymbol{B}$, is identical to its Roe average

$$\bar{p} = \frac{p_l + p_r}{2}. \tag{3.79}$$

The eigenvalues of the Roe matrices are 0 and $\pm\hat{c}$, where the speed of sound $\hat{c}$ is given by

$$\hat{c} = \sqrt{\frac{\gamma\hat{p}}{\hat{\nu}}} \tag{3.80}$$

and

$$\hat{c} = \sqrt{\frac{(\gamma-1)\bar{p} + \hat{p}}{\hat{\nu}}} \tag{3.81}$$

for the conservative and non-conservative formulations, respectively. Note that they are equal for the present definition of $\bar{p}$.

The fractional-step method

We will solve the non-conservative system (3.72) with a numerical solver which solves successively the conservative fluxes and the non-conservative term. The conservative part of the system

$$\begin{aligned} \nu_t - u_x &= 0, \\ u_t + p_x &= 0, \\ \varepsilon_t &= 0, \end{aligned} \tag{3.82}$$

is solved with a Roe scheme, where the Roe averages are still given by (3.76). The eigenvalues are still 0 and $\pm\hat{c}$, but now the speed of sound is

$$\hat{c} = \sqrt{\frac{\hat{p}}{\hat{\nu}}}. \tag{3.83}$$

The non-conservative term in the third equation of (3.72)

$$\varepsilon_t = -p(u)_x \tag{3.84}$$

is solved as a source term alternatively with the conservative flux through

$$\varepsilon_i^{n+1} = \varepsilon_i^n - p_i^n \frac{u_{i+1}^n - u_{i-1}^n}{2\Delta x}\Delta t. \tag{3.85}$$

The results are shown on Figure 3.4. The curve in plain line is the solution of the conservative formulation. The dashed curve is the solution of the non-conservative formulation solved with the *formally path-consistent* approach. As mentioned in [1], the right discontinuity of the dashed curve violates the Rankine-Hugoniot condition prescribed by the integration path of the non-conservative factors. The dotted curve is the solution of the third method, solving the non-conservative terms as source terms. It produces a solution very similar to the dashed curve. Thus, solving the non-conservative terms with a fractional step method does not circumvent the problem of wrong wave velocity and wrong height of the intermediate plateau.

3.4. Summary

The numerical methods presented in this chapter are tailored for systems of conservation laws. They generally manage to resolve the discontinuities sharply and the Lax-Wendroff theorem assures us that if the method

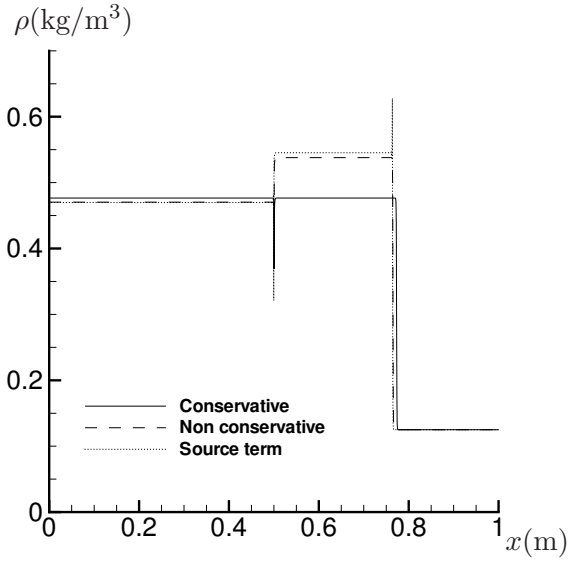

Figure 3.4: Results for the Euler equations in conservative and non-conservative formulations. $t = 0.7s$, CFL $= 0.3$, 1500 cells.

converges, it converges to the right solution. The Roe scheme is the least diffusive of them, however it lacks robustness in some particular cases, due to being non-positively conservative. Its derivation also requires extensive algebraic calculation, reducing its flexibility. Other schemes are positively-conservative, thus more robust, like the HLL scheme and its variations, and the VFRoe scheme. They are nevertheless more diffusive. The MUSTA scheme, despite being computationally expensive, seems to be a good option, due to its robustness and its simplicity and flexibility. As for the non-conservative terms, they are still a challenge to solve.

Now that the physical models and the numerical methods to solve them have been presented, we will summarise the contributions of this thesis in the next chapter.

4 Summary of the contributions

4.1. Paper A

Numerical Resolution of CO_2 Transport Dynamics [54]

Published in the proceedings of the conference Mathematics for Industry '09, San Francisco, USA, October 09-10, 2009.

Authors: Alexandre Morin, Peder K. Aursand, Tore Flåtten and Svend T. Munkejord.

In this paper, we derived a partially-analytical high-resolution scheme for the N-phase drift-flux model with a mixture energy equation. The thermodynamic description is treated as "black box" relations, therefore, any equation of state and mixing rule can be used in the derived framework. Phase change may also be incorporated. Classically, the phases are in mechanical equilibrium. They are in addition in thermal equilibrium, since only a mixture energy equation describes energy transport. The phase velocities have to be recovered from the mixture velocity with an algebraic relation. After having derived the quasilinear formulation of the model, we were able to analyse its eigenstructure. It is composed of N entropy waves having as associated eigenvalues the mixture velocity, and two pressure waves, having as eigenvalues the relative sound speed of the model. All the eigenvectors are given analytically as functions of thermodynamic differentials. Then, a Roe scheme with the higher-order wave-limiter extension is derived. Analytical Roe averages are given for most of the variables; only a few thermodynamic variables have to be averaged numerically. This keeps the generality of the derivation for any thermodynamic description. We suggest a simple numerical procedure to evaluate these averages. We then present the results of some test cases to show the convergence properties of the Roe scheme compared to the MUSTA method applied to the same model. We also illustrate why an ac-

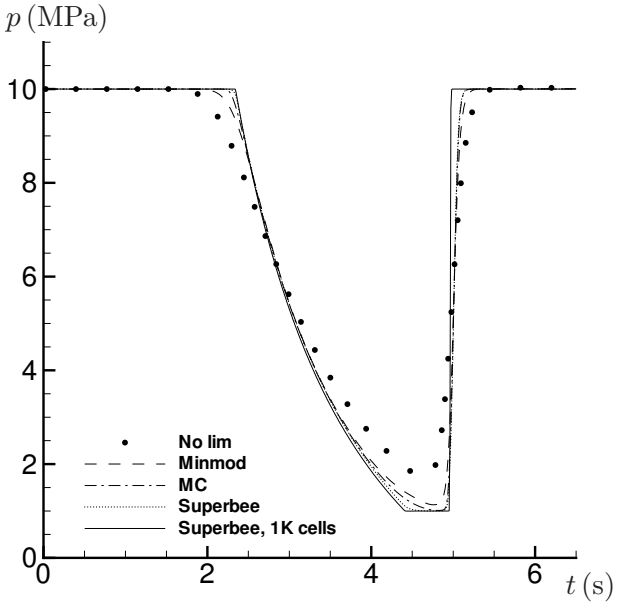

Figure 4.1: Depressurisation case. Pressure as a function of time at $x = 450\,\mathrm{m}$. Roe method, 100 cells. CFL 0.5. Comparison of different flux limiters, and no flux limiter.

curate numerical scheme is crucial to simulate fast depressurisation cases, like for example the crack arrest problem. This is shown on Figure 4.1, where we compare a first-order method ("No lim") to second-order methods.

Personal contributions: In this work, I participated in the implementation of the scheme in our in-house finite-volume-method code initiated by Svend Tollak Munkejord. I ran some of the test-cases and produced curves, and wrote the section on numerical simulations. I wrote the rest of the paper from a note on the derivation. I presented it at the conference.

4.2. Paper B

On Solutions to Equilibrium Problems for Systems of Stiffened Gases [25]

Published in SIAM Journal on Applied Mathematics, Vol. 71 (2011), pp. 41–67.

Authors: Tore Flåtten, Alexandre Morin and Svend T. Munkejord.

In this paper, we derive a method to solve the equilibrium state of a mixture of N immiscible fluids described by the stiffened gas equation of state. The problem that we wish to solve is to evaluate the thermodynamic state of the fluids knowing their fluid-mechanical properties, which are the partial densities and internal energies. Two cases are treated, one with thermal equilibrium, the other without. In both cases, the mixture is in mechanical equilibrium, which means that all the fluids are at the same pressure. In addition, existence and uniqueness of the solution is discussed.

The stiffened gas equation of state is a local approximation of the thermodynamical properties of a fluid around a given reference state, based on the ideal gas equation of state. It can be written as

$$p(\rho, e) = (\gamma - 1)\rho(e - e_*) - \gamma p_\infty, \tag{4.1}$$

where p is the pressure, ρ is the density and e is the specific internal energy of the fluid. γ is the heat capacity ratio, while e_* is the zero point for the internal energy and p_∞ is the "stiffness" parameter, which modulates the compressibility of the fluid. In addition, the volume fraction of the phases in the mixture is denoted by α_i.

The first step in deriving the solution methods is to reduce both problems to the solution of a monotonic function of one variable. In the problem without thermal equilibrium, we know the partial densities $m_i = \alpha_i \rho_i$ and the internal energies $E_i = \alpha_i \rho_i e_i$. We can reduce the problem to a function of the pressure

$$f(\hat{p}) = \sum_{i=1}^{N} \frac{(\gamma_i - 1)(E_i - m_i e_{*,i})}{\hat{p} + \gamma_i p_{\infty,i}}. \tag{4.2}$$

The equilibrium mixture pressure p must satisfy

$$f(p) = 1. \tag{4.3}$$

The problem has a unique physically valid solution as soon as a set of restrictions stated in the article is satisfied.

For the problem with thermal equilibrium, we know the partial densities $m_i = \alpha_i \rho_i$ and the mixture internal energy $E = \sum_{i=1}^{N} \alpha_i \rho_i e_i$. The problem is also reduced to a function of the pressure

$$g(\hat{p}) = \sum_{i=1}^{N} \frac{\gamma_i - 1}{\gamma_i} \frac{m_i c_{p,i}}{\sum_{j=1}^{N} m_j c_{p,j}} \frac{E + \hat{p} - \sum_{j=1}^{N} m_j e_{*,j}}{\hat{p} + p_{\infty,i}}. \tag{4.4}$$

where $c_{p,i}$ is the specific heat capacity at constant pressure. The equilibrium mixture pressure p must satisfy

$$g(p) = 1. \tag{4.5}$$

The problem has a unique physically valid solution as soon as the restrictions stated in the article are satisfied.

Finally, numerical algorithms based on Newton's method are proposed to solve the scalar pressure equations. Second order convergence is shown on some examples.

Personal contributions: I initiated this work by deriving an algorithm which evaluates the primary variables from the conserved variables in the N-phase drift-flux model. I had reduced the equation system to two equations, solved by Newton-Raphson iterations. Then, Tore Flåtten reduced the systems to one pressure equation and derived consistency conditions.

4.3. Paper C

Wave Propagation in Multicomponent Flow Models [24]

Published in SIAM Journal on applied Mathematics, Vol. 70 (2010), pp. 2861-2882.

Authors: Tore Flåtten, Alexandre Morin and Svend T. Munkejord.

This paper follows up on the drift-flux model for mixtures of N phases. It compares the version with instantaneous thermal equilibrium with the version where the equilibrium is reached at a finite rate, called relaxation model. Both models are composed of N phasic mass transport equations and one mixture momentum transport equation. In addition, there is

one mixture total energy transport equation for the model in instantaneous equilibrium, and N phasic total energy transport equations for the relaxation model.

We are interested in comparing the wave structure of these two models, to assess the effect of thermal relaxation on wave propagation. First of all, taking advantage of the decomposition of the relaxation system, we find that there are $2N-1$ waves with velocity v, amongst which N entropy waves and $N-1$ mass-fraction waves, while the remaining two are pressure waves with velocities $v \pm \hat{c}$. Here, the mixture speed of sound is given by

$$\hat{c}^2 = \left(\rho \sum_{i=1}^{N} \frac{\alpha_i}{\rho_i c_i^2} \right)^{-1}, \tag{4.6}$$

where $\rho = \sum_{i=1}^{N} \alpha_i \rho_i$ is the mixture density, α_i is the volume fraction of component i, ρ_i its density and c_i its speed of sound given by the equation of state. The equilibrium system has $N+2$ waves, amongst which $N-1$ mass-fraction waves and one entropy wave, all travelling at velocity v, and two pressure waves with velocity $v \pm \tilde{c}$. The mixture sound velocity of the equilibrium model is given by

$$\tilde{c}^{-2} = \hat{c}^{-2} + \rho \left(T \sum_{i=1}^{N} C_{p,i} \right)^{-1} \sum_{j>i}^{N} C_{p,i} C_{p,j} (\zeta_j - \zeta_i)^2, \tag{4.7}$$

where $Y_i = \alpha_i \rho_i / \rho$ is the mass fraction, T is the temperature, $C_{p,i}$ is the extensive heat capacity $\alpha_i \rho_i c_{p,i}$, and the thermodynamical parameter ζ_i is defined as

$$\zeta_i = \left(\frac{\partial T}{\partial p} \right)_{s_i} = -\frac{1}{\rho_i^2} \left(\frac{\partial \rho_i}{\partial s_i} \right)_p. \tag{4.8}$$

One interesting result to verify with this model comparison is that the subcharacteristic condition is fulfilled. It is a required condition for the stability of the relaxation process. It states that the wave speeds in the equilibrium model should be not be greater than the speeds of the corresponding waves in the relaxation model. It is trivially fulfilled for the waves with velocity v. For the pressure waves, the speeds of sound have

to be compared. From (4.7), we can write that

$$\tilde{c}^{-2} - \hat{c}^{-2} = \rho \left(T \sum_{i=1}^{N} C_{p,i} \right)^{-1} \sum_{j>i}^{N} C_{p,i} C_{p,j} (\zeta_j - \zeta_i)^2, \tag{4.9}$$

which is strictly non-negative since $C_{p,i} > 0$.

Then, the quasilinear formulation for the equilibrium model is derived.

Personal contributions: In this work, I contributed by implementing and numerically testing the Jacobian matrix.

4.4. Paper D

Towards a Formally Path-Consistent Roe Scheme for the Six-Equation Two-Fluid Model [56]

Published in AIP Conference Proceedings, Vol. 1281 (2010), pp. 71–74.

Authors: Alexandre Morin, Tore Flåtten and Svend T. Munkejord.

This paper presents the derivation of a partially-analytical Roe scheme for the six-equation two-fluid model. This model contains non-conservative terms which are a challenge for numerical methods. The strength of the derivation is that the Roe averages are valid for any averaging formula for the non-conservative terms. Also, we give analytical Roe averages for most of the variables, independently of the thermodynamic description of the phases. The averaging of the remaining variables is dependent on the equations of state, and has generally to be done numerically. We split the flux function into two parts, the convective part and the pressure part. The variables without analytical Roe averages must satisfy a reduced Roe condition derived from the pressure part of the Roe condition

$$\hat{\boldsymbol{M}} \left(\boldsymbol{U}^{\mathrm{L}}, \boldsymbol{U}^{\mathrm{R}} \right) \left(\boldsymbol{U}^{\mathrm{R}} - \boldsymbol{U}^{\mathrm{L}} \right) = \boldsymbol{W} \left(\boldsymbol{U}^{\mathrm{R}} \right) - \boldsymbol{W} \left(\boldsymbol{U}^{\mathrm{L}} \right), \tag{4.10}$$

where $\boldsymbol{U}$ is the vector of conserved variables, $\hat{\boldsymbol{M}}$ is the Roe-averaged matrix of the pressure part of the fluxes and $\boldsymbol{W}$ is the pressure-part flux function. The exponents L and R designate the left and right cells. This Roe condition is simplified into two scalar conditions dependent on – but valid for any – equation of state.

Personal contributions: I started to derive the Jacobian matrix of the model, and received help from Tore Flåtten to complete the pressure part

of the Jacobian ($\boldsymbol{M} = \partial_{\boldsymbol{U}} \boldsymbol{W}(\boldsymbol{U})$). Then, Tore Flåtten derived the Roe averages. I wrote the paper. I implemented the scheme and ran test cases. I presented the work at the ICNAAM 2010 conference.

4.5. Paper E

A Roe Scheme for a Compressible Six-Equation Two-Fluid Model [57]

Submitted to International Journal for Numerical Methods in Fluids, 2012.

Authors: Alexandre Morin, Tore Flåtten and Svend T. Munkejord.

This paper extends and completes the previous one. It presents a partially-analytical Roe scheme for the six-equation two-fluid model. While in the previous paper, only the derivation results of the Roe averages were presented, the present paper gives the details. First the necessary differentials to express the model in quasilinear formulation are derived. Then, we show that the Roe averages presented fulfill the Roe conditions, in particular

$$\hat{\boldsymbol{A}}\left(\boldsymbol{U}^{\mathrm{L}}, \boldsymbol{U}^{\mathrm{R}}\right)\left(\boldsymbol{U}^{\mathrm{R}} - \boldsymbol{U}^{\mathrm{L}}\right) = \boldsymbol{F}_c\left(\boldsymbol{U}^{\mathrm{R}}\right) - \boldsymbol{F}_c\left(\boldsymbol{U}^{\mathrm{L}}\right) + \overline{\boldsymbol{B}}\left(\boldsymbol{U}^{\mathrm{L}}, \boldsymbol{U}^{\mathrm{R}}\right)\left(\boldsymbol{W}\left(\boldsymbol{U}^{\mathrm{R}}\right) - \boldsymbol{W}\left(\boldsymbol{U}^{\mathrm{L}}\right)\right) \quad (4.11)$$

where $\boldsymbol{U}$ is the vector of conserved variables, $\hat{\boldsymbol{A}}$ is the Roe-averaged Jacobian of the fluxes, $\boldsymbol{F}_c$ is the convective part of the flux function, $\overline{\boldsymbol{B}}$ is the averaged matrix of the factors of the non-conservative terms and $\boldsymbol{W}$ is the non-conservative flux function, containing the so-called pressure contributions of the fluxes. The exponents L and R designate the left and right cells. The condition (4.11) may be split in two, and $\overline{\boldsymbol{B}}$ cancels using a clever definition of the Roe-averaged Jacobian of the pressure part $\hat{\boldsymbol{A}}_p = \overline{\boldsymbol{B}}\hat{\boldsymbol{M}}$.

$$\hat{\boldsymbol{A}}_c\left(\boldsymbol{U}^{\mathrm{L}}, \boldsymbol{U}^{\mathrm{R}}\right)\left(\boldsymbol{U}^{\mathrm{R}} - \boldsymbol{U}^{\mathrm{L}}\right) = \boldsymbol{F}_c\left(\boldsymbol{U}^{\mathrm{R}}\right) - \boldsymbol{F}_c\left(\boldsymbol{U}^{\mathrm{L}}\right) \quad (4.12)$$

$$\hat{\boldsymbol{M}}\left(\boldsymbol{U}^{\mathrm{L}}, \boldsymbol{U}^{\mathrm{R}}\right)\left(\boldsymbol{U}^{\mathrm{R}} - \boldsymbol{U}^{\mathrm{L}}\right) = \boldsymbol{W}\left(\boldsymbol{U}^{\mathrm{R}}\right) - \boldsymbol{W}\left(\boldsymbol{U}^{\mathrm{L}}\right) \quad (4.13)$$

Therefore, the derivation is independent of the averaging method for the factor matrix of the non-conservative terms $\overline{\boldsymbol{B}}$. Only two scalar conditions remain after simplification, that the remaining equation-of-state-dependent variables must fulfill.

A pitfall arising with the six-equation two-fluid model is that the model is resonant when the gas and liquid velocities are equal to each other. Resonance occurs when two or more eigenvalues are identical and their associated eigenspace loses at least one dimension. Consequently, the Jacobian matrix $\boldsymbol{A}$ of the fluxes becomes non-diagonalisable. The problem is that the Roe scheme uses the Jacobian matrix eigenstructure. However, we explain why this only is an apparent problem. The eigenspace associated with the eigenvalues v when $v_\mathrm{g} = v_\ell = v$ collapses because the volume-fraction waves become identical. Therefore, one eigenvector appears twice, making the matrix of eigenvectors singular. We construct and justify a fix to this problem.

Subsequently, a second-order extension of the scheme using the wave limiter approach is presented. The original version cannot be applied, because of the difficulty to identify the order of the waves in the numerical diagonalisation. We thus found a modified version and applied it to the scheme.

Numerical results are then presented. Because we are aware that non-conservative terms pose problems for the accurate resolution of the waves, the first test case investigates the propagation velocity of all the six waves. We show that only a small discrepancy is noticeable for one of the waves. Then, some classical test cases are presented, Toumi's shock tube (cf. Figure 4.2a), the moving Gauss curve to evaluate the convergence order on smooth regions and the water faucet (cf. Figure 4.2b).

Personal contributions: This is the continuation of the previous paper. The Roe scheme (Sections 2 to 4) was derived by Tore Flåtten. The other sections are mine. I implemented the scheme in the in-house finite-volume-method code initiated by Svend Tollak Munkejord. I derived the fix for resonance, and justified why it works. I added the second order extension with wave limiters. Finally, I ran the test cases and produced the curves. The results for the MUSTA scheme are from Svend Tollak Munkejord.

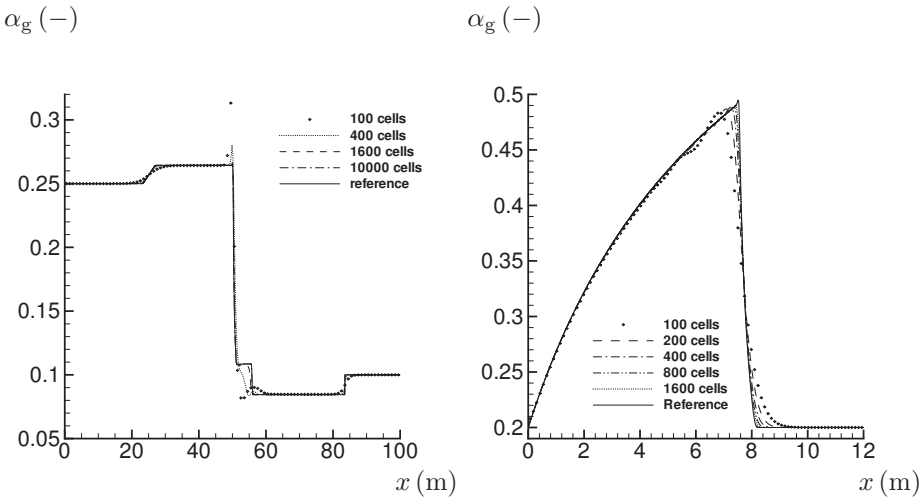

(a) Toumi's shock tube. Gas volume fraction. Minmod limiter. $t = 0.06s$. CFL=0.5.

(b) Water faucet. Gas volume fraction. Minmod limiter. $t = 0.6s$. CFL=0.5.

Figure 4.2: Numerical results for the Roe scheme on the six-equation two-fluid model.

4.6. Paper F

On Interface Transfer Terms in Two-Fluid Models [23]

Published in International Journal of Multiphase Flow, Vol. 45 (2012), pp. 24–29.

Authors: Tore Flåtten and Alexandre Morin.

The two-fluid model is known for not being hyperbolic in its classical form. Though regularisations of the model exist to obtain a functioning model, a better insight in the physical and mathematical explanations of this fact could help improving the formulation of the model. This has already been extensively discussed in the literature, without the debate reaching a final conclusion. The main idea discussed in the paper is that the often used regularisation terms may – and generally do – make the model violate the second law of thermodynamics.

We first construct a two-phase flow model from the classical assump-

tions of conservation of phasic masses, mixture momentum and mixture energy, plus the assumptions of thermodynamical reversibility for smooth solutions. Adding the assumption that entropy follows the transport equation

$$\frac{\partial \alpha_k \rho_k s_k}{\partial t} + \frac{\partial \alpha_k \rho_k s_k v_k}{\partial x} = 0, \tag{4.14}$$

we recover the classical formulation of the six-equation two-fluid model, which is not hyperbolic. Now, the usual regularisations of this model involve an extra differential term $\mathcal{M}_k$ in the momentum transport equations

$$\frac{\partial \alpha_k \rho_k v_k}{\partial t} + \frac{\partial \alpha_k \rho_k v_k^2}{\partial x} + \alpha_k \frac{\partial p}{\partial x} + \mathcal{M}_k = 0, \tag{4.15}$$

where $k = \mathrm{g}$ or $k = \ell$ and $\mathcal{M}_\mathrm{g} = -\mathcal{M}_\ell$. The present derivation shows that such regularised models cannot respect both the conservation assumptions and (4.14).

Then, we investigated the consequences of relaxing the assumption that entropy follows the transport equation (4.14). We used instead

$$\frac{\partial \alpha_k \rho_k s_k}{\partial t} + \frac{\partial \alpha_k \rho_k s_k v_k}{\partial t} = \sigma_k, \tag{4.16}$$

where σ_k may be some conservative differential term. We found that a model could respect the conservation of all the required quantities, while at the same time respect the thermodynamical reversibility, if $\mathcal{M}_k$ in (4.15) is defined as

$$\mathcal{M}_\mathrm{g} = T(v_\mathrm{g} - v_\ell)\frac{\partial W}{\partial x} + 2WT\frac{\partial (v_\mathrm{g} - v_\ell)}{\partial x}, \tag{4.17}$$

where $W(\boldsymbol{U})$ is defined through

$$Z(\boldsymbol{U}) = W(\boldsymbol{U})(v_\mathrm{g} - v_\ell)^2, \tag{4.18}$$

and $Z(\boldsymbol{U})$ is some potential function. This is not a tool to construct a hyperbolic model, but it is a convenient tool to test the thermodynamic consistency of a model. Amongst other things, it shows that a regularisation term consistent with thermodynamics must contain terms of the form $\partial_x v_k$.

Then, the interpretation of the interface transfer terms in the energy balance equations is discussed. It is not really an energy transfer term, but rather a heat and kinetic energy transfer term.

Personal contributions: The first part of this paper is based on my work. I derived the two-fluid model from the basic conservation requirements, leading to relation (24). I remarked that, when the assumption (4.14) is made, the only physically relevant two-fluid model is the standard non-hyperbolic model. Then, Tore Flåtten studied the consequences of relaxing the entropy assumption, and derived relation (36). Section 6 is Tore Flåtten's work.

4.7. Paper G

A Two-Fluid Four-Equation Model with Instantaneous Thermodynamical Equilibrium [55]

Submitted to SIAM Journal on Applied Mathematics, 2012.

Authors: Alexandre Morin and Tore Flåtten.

The motivation for this work was to be able to use the Span-Wagner equilibrium equation of state for mixtures of CO_2. We derived the four-equation two-fluid model, where the phases are at all times at mechanical, thermal and chemical equilibrium. The model was derived from the five-equation two-fluid model with instantaneous thermal equilibrium by performing the instantaneous chemical relaxation through phase change. First, phase change comes with an exchange of momentum at the interface. By deriving the entropy transport equation, we are able to specify the interfacial velocity.

Then, we write the equilibrium model. It contains time derivatives, which we transform into spatial derivatives. The model is then written in quasilinear formulation by deriving the differentials of the components of the conservative flux function, as well as of the non-conservative flux function.

Our derivation completes a hierarchy of models presented in the literature. The hierarchy is represented in Figure 4.3. A remarkable fact is that the instantaneous relaxation of a variable in a model affects the speed of sound of the model by a factor independently of the order in which the relaxations are performed. For example, for the velocity relaxation, we

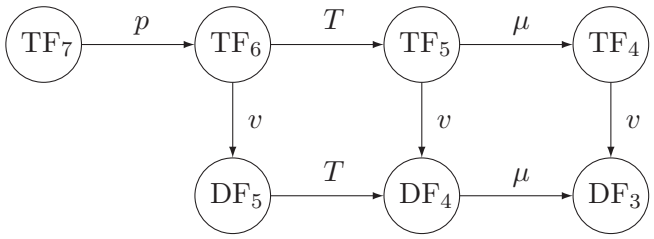

Figure 4.3: Hierarchy of the two-phase flow models. TF: two-phase model. DF: drift-flux model. Index: Number of conservation equations. p, T, μ and v designate the relaxed variable.

have

$$\frac{c_{\mathrm{TF4}}}{c_{\mathrm{DF3}}} = \frac{c_{\mathrm{TF5}}}{c_{\mathrm{DF4}}} = \frac{c_{\mathrm{TF6}}}{c_{\mathrm{DF5}}}, \tag{4.19}$$

where c is the speed of sound of a model following the naming convention in Figure 4.3 of the present chapter. We are also able to verify that the four-equation two-fluid model satisfies the subcharacteristic condition with the other models of the hierarchy.

Finally, this model as the other two-fluid models is not hyperbolic when the gas and liquid velocities are different from each other. We have to use a regularisation term. Using a perturbation method, we find an expression for the pressure difference in the interfacial pressure regularisation term.

Personal contributions: This paper is mostly my work, helped by useful discussions and suggestions from Tore Flåtten.

4.8. Paper H

Pipeline Flow Modelling with Source Terms due to Leakage: The Straw Method [58]

Accepted in Energy Procedia, proceedings of the sixth Trondheim Conference on CO_2 Capture and Storage, 2012.

Authors: Alexandre Morin, Steinar Kragset and Svend T. Munkejord

This paper differs in spirit from the other contributions and is the most applied one of the series. We try to evaluate the flow rate of a pressurised

two-phase mixture through a crack in a pipeline wall. For the single-phase case, the choked-flow theory gives an analytical formula for the flow rate through an orifice. It is composed of two regimes. If the pressure difference on each side of the orifice is under a given threshold, the flow rate is dependent on the pressure difference. Otherwise, the flow rate becomes independent of the downwind pressure. The pressure-difference threshold is reached when the flow velocity at the orifice is equal to the speed of sound. For a two-phase flow, the concept is similar, but obtaining general analytical expressions with a "black box" equation of state is not possible. We therefore wish to develop a numerical method. In the present paper, we present the method and apply it to the single-phase case, for which we have analytical results that we use for comparison.

The Euler equations with source terms for the escaping flow read

$$\frac{\partial \rho}{\partial t} + \frac{\partial \rho u}{\partial x} = -\zeta_e, \tag{4.20}$$

$$\frac{\partial \rho u}{\partial t} + \frac{\partial \rho u^2}{\partial x} + \frac{\partial p}{\partial x} = -u\zeta_e, \tag{4.21}$$

$$\frac{\partial E}{\partial t} + \frac{\partial (E+p)u}{\partial x} = -(E_e + p_e)\frac{1}{\rho_e}\zeta_e, \tag{4.22}$$

where ρ is the density, u the velocity, p the pressure, $E = \rho(e + u^2/2)$ and e the internal energy. ζ_e is the mass flow through the crack. The subscript e designates the state at the orifice, on the inside, as opposed to the other quantities which are averages in the tube. The problem is to evaluate both the flow rate and the fluid state at the orifice.

The straw method models the fracture as a series of transversal tubes – or straws – plugged in the pipe. The diameter of the straws represents the crack opening. The key to the method is the definition of the boundary conditions. They should reproduce the features of the flow through an orifice. Figure 4.4 shows the modelling assumptions. The flow upwind of the orifice is modelled as if it was a convergent nozzle, where the pressure gradient accelerates the fluid. At the orifice, if the flow is subsonic, the downwind pressure is the atmospheric pressure. If the pressure difference should prescribe a speed higher than the sound speed, the pressure at the orifice remains such that the flow is exactly sonic. Then, the fluid reaches atmospheric pressure in a jet that we do not model. Therefore, the inlet boundary condition performs a Bernoulli-like expansion, where

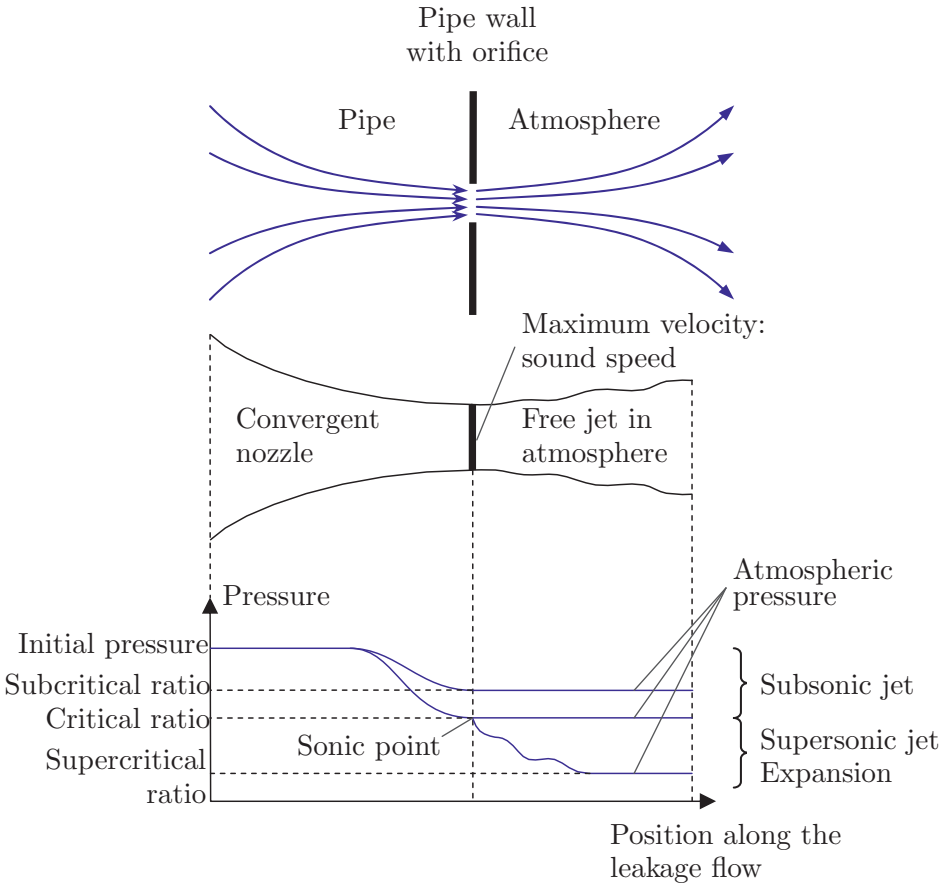

Figure 4.4: Top: real situation of a leak across an orifice in the pipe wall. Middle: model of the leakage flow using a convergent nozzle and a free jet in atmosphere. Bottom: Pressure profile in the adopted model, depending on the ratio of the internal pressure to the surrounding (atmospheric) pressure.

the fluid is accelerated at constant "total enthalpy" $H = \rho(h + u^2/2)$, where h is the specific enthalpy. The outlet boundary condition will intrinsically juggle with the sub- and supercritical regimes. However, to stabilise the convergence, and since we are only interested in the steady

state, a correction is applied to the outlet pressure. This correction naturally disappears in steady state. In the case of two-phase flows, there may be phase change in the fracture flow. This can happen within the straws. This is the strength of this method, which gives flexibility in the modelling of phase change.

The numerical results show a perfect match at numerical precision between the straw method and the choked flow theory.

Personal contributions: The analytical expressions for the single-phase flow through a fracture are from Steinar Kragset. Svend Tollak Munkejord had started to implement the straw method. I completed it by defining the relevant boundary conditions depending on the flow velocity. The pressure correction to speed up convergence is from me. I performed the numerical tests and presented the poster at the conference.

5 Conclusions and continuation

The present thesis contributed to the derivation and implementation of some two-phase flow models and numerical methods to solve them. The Roe method was applied to the N-phase drift-flux model in Paper A. Then in Paper B, a method was derived to compute the equilibrium state of a mixture composed of phases following stiffened gas equations of state. In Paper C, we compared the wave propagation in the model from Paper A and in the thermal-relaxation model that leads to this model. Then in Papers D and E, a Roe scheme was derived for the six-equation two-fluid model. Paper F deals with a known issue with this model, the fact that it is not hyperbolic in its basic formulation. It does not solve the problem, but clarifies the interaction between the regularisation term and the thermodynamic consistency of the model. In Paper G, a new model is derived, the four-equation two-fluid model, where the phases are at equilibrium at all times. Finally, in Paper H, a numerical method is presented, to evaluate the mass flow through a fracture in a pipe.

This work raised some problems and questions. First, in Paper G, a nomenclature of two-phase flow models was presented, containing two-fluid and drift-flux models, with various equilibrium assumptions. One can wonder what the best choice of model is. The crack arrest problem involves fast transients, and the assumptions of instantaneous equilibria can be questioned. On the other hand, however physically relevant a model is, experimental data is required to determine the parameters. For example, the Span-Wagner equation of state describes accurately mixtures of CO_2 only at equilibrium, therefore the four-equation two-fluid model was derived. A six-equation or even seven-equation two-fluid model may be a better description for fast transients, however, an accurate equation of state for CO_2 in liquid and gas phases would be needed. In addition, models should be provided for how the equilibria are reached. Allowing the phases to be out of chemical equilibrium and providing a wrong phase-

change model is not necessarily better than assuming instantaneous chemical equilibrium. Therefore, the choice of fluid-dynamical model should be done by considering the physics that is to be modelled, but also the available submodels for thermodynamics, heat transfer, friction, phase change *etc.*

Another question arises from the non-hyperbolicity of the two-fluid models. This fact questions the physical validity of the models. These models may be regularised for example with an interfacial pressure difference term, with a pressure difference that is small compared to the phase pressures. The problem could also be avoided by using a drift-flux model. However, in the drift-flux model, the phases are not as mechanically independent from each other as they are in the two-fluid model. Hence, using the two-fluid model with a regularisation term may still be a better alternative. The seven-equation two-pressure model may also be an alternative, as it is hyperbolic and its eigenstructure is known. The drawback is that a mechanical model at the interface is needed, and it is not clear which one to use. This strategy is not necessarily a better choice than to assume instantaneous mechanical equilibrium and use a regularisation term. Some work could be carried out on the regularisation term using the tools and insights of Paper F on the interfacial terms. The paper shows that only terms containing spatial derivatives of the velocity could respect the second law of thermodynamics, while these terms have not received as much attention as interfacial pressure terms in the litterature. Virtual mass forces terms may be a starting point.

When it comes to the numerical methods, Paper A illustrates the importance of accurate numerical methods to solve the crack arrest problem. Otherwise, the smearing of the waves may cause a wrong resolution of the features of the flow. The thesis has mainly concentrated on the Roe scheme, which has been compared to the MUSTA method in Paper E. The Roe method has a clear advantage in term of sharp resolution of the waves. However, it requires extensive derivation work, and its application to the two-fluid models poses problems due to the eigenstructure not being known analytically. It also suffers from a lack of robustness in some particular cases, for example close to single-phase states. On the other hand, the MUSTA method is easy to implement and rather robust, but less accurate and more computationally expensive. The very recent adaptation of the HLL scheme with wave reconstruction to the six-equation

two-fluid model by Kumbaro [46] seems interesting and should be tried.

The last concern is the resolution of the non-conservative terms. The numerical methods for conservation laws may lead to a wrong resolution of the waves, which is particularly problematic for the crack-arrest problem. Further work is needed here, to try and correct the finite-volume method. The front tracking method for conservation laws could also be tried, as it is expected that it would perform better on the non-conservative terms. However, in its current form, it requires an exact Riemann solver. To apply it to the six-equation two-fluid model, for example, one should try and see if linearised Riemann problems could be solved instead.

Recommendations for further work

- Run the four-equation two-fluid model with the Span-Wagner equation of state, and compare the results to experimental data, to assess the consequences of the full-equilibrium assumption.
- Study why the instantaneous mechanical relaxation of the seven-equation two-fluid model gives a non-hyperbolic six-equation model, if this is due to a wrong entropy creation in the relaxation process (cf. Chen *et. al.* [11, 12]).
- Related to the point over, try to find differential terms in the regularisation term of the six-equation two-fluid model which make the model both hyperbolic and physically relevant, using the results of Paper F.
- Implement and assess the modified HLL method described by Kumbaro in [46], and compare its performances against the Roe method described in Paper E.
- Try to correct the finite-volume method for non-conservative systems.
- Assess the feasibility of using the front-tracking method to solve the six-equation two-fluid model, or any other model for which no solution of the Riemann problem is known.

Bibliography

[1] R. Abgrall and S. Karni, *A comment on the computation of non-conservative products*, J. Comput. Phys. **229** (2010), pp. 2759–2763.

[2] P. K. Aursand, S. Evje, T. Flåtten, K. E. T. Giljarhus, and S. T. Munkejord, *An exponential time-differencing method for monotonic relaxation systems*, Submitted (2011).

[3] M. R. Baer and J. W. Nunziato, *A two-phase mixture theory for the deflagration-to-detonation transition (DDT) in reactive granular materials*, Int. J. Multiphase Flow **12** (1986), pp. 861–889.

[4] S. Banerjee and A. M. C. Chan, *Separated flow models – I. analysis of the averaged and local instantaneous formulations*, Int. J. Multiphase Flow **6** (1980), pp. 1–24.

[5] K. H. Bendiksen, *An experimental investigation of the motion of long bubbles in inclined tubes*, Int. J. Multiphase Flow **10** (1984), pp. 467–483.

[6] K. H. Bendiksen, D. Malnes, R. Moe, and S. Nuland, *The dynamic two-fluid model OLGA: Theory and application*, SPE Prod. Eng. **6** (1991), pp. 171–180.

[7] S. Benzoni-Gavage, *Analyse numérique des modèles hydrodynamiques d'écoulements diphasiques instationnaires dans les réseaux de production pétrolière*, Ph.D. thesis, ENS Lyon, France, 1991.

[8] D. Bestion, *The physical closure laws in the CATHARE code*, Nuclear Engineering and Design **124** (1990), pp. 229–245.

[9] M. J. Castro, P. G. LeFloch, M. L. Muñoz-Ruiz, and C. Parés, *Why many theories of shock waves are necessary: Convergence error in formally path-consistent schemes*, J. Comput. Phys. **227** (2008), pp. 8107–8129.

[10] C.-H. Chang and M.-S. Liou, *A robust and accurate approach to computing compressible multiphase flow: Stratified flow model and AUSM$^+$-up scheme*, J. Comput. Phys. **225** (2007), pp. 850–873.

[11] G.-Q. Chen, *Relaxation limit for conservation laws*, Z. Angew. Math. Mech. **76** (1996), pp. 381–384.

[12] G.-Q. Chen, C. D. Levermore, and T.-P. Liu, *Hyperbolic conservation laws with stiff relaxation terms and entropy*, Comm. Pure Appl. Math. **47** (1994), pp. 787–830.

[13] F. Coquel, K. El Amine, and E. Godlewski, *A numerical method using upwind schemes for the resolution of two-phase flows*, J. Comput. Phys. **136** (1997), pp. 272–288.

[14] J. Cortes, A. Debussche, and I. Toumi, *A density perturbation method to study the eigenstructure of two-phase flow equation systems*, J. Comput. Phys. **147** (1998), pp. 463–484.

[15] T. Danielson, K. Bansal, B. Djoric, E. D. Duret, S. Johansen, and Ø. Hellan, *Testing and qualification of a new multiphase flow simulator*, Offshore Technology Conference, Houston, Texas, USA, 2–5 May (2011).

[16] E. Delnoij, F. A. Lammers, J. A. M. Kuipers, and W. P. M van Swaaij, *Dynamic simulation of dispersed gas-liquid two-phase flow using a discrete bubble model*, Chemical Engineering Science **52** (1997), pp. 1429–1458.

[17] D. A. Drew and S. L. Passman, *Theory of multicomponent fluids*, Applied Mathematical Sciences, vol. 135, Springer-Verlag, New-York, 1999, ISBN 0-387-98380-5.

[18] M. Dumbser and E. F. Toro, *A simple extension of the Osher Riemann solver to non-conservative hyperbolic systems*, J. Sci. Comput. **48** (2011), pp. 70–88.

[19] B. Einfeldt, *On Godunov-type methods for gas dynamics*, SIAM Journal on Numerical Analysis **25** (1988), pp. 294–318.

[20] S. Evje and T. Flåtten, *Hybrid flux-splitting schemes for a common two-fluid model*, J. Comput. Phys. **192** (2003), pp. 175–210.

[21] U. S. Fjordholm and S. Mishra, *Accurate numerical discretizations of non-conservative hyperbolic systems*, ESAIM: Mathematical Modelling and Numerical Analysis **46** (2012), pp. 187–206.

[22] T. Flåtten and H. Lund, *Relaxation two-phase flow models and the subcharacteristic condition*, Mathematical Models and Methods in Applied Sciences **21** (2011), pp. 2379–2407.

[23] T. Flåtten and A. Morin, *On interface transfer terms in two-fluid models*, International Journal of Multiphase Flow **45** (2012), pp. 24–29.

[24] T. Flåtten, A. Morin, and S. T. Munkejord, *Wave propagation in multicomponent flow models*, SIAM J. Appl. Math. **70** (2010), pp. 2861–2882.

[25] T. Flåtten, A. Morin, and S. T. Munkejord, *On solutions to equilibrium problems for systems of stiffened gases*, SIAM Journal on Applied Mathematics **71** (2011), pp. 41–67.

[26] T. Flåtten and S. T. Munkejord, *The approximate Riemann solver of roe applied to a drift-flux two-phase flow model*, ESAIM: Mathematical Modelling and Numerical Analysis **40** (2006), pp. 735–764.

[27] F. França and R. T. Lahey Jr., *The use of drift-flux techniques for the analysis of horizontal two-phase flows*, International Journal of Multiphase Flow **18** (1992), pp. 787–801.

[28] T. Gallouet and J.-M. Masella, *Un schema de Godunov approche*, C.R. Acad. Sci. Paris, Serie I **323** (1996), pp. 77–84.

[29] D. Gidaspow, *Modeling of two-phase flow. round table discussion (rt-1-2)*, Proc. 5th Int. Heat Transfer Conf. VII (1974), p. 163.

[30] J. Glimm, *Solutions in the large for nonlinear hyperbolic systems of equations*, Commun. Pure Appl. Math. **18** (1965), pp. 697–715.

[31] A. Harten and J. M. Hyman, *Self adjusting grid methods for one-dimensional hyperbolic conservation laws*, Journal of Computational Physics **50** (1983), pp. 235–269.

[32] A. Harten, P. D. Lax, and B. van Leer, *On upstream differencing and Godunov-type schemes for hyperbolic conservation laws*, SIAM Rev **25** (1983), pp. 35–61.

[33] T. Hibiki and M. Ishii, *Distribution parameter and drift velocity of drift-flux model in bubbly flow*, International Journal of Heat and Mass Transfer **45** (2002), pp. 707–721.

[34] H. Holden and N. H. Risebro, *Front tracking for hyperbolic conservation laws*, second version ed., Springer Verlag, Berlin, 2007, ISBN 978-3-540-43289-0.

[35] T. Y. Hou and P. G. Le Floch, *Why non-conservative schemes converge to wrong solutions: Error analysis*, Mathematics of Computation **62** (1994), pp. 497–530.

[36] International Energy Agency (IEA), *Energy technology perspectives*, 2010, ISBN 978-92-64-08597-8.

[37] M. Ishii, *Thermo-fluid dynamics theory of two-phase flow*, Eyrolles, Paris, 1975.

[38] M. Ishii and K. Mishima, *Two-fluid model and hydrodynamic constitutive relations*, Nuclear Engineering and Design **82** (1984), pp. 107–126.

[39] H. Jin, J. Glimm, and D. H. Sharp, *Compressible two-pressure two-phase flow models*, Physics Letters A **353** (2006), pp. 469–474.

[40] H. Jin, J. Glimm, and D. H. Sharp, *Entropy of averaging for compressible two-pressure two-phase flow models*, Physics Letters A **360** (2006), pp. 114–121.

[41] A. V. Jones and A. Prosperetti, *On the suitability of first-order differential models for two-phase flow prediction*, Int. J. Multiphase Flow **11** (1985), pp. 133–148.

[42] Jožef Stefan Insitute, Ljubljana, Slovenia, *WAHA3 code manual, JSI Report IJS-DP-8841*, 2004.

[43] K. H. Karlsen, C. Klingenberg, and N. H. Risebro, *A relaxation system for conservation laws with a discontinuous coefficient*, Math. Comput. **73** (2004), pp. 1235–1259.

[44] S. Karni, *Viscous shock profiles and primitive formulations*, SIAM J. Numer. Anal. **29** (1992), pp. 1592–1609.

[45] S. Karni, E. Kirr, A. Kurganov, and G. Petrova, *Compressible two-phase flows by central and upwind schemes*, ESAIM: M2AN **38** (2004), pp. 477–493.

[46] A. Kumbaro, *Simplified eigenstructure decomposition solver for the simulation of two-phase flow systems*, Computers & Fluids **64** (2012), pp. 19–33.

[47] A. Kumbaro and M. Ndjinga, *Influence of interfacial pressure term on the hyperbolicity of a general multifluid model*, Journal of Computational Multiphase Flows **3** (2011), pp. 177–195.

[48] R. T. Lahey Jr., L. Y. Cheng, D. A. Drew, and J. E. Flaherty, *The effect of virtual mass on the numerical stability of accelerating two-phase flows*, AIChE 71st Annual Meeting at Miami Beach, Florida (1978).

[49] P. D. Lax and B. Wendroff, *Systems of conservation laws*, Comm. Pure Appl. Math. **13** (1960), pp. 217–237.

[50] R. J. Leveque, *Finite volume method for hyperbolic problems*, Cambridge University Press, New York, USA, 2002, ISBN 978-0-521-00924-9.

[51] T.-P. Liu, *Hyperbolic conservation laws with relaxation*, Commun. Math. Phys. **108** (1987), pp. 153–175.

[52] H. Lund and T. Flåtten, *Equilibrium conditions and sound velocities in two-phase flows*, SIAM Annual Meeting 2010 (Pittsburg, Pennsylvania, USA) (2010).

[53] P. J. Martínez Ferrer, T. Flåtten, and S. T. Munkejord, *On the effect of temperature and velocity relaxation in two-phase flow models*, ESAIM-Math. Model. Num. **46** (2012), pp. 411–442.

[54] A. Morin, P. K. Aursand, T. Flåtten, and S. T. Munkejord, *Numerical resolution of CO_2 transport dynamics*, Mathematics for Industry '09, San Francisco, USA, 09-10/10 (2009).

[55] A. Morin and T. Flåtten, *A two-fluid four-equation model with instantaneous thermodynamical equilibrium*, Submitted (2012).

[56] A. Morin, T. Flåtten, and S. T. Munkejord, *Towards a formally path-consistent Roe scheme for the six-equation two-fluid model*, AIP Conference Proceedings **1281** (2010), pp. 71–74.

[57] A. Morin, T. Flåtten, and S. T. Munkejord, *A Roe scheme for a compressible six-equation two-fluid model*, Submitted (2012).

[58] A. Morin, S. Kragset, and S. T. Munkejord, *Pipeline flow modelling with source terms due to leakage: The straw method*, Accepted for publication in Energy Procedia (2012).

[59] S. T. Munkejord, *Analysis of the two-fluid model and the drift-flux model for numerical calculation of two-phase flow*, Doctoral Theses at NTNU, 2005:219.

[60] S. T. Munkejord, *Comparison of Roe-type methods for solving the two-fluid model with and without pressure relaxation*, Comput. & Fluids **36** (2007), pp. 1061–1080.

[61] S. T. Munkejord, S. Evje, and T. Flåtten, *The multi-stage centred-scheme approach applied to a drift-flux two-phase flow model*, Int. J. Numer. Meth. Fluids **52** (2006), pp. 679–705.

[62] S. T. Munkejord, S. Evje, and T. Flåtten, *A MUSTA scheme for a nonconservative two-fluid model*, SIAM J. Sci. Comput. **31** (2009), pp. 2587–2622.

[63] A. Murrone and H. Guillard, *A five equation reduced model for compressible two phase flow problems*, J. Comput. Phys. **202** (2005), pp. 664–698.

[64] R. Natalini, *Recent results on hyperbolic relaxation problems. analysis of systems of conservation laws*, Chapman & Hall/CRC Monogr. Surv. Pure Appl. Math. (1999), pp. 128–198.

[65] M. Ndjinga, A. Kumbaro, F. De Vuyst, and P. Laurent-Gengoux, *Influence of interfacial forces on the hyperbolicity of the two-fluid model*, 5th International Symposium on Multiphase Flow, Heat Mass Transfer and Energy Conversion, ISMF05,Xian, China, 3-6 July (2005).

[66] M. Ndjinga, A. Kumbaro, F. De Vuyst, and P. Laurent-Gengoux, *Numerical simulation of hyperbolic two-phase flow models using a Roe-type solver*, Nuclear Engineering and Design **238** (2008), pp. 2075–2083.

[67] *National institute of standards and technology (NIST)*, `http://webbook.nist.gov/cgi/cbook.cgi?ID=C124389&Units=SI&Mask=4`.

[68] H. O. Nordhagen, S. Kragset, T. Berstad, A. Morin, C. Dørum, and S. T. Munkejord, *A new coupled fluid-structure modelling methodology for running ductile fracture*, Computers & Structures **94** (2012), pp. 13–21.

[69] H. Paillère, C. Corre, and J. R. García Cascales, *On the extension of the AUSM$^+$ scheme to compressible two-fluid models*, Comput. & Fluids **32** (2003), pp. 891–916.

[70] C. Parés, *Numerical methods for non-conservative hyperbolic systems: A theoretical framework*, SIAM J. Numer. Anal. **44** (2006), pp. 300–321.

[71] L. Pareschi and G. Russo, *Implicit-explicit Runge-Kutta schemes and applications to hyperbolic systems with relaxation*, J. Sci. Comput. **25** (2005), pp. 129–155.

[72] H. Pokharna, M. Mori, and V. H. Ransom, *Regularization of two-phase flow models: A comparison of numerical and differential approaches*, Journal Of Computational Physics **134** (1997), pp. 282–295.

[73] A. Prosperetti and A. V. Jones, *The linear stability of general two-phase flow models ii*, Int. J. Multiphase Flow **13** (1987), pp. 161–171.

[74] V. H. Ransom and D. L. Hicks, *Hyperbolic two-pressure models for two-phase flow*, Journal of Computational Physics **53** (1984), pp. 124–151.

[75] V. H. Ransom *et. al.*, *RELAP5/MOD3 code manual, NUREG/CR-5535*, Idaho National Engineering Laboratory, ID, 1995.

[76] G. A. Reigstad and T. Flåtten, *An improved Roe solver for the drift-flux two-phase flow model*, 8^{th} International Conference on CFD in Oil & Gas, Metallurgical and Process Industries, SINTEF/NTNU, Trondheim NORWAY, 21-23 June (2011).

[77] P. L. Roe, *Approximate Riemann solvers, parameter vectors, and difference schemes*, Journal of Computational Physics **135** (1981), pp. 250–258.

[78] J. E. Romate, *An approximate Riemann solver for a two-phase flow model with numerically given slip relation*, Computers and Fluids **27** (1998), pp. 455–477.

[79] R. Saurel and A. Abgrall, *A multiphase godunov method for compressible multifluid and multiphase flows*, Journal of Computational Physics **150** (1999), pp. 425–467.

[80] R. Saurel, S. Gavrilyuk, and F. Renaud, *A multiphase model with internal degrees of freedom: application to shock–bubble interaction*, J. Fluid Mech **495** (2003), pp. 283–321.

[81] R. Saurel, F. Petitpas, and R. Abgrall, *Modelling phase transition in metastable liquids: application to cavitating and flashing flows*, J. Fluid Mech. **607** (2008), pp. 313–350.

[82] J. H. Song and M. Ishii, *The well-posedness of incompressible one-dimensional two-fluid model*, International Journal of Heat and Mass Transfer **43** (2000), pp. 2221–2231.

[83] J. H. Song and M. Ishii, *On the stability of a one-dimensional two-fluid model*, Nuclear Engineering and Design **204** (2001), pp. 101–115.

[84] H. Städtke, *Gasdynamic aspects of two-phase flow*, Wiley-VCH, 2006, ISBN 3-527-40578-X.

[85] H. B. Stewart and B. Wendroff, *Two-phase flow: Models and methods*, J. Comput. Phys. **56** (1984), pp. 363–409.

[86] J. H. Stuhmiller, *The influence of interfacial pressure forces on the character of two-phase flow model equations*, Int. J. Multiphas. Flow **3** (1977), pp. 551–560.

[87] E. Tadmor, *The numerical viscosity of entropy stable schemes for systems of conservation laws*, I. Math. Comp. **49** (1987), pp. 91–103.

[88] E. Tadmor, *Entropy stability theory for difference approximations of nonlinear conservation laws and related time-dependent problems*, Acta Numer. **12** (2003), pp. 451–512.

[89] V. A. Titarev and E. F. Toro, *MUSTA schemes for multi-dimensional hyperbolic systems: Analysis and improvements*, Int. J. Numer. Meth. Fluids **49** (2005), pp. 117–147.

[90] E. F. Toro, *Riemann solvers and numerical methods for fluid dynamics*, second edition ed., Springer-Verlag, Berlin, 1999, ISBN 3-540-65966-8.

[91] E. F. Toro, *MUSTA: A multi-stage numerical flux*, Appl. Numer. Math **56** (2006), pp. 1464–1479.

[92] E. F. Toro, M. Spruce, and W. Speares, *Restoration of the contact surface in the HLL-riemann solver*, Shock Waves **4** (1994), pp. 25–34.

[93] I. Toumi and A. Kumbaro, *An approximate linearized Riemann solver for a two-fluid model*, J. Comput. Phys **124** (1996), pp. 286–300.

[94] Q. H. Tran, M. Baudin, and F. Coquel, *A relaxation method via the Born-Infeld system*, Math. Mod. Meth. Appl. S. **19** (2009), pp. 1203–1240.

[95] K. Ueyama, *A study of two-fluid model equations*, J. Fluid Mech. **690** (2012), pp. 474–498.

[96] B. van Leer, *Towards the ultimate conservative difference scheme V. a second-order sequel to Godunovs method*, Journal Of Computational Physics **135** (1997), pp. 229–248.

[97] G.-S. Yeom and K.-S Chang, *Numerical simulation of two-fluid two-phase flows by HLL scheme using an approximate Jacobian matrix*, Numerical Heat Transfer, Part B **49** (2006), pp. 155–177.

[98] G.-S. Yeom and K.-S Chang, *Two-dimensional two-fluid two-phase flow simulation using an approximate Jacobian matrix for HLL scheme*, Numerical Heat Transfer, Part B **56** (2009), pp. 372–392.

[99] N. Zuber, *On the dispersed two-phase flow on the laminar flow regime*, Chem. Engrg. Sci. **19** (1964), p. 897.

[100] N. Zuber and J. A. Findlay, *Average volumetric concentration in two-phase flow systems*, J. Heat Transfer (1965), pp. 453–468.

A Numerical Resolution of CO2 Transport Dynamics

Alexandre Morin, Peder K. Aursand, Tore Flåtten and Svend T. Munkejord.
Proceedings of the SIAM Mathematics for industry '09 conference, San Francisco, CA, USA. 9–10 Oct. 2009.

Numerical Resolution of CO_2 Transport Dynamics

Alexandre Morin* Peder K. Aursand† Tore Flåtten† Svend T. Munkejord†

Abstract

We consider a hyperbolic system of conservation laws describing multicomponent flows through a transport pipeline, with applications to CO_2 transport and storage. We demonstrate that numerical dissipation easily leads to an underestimation of the amplitude of pressure pulses and the resulting pipe strain. We argue that recently developed high-resolution methods, particularly adapted to our current model, are essential tools for an accurate operations analysis.

1 Introduction

An important factor in carbon dioxide (CO_2) capture and storage (CCS) is the transport between the point of capture and the point of storage. A main focus of the newly established BIGCCS centre [2], a consortium consisting of international universities, research institutions and industry partners, is the development of coupled fluid-mechanical and thermodynamic models with material science models to simulate crack propagation in CO_2 pipelines.

Such pipe flow will take place at high pressures, where the CO_2 is in a supercritical (liquid-like) state. Due to failure, or planned maintenance, the pipe can be depressurized, leading to cooling. If the temperature becomes low enough, the pipe material may become brittle, causing a rupture and much damage. Therefore, for a proper pipeline design, it is necessary to be able to estimate the pipe cooling during depressurization.

This requires the formulation of adequate thermodynamic and fluid-mechanical models, and an accurate numerical solution of these models. Hence potential errors in the operations analysis may arise from two separate sources:

- *Modelling errors*, i.e. failure of the underlying mathematical models to correctly capture physical reality;
- *Numerical errors*, i.e. failure of the chosen numerical method to represent the correct solution of the mathematical problem to a satisfactory degree of accuracy.

The models of interest typically take the form of systems of hyperbolic partial differential equations [9]. It is well known in the scientific community that artificial diffusion, needed to stabilize the numerical solution, may lead to severe loss of accuracy [7].

With this paper, we wish to increase awareness towards the fact that even a highly accurate *mathematical* model may produce untrustworthy results if proper *numerical* methods are not employed for industrial simulations. To this end, we compare an *upwind high-resolution* scheme with a *central first-order* scheme, namely the MUSTA scheme previously investigated for the current model in [9].

Our upwind scheme will be based on the approximate Riemann solver of Roe [10], and high resolution will be obtained by the *wave-limiter* approach of LeVeque [7].

In order to construct our Roe scheme, we must overcome the difficulty that our thermodynamic state relations are generally highly complex. They may consist of a combination of analytical state equations, mixing rules, and tabular interpolations. For all practical purposes, we must be able to treat our interface to thermodynamics as a black box.

In situations like these, *fully numerical* Roe schemes are often applied [12]. However, for reasons of simplicity and efficiency, we wish to consider a more analytical strategy where the Roe matrix involves only *partially numerical* constructions. To this end, we will largely follow the approach of Abgrall [1], and use an idea suggested by Glaister [6] for incorporating a general pressure function into our Roe scheme.

Our paper is organized as follows: In Section 2, we describe the governing equations of our multicomponent model. In Section 2.1, we discuss in some detail the particular thermodynamic submodels chosen for the purposes of this paper. In Section 2.2.1, we analytically derive the velocities and composition of the various waves associated with the model.

In Section 3, we derive our Roe solver. In Section 3.2.2 we describe more precisely how we are able to

*Dept. of Energy and Process Engineering, Norwegian University of Science and Technology (NTNU), NO-7491 Trondheim, Norway

†SINTEF Energy Research, NO-7465 Trondheim, Norway.

Email: Alexandre.Morin@sintef.no, pederka@stud.ntnu.no, Tore.Flatten@sintef.no, Svend.T.Munkejord@sintef.no.

incorporate a general black-box pressure function into the scheme in a smooth manner.

In Section 4, we present some numerical simulations, where we compare our high-resolution Roe scheme to a MUSTA scheme. In Sections 4.1–4.2, we focus on a couple of *shock tube* problems in order to illustrate the behaviour of the schemes on the individual waves. In Section 4.3, we present a case more relevant for industrial applications, where we study the effect of depressurization of a pipe.

Finally, our work is summarized in Section 5.

2 The Model

We consider flows of N different chemical species (components) along a transport pipeline. The model we will be studying assumes that the flow variables are averaged over the pipe cross section. Hence spatial dependence is only along the x-axis, and we obtain a system of conservation laws in the form

$$\frac{\partial \boldsymbol{U}}{\partial t} + \frac{\partial \boldsymbol{F}(\boldsymbol{U})}{\partial x} = \boldsymbol{Q}(\boldsymbol{U}), \tag{2.1}$$

to be solved for the unknown vector $\boldsymbol{U}$. Here $\boldsymbol{U}$ is the vector of conserved variables, $\boldsymbol{F}$ is the vector of fluxes, and $\boldsymbol{Q}$ is the vector of sources.

Our model is similar to the one studied by Abgrall [1]. It consists of $N+2$ separate conservation equations; one for the masses of each component, as well as conservation equations for the total momentum and energy of the mixture. More precisely, we have

- *Conservation of mass:*

$$\frac{\partial m_i}{\partial t} + \frac{\partial}{\partial x}\left(m_i v\right) = 0 \quad \forall i \in \{1, \ldots, N\}, \tag{2.2}$$

- *Conservation of momentum:*

$$\frac{\partial \rho v}{\partial t} + \frac{\partial}{\partial x}\left(\rho v^2 + p\right) = Q_v, \tag{2.3}$$

- *Conservation of energy:*

$$\frac{\partial E}{\partial t} + \frac{\partial}{\partial x}\left(v(E+p)\right) = Q_e. \tag{2.4}$$

Herein, the nomenclature is as follows:

m_i	-	partial density of component i	$\mathrm{kg/m^3}$,
ρ	-	density of the mixture	$\mathrm{kg/m^3}$,
v	-	velocity of the mixture	m/s,
p	-	common pressure	Pa,
e_i	-	internal energy of component i	$\mathrm{m^2/s^2}$,
E	-	total energy of the mixture	$\mathrm{kg/(m{\cdot}s^2)}$,
Q_v	-	momentum source terms	$\mathrm{kg/(m^2{\cdot}s^2)}$,
Q_e	-	energy source terms	$\mathrm{kg/(m{\cdot}s^3)}$.

Furthermore, the following relations hold:

$$\rho = \sum_{i=1}^{N} m_i, \tag{2.5}$$

$$E = \frac{1}{2}\rho v^2 + \sum_{i=1}^{N} m_i e_i. \tag{2.6}$$

2.1 Thermodynamic Relations. An essential feature of the numerical methods presented in this paper is that they are straightforwardly applicable to an arbitrary thermodynamic description of the mixture, including the possibility of phase transitions for each component. Hence, we will generally assume only that the mixture is at all times in thermodynamic equilibrium, and that there exists state relations

$$p = p(\epsilon, m_1, \ldots, m_N), \tag{2.7}$$

$$T = T(\epsilon, m_2, \ldots, m_N) \tag{2.8}$$

for the pressure and temperature of the mixture. Herein,

$$\epsilon = \sum_{i=1}^{N} m_i e_i. \tag{2.9}$$

However, in order to present reproducible results, the thermodynamics used for the simulations of this paper will be based on two simplifying assumptions:

1. The components are assumed to be immiscible;
2. Each component follows a *stiffened gas* equation of state, as described by Menikoff [8].

Note that none of these simplifying assumptions are required to derive the numerical solver.

The assumption of immiscibility implies that each component follows separate pressure and temperature laws:

$$p = p(\rho_i, e_i) \quad \forall i, \tag{2.10}$$

$$T = T(\rho_i, e_i) \quad \forall i, \tag{2.11}$$

where ρ_i is the density of component i. The stiffened gas EOS is fully defined by its *Helmholtz free energy*:

$$A(\rho, T) = c_v T(1 - \ln(T/T_0) + (\gamma - 1)\ln(\rho/\rho_0)) - s_0 T + \frac{p_\infty}{\rho}, \tag{2.12}$$

where the parameters c_v, γ, p_∞, T_0, ρ_0 and s_0 are constants. From this we can derive the pressure law

$$p(\rho_i, e_i) = (\gamma_i - 1)\rho_i e_i - \gamma_i p_{\infty,i}, \tag{2.13}$$

as well as the temperature law

$$c_{v,i} T = e_i - \frac{p_{\infty.i}}{\rho_i} \tag{2.14}$$

for each component i.

2.2 Quasilinear Formulation. In this section, we rewrite the system (2.2)–(2.4) in *quasilinear* form:

$$\frac{\partial \boldsymbol{U}}{\partial t} + \boldsymbol{A}(\boldsymbol{U})\frac{\partial \boldsymbol{U}}{\partial x} = \boldsymbol{Q}(\boldsymbol{U}), \tag{2.15}$$

i.e. we obtain the matrix $\boldsymbol{A}$ given by

$$\boldsymbol{A}(\boldsymbol{U}) = \frac{\partial \boldsymbol{F}(\boldsymbol{U})}{\partial \boldsymbol{U}}. \tag{2.16}$$

This will form the basis for the derivation of our Roe scheme in Section 3.2. The derivation is a generalization of the results of Abgrall [1], who considered a system of ideal gases with phase transition. However, whereas Abgrall's construction assumes that the pressure is given by Dalton's law, our Roe scheme allows for a general pressure function as described in Section 3.2.

First, we will find it convenient to split the flux vector into convective and pressure terms as follows:

$$\boldsymbol{F}(\boldsymbol{U}) = \boldsymbol{F}_{\mathrm{c}}(\boldsymbol{U}) + \boldsymbol{F}_p(\boldsymbol{U}), \tag{2.17}$$

where

$$\boldsymbol{F}_{\mathrm{c}}(\boldsymbol{U}) = v\boldsymbol{U} \tag{2.18}$$

and

$$\boldsymbol{F}_p(\boldsymbol{U}) = \begin{bmatrix} 0 \\ 0 \\ \vdots \\ 0 \\ p \\ pv \end{bmatrix}, \qquad \boldsymbol{U} = \begin{bmatrix} m_1 \\ m_2 \\ \vdots \\ m_N \\ \rho v \\ E \end{bmatrix} = \begin{bmatrix} U_1 \\ U_2 \\ \vdots \\ U_N \\ U_{N+1} \\ U_{N+2} \end{bmatrix}. \tag{2.19}$$

Then we may write

$$\boldsymbol{A}(\boldsymbol{U}) = \boldsymbol{A}_{\mathrm{c}}(\boldsymbol{U}) + \boldsymbol{A}_p(\boldsymbol{U}), \tag{2.20}$$

where

$$\boldsymbol{A}_{\mathrm{c}}(\boldsymbol{U}) = \frac{\partial \boldsymbol{F}_{\mathrm{c}}(\boldsymbol{U})}{\partial \boldsymbol{U}} \qquad \text{and} \qquad \boldsymbol{A}_p(\boldsymbol{U}) = \frac{\partial \boldsymbol{F}_p(\boldsymbol{U})}{\partial \boldsymbol{U}}. \tag{2.21}$$

Proposition 1. *The convective Jacobian matrix* $\boldsymbol{A}_{\mathrm{c}}(\boldsymbol{U})$ *can be written as*

$$\boldsymbol{A}_{\mathrm{c}} = \begin{bmatrix} (1-Y_1)v & -Y_1 v & \dots & -Y_1 v & Y_1 & 0 \\ -Y_2 v & (1-Y_2)v & \dots & -Y_2 v & Y_2 & 0 \\ \vdots & \ddots & \ddots & \vdots & \vdots & \vdots \\ -Y_N v & -Y_N v & \dots & (1-Y_N)v & Y_N & 0 \\ -v^2 & -v^2 & \dots & -v^2 & 2v & 0 \\ -\mathcal{E}v & -\mathcal{E}v & \dots & -\mathcal{E}v & \mathcal{E} & v \end{bmatrix} \tag{2.22}$$

where

$$\mathcal{E} = \frac{E}{\rho} \tag{2.23}$$

and

$$Y_i = \frac{m_i}{\rho}. \tag{2.24}$$

Proof. From (2.18) we obtain

$$\mathrm{d}\boldsymbol{F}_{\mathrm{c}} = v\,\mathrm{d}\boldsymbol{U} + \boldsymbol{U}\,\mathrm{d}v, \tag{2.25}$$

which together with (2.5) and

$$\mathrm{d}v = \frac{1}{\rho}\left(\mathrm{d}(\rho v) - v\,\mathrm{d}\rho\right) \tag{2.26}$$

yields the result.

Proposition 2. *Define*

$$\mathcal{P}_i = \left(\frac{\partial p}{\partial m_i}\right)_{m_{j\neq i},\epsilon} \qquad i \in \{1,\dots,N\} \tag{2.27}$$

and

$$\mathcal{P}_\epsilon = \left(\frac{\partial p}{\partial \epsilon}\right)_{m_1,\dots,m_N} \tag{2.28}$$

so that (2.7) *can be written in differential form as*

$$\mathrm{d}p = \mathcal{P}_\epsilon\,\mathrm{d}\epsilon + \sum_{i=1}^{N} \mathcal{P}_i\,\mathrm{d}m_i. \tag{2.29}$$

Then the pressure Jacobian matrix $\boldsymbol{A}_p(\boldsymbol{U})$ *can be written as*

$$\boldsymbol{A}_p^{\mathrm{T}} = \begin{bmatrix} 0 & 0 & \dots & 0 & a_1 & v\left(a_1 - \frac{p}{\rho}\right) \\ 0 & 0 & \dots & 0 & a_2 & v\left(a_2 - \frac{p}{\rho}\right) \\ \vdots & \ddots & \ddots & \vdots & \vdots & \vdots \\ 0 & 0 & \dots & 0 & a_N & v\left(a_N - \frac{p}{\rho}\right) \\ 0 & 0 & \dots & 0 & -v\mathcal{P}_\epsilon & \frac{p}{\rho} - v^2\mathcal{P}_\epsilon \\ 0 & 0 & \dots & 0 & \mathcal{P}_\epsilon & v\mathcal{P}_\epsilon \end{bmatrix}, \tag{2.30}$$

where

$$a_i = \mathcal{P}_i + \frac{1}{2}v^2\mathcal{P}_\epsilon \quad \forall i \in \{1,\dots,N\}. \tag{2.31}$$

Proof. From (2.6) and (2.26) we can derive the differential

$$\mathrm{d}E = \mathrm{d}\epsilon - \frac{1}{2}v^2\sum_{i=1}^{N}\mathrm{d}m_i + v\,\mathrm{d}(\rho v), \tag{2.32}$$

by which we may rewrite (2.29) as

$$\mathrm{d}p = \sum_{i=1}^{N}\left(\mathcal{P}_i + \frac{1}{2}v^2\mathcal{P}_\epsilon\right)\mathrm{d}U_i - v\mathcal{P}_\epsilon\,\mathrm{d}U_{N+1} + \mathcal{P}_\epsilon\,\mathrm{d}U_{N+2}. \tag{2.33}$$

The result follows from (2.33) together with

$$\mathrm{d}(pv) = p\,\mathrm{d}v + v\,\mathrm{d}p. \tag{2.34}$$

2.2.1 Eigenstructure. In this section, we analytically derive the eigenstructure of the matrix

$$\boldsymbol{A} = \begin{bmatrix} A_{11} & A_{12} & \dots & A_{1,N+2} \\ A_{21} & A_{22} & \dots & A_{2,N+2} \\ \vdots & \vdots & \ddots & \vdots \\ A_{N+2,1} & A_{N+2,2} & \dots & A_{N+2,N+2} \end{bmatrix} \tag{2.35}$$

given by (2.20), (2.22) and (2.30).

PROPOSITION 3. *The velocity v is an eigenvalue of the matrix $\boldsymbol{A}$, and the dimension $\mathcal{D}_v$ of the corresponding eigenspace satisfies*

$$\mathcal{D}_v \geq N. \tag{2.36}$$

Proof. We look for eigenvectors satisfying

$$\boldsymbol{A}\boldsymbol{\omega} = v\boldsymbol{\omega}, \tag{2.37}$$

where

$$\boldsymbol{\omega} = \begin{bmatrix} \omega_1 \\ \omega_2 \\ \vdots \\ \omega_N \\ \omega_{N+1} \\ \omega_{N+2} \end{bmatrix}. \tag{2.38}$$

Now observe that the equations

$$\sum_{j=1}^{N+2} A_{ij}\omega_j = v\omega_i \tag{2.39}$$

reduce to

$$\omega_{N+1} = v\sum_{j=1}^{N} \omega_j \tag{2.40}$$

for all $i \in \{1, \dots, N\}$ and

$$\sum_{i=1}^{N} \mathcal{P}_i\omega_i - \frac{1}{2}v\mathcal{P}_\epsilon\omega_{N+1} + \mathcal{P}_\epsilon\omega_{N+2} = 0 \tag{2.41}$$

for $i \in \{N+1, N+2\}$. Hence there are at most 2 independent linear constraints on the elements of $\boldsymbol{\omega}$, and

$$\mathcal{D}_v \geq (N+2) - 2 = N. \tag{2.42}$$

PROPOSITION 4. *Assume that $\mathcal{P}_1, \dots, \mathcal{P}_N$ and $\mathcal{P}_\epsilon$ are all strictly positive. Then the eigenspace corresponding to the eigenvalue $\lambda = v$ is spanned by the basis vectors $\boldsymbol{\omega}^i$, where*

$$\omega_j^i = \begin{cases} \mathcal{P}_N & \text{if} \quad j = i, \\ -\mathcal{P}_i & \text{if} \quad j = N, \\ v\left(\mathcal{P}_N - \mathcal{P}_i\right) & \text{if} \quad j = N+1, \\ \frac{1}{2}v^2\left(\mathcal{P}_N - \mathcal{P}_i\right) & \text{if} \quad j = N+2, \\ 0 & \text{otherwise} \end{cases} \tag{2.43}$$

for $i \in \{1, \dots, N-1\}$ and

$$\omega_j^N = \begin{cases} \mathcal{P}_\epsilon & \text{if} \quad j = 1, \\ v\mathcal{P}_\epsilon & \text{if} \quad j = N+1, \\ \frac{1}{2}v^2\mathcal{P}_\epsilon - \mathcal{P}_1 & \text{if} \quad j = N+2, \\ 0 & \text{otherwise.} \end{cases} \tag{2.44}$$

Proof. Observe that when $\mathcal{P}_\epsilon$ is strictly positive, the constraints (2.40) and (2.41) are linearly independent, hence

$$\mathcal{D}_v = N. \tag{2.45}$$

Furthermore, note that the constraints (2.40)–(2.41) are satisfied, so (2.43) and (2.44) are in the eigenspace corresponding to $\lambda = v$.

Also, the $N-1$ vectors described by (2.43) are linearly independent since $\omega_j^j \neq 0$, $\omega_j^{i\neq j} = 0$ for all $j \in \{1, \dots, N\}$. Finally, (2.44) is linearly independent of the set (2.43), as all linear combinations of vectors in the form (2.43) satisfy

$$\forall i \in \{1, ..., N-1\} \quad \sum_{j=1}^{N} \mathcal{P}_j\omega_j^i = 0, \tag{2.46}$$

which is not satisfied by (2.44).

In conclusion, the N vectors described by (2.43)–(2.44) are linearly independent and reside in the N-dimensional eigenspace corresponding to $\lambda = v$. Hence they form a basis for this space.

PROPOSITION 5. *The matrix $\boldsymbol{A}$ has two eigenvalues given by*

$$\lambda = v \pm \tilde{c}, \tag{2.47}$$

where

$$\tilde{c} = \sqrt{\sum_{i=1}^{N} Y_i\mathcal{P}_i + \frac{\epsilon + p}{\rho}\mathcal{P}_\epsilon}. \tag{2.48}$$

Proof. We look for eigenvectors satisfying

$$\boldsymbol{A}\boldsymbol{\omega} = (v+s)\boldsymbol{\omega}, \tag{2.49}$$

where s is assumed to be non-zero. Now observe that the equations

$$\sum_{j=1}^{N+2} A_{ij}\omega_j = (v+s)\,\omega_i \tag{2.50}$$

may be simplified to yield the constraints

$$(v+s)\omega_j = Y_j\omega_{N+1} \quad \forall j \in \{1,\dots,N\}, \tag{2.51}$$

$$(v+s)\mathcal{P}_\epsilon\omega_{N+2} = \left(s^2 - \sum_{i=1}^{N}\mathcal{P}_i Y_i + v\left(s+\frac{1}{2}v\right)\right)\omega_{N+1}, \tag{2.52}$$

$$\left(\mathcal{P}_\epsilon\frac{\epsilon+p}{\rho} - s^2 + \sum_{i=1}^{N}\mathcal{P}_i Y_i\right)\omega_{N+1} = 0. \tag{2.53}$$

Furthermore, observe that (2.51)–(2.53) allow for non-trivial solutions if

$$s^2 = \sum_{i=1}^{N}\mathcal{P}_i Y_i + \frac{\epsilon+p}{\rho}\mathcal{P}_\epsilon, \tag{2.54}$$

or by (2.48):

$$s = \pm\tilde{c}. \tag{2.55}$$

PROPOSITION 6. *The eigenvectors corresponding to the eigenvalues $v \pm \tilde{c}$ can be expressed as*

$$\omega_j^{\pm} = \begin{cases} Y_j & \text{if} \quad j \le N \\ v \pm \tilde{c} & \text{if} \quad j = N+1 \\ \frac{\epsilon+p}{\rho} + \frac{1}{2}v^2 \pm v\tilde{c} & \text{if} \quad j = N+2. \end{cases} \tag{2.56}$$

Proof. The constraints (2.51)–(2.53) can be simplified by use of (2.55) to

$$(v \pm \tilde{c})\omega_j = Y_j\omega_{N+1}, \tag{2.57}$$

$$(v \pm \tilde{c})\omega_{N+2} = \left(\frac{\epsilon+p}{\rho} + \frac{1}{2}v^2 \pm v\tilde{c}\right)\omega_{N+1}, \tag{2.58}$$

which are satisfied by (2.56).

2.2.2 Primary variables. While the translation of the primary variables into the vector of conserved variables U is straightforward, the opposite direction is not. It involves the resolution of the system consisting of the definition of the conserved variables (U in equation (2.19)), two state equations per component (equations (2.13) and (2.14)) and the fact that the sum of the volume fractions is equal to one:

$$\sum_{i=1}^{N}\frac{U_i}{\rho_i} = 1. \tag{2.59}$$

First of all, the velocity is trivially found through

$$v = \frac{U_{N+1}}{\sum_{i=1}^{N}U_i}. \tag{2.60}$$

In order for the rest to be solved, it is reduced to a system of two equations. First, a relation between the density of the component $i = 2, N$ and that of the component 1 is:

$$\rho_i = \frac{\frac{\gamma_1-1}{\gamma_1}c_{p,1}}{\frac{\gamma_i-1}{\gamma_i}c_{p,i}}\rho_1 - \frac{p_{\infty,1}-p_{\infty,i}}{\frac{\gamma_i-1}{\gamma_i}c_{p,i}T}. \tag{2.61}$$

Then we can write

$$f_1 = \left(1 - \sum_{i=2}^{N}\frac{U_i}{\rho_i}\right)\rho_1 - U_1, \tag{2.62}$$

$$f_2 = \sum_{i=1}^{N}U_i\left(e_i + \frac{1}{2}v^2\right) - U_{N+2}. \tag{2.63}$$

This system can be solved for ρ_1 and T using a Newton algorithm. The remaining variables follow from (2.61) and the equations of state.

3 Numerical Methods

A rough classification of finite volume methods for hyperbolic conservation laws separates between *central methods*, which are straightforward yet diffusive, and *upwind methods*, which are more accurate but can be algebraically cumbersome. A central-type method, the *MUSTA* scheme introduced by Toro [13], was employed in [9] for our current model.

The purpose of this paper is to adapt the Riemann solver of Roe [10] to our particular application. Roe's solver is a convenient upwind method, as it requires only the solution of a *linear* Riemann problem at each cell interface; see [10] for details.

For a related model, a Roe scheme has already been proposed by Abgrall [1], and we will closely follow his approach. The modification presented here allows us to construct a Roe scheme for *arbitrary* equations of state, as described in more detail in Section 3.2.2.

3.1 The Roe Method. Roe's method relies upon the construction of a matrix $\hat{\boldsymbol{A}}$ satisfying the following properties:

R1: $\hat{\boldsymbol{A}}(\boldsymbol{U}^{\mathrm{L}},\boldsymbol{U}^{\mathrm{R}})(\boldsymbol{U}^{\mathrm{R}}-\boldsymbol{U}^{\mathrm{L}}) = \boldsymbol{F}(\boldsymbol{U}^{\mathrm{R}}) - \boldsymbol{F}(\boldsymbol{U}^{\mathrm{L}})$;

R2: $\hat{\boldsymbol{A}}(\boldsymbol{U}^{\mathrm{L}},\boldsymbol{U}^{\mathrm{R}})$ is diagonalizable with real eigenvalues;

R3: $\hat{\boldsymbol{A}}(\boldsymbol{U}^{\mathrm{L}},\boldsymbol{U}^{\mathrm{R}}) \to \frac{\partial \boldsymbol{F}}{\partial \boldsymbol{U}}$ smoothly as $\boldsymbol{U}^{\mathrm{L}},\boldsymbol{U}^{\mathrm{R}} \to \boldsymbol{U}$.

We now consider a computational grid with space index j and time index n, such that

$$x_j = x_0 + j\Delta x \tag{3.64}$$

and

$$t^n = t_0 + n\Delta t. \tag{3.65}$$

The Roe scheme can now be written in *flux-conservative* form:

$$\frac{\boldsymbol{U}_j^{n+1}-\boldsymbol{U}_j^n}{\Delta t}+\frac{\boldsymbol{F}_{j+1/2}-\boldsymbol{F}_{j-1/2}}{\Delta x}=\boldsymbol{Q}_j^n, \tag{3.66}$$

where the first-order numerical flux $\boldsymbol{F}_{j+1/2}$ is given by

$$\boldsymbol{F}_{j+1/2}=\frac{1}{2}\left(\boldsymbol{F}(\boldsymbol{U}_j^n)+\boldsymbol{F}(\boldsymbol{U}_{j+1}^n)\right)+\left|\hat{\boldsymbol{A}}\right|\left(\boldsymbol{U}_{j+1}^n-\boldsymbol{U}_j^n\right) \tag{3.67}$$

where the "absolute value" of the matrix $\hat{\boldsymbol{A}}$ is given by

$$\left|\hat{\boldsymbol{A}}\right|=\hat{\boldsymbol{R}}\left|\hat{\boldsymbol{\Lambda}}\right|\hat{\boldsymbol{R}}^{-1}, \tag{3.68}$$

with

$$\left|\hat{\boldsymbol{\Lambda}}\right|=\operatorname{diag}(|\lambda_1|,|\lambda_2|,\ldots,|\lambda_{N+2}|), \tag{3.69}$$

where λ_i are the eigenvalues of $\hat{\boldsymbol{A}}$, and $\hat{\boldsymbol{R}}$ is the matrix of eigenvectors that diagonalizes $\hat{\boldsymbol{A}}$.

3.1.1 High Resolution. There are several ways of obtaining high resolution in the numerical solution. By "high resolution" we here mean second-order accuracy in smooth portions of the solution, and no spurious oscillations. In this work, we employ the method of characteristic flux-limiting described in LeVeque [7, Chapter 15] because of its accuracy and efficiency. Herein, the numerical scheme is formulated as

$$\begin{aligned}\boldsymbol{U}_j^{n+1}=\boldsymbol{U}_j^n-\frac{\Delta t}{\Delta x}\Big(\mathcal{A}^-\Delta\boldsymbol{U}_{j+1/2}+\mathcal{A}^+\Delta\boldsymbol{U}_{j-1/2}\Big)\\ -\frac{\Delta t}{\Delta x}\Big(\tilde{\boldsymbol{F}}_{j+1/2}-\tilde{\boldsymbol{F}}_{j-1/2}\Big),\end{aligned} \tag{3.70}$$

where the symbol $\mathcal{A}^-\Delta\boldsymbol{U}_{j+1/2}$ denotes the net effect of all left-going waves at $x_{j+1/2}$, and $\mathcal{A}^+\Delta\boldsymbol{U}_{j-1/2}$ measures the net effect of all right-going waves at $x_{j-1/2}$. The second-order correction $\tilde{\boldsymbol{F}}_{j+1/2}$ is defined in the following.

For the Roe solver, we have the interpretation that

$$\mathcal{A}^\pm\Delta\boldsymbol{U}_{j+1/2}=\hat{\boldsymbol{A}}^\pm_{j+1/2}(\boldsymbol{U}_{j+1}-\boldsymbol{U}_j). \tag{3.71}$$

Herein,

$$\hat{\boldsymbol{A}}^\pm_{j+1/2}=\hat{\boldsymbol{R}}_{j+1/2}\hat{\boldsymbol{\Lambda}}^\pm_{j+1/2}\hat{\boldsymbol{R}}^{-1}_{j+1/2}, \tag{3.72}$$

where $\hat{\boldsymbol{R}}_{j+1/2}$ is the matrix having the right eigenvectors $\hat{\boldsymbol{r}}_{j+1/2}$ of $\hat{\boldsymbol{A}}_{j+1/2}$ as its columns, and $\hat{\boldsymbol{\Lambda}}^+_{j+1/2}$ and $\hat{\boldsymbol{\Lambda}}^-_{j+1/2}$ are the diagonal matrices containing the positive and negative eigenvalues, respectively, of $\hat{\boldsymbol{A}}_{j+1/2}$. Further, to satisfy the condition R1, we must have that

$$\hat{\boldsymbol{A}}_{j+1/2}(\boldsymbol{U}_{j+1}-\boldsymbol{U}_j)=\sum_{p=1}^{N+2}\lambda^p_{j+1/2}\mathcal{W}^p_{j+1/2}, \tag{3.73}$$

where $\mathcal{W}^p_{j+1/2}$ is the pth wave arising in the solution to the Riemann problem at $x_{j+1/2}$. The approximate Riemann solution consists of $N+2$ waves proportional to the right eigenvectors $\hat{\boldsymbol{r}}_{j+1/2}$, propagating with speeds equal to the eigenvalues, $\lambda^p_{j+1/2}$, of $\hat{\boldsymbol{A}}_{j+1/2}$. The proportionality coefficients $\beta^p_{j+1/2}$ can be found by solving the linear system

$$\boldsymbol{U}_{j+1}-\boldsymbol{U}_j=\sum_{p=1}^{N+2}\beta^p_{j+1/2}\hat{\boldsymbol{r}}^p_{j+1/2}, \tag{3.74}$$

and $\beta^p_{j+1/2}$ can be interpreted as wave strengths.

The flux vector $\tilde{\boldsymbol{F}}_{j+1/2}$ is the higher-order correction. It is given by

$$\tilde{\boldsymbol{F}}_{j+1/2}=\frac{1}{2}\sum_{p=1}^{N+2}\left|\lambda^p_{j+1/2}\right|\Big(1-\frac{\Delta t}{\Delta x}\left|\lambda^p_{j+1/2}\right|\Big)\widetilde{\mathcal{W}}^p_{j+1/2}, \tag{3.75}$$

where $\widetilde{\mathcal{W}}^p_{j+1/2}$ is a limited version of the wave $\mathcal{W}^p_{j+1/2}$. The limited waves $\widetilde{\mathcal{W}}^p_{j+1/2}$ are found by comparing the wave $\mathcal{W}^p_{j+1/2}$ with the upwind wave $\mathcal{W}^p_{J+1/2}$ [7, see Section 9.13], where

$$J=\begin{cases}j-1 & \text{if } \lambda^p_{j+1/2}\geq 0,\\ j+1 & \text{if } \lambda^p_{j+1/2}<0.\end{cases} \tag{3.76}$$

We write

$$\widetilde{\mathcal{W}}^p_{j+1/2}=\phi(\theta^p_{j+1/2})\mathcal{W}^p_{j+1/2}, \tag{3.77}$$

where ϕ is a flux-limiter function, and $\theta^p_{j+1/2}$ is a measure of the smoothness of the pth characteristic component of the solution:

$$\theta^p_{j+1/2}=\frac{\mathcal{W}^p_{J+1/2}\cdot\mathcal{W}^p_{j+1/2}}{\mathcal{W}^p_{j+1/2}\cdot\mathcal{W}^p_{j+1/2}}, \tag{3.78}$$

where $\cdot$ denotes the scalar product in $\mathbb{R}^{N+2}$.

In Section 4, we will employ the minmod limiter, see [11],

$$\phi(\theta)=\operatorname{minmod}(1,\theta), \tag{3.79}$$

where

$$\operatorname{minmod}(a,b)=\begin{cases}0 & \text{if } ab\leq 0,\\ a & \text{if } |a|<|b| \text{ and } ab>0,\\ b & \text{if } |a|\geq|b| \text{ and } ab>0,\end{cases} \tag{3.80}$$

the monotonized central-difference (MC) limiter [14],

$$\phi(\theta)=\max(0,\min((1+\theta)/2,2,2\theta)), \tag{3.81}$$

and the superbee limiter [11],

$$\phi(\theta)=\max(0,\min(1,2\theta),\min(2,\theta)), \tag{3.82}$$

(see also [7, Section 6.11]).

3.2 A Semi-Analytical Roe Matrix. In this section, we construct a Roe matrix in the so-called *quasi-Jacobian* form [4], following closely the approach of Abgrall [1]. We will take advantage of the flux splitting (2.17), and write the Roe matrix as

$$\hat{\boldsymbol{A}} = \hat{\boldsymbol{A}}_{\mathrm{c}} + \hat{\boldsymbol{A}}_{\mathrm{p}}. \tag{3.83}$$

PROPOSITION 7. *The convective Roe matrix given by* (3.84)

$$\hat{\boldsymbol{A}}_{\mathrm{c}} = \begin{bmatrix} (1-\hat{Y}_1)\hat{v} & -\hat{Y}_1\hat{v} & \dots & -\hat{Y}_1\hat{v} & \hat{Y}_1 & 0 \\ -\hat{Y}_2\hat{v} & (1-\hat{Y}_2)\hat{v} & \dots & -\hat{Y}_2\hat{v} & \hat{Y}_2 & 0 \\ \vdots & \ddots & \ddots & \vdots & \vdots & \vdots \\ -\hat{Y}_N\hat{v} & -\hat{Y}_N\hat{v} & \dots & (1-\hat{Y}_N)\hat{v} & \hat{Y}_N & 0 \\ -\hat{v}^2 & -\hat{v}^2 & \dots & -\hat{v}^2 & 2\hat{v} & 0 \\ -\hat{\mathcal{E}}\hat{v} & -\hat{\mathcal{E}}\hat{v} & \dots & -\hat{\mathcal{E}}\hat{v} & \hat{\mathcal{E}} & \hat{v} \end{bmatrix}$$

where

$$\hat{Y}_i = \frac{\sqrt{\rho_j}Y_{i,j} + \sqrt{\rho_{j+1}}Y_{i,j+1}}{\sqrt{\rho_j} + \sqrt{\rho_{j+1}}}, \tag{3.85}$$

$$\hat{v} = \frac{\sqrt{\rho_j}v_j + \sqrt{\rho_{j+1}}v_{j+1}}{\sqrt{\rho_j} + \sqrt{\rho_{j+1}}}, \tag{3.86}$$

$$\hat{\mathcal{E}} = \frac{\sqrt{\rho_j}\hat{\mathcal{E}}_j + \sqrt{\rho_{j+1}}\hat{\mathcal{E}}_{j+1}}{\sqrt{\rho_j} + \sqrt{\rho_{j+1}}}, \tag{3.87}$$

satisfies the Roe condition

$$\hat{\boldsymbol{A}}_{\mathrm{c},j+1/2}(\boldsymbol{U}_{j+1} - \boldsymbol{U}_j) = \boldsymbol{F}_{\mathrm{c}}(\boldsymbol{U}_{j+1}) - \boldsymbol{F}_{\mathrm{c}}(\boldsymbol{U}_j). \tag{3.88}$$

Proof. As described in [1, 3], this result can be derived using Roe's approach [10] with the parameter vector:

$$\boldsymbol{q} = \sqrt{\rho}\begin{bmatrix} Y_1 \\ \vdots \\ Y_N \\ v \\ \hat{\mathcal{E}} \end{bmatrix}. \tag{3.89}$$

3.2.1 The Pressure Roe Matrix. We write the Roe matrix $\hat{\boldsymbol{A}}_p$ as (3.90)

$$\hat{\boldsymbol{A}}_p^{\mathrm{T}} = \begin{bmatrix} 0 & 0 & \dots & 0 & \hat{a}_1 & \hat{v}\left(\hat{a}_1 - \widehat{\left[\frac{p}{\rho}\right]}\right) \\ 0 & 0 & \dots & 0 & \hat{a}_2 & \hat{v}\left(\hat{a}_2 - \widehat{\left[\frac{p}{\rho}\right]}\right) \\ \vdots & \ddots & \ddots & \vdots & \vdots & \vdots \\ 0 & 0 & \dots & 0 & \hat{a}_N & \hat{v}\left(\hat{a}_N - \widehat{\left[\frac{p}{\rho}\right]}\right) \\ 0 & 0 & \dots & 0 & -\hat{v}\hat{\mathcal{P}}_\epsilon & \widehat{\left[\frac{p}{\rho}\right]} - \hat{v}^2\hat{\mathcal{P}}_\epsilon \\ 0 & 0 & \dots & 0 & \hat{\mathcal{P}}_\epsilon & \hat{v}\hat{\mathcal{P}}_\epsilon \end{bmatrix},$$

where

$$\hat{a}_i = \hat{\mathcal{P}}_i + \frac{1}{2}\hat{v}^2\hat{\mathcal{P}}_\epsilon \quad \forall i \in \{1, \dots, N\}. \tag{3.91}$$

PROPOSITION 8. *The pressure Roe matrix given by* (3.90) *satisfies the Roe condition*

$$\hat{\boldsymbol{A}}_{p,j+1/2}(\boldsymbol{U}_{j+1} - \boldsymbol{U}_j) = \boldsymbol{F}_p(\boldsymbol{U}_{j+1}) - \boldsymbol{F}_p(\boldsymbol{U}_j), \tag{3.92}$$

provided that $\hat{v}$ *is given by* (3.86)*, and*

$$\widehat{\left[\frac{p}{\rho}\right]} = \frac{\sqrt{\rho_{j+1}}p_j + \sqrt{\rho_j}p_{j+1}}{\sqrt{\rho_{j+1}}\rho_j + \sqrt{\rho_j}\rho_{j+1}}, \tag{3.93}$$

and the subcondition

$$\hat{\mathcal{P}}_\epsilon(\epsilon_{j+1} - \epsilon_j) + \sum_{i=1}^{N}\hat{\mathcal{P}}_i(m_{i,j+1} - m_{i,j}) = p_{j+1} - p_j \tag{3.94}$$

is satisfied.

Proof. The result may be verified by substituting (2.19) and (3.90) with (3.86), (3.93) and (3.94) into (3.92).

3.2.2 The Roe-Averaged Pressure Derivative. We have now reduced the problem to finding a suitable Roe-type average of the form (3.94) for the pressure function $p(\epsilon, m_1, \dots, m_N)$. In general, these averages can be calculated analytically for any given case of an analytical pressure function $p(\epsilon, m_1, \dots, m_N)$.

However, as the purpose of this paper is to keep the method as general as possible, we will use an approach similar in spirit to the suggestion of Glaister [6]. In particular, our approach here is identical to the one used in [5] for a different model.

Following [5], we first introduce the symbol $\Delta_{(r)}$ given by

$$\begin{aligned}\Delta_{(r)}p(\boldsymbol{q}^{\mathrm{L}}, \boldsymbol{q}^{\mathrm{R}}) = {} & p(q_1^{\mathrm{R}}, \dots, q_r^{\mathrm{R}}, q_{r+1}^{\mathrm{L}}, \dots, q_M^{\mathrm{L}}) \\ & - p(q_1^{\mathrm{R}}, \dots, q_{r-1}^{\mathrm{R}}, q_r^{\mathrm{L}}, \dots, q_M^{\mathrm{L}}),\end{aligned} \tag{3.95}$$

where the $(M = N + 1)$-vector $\boldsymbol{q}$ is given by

$$\boldsymbol{q} = \begin{bmatrix} m_1 \\ \vdots \\ m_N \\ \epsilon \end{bmatrix}. \tag{3.96}$$

We then have that (3.97)

$$\hat{\mathcal{P}}_r = \begin{cases} \frac{\Delta_{(r)}p(\boldsymbol{q}^{\mathrm{L}}, \boldsymbol{q}^{\mathrm{R}})}{q_r^{\mathrm{R}} - q_r^{\mathrm{L}}} & \text{for } q_r^{\mathrm{L}} \neq q_r^{\mathrm{R}} \\ \frac{\partial p}{\partial q_r}(q_1^{\mathrm{R}}, \dots, q_{r-1}^{\mathrm{R}}, q_r^{\mathrm{L}}, \dots, q_M^{\mathrm{L}}) & \text{otherwise} \end{cases}$$

satisfies the condition (3.94) for all functions $p(m_1, \dots, m_N, \epsilon)$. Furthermore, the Roe condition

Table 1: EOS parameters employed in the present calculations.

	γ_i (–)	$p_{\infty,i}$ (MPa)	$c_{p,i}$ (kJ/(kg K))
carbon dioxide (1)	1.03	13.47	3.877
water (2)	2.85	833.02	4.155
methane (3)	1.23	10.94	2.930

Table 2: Initial state in the moving-discontinuity problem.

Quantity	Symbol (unit)	Left	Right
CO_2 vol. frac.	α_1 (–)	0.8	0.2
Water vol. frac.	α_2 (–)	0.2	0.8
Velocity	v (m/s)	10	10
Pressure	p (MPa)	10	10
Temperature	T (K)	310	310

R3 is also satisfied; see [5] for details. The condition R2 is satisfied provided the sound velocity $\tilde{c}$ is real, or equivalently that s as given by (2.54) satisfies

$$s^2 \geq 0. \tag{3.98}$$

Note in particular that this is the case if $\hat{\mathcal{P}}_1, \ldots, \hat{\mathcal{P}}_N$ and $\hat{\mathcal{P}}_\epsilon$ are all strictly positive. This assumption is also made in Proposition 4.

4 Numerical Simulations

In this section, the Roe scheme is tested with respect to stability, accuracy and robustness. Further, it is compared to an independent scheme, namely the MUSTA scheme described by Munkejord *et al.* [9].

The equation-of-state parameters have been adapted to carbon dioxide (component 1), water (component 2) and methane (component 3) at 10 MPa and 310 K, and are shown in Table 1.

4.1 Moving discontinuity. We consider a case which tests how the numerical method captures a moving discontinuity. Initially, all variables are uniform, except for a discontinuity in the volume fraction in the middle of the tube, see Table 2. Ideally, the numerical method should advect the volume-fraction discontinuity without smearing it.

Calculations have been performed with the Roe scheme and the two-stage two-cell MUSTA scheme using a CFL number of $r = 0.9$ on various grids. Figure 1 shows the CO_2 volume fraction at $t = 1.5$ s. Both numerical schemes behave well, without introducing spurious oscillations. However, the MUSTA scheme is more dissipative than the Roe scheme. In this case, the MUSTA scheme gives roughly the same solution on an 800-cell grid as that produced with the Roe scheme on a 100-cell grid.

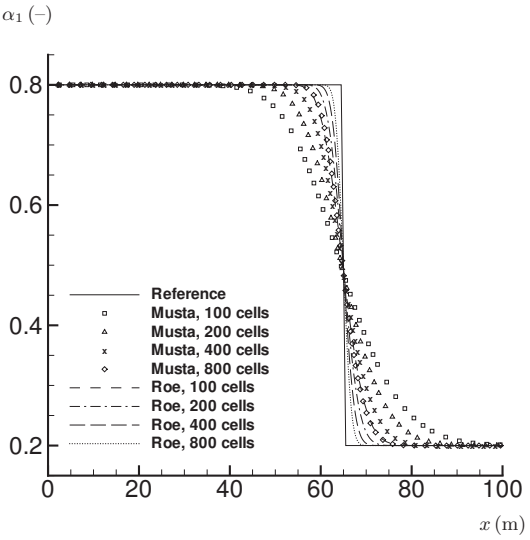

Figure 1: Moving-discontinuity problem. CO_2 volume fraction for the MUSTA and Roe schemes. $r = 0.9$.

Table 3: Initial state in the shock-tube problem.

Quantity	Symbol (unit)	Left	Right
CO_2 vol. frac.	α_1 (–)	0.9	0.9
Water vol. frac.	α_2 (–)	0.04	0.04
Methane vol. frac.	α_3 (–)	0.06	0.06
Velocity	v (m/s)	0	0
Pressure	p (MPa)	1.5	0.9
Temperature	T (K)	310	310

4.2 Shock Tube. The present test case is a Riemann problem set up to investigate basic consistency properties of the Roe scheme. The physical interpretation is a tube divided by a membrane in the middle. At $t = 0$, the membrane ruptures, and the flow starts evolving. The initial conditions are given in Table 3.

Calculations have been performed on various grids using a CFL number of $r = 0.9$. Figures **??**–3 display the physical variables at $t = 0.1$ s. The reference solution has been obtained using the two-stage two-cell MUSTA scheme on a fine grid of 20 000 cells. The figures show that the solution calculated using the Roe

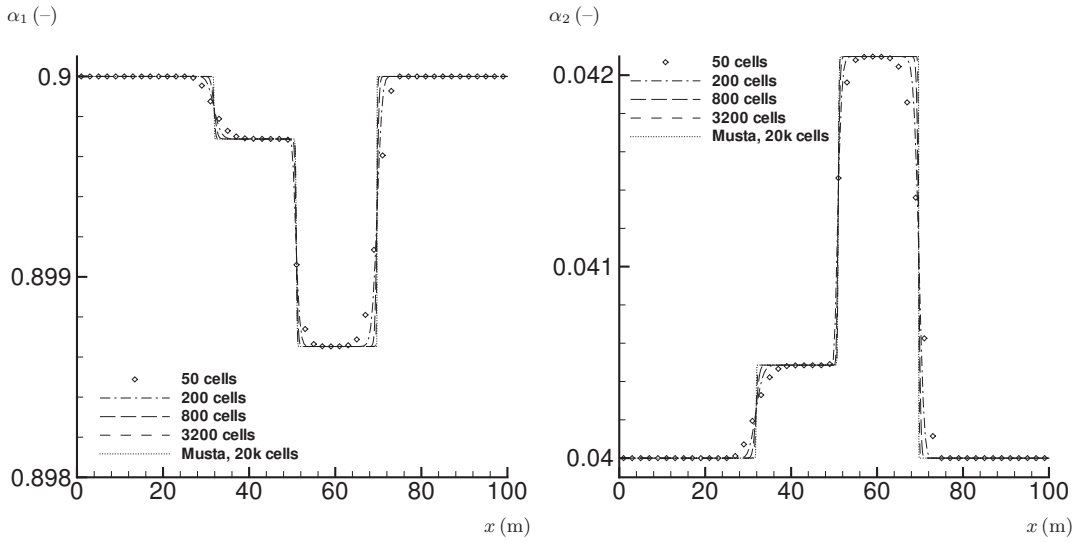

(a) Carbon dioxide volume fraction

(b) Water volume fraction

Figure 2: Shock-tube problem. Convergence of the Roe scheme, $r = 0.9$. Volume fractions.

scheme converges towards the reference solution without oscillations.

4.3 Depressurization Case. This test case is an example of a possible industrial application. It simulates the instantaneous depressurization of a tube at its right end, followed by a repressurization at the previous pressure. This creates a low-pressure wave propagating to the left. In this case where only liquids are involved, this is accompanied by a slight temperature decrease. However, things change for a system where phase change is allowed, which finds direct application in industry. The low-pressure wave would lead to an evaporation, and thus to a strong cooling. This cooling is of interest when one wishes to evaluate the mechanical properties of a metal pipe, for example. As the cooling is sensitive to the amplitude of the pressure wave, it becomes critically important to numerically reproduce such waves correctly.

The case consists of a 1000 m long pipe filled with an initially motionless mixture at 10 MPa and 300 K. The mixture is composed of carbon dioxide, water and methane with initial volume fractions respectively being 0.9, 0.09 and 0.01. The component properties used are shown in Table 1. At $t = 0$ s, the pressure is instantaneously decreased to 1 MPa, and set back to 10 MPa at $t = 2$ s. The boundary conditions used are designed to respect the information propagation. This model includes five conservation equations, therefore five independent quantities are advected in waves. Two of those are mass fractions waves, one is the mixture entropy wave and two are sound waves. Depending on their propagation direction, they will either be created or disappear at the boundary. In this case, where the velocity is always positive or zero, four of the waves leave the domain at the right; the last one - the left-going sound wave - enters it. Consequently, the last cell at the right of the domain is copied into a ghost boundary cell. The required pressure is then set in this boundary cell at constant mass fractions and mixture entropy.

Figures 4–5 show the result of calculations that have been performed on a grid of 100 cells, except the reference solution which uses 1000 cells. The pressure is recorded at a position of 450 m from the right, over 6.5 s.

Several methods have been compared to evaluate their ability to preserve the amplitude of the low-pressure wave. Figure 4 shows the results for the MUSTA method and the Roe method without limiters, which are both first order. The three curves are almost superimposed and a significant smoothing of the pressure wave can be seen. The Roe method is then made second order by adding flux limiters.

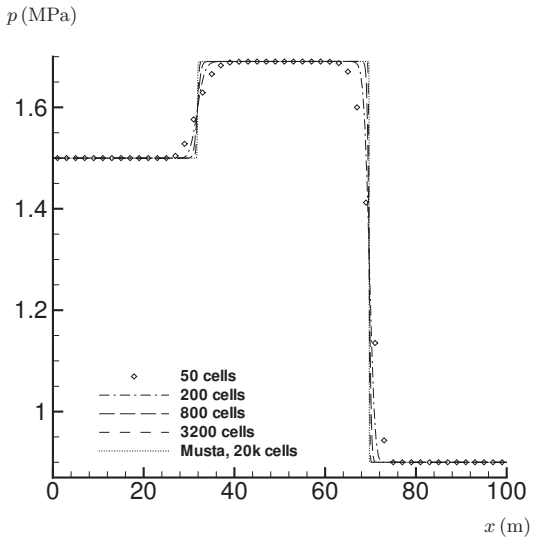

(a) Pressure

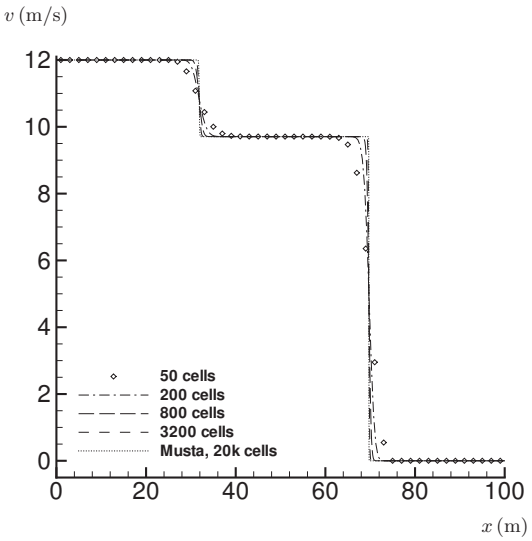

(b) Velocity

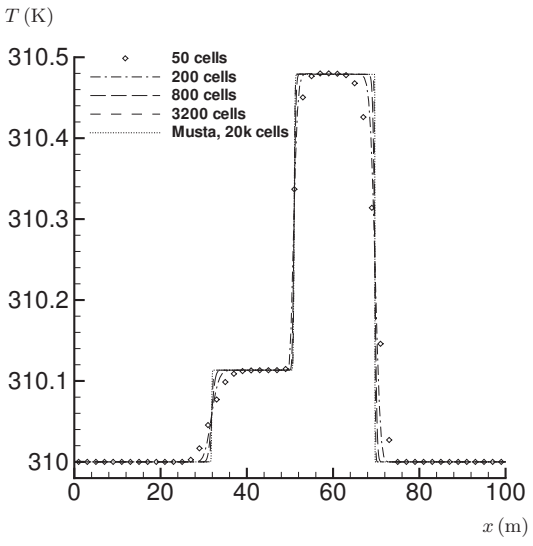

(e) Temperature

Figure 3: Shock-tube problem. Convergence of the Roe scheme, $r = 0.9$. Pressure, velocity and temperature.

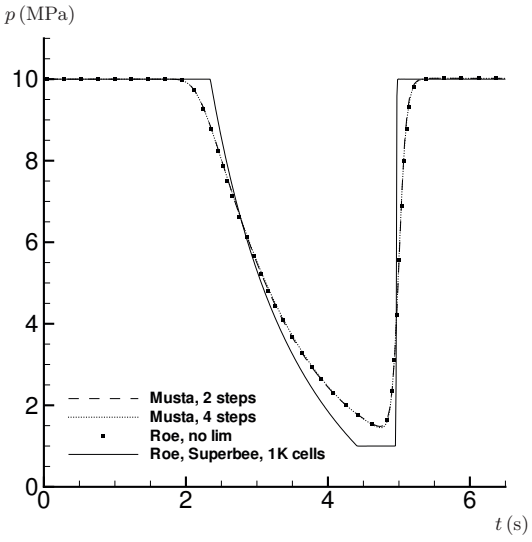

Figure 4: Depressurization case. Pressure as a function of time at $x = 450\,\mathrm{m}$. Comparison of the first-order Musta and Roe methods. 100 cells, $r = 0.9$.

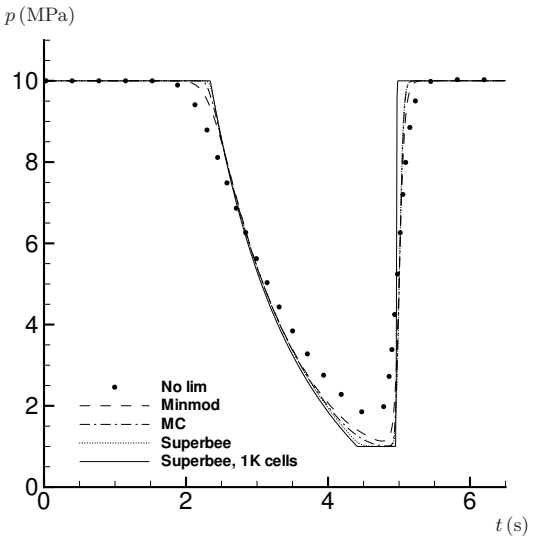

(a) Different flux limiters, $r = 0.5$.

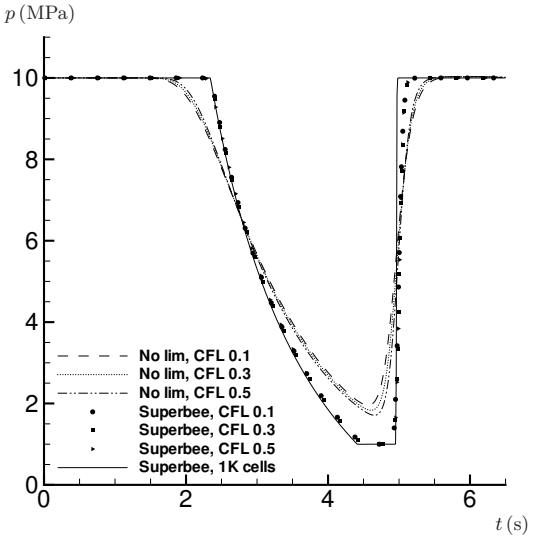

(b) Effect of varying CFL number with and without flux limiters.

Figure 5: Depressurization case. Pressure as a function of time at $x = 450\,\mathrm{m}$. Roe method, 100 cells.

In Figure 5(a), the results for three different flux limiters (minmod, monotonized central-difference (MC) and superbee) are compared to the version without limiters (No lim). MC performs quite well, but the best in this case is superbee. Here, the shape of the pressure wave is well conserved. Finally, the influence of the CFL number, r, deserves discussion. It may have a significant effect on the numerical viscosity. Since only a global limit can be imposed, the actual local CFL number can be very different along the computational domain. Therefore, methods maintaining accuracy for low CFL numbers are needed. Figure 5(b) shows that the flux limiters added to the Roe scheme, here superbee, make it basically insensitive to the CFL number, while the first-order scheme becomes more diffusive as the CFL number decreases.

Additionally, a grid refinement test has been performed on the Roe method with superbee limiter (Figure 6). It shows that already with 100 cells, the shock resolution is quite sharp.

5 Summary

We have presented a formulation of the approximate Riemann solver of Roe for a multicomponent flow model, allowing for a general formulation of the thermodynamic closure relations. We have incorporated high resolution (second order accuracy for smooth solutions)

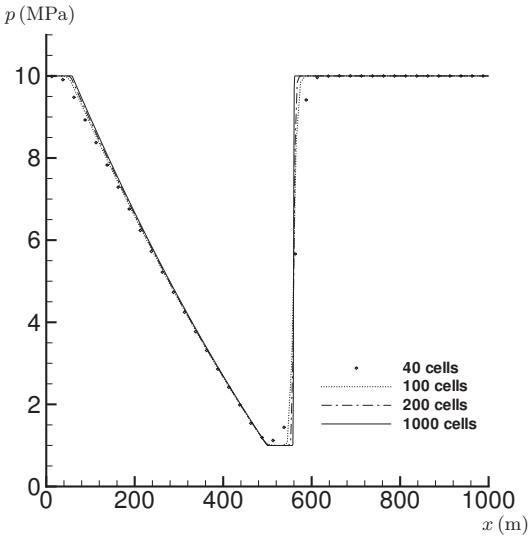

Figure 6: Depressurization case. Pressure as a function of position at $t = 4.9\,\mathrm{s}$. Grid refinement for the Roe method with superbee limiter, $r = 0.5$.

by means of the *wave limiter* approach. Our solver is relatively efficient, as an analytical formulation of its eigenstructure is available.

By numerical simulations, we have compared our solver to a more straightforward first-order central scheme. The results clearly show that numerical dissipation, which introduces a significant amount of error for the first-order scheme, may be satisfactorily controlled with our high-resolution Roe solver.

In particular, we have presented a case representing the effect of depressurization of a pipe relevant for the industry. Using a computational grid that would be representative for industrial simulations, we have seen that the central scheme underestimates the maximum amplitude of a pressure pulse by as much as 9.5 percent, whereas the high-resolution Roe scheme is able to capture the pulse with a high degree of accuracy.

Hence, we conclude that a proper choice of a numerical method plays an integral part in industrial operations analysis and simulation.

Acknowledgements

The first author has received a PhD grant from the BIGCCS Centre [2] and the work of the remaining authors was financed through the CO_2 Dynamics project. The authors acknowledge the support from the Research Council of Norway, Aker Solutions, ConocoPhilips Skandinavia AS, Det Norske Veritas AS, Gassco AS, Hydro Aluminium AS, Shell Technology AS, Statkraft Development AS, StatoilHydro Petroleum AS, TOTAL E&P Norge AS and Vattenfall Research and Development AB.

References

[1] R. Abgrall, *An extension of Roe's upwind scheme to algebraic equilibrium real gas models*, Comput. Fluids 19 (1991), pp. 171–182.

[2] BIGCCS, *International CCS Research Centre*, `http://www.sintef.no/Projectweb/BIGCCS/`

[3] D. Chargy, R. Abgrall, L. Fezoui and B. Larrouturou, *Comparisons of several upwind schemes for multi-component one-dimensional inviscid flows*, Rapports de Recherche N° 1253, INRIA, France, 1990.

[4] P. Cinnella, *Roe-type schemes for dense gas flow computations*, Comput. Fluids 35 (2006), pp. 1264–1281.

[5] T. Flåtten and S. T. Munkejord, *The approximate Riemann solver of Roe applied to a drift-flux two-phase flow model*, ESAIM-Math. Model. Num., 40 (2006), pp. 735–764.

[6] P. Glaister, *An approximate linearized Riemann solver for the Euler equations for real gases*, J. Comput. Phys. 74 (1988), pp. 382–408.

[7] R. J. LeVeque, *Finite Volume Methods for Hyperbolic Problems*, Cambridge University Press, Cambridge, UK, 2002.

[8] R. Menikoff, *Empirical EOS for solids*, in Shock Wave Science and Technology Reference Library, Volume 2 - Solids I, Springer Berlin Heidelberg New York, 2007, pp. 143–188.

[9] S. T. Munkejord, J. P. Jakobsen, A. Austegard and M. J. Mølnvik, *Thermo- and fluid-dynamical modeling of two-phase multi-component carbon dioxide mixtures*, Energy Procedia, 1 (2009), pp. 1649–1656.

[10] P. L. Roe, *Approximate Riemann solvers, parameter vectors, and difference schemes*, J. Comput. Phys., 43 (1981), pp. 357–372.

[11] P. L. Roe, *Some contributions to the modeling of discontinuous flows*, Lect. Appl. Math., 22 (1985), pp. 163–193.

[12] J. E. Romate, *An approximate Riemann solver for a two-phase flow model with numerically given slip relation*, Comput. Fluids, 27 (1998), pp. 455–477.

[13] E. F. Toro, *MUSTA: A multi-stage numerical flux*, Appl. Numer. Math., 56 (2006), pp. 1464–1479.

[14] B. van Leer, *Towards the ultimate conservative difference scheme IV. New approach to numerical convection,* J. Comput. Phys., 23 (1977), pp. 276-299.

B On Solutions to Equilibrium Problems for Systems of Stiffened Gases

Tore Flåtten, Alexandre Morin and Svend T. Munkejord.
SIAM Journal on Applied Mathematics, Volume 71, No. 1, pp. 41-67, 2011.

SIAM J. APPL. MATH.
Vol. 71, No. 1, pp. 41–67
© 2011 Society for Industrial and Applied Mathematics

ON SOLUTIONS TO EQUILIBRIUM PROBLEMS FOR SYSTEMS OF STIFFENED GASES*

TORE FLÅTTEN†, ALEXANDRE MORIN‡, AND SVEND TOLLAK MUNKEJORD†§

Abstract. We consider an isolated system of N immiscible fluids, each following a stiffened-gas equation of state. We consider the problem of calculating equilibrium states from the conserved fluid-mechanical properties, i.e., the partial densities and internal energies. We consider two cases; in each case mechanical equilibrium is assumed, but the fluids may or may not be in thermal equilibrium. For both cases, we address the issues of existence, uniqueness, and physical validity of equilibrium solutions. We derive necessary and sufficient conditions for physically valid solutions to exist, and prove that such solutions are unique. We show that for both cases, physically valid solutions can be expressed as the root of a monotonic function in one variable. We then formulate efficient algorithms which unconditionally guarantee global and quadratic convergence toward the physically valid solution.

Key words. stiffened gas, existence, uniqueness

AMS subject classifications. 76T30, 26C15

DOI. 10.1137/100784321

1. Introduction. Due to its simplicity and suitability for fluid-mechanical applications, the stiffened-gas equation of state advocated by Menikoff [7] and Menikoff and Plohr [8] has found widespread use in the computational fluid dynamics community [4, 6, 17]. In particular, many authors consider it a useful basis for simulating multicomponent flow problems [1, 3, 11, 12, 14, 16]. This observation motivates our current work.

For a given fluid, the stiffened-gas equation of state can be written as a pressure law:

$$p(\rho, e) = (\gamma - 1)\rho(e - e_*) - \gamma p_\infty, \tag{1}$$

where p is the pressure, ρ is the density, and e is the specific internal energy of the fluid. The parameters γ, e_*, and p_∞ are constants specific to the fluid. Herein, e_* defines the zero point for the internal energy and becomes relevant when phase transitions are involved. The parameter p_∞ leads to the "stiffened" properties compared to ideal gases; a large value of p_∞ implies near-incompressible behavior. Note in particular that for $p_\infty = 0$ an ideal-gas law is recovered.

In this paper, we consider N immiscible fluids, each governed by the stiffened-gas law (1) while sharing a common volume V. Now let M_i be the total mass of fluid i

*Received by the editors January 28, 2010; accepted for publication (in revised form) October 18, 2010; published electronically January 4, 2011. This work was financed through the CO_2 Dynamics project, and was supported by the Research Council of Norway (189978, 193816), Aker Solutions, ConocoPhilips Skandinavia AS, Det Norske Veritas AS, Gassco AS, GDF SUEZ E&P Norge AS, Hydro Aluminium AS, Shell Technology AS, Statkraft Development AS, Statoil Petroleum AS, TOTAL E&P Norge AS, and Vattenfall AB.

http://www.siam.org/journals/siap/71-1/78432.html

†SINTEF Energy Research, Sem Sælands vei 11, NO-7465 Trondheim, Norway (Tore.Flatten@sintef.no, stm@pvv.org).

‡Department of Energy and Process Engineering, Norwegian University of Science and Technology (NTNU), NO-7491 Trondheim, Norway (Alexandre.Morin@sintef.no). This author's work was supported by a Ph.D. grant from the BIGCCS Centre.

§Corresponding author.

Copyright © by SIAM. Unauthorized reproduction of this article is prohibited.

in the volume V. We may then define *partial densities* m_i as

$$m_i = \frac{M_i}{V}. \tag{2}$$

Furthermore, let V_i be the total volume occupied by the fluid i, defined by

$$V_i = \frac{M_i}{\rho_i}, \tag{3}$$

where ρ_i is the density of fluid i. We may then define the *volume fractions* α_i as

$$\alpha_i = \frac{V_i}{V}, \tag{4}$$

where consistency requires that

$$\sum_{i=1}^{N} \alpha_i = 1. \tag{5}$$

From (2)–(4) it now follows that the partial densities can be written as

$$m_i = \rho_i \alpha_i. \tag{6}$$

Furthermore, each fluid has a partial internal energy density E_i given by

$$E_i = m_i e_i, \tag{7}$$

and the total internal energy density in the volume V is

$$E = \sum_{i=1}^{N} E_i. \tag{8}$$

Fluid-mechanical models are typically expressed as partial differential equations representing conservation or balance laws. The solution vector obtained from these equations will typically provide us with the partial densities (6) and energies (7) or (8). From this information, our task is to calculate the proper physical equilibrium states.

In this paper, we will consider two cases, summarized as follows.

PROBLEM 1. *The partial densities* (6) *are known for each of the N fluids. The internal energies* (7) *are also known for each of the N fluids. In addition, we assume that the fluids are in mechanical equilibrium; they all have the same pressure. Our task is to calculate the pressure p and the temperatures T_i for each fluid as well as the volume fractions α_i.*

This problem is more precisely defined in section 3.

PROBLEM 2. *The partial densities* (6) *are known for each of the N fluids. The total internal energy* (8) *is known for the mixture. In addition, we assume that the fluids are in mechanical* and *thermal equilibrium; they all have the same pressure and temperature. Our task is to calculate the pressure p, the common temperature T, as well as the volume fractions α_i.*

This problem is more precisely defined in section 4.

These problems have been encountered and solved by many authors [2, 3, 9, 10, 13, 15], although the number of fluids has often been limited to $N = 2$. Our current paper is motivated by the observation that a complete discussion of the question of

Copyright © by SIAM. Unauthorized reproduction of this article is prohibited.

existence, uniqueness, and physical validity of solutions to such general equilibrium problems for N fluids seems so far to be lacking in the literature.

A main result of this paper is a proof that, for any system of stiffened gases, if physically valid (in a sense that will be made precise) solutions to the equilibrium Problems 1 and 2 exist, they are unique. This should not be surprising; in many cases, existence and uniqueness can be established directly by thermodynamic stability theory if the equilibrium solution corresponds to the minimum of some free energy for the system. One may then apply convexity arguments as described, for instance, in [5].

However, in this paper we are also interested in obtaining *explicit* conditions for physically valid solutions to exist, as well as practical algorithms for obtaining these solutions. Toward this aim, a simple constructive approach will turn out to be fruitful. A main idea behind our approach is the observation that, although the problems are highly nonlinear, the stiffened-gas equation of state is in itself sufficiently linear to allow the volume fractions to be expressed without an explicit temperature dependence. This has been done in (42) and (79); see below.

This strategy allows for reducing Problems 1 and 2 to finding the root of a monotonic function in one variable, for which existence and uniqueness follow directly from elementary arguments. Robust and efficient numerical solvers can also be rather straightforwardly constructed.

Our paper is organized as follows. In section 2, we review the stiffened-gas equation of state as presented by Menikoff and Plohr [7, 8]. In section 3, we address equilibrium Problem 1; here equal pressures are assumed, but the fluids have independent temperatures. A key equation is (42), which allows us to directly construct a monotonic function whose root is our required solution.

In section 4 we address the case where both mechanical and thermal equilibrium are assumed; this is Problem 2 described above. Here we use (79) for the construction of our monotonic function, which in this case requires an additional mathematical transformation detailed in section 4.1.1. For both problems, we derive sufficient and necessary conditions for physically valid solutions to exist, and uniqueness follows from monotonicity.

In section 5, we take advantage of some well-established properties of the Newton–Raphson method. In particular, we show how our problems may be formulated to yield numerical solution algorithms which unconditionally guarantee global and quadratic convergence.

In section 6, we present numerical examples to verify and illustrate the results derived in section 5. Finally, we briefly summarize our results in section 7.

2. The stiffened-gas equation of state. In this section, we briefly review some properties of the *stiffened-gas* equation of state considered in this paper. We refer to the work of Menikoff and Plohr [8] for a more in-depth discussion, particularly regarding the physical basis for this model.

For a given fluid, the stiffened-gas equation of state is fully defined by the *Helmholtz free energy* [7]:

$$A(\rho, T) = c_V T \left(1 - \ln\left(\frac{T}{T_0}\right) + (\gamma - 1)\ln\left(\frac{\rho}{\rho_0}\right)\right) - s_0 T + \frac{p_\infty}{\rho} + e_*, \tag{9}$$

where the parameters c_V, γ, p_∞, T_0, ρ_0, s_0, and e_* are constants specific to the fluid. Here e_* is used to define the zero point of energy, which becomes relevant when phase transitions are involved. Although phase transitions will not be considered in this

Copyright © by SIAM. Unauthorized reproduction of this article is prohibited.

paper, we include this parameter for completeness.

2.1. Entropy. From (9) we can derive the entropy

$$s(\rho,T) = -\left(\frac{\partial A}{\partial T}\right)_\rho = c_V \ln\left(\frac{T}{T_0}\left(\frac{\rho_0}{\rho}\right)^{\gamma-1}\right) + s_0. \tag{10}$$

Note that

$$s_0 = s(\rho_0, T_0). \tag{11}$$

Hence the stiffened-gas equation of state can be interpreted as a *local linearization* near the state (ρ_0, T_0), where the entropy is s_0.

2.2. Heat capacity. The intensive internal energy is given by

$$e(\rho,T) = A + Ts = c_V T + \frac{p_\infty}{\rho} + e_*, \tag{12}$$

from which we immediately see that c_V is the *specific isochoric heat capacity*:

$$c_V = \left(\frac{\partial e}{\partial T}\right)_\rho. \tag{13}$$

2.3. Pressure. The pressure is obtained by

$$p(\rho,T) = \rho^2\left(\frac{\partial A}{\partial \rho}\right)_T = \rho(\gamma-1)c_V T - p_\infty. \tag{14}$$

By (12), this can be written as the pressure law (1):

$$p(\rho,e) = (\gamma-1)\rho(e-e_*) - \gamma p_\infty, \tag{15}$$

and we also obtain the energy in terms of pressure and temperature:

$$e(p,T) = c_V T\frac{p+\gamma p_\infty}{p+p_\infty} + e_*. \tag{16}$$

Note that positive densities and energies do not generally guarantee positivity of the pressure.

2.4. Ratio of specific heats. Substituting (14) into (10), we obtain

$$s(p,T) = \gamma c_V \ln\left(\frac{T}{T_0}\left(\frac{p_0+p_\infty}{p+p_\infty}\right)^{1-1/\gamma}\right) + s_0, \tag{17}$$

where

$$p_0 = p(\rho_0, T_0). \tag{18}$$

Now

$$c_p = T\left(\frac{\partial s}{\partial T}\right)_p = \gamma c_V; \tag{19}$$

hence γ is the *ratio of specific heats*

$$\gamma = \frac{c_p}{c_V}, \tag{20}$$

and it follows that c_p is constant.

Copyright © by SIAM. Unauthorized reproduction of this article is prohibited.

2.5. Sound velocity. Now if we introduce the constant

$$K = \frac{e^{s_0/c_p}}{T_0} \left(p_0 + p_\infty\right)^{1-1/\gamma}, \tag{21}$$

we can write (17) more conveniently as

$$s(p,T) = c_p \ln\left(KT\left(p + p_\infty\right)^{1/\gamma - 1}\right). \tag{22}$$

Then from (14) we get the relation

$$s(p,\rho) = c_p \ln\left(K\frac{(p+p_\infty)^{1/\gamma}}{\rho(\gamma-1)c_V}\right). \tag{23}$$

Hence

$$\mathrm{d}s = \frac{c_p}{\gamma(p+p_\infty)}\,\mathrm{d}p - \frac{c_p}{\rho}\,\mathrm{d}\rho \tag{24}$$

and

$$c^2 = \left(\frac{\partial p}{\partial \rho}\right)_s = \gamma\frac{p+p_\infty}{\rho}. \tag{25}$$

Hence p_∞ can be interpreted as a parameter that "stiffens" an ideal gas by increasing its sound velocity.

We further note that from (12) and (14) we get a simple expression for the specific enthalpy:

$$h = e + \frac{p}{\rho} = c_p T + e_*. \tag{26}$$

From this and (15), expression (25) can be written as

$$c^2 = (\gamma - 1)c_p T. \tag{27}$$

2.6. Physical considerations. We note that the various parameters of the stiffened-gas equation of state cannot be chosen freely if physically correct thermodynamic behavior is to be reproduced. Throughout this paper, we will consistently make the assumption that the parameters satisfy the following standard restrictions, which follow from thermodynamic stability theory.

RESTRICTION 1. *We require*

$$c_V > 0 \tag{28}$$

and

$$\gamma > 1 \tag{29}$$

for the stiffened-gas equation of state to be physically valid.

Copyright © by SIAM. Unauthorized reproduction of this article is prohibited.

3. Mechanical equilibrium. In this section, we consider a mixture of N fluids, each following its separate stiffened-gas equation of state (9). We assume that the fluids are immiscible, in the sense that the equation of state is not affected by the mixing. We here assume that the fluids reach instantaneous mechanical equilibrium, but heat transfer is dynamically modelled. Hence the fluids possess individual temperatures.

For each fluid $i \in \{1, \dots, N\}$, the following information is known to us:

- The partial densities $m_i = \rho_i \alpha_i$.
- The internal energies $E_i = m_i e_i$.

Herein, the densities are given by (14),

$$\rho_i = \frac{p + p_{\infty,i}}{(\gamma_i - 1) c_{V,i} T_i} \quad \forall i, \tag{30}$$

the volume fractions are given by (4), and the internal energies are given by (12),

$$e_i = c_{V,i} T_i + \frac{p_{\infty,i}}{\rho_i} + e_{*,i}. \tag{31}$$

Definition 1 (Problem 1). *Given the information above, our task is to calculate the common pressure p, the temperatures T_i, and the volume fractions α_i.*

Such a problem is considered, for instance, in [3, 10, 13]. We now define the following classes of solutions.

Definition 2. *A* valid *solution to Problem* 1 *is a solution that satisfies*

$$\alpha_i \in (0, 1] \quad \forall i \tag{32}$$

and

$$\sum_{i=1}^{N} \alpha_i = 1. \tag{33}$$

A physically valid *solution to Problem* 1 *is a valid solution that satisfies*

$$0 < \rho_i < \infty, \tag{34}$$

$$0 < T_i < \infty, \tag{35}$$

$$e_{*,i} < e_i < \infty \tag{36}$$

for all i.

A strictly valid *solution to Problem* 1 *is a physically valid solution that satisfies*

$$p > 0. \tag{37}$$

Note that, by Definition 2, nonpositive partial densities (6) cannot yield physically valid solutions. Hence we have the following.

Restriction 2. *Physically valid solutions require*

$$m_i > 0 \quad \forall i. \tag{38}$$

With (36), this immediately yields the following additional restriction.

Restriction 3. *Physically valid solutions require*

$$E_i - m_i e_{*,i} = m_i (e_i - e_{*,i}) > 0 \quad \forall i. \tag{39}$$

Copyright © by SIAM. Unauthorized reproduction of this article is prohibited.

Furthermore, we make the following observation.

LEMMA 1. *Any physically valid solution must satisfy*

$$p \in \mathcal{P}_1, \quad \textit{where} \quad \mathcal{P}_1 = \left(-\min_i p_{\infty,i}, +\infty\right). \tag{40}$$

Proof. The lemma follows directly from Restriction 1 and from (34) applied to (30). ∎

REMARK 1. *Note that if*

$$\min_i p_{\infty,i} \geq 0, \tag{41}$$

then it follows from Restriction 1*, Lemma* 1*, and* (16) *that the condition* (36) *is superfluous; it follows directly from* (34)*.*

3.1. Mathematical formulation of the problem. Multiplying (15) with α_i and using (6)–(7), we obtain

$$\alpha_i = \frac{(\gamma_i - 1)(E_i - m_i e_{*,i})}{p + \gamma_i p_{\infty,i}}, \tag{42}$$

from which we immediately obtain the following.

LEMMA 2. *Any physically valid solution must satisfy*

$$p \in \left(-\min_i (\gamma_i p_{\infty,i}), +\infty\right). \tag{43}$$

Proof. In order for (32) to be satisfied by (42), it follows from Restrictions 1 and 3 that we must have

$$p + \gamma_i p_{\infty,i} > 0 \qquad \forall i, \tag{44}$$

which is equivalent to (43). ∎

An equation for the pressure is now found by imposing the condition that the volume fractions (42) must sum to 1. In other words, if we consider the function

$$f(\hat{p}) = \sum_{i=1}^{N} \frac{(\gamma_i - 1)(E_i - m_i e_{*,i})}{\hat{p} + \gamma_i p_{\infty,i}}, \tag{45}$$

the required pressure p must satisfy

$$f(p) = 1. \tag{46}$$

LEMMA 3. *The equation*

$$f(\hat{p}) = 1 \tag{47}$$

has a unique solution for $\hat{p}$ *satisfying*

$$\hat{p} \in \mathcal{P}_2, \quad \textit{where} \quad \mathcal{P}_2 = \left(-\min_i (\gamma_i p_{\infty,i}), +\infty\right). \tag{48}$$

Proof. We note that $f(\hat{p})$ is a rational function without poles in the interval $\mathcal{P}_2$. Hence $f(\hat{p})$ is C^∞-smooth in this interval, and its first derivative is

$$\frac{\mathrm{d}f}{\mathrm{d}\hat{p}} = -\sum_{i=1}^{N} \frac{(\gamma_i - 1)(E_i - m_i e_{*,i})}{(\hat{p} + \gamma_i p_{\infty,i})^2}. \tag{49}$$

Copyright © by SIAM. Unauthorized reproduction of this article is prohibited.

From (29) and Restriction 3 it follows that $f'(\hat{p}) < 0$ throughout the interval $\mathcal{P}_2$. Furthermore, note that $f(\hat{p}) \to +\infty$ as $\hat{p} \to -\min_i (\gamma_i p_{\infty,i})^+$. Also,

$$\lim_{\hat{p}\to+\infty} f(\hat{p}) = 0. \tag{50}$$

Uniqueness and existence of the solution to (47) in the interval $\mathcal{P}_2$ follow. ∎

We now know that $f(\hat{p}) = 1$ has a unique solution in the interval $\mathcal{P}_2$. However, Lemma 1 tells us that the solution must also lie in the interval $\mathcal{P}_1$ for the solution to be physically valid. This is trivially satisfied if

$$\min_i p_{\infty,i} \leq 0. \tag{51}$$

Otherwise, we observe that $f(\hat{p})$ is monotonically decreasing in the interval $\mathcal{P}_1$. We must then have

$$\lim_{\hat{p}\to-\min_i p^+_{\infty,i}} f(\hat{p}) > 1 \tag{52}$$

for a physically valid solution to exist. Together with (45), this yields the following restriction.

RESTRICTION 4. *Physically valid solutions require either*

$$\min_i p_{\infty,i} \leq 0 \tag{53}$$

or

$$\sum_{i=1}^{N} \frac{(\gamma_i - 1)(E_i - m_i e_{*,i})}{\gamma_i p_{\infty,i} - \min_j p_{\infty,j}} > 1. \tag{54}$$

To recapitulate, we have the following claim.

LEMMA 4. *If Problem* 1 *has a physically valid solution in the sense of Definition* 2*, then E_i and m_i satisfy Restrictions* 2–4.

Proof. From (6), (32), and (34) it follows that Restriction 2 is satisfied. Restriction 3 follows from (36) and Restriction 2. By Lemmas 1 and 2, it follows from the monotonicity of f that Restriction 4 is satisfied. ∎

Furthermore, the converse also holds, as given next.

LEMMA 5. *Problem* 1 *has a physically valid solution in the sense of Definition* 2 *if E_i and m_i satisfy Restrictions* 2–4.

Proof. Lemma 3 guarantees the existence of a solution satisfying (33). Furthermore, from (42), Lemma 2, and Restrictions 1 and 3 it follows that (32) is satisfied. Hence the solution is valid.

Given that (32) is satisfied, it follows from Restriction 2 and (6) that (34) is satisfied. Furthermore, Restriction 4 guarantees that (40) is satisfied. Given that (34) is satisfied, it now follows from (30) that (35) is satisfied. Finally, from (16), Restriction 1, and Lemmas 1–2 it follows that (36) is satisfied. Hence the solution is physically valid. ∎

We are now in position to conclude the following.

PROPOSITION 1. *Problem* 1 *has a physically valid solution in the sense of Definition* 2 *if and only if E_i and m_i satisfy Restrictions* 2–4. *This solution is unique.*

Proof. By Lemmas 4 and 5, all that remains is to prove uniqueness. Uniqueness of the pressure follows directly from Lemma 3. Then the volume fractions are uniquely determined by (42). Multiply (31) by m_i to obtain

$$E_i = m_i c_{V,i} T_i + \alpha_i p_{\infty,i} + m_i e_{*,i}, \tag{55}$$

and it follows that T_i is uniquely determined for all i. ∎

Copyright © by SIAM. Unauthorized reproduction of this article is prohibited.

3.2. Positivity of the pressure. We note that Definition 2 of physically valid solutions allows for negative pressures. This is consistent with the view that a *stiffened* gas is obtained by shifting the zero point of pressure for an *ideal* gas. In particular, all derived thermodynamic quantities are well defined as long as $p + p_{\infty,i}$ remains positive; see, for instance, (17) and (30).

Hence there is no immediate reason to discard negative-pressure solutions as unphysical. However, one may easily envisage situations in which positivity of the pressure must be enforced, for instance if the stiffened gas mixture is to be used in conjunction with other models. We now observe the following.

RESTRICTION 5. *A physically valid solution to Problem* 1 *is a strictly valid solution in the sense of Definition* 2 *if and only if one of the following requirements is satisfied: either*

$$\min_i p_{\infty,i} \leq 0 \tag{56}$$

or

$$\sum_{i=1}^{N} \frac{E_i - m_i e_{*,i}}{p_{\infty,i}} \frac{\gamma_i - 1}{\gamma_i} > 1. \tag{57}$$

Proof. If (56) holds, it follows from Lemma 1 that any physically valid solution is also a strictly valid solution. Otherwise, since $f(\hat{p})$ as given by (45) is a strictly decreasing function for $\hat{p} > 0$, it follows that a positive solution to (47) requires

$$f(0) > 1. \tag{58}$$

This is precisely the condition (57). Conversely, if the solution satisfies $p \leq 0$, then $f(0) \leq 1$. ∎

Furthermore, we may make a more precise statement, as follows.

PROPOSITION 2. *Problem* 1 *has a strictly valid solution in the sense of Definition* 2 *if and only if* E_i *and* m_i *satisfy Restrictions* 2–3 *as well as Restriction* 5. *This solution is unique.*

Proof. Note that by (29) and Restriction 3, the following inequality holds whenever $\min_i p_{\infty,i} > 0$:

$$\sum_{i=1}^{N} \frac{(\gamma_i - 1)(E_i - m_i e_{*,i})}{\gamma_i p_{\infty,i} - \min_j p_{\infty,j}} > \sum_{i=1}^{N} \frac{E_i - m_i e_{*,i}}{p_{\infty,i}} \frac{\gamma_i - 1}{\gamma_i}. \tag{59}$$

Hence Restriction 5 implies Restriction 4. The result now follows from Proposition 1 and Restriction 5. ∎

4. Thermal and mechanical equilibrium. In this section, we consider a modified problem where the additional assumption is made that the fluids are in thermal equilibrium. We again consider a mixture of N immiscible fluids, each following its separate stiffened-gas equation of state (9).

For each fluid $i \in \{1, \ldots, N\}$, the following information is known to us:

- The partial densities $m_i = \rho_i \alpha_i$.
- The total energy density of the mixture $E = \sum_{i=1}^{N} m_i e_i$.

Herein, the densities are given by (14),

$$\rho_i = \frac{p + p_{\infty,i}}{(\gamma_i - 1) c_{V,i} T} \quad \forall i, \tag{60}$$

Copyright © by SIAM. Unauthorized reproduction of this article is prohibited.

and the internal energies are given by (12),

$$e_i = c_{V,i}T + \frac{p_{\infty,i}}{\rho_i} + e_{*,i}. \tag{61}$$

Definition 3 (Problem 2). *Given the information above, our task is to calculate the common pressure p, the common temperature T, and the volume fractions α_i.*

This problem is considered in [2, 9]. Analogously to section 3, we define a hierarchy of classes of solutions below.

Definition 4. *A* valid *solution to Problem* 2 *is a solution that satisfies*

$$\alpha_i \in (0, 1] \quad \forall i \tag{62}$$

and

$$\sum_{i=1}^{N} \alpha_i = 1. \tag{63}$$

A physically valid *solution to Problem* 2 *is a valid solution that satisfies*

$$0 < \rho_i < \infty \quad \forall i, \tag{64}$$

$$0 < T < \infty. \tag{65}$$

A positive-energy *solution to Problem* 2 *is a physically valid solution that satisfies*

$$e_{*,i} < e_i < \infty \quad \forall i. \tag{66}$$

A strictly valid *solution to Problem* 2 *is a physically valid solution that satisfies*

$$p > 0. \tag{67}$$

Remark 2. *Compared to Problem* 1*, here we have chosen to split physically valid solutions into two classes, where positive energies may or may not be imposed. This is done with the aim of completeness, as the separate analysis of these two cases allows for the option of relaxing the requirement* (66)*.*

As in section 3, the following restriction follows from (6).

Restriction 6. *Physically valid solutions require*

$$m_i > 0 \quad \forall i. \tag{68}$$

Remark 3. *Note that in the limit when a component vanishes, i.e.,*

$$\exists j \in \{1, \ldots, N\} : m_j = 0, \tag{69}$$

our analysis can still be applied with a minor modification. Assume that K of the N components satisfy

$$m_j = 0 \quad \forall j \in \{1, \ldots, K\}, \tag{70}$$

where $K < N$. It then follows from (6) *and* (64) *that*

$$\alpha_j = 0 \quad \forall j \in \{1, \ldots, K\}. \tag{71}$$

Copyright © by SIAM. Unauthorized reproduction of this article is prohibited.

We may then replace the problem with an equivalent problem consisting of $M = N-K$ *components, where the volume fractions satisfy*

$$\alpha_r \in (0,1] \quad \forall r \in \{K+1,\dots,N\} \tag{72}$$

and

$$\sum_{r=K+1}^{N} \alpha_r = 1. \tag{73}$$

We may now apply our results to this reduced problem. This consideration is equally valid for Problem 1*, with the understanding that the temperatures* T_j *would then be undefined for the vanishing components.*

Furthermore, as it did for Problem 1, the following result holds.

LEMMA 6. *Any physically valid solution must satisfy*

$$p \in \mathcal{P}_1, \quad \textit{where} \quad \mathcal{P}_1 = \left(-\min_i p_{\infty,i}, +\infty\right). \tag{74}$$

Proof. The lemma follows directly from Restriction 1 and Definition 4 applied to (60). ∎

4.1. Mathematical formulation of the problem. Multiplying (26) with m_i, we obtain

$$\alpha_i \left(\rho_i(e_i - e_{*,i}) + p\right) = m_i c_{p,i} T. \tag{75}$$

Also, (15) can be written as

$$\rho_i(e_i - e_{*,i}) + p = \frac{\gamma_i}{\gamma_i - 1}\left(p + p_{\infty,i}\right); \tag{76}$$

hence

$$\alpha_i \frac{\gamma_i}{\gamma_i - 1}\left(p + p_{\infty,i}\right) = m_i c_{p,i} T. \tag{77}$$

Furthermore, summing (75) over all i yields

$$E + p - \sum_{i=1}^{N} m_i e_{*,i} = T \sum_{i=1}^{N} m_i c_{p,i}. \tag{78}$$

Substituting for T in (77), we obtain

$$\alpha_i = \frac{\gamma_i - 1}{\gamma_i} \frac{m_i c_{p,i}}{\sum_{j=1}^{N} m_j c_{p,j}} \frac{E + p - \sum_{j=1}^{N} m_j e_{*,j}}{p + p_{\infty,i}}. \tag{79}$$

As in section 3, an equation for the pressure is found by imposing the condition that the volume fractions (79) must sum to 1. We introduce the function

$$g(\hat{p}) = \sum_{i=1}^{N} \frac{\gamma_i - 1}{\gamma_i} \frac{m_i c_{p,i}}{\sum_{j=1}^{N} m_j c_{p,j}} \frac{E + \hat{p} - \sum_{j=1}^{N} m_j e_{*,j}}{\hat{p} + p_{\infty,i}}, \tag{80}$$

where the required pressure p must satisfy

$$g(p) = 1. \tag{81}$$

Copyright © by SIAM. Unauthorized reproduction of this article is prohibited.

4.1.1. A simplifying notation. Now note that if we introduce the variables

$$A_i = \frac{\gamma_i - 1}{\gamma_i} \frac{m_i c_{p,i}}{\sum_{j=1}^{N} m_j c_{p,j}}, \tag{82}$$

$$z = E + \hat{p} - \sum_{i=1}^{N} m_i e_{*,i}, \tag{83}$$

$$q_i = p_{\infty,i} - E + \sum_{i=1}^{N} m_i e_{*,i}, \tag{84}$$

then g can be written in the form

$$g(\hat{p}(z)) = \sum_{i=1}^{N} A_i \frac{z}{z + q_i}. \tag{85}$$

We consider now the function

$$\varphi(z(\hat{p})) = g(\hat{p}) - 1 = \sum_{i=1}^{N} A_i \frac{z}{z + q_i} - 1, \tag{86}$$

subject to the constraints

$$A_i \geq 0 \quad \forall i, \tag{87}$$

$$\sum_{i=1}^{N} A_i < 1, \tag{88}$$

$$z \in \mathcal{Z} = \left(-\min_i q_i, +\infty \right), \tag{89}$$

which follow from Restriction 1, Restriction 6, and Lemma 6.

Below, we will derive some results concerning solutions to (81), expressed in the form

$$\varphi(z) = 0. \tag{90}$$

We start by making the observation that

$$\frac{\mathrm{d}\varphi}{\mathrm{d}z} = \sum_{i=1}^{N} A_i \frac{q_i}{(z + q_i)^2}. \tag{91}$$

LEMMA 7. *If*

$$\min_i q_i \geq 0, \tag{92}$$

the equation

$$\varphi(z) = 0 \tag{93}$$

has no solution in the interval $\mathcal{Z}$.

Copyright © by SIAM. Unauthorized reproduction of this article is prohibited.

Proof. We first note that $\varphi(z)$ is a rational function without poles in $\mathcal{Z}$. Hence φ is C^∞-smooth in the interval $\mathcal{Z}$. We further note that from (87), (91), and (92) it follows that

$$\frac{\mathrm{d}\varphi}{\mathrm{d}z} \geq 0 \tag{94}$$

in this interval. Hence

$$\sup_{z\in\mathcal{Z}} \varphi(z) = \lim_{z\to\infty} \varphi(z) = \sum_{i=1}^{N} A_i - 1 < 0, \tag{95}$$

so no solution can exist. ∎

We now consider the case

$$\min_i q_i < 0. \tag{96}$$

Under this condition, $\varphi'(z)$ as given by (91) does not have a definite sign. However, a simple transformation on φ will give us a monotonic function, as stated below.

LEMMA 8. *The function* $\Phi(z)$ *given by*

$$\Phi : z \mapsto z\varphi(z) \tag{97}$$

is monotonicly decreasing in the interval $\mathcal{Z}$.

Proof. We first note that $\Phi(z)$, being the product of two C^∞-smooth functions, is itself C^∞-smooth in $\mathcal{Z}$. Now

$$\frac{\mathrm{d}\Phi}{\mathrm{d}z} = \varphi(z) + z\frac{\mathrm{d}\varphi}{\mathrm{d}z} = \sum_{i=1}^{N} A_i - 1 - \sum_{i=1}^{N} A_i \left(\frac{q_i}{z+q_i}\right)^2 < 0, \tag{98}$$

where we have used (87) and (88). ∎

PROPOSITION 3. *The equation*

$$\varphi(z) = 0 \tag{99}$$

has a solution in the interval $\mathcal{Z}$ *if and only if*

$$\min_i q_i < 0. \tag{100}$$

This solution is unique.

Proof. Assume first that the condition (100) is satisfied. Then all $z \in \mathcal{Z}$ satisfy $z > 0$, and $\Phi(z) = 0$ if and only if $\varphi(z) = 0$. Now

$$\lim_{z\to -\min_i q_i^+} \Phi(z) = +\infty \tag{101}$$

and

$$\lim_{z\to\infty} \Phi(z) = -\infty, \tag{102}$$

and we have already established that $\Phi(z)$ is monotonicly decreasing in $\mathcal{Z}$. Hence, by smoothness, $\Phi(z) = 0$ has precisely one solution in $\mathcal{Z}$ when (100) is satisfied. Lemma 7 completes the proof. ∎

Copyright © by SIAM. Unauthorized reproduction of this article is prohibited.

We have now established sufficient results to formulate our main conclusions. First, we note that from Lemma 7 and (84) we may conclude the following.

RESTRICTION 7. *Physically valid solutions require*

$$E - \sum_{j=1}^{N} m_j e_{*,j} > \min_i p_{\infty,i}. \tag{103}$$

This leads us toward the following proposition.

PROPOSITION 4. *Problem* 2 *has a physically valid solution in the sense of Definition* 4 *if and only if* E *and* m_i *satisfy Restrictions* 6–7. *This solution is unique.*

Proof. We have shown that if a physically valid solution exists, then Restrictions 6–7 are satisfied. Assume now that Restrictions 6–7 are satisfied. Then, from (29) and (82), it follows that (87) is satisfied. Furthermore, from (29) it also follows that (88) is satisfied. Hence it follows from Proposition 3 that (90) has a unique solution in the interval $\mathcal{P}_1$.

It remains to show that this solution is physically valid, and that the full physical state is uniquely determined. Now (81) gives us directly that (63) is satisfied. Furthermore, from (29), (68), (74), (79), and (103) it follows that (62) is satisfied and that all α_i are uniquely determined. From (68), (74), (78), and (103) it follows that (65) is satisfied and that T is uniquely determined.

Finally, from (28), (29), (60), (65), and (74) it follows that (64) is satisfied and that ρ_i is uniquely determined for all i. ∎

4.2. Positivity of the internal energies. In this section, we wish to derive conditions under which physically valid solutions are also positive-energy solutions.

PROPOSITION 5. *A physically valid solution to Problem* 2 *is a positive-energy solution if and only if one of the following requirements is satisfied: either*

$$\min_i p_{\infty,i} \geq 0 \tag{104}$$

or

$$\left(E - \min_j (\gamma_j p_{\infty,j}) - \sum_{j=1}^{N} m_j e_{*,j}\right) \sum_{i=1}^{N} \frac{\gamma_i - 1}{\gamma_i} \frac{m_i c_{p,i}}{p_{\infty,i} - \min_j (\gamma_j p_{\infty,j})} > \sum_{i=1}^{N} m_i c_{p,i}. \tag{105}$$

Proof. From (16), Restriction 1, and Lemma 6, it follows that a necessary and sufficient condition for a physically valid solution to be a positive-energy solution is

$$p \in \left(-\min_i (\gamma_i p_{\infty,i}), +\infty\right), \tag{106}$$

which follows directly from Lemma 6 if (104) holds.

Otherwise, write $g(\hat{p}) = 1$ as

$$\Phi(z(\hat{p})) = z\left(\sum_{i=1}^{N} A_i \frac{z}{z + q_i} - 1\right) = 0. \tag{107}$$

Lemma 8 tells us that $\Phi(z)$ is a strictly decreasing function in the interval $\mathcal{Z}$, corresponding to

$$\hat{p} \in \left(-\min_i p_{\infty,i}, +\infty\right). \tag{108}$$

Copyright © by SIAM. Unauthorized reproduction of this article is prohibited.

Since we now have from (83) that

$$\frac{\mathrm{d}z}{\mathrm{d}\hat{p}} \equiv 1, \tag{109}$$

it follows that a positive-energy solution to (107) requires

$$\Phi\left(z|\hat{p} = -\min_i\left(\gamma_i p_{\infty,i}\right)\right) = \Phi\left(E - \min_i\left(\gamma_i p_{\infty,i}\right) - \sum_{i=1}^{N} m_i e_{*,i}\right) > 0. \tag{110}$$

This is precisely the condition (105). Conversely, if the solution does not satisfy (106), then

$$\Phi\left(E - \min_i\left(\gamma_i p_{\infty,i}\right) - \sum_{i=1}^{N} m_i e_{*,i}\right) \leq 0. \qquad \square \tag{111}$$

4.3. Positivity of the pressure. Just as in section 3, our definition of physically valid solutions is sufficiently weak to allow for a negative pressure. We now consider the stronger constraint that the pressure must remain positive.

RESTRICTION 8. *A physically valid solution to Problem* 2 *is a strictly valid solution in the sense of Definition* 4 *if and only if one of the following requirements is satisfied: either*

$$\min_i p_{\infty,i} \leq 0 \tag{112}$$

or

$$\left(E - \sum_{j=1}^{N} m_j e_{*,j}\right) \sum_{i=1}^{N} \frac{\gamma_i - 1}{\gamma_i} \frac{m_i c_{p,i}}{p_{\infty,i}} > \sum_{i=1}^{N} m_i c_{p,i}. \tag{113}$$

Proof. If (112) holds, it follows from Lemma 6 that any physically valid solution is also a strictly valid solution. Otherwise, write $g(\hat{p}) = 1$ as (107). It then follows from a line of reasoning completely similar to the proof of Proposition 5 that a positive pressure solution to (107) requires

$$\Phi(z|\hat{p} = 0) = \Phi\left(E - \sum_{i=1}^{N} m_i e_{*,i}\right) > 0. \tag{114}$$

This is precisely the condition (113). Conversely, if the solution satisfies $p \leq 0$, then $\Phi(E - \sum_{i=1}^{N} m_i e_{*,i}) \leq 0$. $\square$

This result may be incorporated with Proposition 4 to yield a more compact characterization of strictly valid solutions, as follows.

PROPOSITION 6. *Problem* 2 *has a strictly valid solution in the sense of Definition* 4 *if and only if* E_i *and* m_i *satisfy Restrictions* 6–8. *This solution is unique.*

Proof. The result follows directly from Proposition 4 and Restriction 8. $\square$

COROLLARY 1. *Problem* 2 *has a strictly valid, positive-energy solution in the sense of Definition* 4 *if and only if* E_i *and* m_i *satisfy Restrictions* 6–7, *and in addition one of the following is satisfied:*

1.

$$\min_i p_{\infty,i} > 0 \tag{115}$$

Copyright © by SIAM. Unauthorized reproduction of this article is prohibited.

and

$$\left(E - \sum_{j=1}^{N} m_j e_{*,j}\right) \sum_{i=1}^{N} \frac{\gamma_i - 1}{\gamma_i} \frac{m_i c_{p,i}}{p_{\infty,i}} > \sum_{i=1}^{N} m_i c_{p,i}, \tag{116}$$

2.

$$\min_i p_{\infty,i} < 0 \tag{117}$$

and

$$\left(E - \min_j (\gamma_j p_{\infty,j}) - \sum_{j=1}^{N} m_j e_{*,j}\right) \sum_{i=1}^{N} \frac{\gamma_i - 1}{\gamma_i} \frac{m_i c_{p,i}}{p_{\infty,i} - \min_j (\gamma_j p_{\infty,j})} > \sum_{i=1}^{N} m_i c_{p,i}, \tag{118}$$

3.

$$\min_i p_{\infty,i} = 0. \tag{119}$$

This solution is unique.

Proof. The result follows from Proposition 4 and checking all possible signs of $\min_i p_{\infty,i}$ in Proposition 5 and Restriction 8. ∎

5. Numerical solution algorithms. In this section, we derive second-order solution algorithms for Problems 1 and 2. We will base our approach on the standard Newton–Raphson method. However, we want our algorithms to be unconditionally globally convergent, a property which would not be ensured if we were to use Newton's algorithm directly on the functions f and g given by (45) and (80). Instead, we will make use of the following observation.

PROPOSITION 7. *Consider the equation*

$$f(x) = 0, \qquad x \in \mathcal{S} \subseteq \mathbb{R}. \tag{120}$$

Let $g(x)$ be some C^1-smooth function without roots in $\mathcal{S}$, and let

$$f'(x) \neq 0 \tag{121}$$

in $\mathcal{S}$. Then Newton's method applied to the function

$$F(x) = f(x) \cdot g(x) \tag{122}$$

will yield a quadratically convergent method to a root of f, subject to the standard conditions for quadratic convergence of Newton's method applied to F. Furthermore, Newton's method applied to F will throughout $\mathcal{S}$ be a second-order accurate approximation to Newton's method applied to f.

Proof. The definition of quadratic convergence may be stated as follows:

$$|x^* - x_{n+1}| \leq K |x^* - x_n|^2 \tag{123}$$

for all x_n in some neighborhood close to x^*, where x^* is the root and K is some positive constant. Since the roots of F coincide with the roots of f, and (123) involves only the root x^*, it follows that second-order convergence for F implies second-order convergence for f.

Copyright © by SIAM. Unauthorized reproduction of this article is prohibited.

Furthermore, Newton's method applied to f yields

$$x_{n+1} = x_n - \frac{f(x_n)}{f'(x_n)}. \tag{124}$$

Newton's method applied to F yields

$$\begin{aligned} \tilde{x}_{n+1} &= x_n - \frac{f(x_n)}{f'(x_n)}\left(1 + \frac{f(x_n)g'(x_n)}{f'(x_n)g(x_n)}\right)^{-1} \\ &= x_n - \frac{f(x_n)}{f'(x_n)}\left(1 - \frac{f(x_n)g'(x_n)}{f'(x_n)g(x_n)} + \mathcal{O}(\Delta x^2)\right) \\ &= x_{n+1} + \mathcal{O}(\Delta x^2), \end{aligned} \tag{125}$$

where

$$\Delta x = x_{n+1} - x_n \tag{126}$$

and we have used that

$$f(x_n) = \mathcal{O}(\Delta x). \qquad \square \tag{127}$$

The usefulness of this observation now lies in the possibility that a function F may be found such that the method (125) provides us with better convergence properties than the method (124). In the following, we will use this trick to obtain globally convergent methods for Problems 1 and 2.

To this end, we will use the following classic result.

PROPOSITION 8. *Consider the equation*

$$F(x) = 0, \qquad x \in \mathcal{S} \subseteq \mathbb{R}, \tag{128}$$

where $F(x)$ is at least C^2-smooth. Consider now an interval $\mathcal{T} \subseteq \mathcal{S}$, and assume that (128) *has a root x^* in $\mathcal{T}$, i.e.,*

$$F(x^*) = 0. \tag{129}$$

Assume that for all $x \in \mathcal{T}$ we have

$$F'(x) \neq 0, \tag{130}$$

$$F(x) \cdot F''(x) > 0 \quad \forall x \neq x^*. \tag{131}$$

Then Newton's method converges monotonically and quadratically to x^* for all initial values $x_0 \in \mathcal{T}$.

The reader is referred to [18] and references therein for a review and more general convergence criteria for Newton's method. For our current purposes, Proposition 8 will be sufficient.

5.1. Problem 1. Let p^* be the pressure that solves (46), where $f(\hat{p})$ is given by (45). In the context of Proposition 8, we then have

$$F_a(\hat{p}) = \sum_{i=1}^{N} \frac{(\gamma_i - 1)(E_i - m_i e_{*,i})}{\hat{p} + \gamma_i p_{\infty,i}} - 1, \tag{132}$$

$$F_a'(\hat{p}) = -\sum_{i=1}^{N} \frac{(\gamma_i - 1)(E_i - m_i e_{*,i})}{(\hat{p} + \gamma_i p_{\infty,i})^2}, \tag{133}$$

$$F_a''(\hat{p}) = 2\sum_{i=1}^{N} \frac{(\gamma_i - 1)(E_i - m_i e_{*,i})}{(\hat{p} + \gamma_i p_{\infty,i})^3}. \tag{134}$$

Copyright © by SIAM. Unauthorized reproduction of this article is prohibited.

Newton's method gives

$$\hat{p}_{n+1} = \hat{p}_n - \frac{F_a(\hat{p}_n)}{F_a'(\hat{p}_n)} = \hat{p}_n + \frac{1 - f(\hat{p}_n)}{f'(\hat{p}_n)}, \tag{135}$$

where $f(\hat{p})$ is given by (45) and $f'(\hat{p})$ is given by (49).

LEMMA 9. *Assume that a physically valid solution p^* to Problem 1 exists. Then the method* (135) *converges monotonically and quadratically to p^* for all initial values satisfying*

$$\hat{p}_0 \in \mathcal{P}_3, \quad \textit{where} \quad \mathcal{P}_3 = \left(-\min_i \left(\gamma_i p_{\infty,i}\right), p^* \right]. \tag{136}$$

Proof. It follows from Restriction 1, Lemma 2, and Restriction 3 that in the interval $\mathcal{P}_3$, $F_a'(\hat{p}) < 0$ and F_a is monotonically decreasing. Hence $F_a(\hat{p}) > 0$ for all $\hat{p} \neq p^*$ in this interval. Furthermore, we see from (134) that $F_a''(\hat{p}) > 0$ throughout the interval $\mathcal{P}_3$. Hence the conditions of Proposition 8 apply. ∎

We now turn our attention to initial values satisfying

$$\hat{p}_0 \in [p^*, +\infty). \tag{137}$$

The method (135) then no longer satisfies the convexity requirement (131), and in general we have no guarantee that successive iterates $\hat{p}_n$ will remain in the interval $\mathcal{P}_1$ as given by (40). We will therefore make use of Proposition 7, and we consider instead the function

$$F_b(\hat{p}) = \left(\hat{p} + \min_j \left(\gamma_j p_{\infty,j}\right) \right) F_a(\hat{p}). \tag{138}$$

We then have

$$F_b'(\hat{p}) = f(\hat{p}) - 1 + \left(\hat{p} + \min_j \left(\gamma_j p_{\infty,j}\right) \right) f'(\hat{p}), \tag{139}$$

$$\begin{aligned} F_b''(\hat{p}) &= 2f'(\hat{p}) + \left(\hat{p} + \min_j \left(\gamma_j p_{\infty,j}\right) \right) f''(\hat{p}) \\ &= 2 \sum_{i=1}^{N} \frac{(\gamma_i - 1)(E_i - m_i e_{*,i})}{\left(\hat{p} + \gamma_i p_{\infty,i}\right)^2} \left(\frac{\hat{p} + \min_j \left(\gamma_j p_{\infty,j}\right)}{\hat{p} + \gamma_i p_{\infty,i}} - 1 \right). \end{aligned} \tag{140}$$

Newton's method applied to F_b gives

$$\hat{p}_{n+1} = \hat{p}_n - \frac{F_b(\hat{p}_n)}{F_b'(\hat{p}_n)} = \hat{p}_n + \frac{1 - f(\hat{p}_n)}{f'(\hat{p}_n)} \left(1 - \frac{1 - f(\hat{p}_n)}{f'(\hat{p}_n) \left(\hat{p}_n + \min_j \left(\gamma_j p_{\infty,j}\right) \right)} \right)^{-1}. \tag{141}$$

LEMMA 10. *Assume that a physically valid solution p^* to Problem 1 exists, and that*

$$\gamma_i p_{\infty,i} = \gamma_j p_{\infty,j} = \widetilde{\gamma p_\infty} \qquad \forall i, j \in \{1, \ldots, N\}. \tag{142}$$

Then the method (141) *converges in one step to p^* for all initial values satisfying*

$$\hat{p}_0 \in [p^*, +\infty). \tag{143}$$

Copyright © by SIAM. Unauthorized reproduction of this article is prohibited.

Proof. When (142) holds, the method (141) reduces to

$$\hat{p}_{n+1} = \sum_{i=1}^{N} (\gamma_i - 1)\,(E_i - m_i e_{*,i}) - \widetilde{\gamma p_\infty} \quad \forall n. \tag{144}$$

Substituting into (45) yields

$$f(\hat{p}_{n+1}) = 1. \tag{145}$$

∎

LEMMA 11. *Assume that a physically valid solution p^* to Problem 1 exists. Then the method (141) converges monotonically and at least quadratically to p^* for all initial values satisfying*

$$\hat{p}_0 \in \mathcal{P}_4, \quad \textit{where} \quad \mathcal{P}_4 = [p^*, +\infty)\,. \tag{146}$$

Proof. We know from (49) that $f'(\hat{p}) < 0$ in the interval $\mathcal{P}_1$, and from this it follows that $f(\hat{p}) \leq 1$ in the interval $\mathcal{P}_4$. We then see from Restriction 1 and (138) that $F_b(\hat{p}) < 0$ for all $\hat{p} \neq p^*$ in $\mathcal{P}_4$, and from (139) that $F_b'(\hat{p}) < 0$ in this interval. Furthermore, from Restrictions 1 and 3, Lemma 1, and (140), we see that $F_b''(\hat{p}) < 0$ in $\mathcal{P}_4$, assuming that (142) does not hold. Then the conditions of Proposition 8 apply.

In the case that (142) does in fact hold, the result follows from Lemma 10. ∎

We are now in position to formulate our globally convergent method, as follows.

PROPOSITION 9. *Assume that E_i and m_i satisfy Restrictions 2–4. Then the method*

$$\hat{p}_{n+1} = \hat{p}_n + \frac{1 - f(\hat{p}_n)}{f'(\hat{p}_n)} \left(1 - \frac{1 - f(\hat{p}_n) + |1 - f(\hat{p}_n)|}{2f'(\hat{p}_n)\,(\hat{p}_n + \min_j (\gamma_j p_{\infty,j}))}\right)^{-1}, \tag{147}$$

where $f(\hat{p})$ is given by (45) and $f'(\hat{p})$ is given by (49), converges monotonically and at least quadratically to the unique physically valid solution p^* to Problem 1 for all initial values satisfying

$$\hat{p}_0 \in \mathcal{P}_2, \quad \textit{where} \quad \mathcal{P}_2 = \left(-\min_i (\gamma_i p_{\infty,i}), +\infty\right). \tag{148}$$

Proof. We know from (49) that $f(\hat{p})$ is monotonically decreasing in the interval $\mathcal{P}_2$. Hence we have $f(\hat{p}) \geq 1$ in the interval $\mathcal{P}_3$, and the method (147) reduces to (135) in this interval. Monotonicity also implies that $f(\hat{p}) \leq 1$ in the interval $\mathcal{P}_4$, and the method (147) reduces to (141) in this interval. The result now follows from Lemmas 9–11 and Proposition 1. ∎

5.2. Problem 2. We here focus on Problem 2 as stated in section 4. Now let p^* be the pressure that solves (81), where $g(\hat{p})$ is given by (80). Consider now Newton's method applied to the function φ given by (86), where the parameters are given by (82)–(84). We obtain

$$z_{n+1} = z_n - \frac{\varphi(z_n)}{\varphi'(z_n)}. \tag{149}$$

Now from (85) and (86) it follows that

$$\varphi(z) = g(\hat{p}) - 1. \tag{150}$$

Copyright © by SIAM. Unauthorized reproduction of this article is prohibited.

From (83), (109), and (150) it then follows that the method (149) can be written in the equivalent form

$$\hat{p}_{n+1} = \hat{p}_n + \frac{1 - g(\hat{p}_n)}{g'(\hat{p}_n)}, \tag{151}$$

where $g(\hat{p})$ is given by (80) and $g'(\hat{p})$ is given by

$$g'(\hat{p}) = \sum_{i=1}^{N} \frac{\gamma_i - 1}{\gamma_i} \frac{m_i c_{p,i}}{\sum_{j=1}^{N} m_j c_{p,j}} \frac{p_{\infty,i} - E + \sum_{j=1}^{N} m_j e_{*,j}}{(\hat{p} + p_{\infty,i})^2}. \tag{152}$$

LEMMA 12. *Assume that a physically valid solution p^* to Problem 2 exists. Then the method* (151) *converges monotonically and quadratically to p^* for all initial values satisfying*

$$\hat{p}_0 \in \mathcal{P}_5, \quad \textit{where} \quad \mathcal{P}_5 = \left(-\min_i p_{\infty,i}, p^* \right]. \tag{153}$$

Proof. We consider the method in the equivalent form (149), where the root z^* satisfies

$$z^* = z(p^*), \tag{154}$$

and the condition (153) corresponds to

$$z \in \left(-\min_i q_i, z^* \right]. \tag{155}$$

Now it follows from (98) that $\varphi'(z^*) < 0$, and since z^* is the unique root that satisfies (155), it follows from continuity that

$$\varphi(z) > 0 \qquad \forall z \in \left(-\min_i q_i, z^* \right). \tag{156}$$

Hence it follows from (98) and (100) that

$$\varphi'(z) < 0 \qquad \forall z \in \left(-\min_i q_i, z^* \right]. \tag{157}$$

Differentiating (98) yields

$$\varphi''(z) = \frac{2}{z} \left(\sum_{i=1}^{N} A_i \frac{q_i^2}{(z + q_i)^3} - \varphi'(z) \right), \tag{158}$$

and it follows from (87), (100), and (157) that

$$\varphi''(z) > 0 \qquad \forall z \in \left(-\min_i q_i, z^* \right]. \tag{159}$$

Hence the conditions of Proposition 8 apply. ∎

We now focus on the interval

$$\hat{p}_0 \in [p^*, +\infty). \tag{160}$$

Copyright © by SIAM. Unauthorized reproduction of this article is prohibited.

As noted in section 4.1, $\varphi'(z)$ may become zero in this interval, rendering the method (151) unreliable. We therefore again make use of Proposition 7, and consider instead the function

$$F_c(z) = \left(z + \min_i q_i\right) \Phi(z), \tag{161}$$

where Φ is given by (97). We then have

$$F_c(z(\hat{p})) = \left(\hat{p} + \min_i p_{\infty,i}\right) \left(E + \hat{p} - \sum_{j=1}^{N} m_j e_{*,j}\right) \left(g(\hat{p}) - 1\right), \tag{162}$$

$$\begin{aligned} F_c'(z(\hat{p})) = &\left(2\hat{p} + \min_i p_{\infty,i} + E - \sum_{j=1}^{N} m_j e_{*,j}\right) \left(g(\hat{p}) - 1\right) \\ &+ \left(\hat{p} + \min_i p_{\infty,i}\right) \left(E + \hat{p} - \sum_{j=1}^{N} m_j e_{*,j}\right) g'(\hat{p}). \end{aligned} \tag{163}$$

Newton's method applied to F_c yields

$$\hat{p}_{n+1} = \hat{p}_n - \frac{F_c(z(\hat{p}_n))}{F_c'(z(\hat{p}_n))} = \hat{p}_n + \frac{1 - g(\hat{p}_n)}{g'(\hat{p}_n)} \left(1 - \frac{1 - g(\hat{p}_n)}{g'(\hat{p}_n)} h(\hat{p}_n)\right)^{-1}, \tag{164}$$

where $h(\hat{p})$ is given by

$$h(\hat{p}) = \frac{1}{E + \hat{p} - \sum_{j=1}^{N} m_j e_{*,j}} + \frac{1}{\hat{p} + \min_i p_{\infty,i}}. \tag{165}$$

LEMMA 13. *Assume that a physically valid solution p^* to Problem 2 exists. Then the method* (164) *converges monotonically and quadratically to p^* for all initial values satisfying*

$$\hat{p}_0 \in \mathcal{P}_6, \quad \textit{where} \quad \mathcal{P}_6 = [p^*, +\infty). \tag{166}$$

Proof. By Lemma 6, Lemma 8, and (83)–(84), it follows that

$$F_c(z) < 0 \qquad \forall \hat{p}(z) \in (p^*, +\infty). \tag{167}$$

Furthermore, we have

$$F_c'(z) = \left(z + \min_i q_i\right) \Phi'(z) + \Phi(z), \tag{168}$$

and it follows from Lemma 8 and (83)–(84) that

$$F_c'(z) < 0 \qquad \forall \hat{p}(z) \in [p^*, +\infty). \tag{169}$$

Differentiating (168) yields

$$F_c''(z) = 2\Phi'(z) + \left(z + \min_i q_i\right) \Phi''(z), \tag{170}$$

which by (98) can be written as

$$F_c''(z) = 2\left(\sum_{i=1}^{N} A_i - 1 + \sum_{i=1}^{N} A_i \left(\frac{q_i}{z + q_i}\right)^2 \left(\frac{z + \min_j q_j}{z + q_i} - 1\right)\right). \tag{171}$$

Copyright © by SIAM. Unauthorized reproduction of this article is prohibited.

Hence

$$F_c''(z) < 0 \qquad \forall \hat{p}(z) \in [p^*, +\infty)\,, \tag{172}$$

and the conditions of Proposition 8 apply. ∎

We may now formulate our globally convergent method, as follows.

PROPOSITION 10. *Assume that E_i and m_i satisfy Restrictions 6–7. Then the method*

$$\hat{p}_{n+1} = \hat{p}_n + \frac{1 - g(\hat{p}_n)}{g'(\hat{p}_n)} \left(1 - \frac{1 - g(\hat{p}_n) + |1 - g(\hat{p}_n)|}{2g'(\hat{p}_n)} h(\hat{p}_n)\right)^{-1}, \tag{173}$$

where $g(\hat{p})$ is given by (80), $g'(\hat{p})$ is given by (152), and $h(\hat{p})$ is given by (165), converges monotonically and quadratically to the unique physically valid solution p^* to Problem 2, for all initial values satisfying

$$\hat{p}_0 \in \mathcal{P}_1, \quad \textit{where} \quad \mathcal{P}_1 = \left(-\min_i p_{\infty,i}, +\infty\right). \tag{174}$$

Proof. We know from (157) that $\varphi(z)$ is monotonically decreasing in the interval $\mathcal{P}_5$. Hence we have $g(\hat{p}) \geq 1$ in $\mathcal{P}_5$, and the method (173) reduces to (151) in this interval. In particular, we have that $\varphi'(z(p^*)) < 0$, and since p^* is the unique solution to $g(\hat{p}) = 1$ in the interval $\mathcal{P}_1$, it follows that $g(\hat{p}) \leq 1$ in the interval $\mathcal{P}_6$. Note that the method (173) reduces to (164) in this interval. The result now follows from Lemmas 12–13 and Proposition 4. ∎

6. Numerical examples. The purpose of this section is to numerically demonstrate and verify the results derived above. In particular, our examples will illustrate the quadratic and monotone convergence of our methods. We first define some useful concepts.

DEFINITION 5. *At each step of the Newton iteration, we define the* error $\mathcal{E}_n$ *as*

$$\mathcal{E}_n = \hat{p}_n - p^*. \tag{175}$$

We also define the relative error $\mathcal{R}_n$ *as*

$$\mathcal{R}_n = \left|\frac{\mathcal{E}_n}{p^*}\right|, \tag{176}$$

as well as the local convergence rate $\mathcal{L}_n$*,*

$$\mathcal{L}_n = \frac{\ln|\mathcal{E}_{n+1}/\mathcal{E}_n|}{\ln|\mathcal{E}_n/\mathcal{E}_{n-1}|}. \tag{177}$$

The local convergence rate $\mathcal{L}$ is related to, but generally not identical to, the global convergence order. However, $\mathcal{L}_n$ will approach the global convergence order as we approach the solution.

6.1. Problem 1. We first consider Problem 1 concerning mechanical equilibria; see section 3. This corresponds to multifluid models of the kind treated, e.g., by Paillère, Corre, and García Cascales [13], and we will use their parameters corresponding to water and air as an example. Our input state and the corresponding equilibrium solution are given in Table 1, while the equation-of-state parameters can be found in Table 2. In this case, we have two fluids, $N = 2$.

Copyright © by SIAM. Unauthorized reproduction of this article is prohibited.

TABLE 1
State variables for Problem 1.

Symbol (unit)	Value
$m_1\,(\mathrm{kg/m^3})$	2.252×10^{-1}
$m_2\,(\mathrm{kg/m^3})$	5.000×10^{4}
$E_1\,(\mathrm{J/m^3})$	8.201×10^{2}
$E_2\,(\mathrm{J/m^3})$	1.058×10^{9}
$\alpha_1\,(-)$	0.200
$\alpha_2\,(-)$	0.800
$p\,(\mathrm{MPa})$	0.100
$T_1\,(\mathrm{K})$	308.15
$T_2\,(\mathrm{K})$	308.15

TABLE 2
EOS parameters for Problem 1.

	γ_j (–)	$p_{\infty,j}$ (Pa)	$c_{p,j}$ (J/(kg K))	$e_{*,j}$ (J/(kg))
gas (1)	1.4	0	1008.7	0
liquid (2)	2.8	8.5×10^{8}	4186.0	0

TABLE 3
Convergence for Problem 1 *with* $\hat{p}_0 = 1 \times 10^4\,\mathrm{Pa}$.

n	$\hat{p}_n\,(\mathrm{Pa})$	$\mathcal{E}_n\,(\mathrm{Pa})$	$\mathcal{R}_n\,(-)$	$\mathcal{L}_n$
0	1.000×10^{4}	-9.00×10^{4}	9.00×10^{-1}	–
1	1.900×10^{4}	-8.10×10^{4}	8.10×10^{-1}	2.00
2	3.439×10^{4}	-6.56×10^{4}	6.56×10^{-1}	2.00
3	5.695×10^{4}	-4.30×10^{4}	4.30×10^{-1}	2.00
4	8.147×10^{4}	-1.85×10^{4}	1.85×10^{-1}	2.00
5	9.656×10^{4}	-3.43×10^{3}	3.43×10^{-2}	2.00
6	9.988×10^{4}	-1.17×10^{2}	1.17×10^{-3}	2.00
7	1.000×10^{5}	-1.38×10^{-1}	1.38×10^{-6}	2.00
8	1.000×10^{5}	-1.92×10^{-7}	1.92×10^{-12}	2.00
9	1.000×10^{5}	-3.70×10^{-19}	3.70×10^{-24}	–

We employ the method (147) of Proposition 9. The results are shown in Table 3 for

$$\hat{p}_0 = 1 \times 10^4\,\mathrm{Pa} < p^*, \tag{178}$$

and in Table 4 for

$$\hat{p}_0 = 1 \times 10^{12}\,\mathrm{Pa} > p^*. \tag{179}$$

We observe the expected quadratic convergence, and the monotonicity is verified by $\mathcal{E}_n$ having a constant sign.

The results from Tables 3–4 are graphically illustrated in Figure 1. Figure 1(a) contains the function F_a given by (132), and Figure 1(b) contains the function F_b given by (138). As described in section 5.1, the method (147) is equivalent to the standard Newton–Raphson algorithm applied to these functions. The figure indicates how the established convexity properties ensure the monotone convergence.

Note that for the initial value (178), the unmodified Newton–Raphson method (135) would fail. In particular, the method gives $\hat{p}_1 = -5.2 \times 10^{14}\,\mathrm{Pa}$ and rapidly

Copyright © by SIAM. Unauthorized reproduction of this article is prohibited.

TABLE 4
Convergence for Problem 1 *with* $\hat{p}_0 = 1 \times 10^{12}$ Pa.

n	$\hat{p}_n$ (Pa)	$\mathcal{E}_n$ (Pa)	$\mathcal{R}_n$ (−)	$\mathcal{L}_n$
0	1.000×10^{12}	1.00×10^{12}	1.00×10^{7}	–
1	1.895×10^{9}	1.89×10^{9}	1.89×10^{4}	0.21
2	4.975×10^{8}	4.97×10^{8}	4.97×10^{3}	1.03
3	1.257×10^{8}	1.25×10^{8}	1.25×10^{3}	1.45
4	1.731×10^{7}	1.72×10^{7}	1.72×10^{2}	1.82
5	5.642×10^{5}	4.64×10^{5}	4.64×10^{0}	1.98
6	1.003×10^{5}	3.61×10^{2}	3.61×10^{-3}	2.00
7	1.000×10^{5}	2.19×10^{-4}	2.19×10^{-9}	2.00
8	1.000×10^{5}	8.09×10^{-17}	8.09×10^{-22}	–

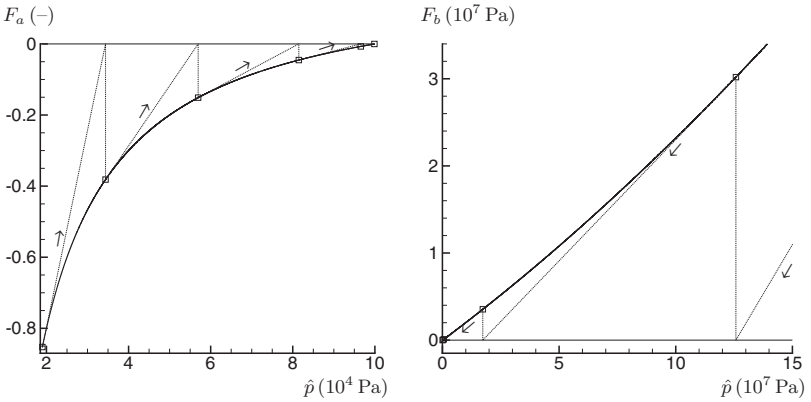

(a) $\hat{p}_0 = 1 \times 10^4$ Pa. (b) $\hat{p}_0 = 1 \times 10^{12}$ Pa.

FIG. 1. *Convergence for Problem* 1 *with the initial value lower (left) and higher (right) than the solution. The arrows indicate the direction of successive iterates.*

diverges. This shows that our modification (147) is in fact *necessary* to obtain global convergence.

6.2. Problem 2. We now consider Problem 2 with mechanical and thermal equilibria; see section 4. As an example we will take the three-component ($N = 3$) mixture whose decompression was studied by Morin et al. [9]. The input state and the corresponding equilibrium solution are shown in Table 5, while the equation-of-state parameters are given in Table 6.

The numerical algorithm (173) of Proposition 10 has been applied. Table 7 shows the result for an initial pressure of

$$\hat{p}_0 = -\min_j p_{\infty,j} = -1.094 \times 10^7 \,\text{Pa} < p^*, \tag{180}$$

while Table 8 presents results for an initial pressure of

$$\hat{p}_0 = 1 \times 10^{10} \,\text{Pa} > p^*. \tag{181}$$

Again the expected convergence order and monotonicity are verified.

Copyright © by SIAM. Unauthorized reproduction of this article is prohibited.

TABLE 5
State variables for Problem 2.

Symbol (unit)	Value
$m_1\,(\mathrm{kg/m^3})$	6.235×10^2
$m_2\,(\mathrm{kg/m^3})$	9.378×10^1
$m_3\,(\mathrm{kg/m^3})$	1.274×10^0
$E\,(\mathrm{J/m^3})$	8.332×10^8
$\alpha_1\,(-)$	0.9
$\alpha_2\,(-)$	0.09
$\alpha_3\,(-)$	0.01
$p\,(\mathrm{MPa})$	10
$T\,(\mathrm{K})$	300

TABLE 6
EOS parameters for Problem 2.

	γ_j (–)	$p_{\infty,j}$ (MPa)	$c_{p,j}$ (J/(kg K))	$e_{*,j}$ (J/(kg))
CO_2 (1)	1.03	13.47	3877	0
Water (2)	2.85	833.02	4155	0
Methane (3)	1.23	10.94	2930	0

TABLE 7
Convergence for Problem 2 with $\hat{p}_0 = -1.094 \times 10^7$ Pa.

n	$\hat{p}_n\,(\mathrm{Pa})$	$\mathcal{E}_n\,(\mathrm{Pa})$	$\mathcal{R}_n\,(-)$	$\mathcal{L}_n$
0	-1.094×10^7	-2.09×10^7	2.09×10^0	–
1	-1.093×10^7	-2.09×10^7	2.09×10^0	2.44
2	-1.092×10^7	-2.09×10^7	2.09×10^0	2.98
3	-1.089×10^7	-2.08×10^7	2.08×10^0	4.35
4	-1.074×10^7	-2.07×10^7	2.07×10^0	6.83
5	-9.791×10^6	-1.97×10^7	1.97×10^0	3.38
6	-6.875×10^6	-1.68×10^7	1.68×10^0	2.05
7	-2.170×10^6	-1.21×10^7	1.21×10^0	2.00
8	3.676×10^6	-6.32×10^6	6.32×10^{-1}	2.00
9	8.293×10^6	-1.70×10^6	1.70×10^{-1}	2.00
10	9.875×10^6	-1.24×10^5	1.24×10^{-2}	2.00
11	9.999×10^6	-6.59×10^2	6.59×10^{-5}	2.00
12	1.000×10^7	-1.85×10^{-2}	1.85×10^{-9}	2.00
13	1.000×10^7	-1.46×10^{-11}	1.46×10^{-18}	–

In Figure 2, the results of Tables 7–8 are represented graphically. The function φ, as given by (150), is presented in Figure 2(a) for the initial value (180). For the initial value (181), Figure 2(b) contains the function F_c as given by (162). As described in section 5.2, the method (173) reduces to the standard Newton–Raphson algorithm applied to these functions. The graphs demonstrate behavior similar to that observed for Problem 1.

As for Problem 1, we observe that the unmodified Newton–Raphson method (151) fails for the initial value (181). It gives $\hat{p}_1 = -4.2 \times 10^{12}\,\mathrm{Pa}$, and then rapidly diverges toward negative infinity. This is due to the unfavorable curvature of φ for $\hat{p} > p^*$, causing the naïve method (151) to cut through the physically relevant part of φ and give a very large negative $\hat{p}_1$. From this there is no recovery.

This underscores the necessity of our modification (173).

Copyright © by SIAM. Unauthorized reproduction of this article is prohibited.

TABLE 8
Convergence for Problem 2 with $\hat{p}_0 = 1 \times 10^{10}$ Pa.

n	$\hat{p}_n$ (Pa)	$\mathcal{E}_n$ (Pa)	$\mathcal{R}_n$ $(-)$	$\mathcal{L}_n$
0	1.000×10^{10}	9.99×10^{9}	9.99×10^{2}	–
1	4.803×10^{9}	4.79×10^{9}	4.79×10^{2}	1.06
2	2.213×10^{9}	2.20×10^{9}	2.20×10^{2}	1.12
3	9.357×10^{8}	9.25×10^{8}	9.25×10^{1}	1.23
4	3.290×10^{8}	3.19×10^{8}	3.19×10^{1}	1.42
5	8.005×10^{7}	7.00×10^{7}	7.00×10^{0}	1.60
6	1.621×10^{7}	6.20×10^{6}	6.20×10^{-1}	1.51
7	1.016×10^{7}	1.60×10^{5}	1.60×10^{-2}	1.90
8	1.000×10^{7}	1.59×10^{2}	1.59×10^{-5}	2.00
9	1.000×10^{7}	1.58×10^{4}	1.58×10^{-11}	2.00
10	1.000×10^{7}	1.58×10^{16}	1.58×10^{-23}	–

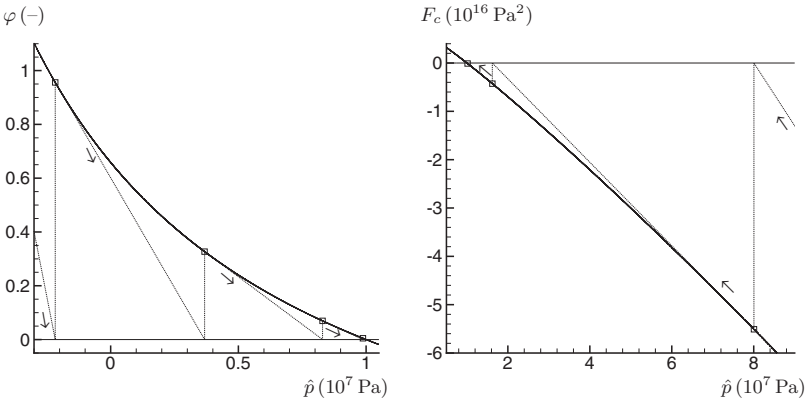

(a) $\hat{p}_0 = -1.094 \times 10^7$ Pa. (b) $\hat{p}_0 = 1 \times 10^{10}$ Pa.

FIG. 2. *Convergence for Problem 2 with the initial value lower (left) and higher (right) than the solution. The arrows indicate the direction of successive iterates.*

7. Summary. We have investigated a general system of N immiscible stiffened gases assumed to be in mechanical equilibrium, meaning that the pressure is identical for all the components. We have considered two cases, one in which the fluids are assumed to have individual temperatures and one in which thermal equilibrium has been assumed.

Under these assumptions, we have considered the problem of calculating the full physical state from knowledge of only the conserved fluid-mechanical parameters. To as large an extent as possible, we have attempted to give a complete exposition of this problem. We have provided some natural definitions of what *physical validity* means for such equilibrium solutions. We have then given the necessary and sufficient conditions for such valid solutions to exist, and we have proved that these solutions are unique.

Finally, we have demonstrated that the problems may be reduced to solving an equation in one unknown. This allows for the construction of robust and efficient

Copyright © by SIAM. Unauthorized reproduction of this article is prohibited.

numerical solvers. In particular, we have formulated explicit Newton–Raphson-type methods which guarantee unconditional quadratic convergence.

Acknowledgments. We are grateful to our colleague Karl Yngve Lervåg for fruitful discussions regarding the Newton–Raphson method. We also thank the anonymous reviewers for their valuable remarks, which led to substantial improvements of the first version of this paper.

REFERENCES

[1] R. Abgrall, *An extension of Roe's upwind scheme to algebraic equilibrium real gas models*, Comput. Fluids, 19 (1991), pp. 171–182.
[2] T. Barberon and P. Helluy, *Finite volume simulation of cavitating flows*, Comput. Fluids, 34 (2005), pp. 832–858.
[3] C.-H. Chang and M.-S. Liou, *A robust and accurate approach to computing compressible multiphase flow: Stratified flow model and AUSM+-up scheme*, J. Comput. Phys., 225 (2007), pp. 840–873.
[4] P. Glaister, *Real gas flows in a duct*, Comput. Math. Appl., 24 (1992), pp. 45–59.
[5] P. Helluy and H. Mathis, *Pressure Laws and Fast Legendre Transform*, preprint, available online from http://hal.archives-ouvertes.fr/hal-00424061/fr/; Math. Models Methods Appl. Sci., to appear.
[6] J.-M. Hérard and O. Hurisse, *Coupling two and one-dimensional unsteady Euler equations through a thin interface*, Comput. Fluids, 36 (2007), pp. 651–666.
[7] R. Menikoff, *Empirical EOS for solids*, in Shock Wave Science and Technology Reference Library, Volume 2 - Solids, Springer-Verlag, Berlin, 2007, pp. 143–188.
[8] R. Menikoff and B. J. Plohr, *The Riemann problem for fluid flow of real materials*, Rev. Modern Phys., 88 (1989), pp. 75–130.
[9] A. Morin, P. K. Aursand, T. Flåtten, and S. T. Munkejord, *Numerical resolution of CO_2 transport dynamics*, in Proceedings of the Fourth SIAM Conference on Mathematics for Industry: Challenges and Frontiers (MI09), San Francisco, CA, 2009, SIAM, Philadelphia, 2009, pp. 108–119; available online from http://www.siam.org/proceedings/industry/2009/mi09_013_morina.pdf.
[10] S. T. Munkejord, S. Evje, and T. Flåtten, *A MUSTA scheme for a nonconservative two-fluid model*, SIAM J. Sci. Comput., 31 (2009), pp. 2587–2622.
[11] Y.-Y. Niu, *Advection upwinding splitting method to solve a compressible two-fluid model*, Internat. J. Numer. Methods Fluids, 36 (2001), pp. 351–371.
[12] Y.-Y. Niu, Y.-C. Lin, and C.-H. Chang, *A further work on multi-phase two-fluid approach for compressible multi-phase flows*, Internat. J. Numer. Methods Fluids, 58 (2008), pp. 879–896.
[13] H. Paillère, C. Corre, and J. R. García Cascales, *On the extension of the AUSM+ scheme to compressible two-fluid models*, Comput. Fluids, 32 (2003), pp. 891–916.
[14] R. Saurel and R. Abgrall, *A simple method for compressible multifluid flows*, SIAM J. Sci. Comput., 21 (1999), pp. 1115–1145.
[15] R. Saurel, F. Petitpas, and R. Abgrall, *Modelling phase transition in metastable liquids: Application to cavitating and flashing flows*, J. Fluid Mech., 607 (2008), pp. 313–350.
[16] K.-M. Shyue, *An efficient shock-capturing algorithm for compressible multicomponent problems*, J. Comput. Phys., 142 (1998), pp. 208–242.
[17] H. Takahira, T. Matsuno, and K. Shuto, *Numerical investigations of shock-bubble interactions in mercury*, Fluid Dyn. Res., 40 (2008), pp. 510–520.
[18] L. Thorlund-Petersen, *Global convergence of Newton's method on an interval*, Math. Methods Oper. Res., 59 (2004), pp. 91–110.

Copyright © by SIAM. Unauthorized reproduction of this article is prohibited.

C Wave Propagation in Multicomponent Flow Models

Tore Flåtten, Alexandre Morin and Svend T. Munkejord.
SIAM Journal on Applied Mathematics, Volume 70, No. 8,
pp. 2861-2882, 2010.

SIAM J. APPL. MATH.
Vol. 70, No. 8, pp. 2861–2882
© 2010 Society for Industrial and Applied Mathematics

WAVE PROPAGATION IN MULTICOMPONENT FLOW MODELS*

TORE FLÅTTEN†, ALEXANDRE MORIN‡, AND SVEND TOLLAK MUNKEJORD§

Abstract. We consider systems of hyperbolic balance laws governing flows of an arbitrary number of components equipped with general equations of state. The components are assumed to be immiscible. We compare two such models: one in which thermal equilibrium is attained through a relaxation procedure, and a fully relaxed model in which equal temperatures are instantaneously imposed. We describe how the relaxation procedure may be made consistent with the second law of thermodynamics. Exact wave velocities for both models are obtained and compared. In particular, our formulation directly proves a general subcharacteristic condition: For an arbitrary number of components and thermodynamically stable equations of state, the mixture sonic velocity of the relaxed system can never exceed the sonic velocity of the relaxation system.

Key words. multicomponent flow, sonic waves, sound velocity, relaxation system

AMS subject classifications. 76T30, 35L60, 35L65

DOI. 10.1137/090777700

1. Introduction.

Dynamic simulations of multicomponent flows often involve nonequilibrium processes. Driving forces towards equilibrium occur in the equations as *relaxation source terms*, which may be extremely stiff if the relaxation time towards equilibrium is small. In this paper, we consider hyperbolic relaxation systems in a form similar to the description by Chen, Levermore, and Liu [7],

$$\frac{\partial \boldsymbol{U}}{\partial t} + \frac{\partial \boldsymbol{F}(\boldsymbol{U})}{\partial x} + \boldsymbol{A}(\boldsymbol{U})\frac{\partial \boldsymbol{W}(\boldsymbol{U})}{\partial x} + \frac{1}{\epsilon}\boldsymbol{R}(\boldsymbol{U}) = 0, \tag{1}$$

to be solved for the unknown M-vector $\boldsymbol{U}$. The system is endowed with an $m \times M$ constant-coefficient matrix $\mathcal{Q}$ with rank $m < M$ such that

$$\mathcal{Q}\boldsymbol{R} = 0 \qquad \forall \boldsymbol{U}. \tag{2}$$

Furthermore, we assume that $\mathcal{Q}\boldsymbol{A}\,\mathrm{d}\boldsymbol{W}$ is an exact differential:

$$\mathcal{Q}\boldsymbol{A}\,\mathrm{d}\boldsymbol{W} = \mathrm{d}\boldsymbol{G}(\boldsymbol{U}). \tag{3}$$

Multiplying (1) on the left by $\mathcal{Q}$ we obtain a conservation law for the reduced variable $\boldsymbol{V} = \mathcal{Q}\boldsymbol{U}$:

$$\frac{\partial \boldsymbol{V}}{\partial t} + \frac{\partial}{\partial x}\left(\mathcal{Q}\boldsymbol{F}(\boldsymbol{U}) + \boldsymbol{G}(\boldsymbol{U})\right) = 0. \tag{4}$$

*Received by the editors November 18, 2009; accepted for publication (in revised form) July 1, 2010; published electronically September 23, 2010. This work was financed through the CO_2 Dynamics project and was supported by the Research Council of Norway (189978, 193816), Aker Solutions, ConocoPhilips Skandinavia AS, Det Norske Veritas AS, Gassco AS, Hydro Aluminium AS, Shell Technology AS, Statkraft Development AS, Statoil Petroleum AS, TOTAL E&P Norge AS, and Vattenfall AB.

http://www.siam.org/journals/siap/70-8/77770.html

†SINTEF Energy Research, Sem Sælands vei 11, NO-7465 Trondheim, Norway (Tore.Flatten@sintef.no).

‡Department of Energy and Process Engineering, Norwegian University of Science and Technology (NTNU), NO-7491 Trondheim, Norway (Alexandre.Morin@sintef.no). The work of this author was supported by a Ph.D. grant from the BIGCCS Centre.

§Corresponding author. SINTEF Energy Research, Sem Sælands vei 11, NO-7465 Trondheim, Norway (stm@pvv.org).

We now assume that each $\boldsymbol{V}$ uniquely determines a local equilibrium value $\boldsymbol{U} = \mathcal{E}(\boldsymbol{V})$, satisfying $\boldsymbol{R}(\mathcal{E}(\boldsymbol{V})) = 0$ as well as

$$\mathcal{Q}\mathcal{E}(\boldsymbol{V}) = \boldsymbol{V} \qquad \forall \boldsymbol{V}. \tag{5}$$

Now (4) can be closed as a reduced system by imposing the local equilibrium condition for $\boldsymbol{U}$, namely,

$$\boldsymbol{U} = \mathcal{E}(\boldsymbol{V}), \tag{6}$$

$$\frac{\partial \boldsymbol{V}}{\partial t} + \frac{\partial \mathcal{F}(\boldsymbol{V})}{\partial x} = 0, \tag{7}$$

where the reduced flux $\mathcal{F}$ is defined by

$$\mathcal{F}(\boldsymbol{V}) \equiv \mathcal{Q}\boldsymbol{F}\left(\mathcal{E}(\boldsymbol{V})\right) + \boldsymbol{G}(\mathcal{E}(\boldsymbol{V})). \tag{8}$$

Chen, Levermore, and Liu [7] studied stability of solutions to such relaxation systems for the special case $\boldsymbol{A} = 0$; i.e., the hyperbolic part of (1) is conservative. In particular, they based their analysis on the requirement that the relaxation term should be *entropy dissipative*.

1.1. The subcharacteristic condition. Central to the question of stability of relaxation systems is the *subcharacteristic condition*, a concept introduced by Liu [13]. Within our formulation, this concept may be defined as follows.

DEFINITION 1. *Let the M eigenvalues of the relaxing system* (1) *be given by*

$$\lambda_1 \leq \cdots \leq \lambda_k \leq \lambda_{k+1} \leq \cdots \leq \lambda_M \tag{9}$$

and the m eigenvalues of the relaxed system (6)–(7) *be given by*

$$\tilde{\lambda}_1 \leq \cdots \leq \tilde{\lambda}_j \leq \tilde{\lambda}_{j+1} \leq \cdots \leq \tilde{\lambda}_m. \tag{10}$$

Herein, the relaxation system (1) *is applied to a local equilibrium state $\boldsymbol{U} = \mathcal{E}(\boldsymbol{V})$ such that*

$$\lambda_k = \lambda_k(\mathcal{E}(\boldsymbol{V})), \qquad \tilde{\lambda}_j = \tilde{\lambda}_j(\boldsymbol{V}). \tag{11}$$

Now let the $\tilde{\lambda}_j$ be interlaced *with λ_k in the following sense: Each $\tilde{\lambda}_j$ lies in the closed interval $[\lambda_j, \lambda_{j+M-m}]$. Then the relaxed system* (6)–(7) *is said to satisfy the* subcharacteristic condition *with respect to* (1).

Chen et al. [7] were able to prove the following: If the relaxation system (1) may be equipped with a convex entropy function that is dissipated by the relaxation term, then the subcharacteristic condition holds. Furthermore, a converse holds for linear systems and general 2×2 systems.

Although the subcharacteristic condition is formally neither a necessary nor sufficient condition for stability *in general*, it is nevertheless an essential condition for linear stability and is in practice required for most physically meaningful relaxation processes. Hence the literature commonly puts a strong focus on this condition; see, for instance, Baudin et al. [4, 5] for an application to a two-phase flow model.

A main result of this paper is a constructive proof that the subcharacteristic condition holds for the models we are studying. We will *not* rely on the technique proposed by Chen et al. [7], as this would involve constructing a convex, mathematical entropy function to be dissipated by the relaxation term. Instead, we will first prove

the weaker result that standard *thermodynamic* entropy is dissipated by the relaxation term, thus verifying the physical consistency of the model.

Then our constructive approach allows us to obtain explicit algebraic expressions for the eigenvalues of the models. By these, it may easily be verified that the subcharacteristic condition holds.

1.2. Weak solutions. A well-known property of hyperbolic systems is the ability to support weak solutions, i.e., solutions containing discontinuities. However, the results of this paper are achieved by considering only classical (smooth) solutions. That is, we assume that our state vectors $\boldsymbol{U}(x,t)$ and $\boldsymbol{V}(x,t)$ are everywhere differentiable. The question of existence and uniqueness of weak solutions of our resulting models (stated in sections 2.1.2 and 2.2) may then be addressed by interpreting the derivatives in the distributional sense.

Although this issue will not be pursued in our paper, we remark that for the general case of nonconservative hyperbolic balance laws, where $\boldsymbol{A}\,\mathrm{d}\boldsymbol{W}$ in (1) is not an exact differential, the study of uniqueness of weak solutions requires an extension of the standard theory for conservative systems. This has been an active area of research in recent years; see, for instance, [6, 8].

1.3. Applications to multiphase flows. In addition to modeling actual physical processes, relaxation systems are significant also from the viewpoint of pure numerical analysis—the relaxation system (1) may be used as a starting point for devising numerical methods for the relaxed system (6)–(7). A classic paper in this respect is the work of Jin and Xin [11], who devised a general method in which a conservative system in the form (7) is recast as the limit $\epsilon \to 0$ of (1), where $M = 2m$ and the hyperbolic part of (1) is fully linear. By this, they were able to construct a numerical method where all nonlinearities are encoded in the source terms. Variations of this approach were applied to the drift-flux two-phase flow model by Evje and Fjelde [10] as well as Baudin et al. [4, 5].

Since the works of Abgrall and Saurel [2, 20], there has been considerable interest in applying various relaxation techniques to multiphase flow models. The starting point for many such investigations is the two-pressure two-fluid model [3, 19].

•*Conservation of mass:*

$$\frac{\partial}{\partial t}\left(\rho_{\mathrm{g}}\alpha_{\mathrm{g}}\right) + \frac{\partial}{\partial x}\left(\rho_{\mathrm{g}}\alpha_{\mathrm{g}}v_{\mathrm{g}}\right) = 0, \tag{12}$$

$$\frac{\partial}{\partial t}\left(\rho_{\ell}\alpha_{\ell}\right) + \frac{\partial}{\partial x}\left(\rho_{\ell}\alpha_{\ell}v_{\ell}\right) = 0. \tag{13}$$

•*Balance of momentum:*

$$\frac{\partial}{\partial t}\left(\rho_{\mathrm{g}}\alpha_{\mathrm{g}}v_{\mathrm{g}}\right) + \frac{\partial}{\partial x}\left(\rho_{\mathrm{g}}\alpha_{\mathrm{g}}v_{\mathrm{g}}^2 + \alpha_{\mathrm{g}}p_{\mathrm{g}}\right) - p^{\mathrm{i}}\frac{\partial \alpha_{\mathrm{g}}}{\partial x} = \mu_v(v_{\ell} - v_{\mathrm{g}}), \tag{14}$$

$$\frac{\partial}{\partial t}\left(\rho_{\ell}\alpha_{\ell}v_{\ell}\right) + \frac{\partial}{\partial x}\left(\rho_{\ell}\alpha_{\ell}v_{\ell}^2 + \alpha_{\ell}p_{\ell}\right) - p^{\mathrm{i}}\frac{\partial \alpha_{\ell}}{\partial x} = \mu_v(v_{\mathrm{g}} - v_{\ell}). \tag{15}$$

•*Balance of energy:*

$$\frac{\partial}{\partial t}\left(\rho_{\mathrm{g}}\alpha_{\mathrm{g}}\left(\frac{1}{2}v_{\mathrm{g}}^2 + e_{\mathrm{g}}\right)\right) + \frac{\partial}{\partial x}\left(\rho_{\mathrm{g}}\alpha_{\mathrm{g}}v_{\mathrm{g}}\left(\frac{1}{2}v_{\mathrm{g}}^2 + e_{\mathrm{g}} + \frac{p_{\mathrm{g}}}{\rho_{\mathrm{g}}}\right)\right) + p^{\mathrm{i}}\frac{\partial \alpha_{\mathrm{g}}}{\partial t} = \mu_v v^{\mathrm{i}}(v_{\ell} - v_{\mathrm{g}}), \tag{16}$$

$$\frac{\partial}{\partial t}\left(\rho_{\ell}\alpha_{\ell}\left(\frac{1}{2}v_{\ell}^2 + e_{\ell}\right)\right) + \frac{\partial}{\partial x}\left(\rho_{\ell}\alpha_{\ell}v_{\ell}\left(\frac{1}{2}v_{\ell}^2 + e_{\ell} + \frac{p_{\ell}}{\rho_{\ell}}\right)\right) + p^{\mathrm{i}}\frac{\partial \alpha_{\ell}}{\partial t} = \mu_v v^{\mathrm{i}}(v_{\mathrm{g}} - v_{\ell}). \tag{17}$$

•*Evolution of volume fraction:*

$$\frac{\partial \alpha_{\mathrm{g}}}{\partial t} + v^{\mathrm{i}} \frac{\partial \alpha_{\mathrm{g}}}{\partial x} = \mu_p (p_{\mathrm{g}} - p_\ell). \tag{18}$$

Herein, we use the following nomenclature for phase $k \in \{\mathrm{g}, \ell\}$:

ρ_k - density of phase k,
p_k - pressure of phase k,
v_k - velocity of phase k,
α_k - volume fraction of phase k,
e_k - specific internal energy of phase k,
p^{i} - pressure at the gas-liquid interface,
v^{i} - local velocity at the gas-liquid interface.

Furthermore, μ_v and μ_p are relaxation coefficients and the following relation holds:

$$\alpha_{\mathrm{g}} + \alpha_\ell = 1. \tag{19}$$

Munkejord [15] fixed $\mu_v = 0$ and studied the resulting relaxation system for $\mu_p \to \infty$, with an emphasis on assessing a relaxation scheme based on the Roe Riemann solver, and performing computations with finite μ_p. Here the energy equations were neglected.

Murrone and Guillard [16] and several other authors [9, 12, 21, 22] have performed analytical and numerical studies of the full relaxation process where both $\mu_p \to \infty$ and $\mu_v \to \infty$. This results in a five-equation simplified system also briefly described by Stewart and Wendroff [24]. This system may be written in the following form [16]:

$$\frac{\partial}{\partial t}(\rho_{\mathrm{g}} \alpha_{\mathrm{g}}) + \frac{\partial}{\partial x}(\rho_{\mathrm{g}} \alpha_{\mathrm{g}} v) = 0, \tag{20}$$

$$\frac{\partial}{\partial t}(\rho_\ell \alpha_\ell) + \frac{\partial}{\partial x}(\rho_\ell \alpha_\ell v) = 0, \tag{21}$$

$$\frac{\partial}{\partial t}(\rho v) + \frac{\partial}{\partial x}(\rho v + p) = 0, \tag{22}$$

$$\frac{\partial E}{\partial t} + \frac{\partial}{\partial x}\left(v(E+p)\right) = 0, \tag{23}$$

$$\frac{\partial \alpha_{\mathrm{g}}}{\partial t} + v \frac{\partial \alpha_{\mathrm{g}}}{\partial x} = \frac{\alpha_{\mathrm{g}} \alpha_\ell (\rho_\ell c_\ell^2 - \rho_{\mathrm{g}} c_{\mathrm{g}}^2)}{\alpha_\ell \rho_{\mathrm{g}} c_{\mathrm{g}}^2 + \alpha_{\mathrm{g}} \rho_\ell c_\ell^2} \frac{\partial v}{\partial x}, \tag{24}$$

where the mixture density ρ is given by

$$\rho = \rho_{\mathrm{g}} \alpha_{\mathrm{g}} + \rho_\ell \alpha_\ell, \tag{25}$$

the mixture total energy E is given by

$$E = \rho_{\mathrm{g}} \alpha_{\mathrm{g}} e_{\mathrm{g}} + \rho_\ell \alpha_\ell e_\ell + \frac{1}{2} \rho v^2, \tag{26}$$

and v and p are the velocity and pressure common to both phases. In addition to p, v, and α_{g}, the independent physical variables are here the temperatures T_{g} and T_ℓ.

1.4. Outline of this paper. This paper is motivated by the observation that most existing works related to the model (20)–(24) assume that the number of independent phases is fixed to 2. We are interested in generalizing this model to apply to an arbitrary number of components, and then applying relaxation heat-transfer terms

that will drive the model towards thermal equilibrium. In the fully relaxed limit, we then recover the *homogeneous equilibrium model*, studied, for instance, in [1, 18].

The usefulness of such an extension is twofold:

1. Several immiscible fluids may coexist without being in thermal equilibrium, and modeling individual temperatures for each species may be required. For instance, this can occur for mixtures of hydrocarbons and water relevant for the petroleum industry.
2. Direct equilibrium calculations for multicomponent mixtures are computationally expensive. Therefore, relaxation schemes based on nonequilibrium models may provide benefits in terms of efficiency compared to solving equilibrium models directly.

This paper is organized as follows: In section 2, we detail the models we will be working with. In section 2.1, we present the $(2N+1)$-equation relaxation model for N components involving N individual temperatures. We derive necessary and sufficient restrictions on the relaxation terms imposed by the first and second laws of thermodynamics. In section 2.1.2, we explicitly state our model in the form (1). In section 2.1.3, we show that our model reduces to the standard five-equation model for the special case $N = 2$. In section 2.2, we explicitly perform the relaxation procedure to recover the reduced form (6)–(7).

In sections 3.1–3.2, we obtain exact expressions for the wave velocities of the models. Our formulation allows for a direct proof that the subcharacteristic condition as stated in Definition 1 is satisfied. This is stated in section 3.2.4.

For completeness, we derive an explicit quasi-linear formulation of the relaxed system in section 3.3. In section 4, we summarize and comment on the results of our paper.

2. The models. The foundation for the models we consider in this paper consists of one mass conservation equation for each component,

$$\frac{\partial}{\partial t}\left(\rho_i \alpha_i\right) + \frac{\partial}{\partial x}\left(\rho_i \alpha_i v\right) = 0 \quad \forall i \in \{1, \ldots, N\}, \tag{27}$$

as well as a conservation equation for the total momentum of the mixture,

$$\frac{\partial \rho v}{\partial t} + \frac{\partial}{\partial x}\left(\rho v^2 + p\right) = 0, \tag{28}$$

where for the purposes of this analysis we neglect any momentum source terms. Here

ρ_i - density of component i,
ρ - density of the mixture,
v - velocity of the mixture,
α_i - volume fraction of component i,
p - pressure common to all components,

and the following relations hold:

$$\rho = \sum_{i=1}^{N} \rho_i \alpha_i, \tag{29}$$

$$\sum_{i=1}^{N} \alpha_i = 1. \tag{30}$$

We remind the reader that throughout the paper all derivatives will be interpreted in the classical (i.e., nondistributional) sense. We now state some observations that will prove useful later.

LEMMA 1. *The mixture density evolution equation can be written as*

$$\frac{\partial \rho}{\partial t} + \frac{\partial}{\partial x}(\rho v) = 0, \tag{31}$$

and the evolution equation for the mass fraction

$$Y_i = \frac{\rho_i \alpha_i}{\rho} \tag{32}$$

can be written as an advection equation:

$$\frac{\partial Y_i}{\partial t} + v \frac{\partial Y_i}{\partial x} = 0. \tag{33}$$

Proof. Sum (27) over all i to obtain (31). Write

$$\rho_i \alpha_i = \rho Y_i \tag{34}$$

and use (27) and (31) to recover (33). ∎

Remark 1. Note that since

$$\sum_{i=1}^{N} Y_i = 1, \tag{35}$$

we have only $N-1$ independent mass fraction equations, expressible in vector form

$$\frac{\partial \boldsymbol{Y}}{\partial t} + v \frac{\partial \boldsymbol{Y}}{\partial x} = 0, \tag{36}$$

where

$$\boldsymbol{Y} = \begin{bmatrix} Y_1 \\ \vdots \\ Y_{N-1} \end{bmatrix}. \tag{37}$$

LEMMA 2. *The following momentum evolution equation is valid for each component i:*

$$\frac{\partial}{\partial t}\left(\rho_i \alpha_i v\right) + \frac{\partial}{\partial x}\left(\rho_i \alpha_i v^2\right) + \frac{\rho_i \alpha_i}{\rho}\frac{\partial p}{\partial x} = 0. \tag{38}$$

Proof. We have

$$\mathrm{d}(\rho_i \alpha_i v) = \rho_i \alpha_i \,\mathrm{d}v + v\,\mathrm{d}(\rho_i \alpha_i) \tag{39}$$

and also

$$\mathrm{d}v = \frac{1}{\rho}\left(\mathrm{d}(\rho v) - v\,\mathrm{d}\rho\right). \tag{40}$$

Substituting (40) into (39), and using (27)–(28) and (31), we obtain

$$\frac{\partial}{\partial t}\left(\rho_i \alpha_i v\right) + \frac{\rho_i \alpha_i}{\rho}\left(\frac{\partial}{\partial x}(\rho v^2 + p) - v\frac{\partial}{\partial x}(\rho v)\right) + v\frac{\partial}{\partial x}(\rho_i \alpha_i v) = 0, \tag{41}$$

which simplifies to

$$\frac{\partial}{\partial t}(\rho_i\alpha_i v) + \rho_i\alpha_i v\frac{\partial v}{\partial x} + \frac{\rho_i\alpha_i}{\rho}\frac{\partial p}{\partial x} + v\frac{\partial}{\partial x}(\rho_i\alpha_i v) = 0 \tag{42}$$

by expansion of derivatives. Lemma 2 now follows from the product rule for derivatives. □

LEMMA 3. *The velocity evolution equation can be formulated as follows:*

$$\frac{\partial v}{\partial t} + v\frac{\partial v}{\partial x} + \frac{1}{\rho}\frac{\partial p}{\partial x} = 0, \tag{43}$$

and the following kinetic energy evolution equation is valid for each component i:

$$\frac{\partial}{\partial t}\left(\frac{1}{2}\rho_i\alpha_i v^2\right) + \frac{\partial}{\partial x}\left(\frac{1}{2}\rho_i\alpha_i v^3\right) + \frac{\rho_i\alpha_i v}{\rho}\frac{\partial p}{\partial x} = 0. \tag{44}$$

Proof. Expand derivatives in (38) and use (27) to obtain (43). Furthermore, expand the time derivative of (44) as

$$\frac{\partial}{\partial t}\left(\frac{1}{2}\rho_i\alpha_i v^2\right) = \frac{1}{2}v\frac{\partial}{\partial t}(\rho_i\alpha_i v) + \frac{1}{2}\rho_i\alpha_i v\frac{\partial v}{\partial t}. \tag{45}$$

If we now substitute (38) and (43) into (45), we recover (44) after collecting derivatives. □

2.1. Relaxation system. In this section, we derive separate energy evolution equations for each component, where heat is transferred between the components at a rate proportional to their temperature difference. We start with the assumption that in Lagrangian coordinates, entropy change is due only to the heat-transfer terms,

$$\rho_i\alpha_i T_i\left(\frac{\partial s_i}{\partial t} + v\frac{\partial s_i}{\partial x}\right) = \sum_{j\neq i} H_{ij}(T_j - T_i), \tag{46}$$

where

$$s_i = s_i(p, T_i) \tag{47}$$

is the specific entropy of component i. We further assume that the relaxation coefficients H_{ij} are independent of the temperatures T_k. From (46), we may then derive energy evolution equations for each component, using the kinetic energy equation (44) and the fundamental thermodynamic differential

$$\mathrm{d}e_i = T_i\,\mathrm{d}s_i + \frac{p}{\rho_i^2}\,\mathrm{d}\rho_i. \tag{48}$$

PROPOSITION 1. *To be consistent with the second law of thermodynamics, the relaxation coefficients H_{ij} must satisfy*

$$H_{ij} = H_{ji} \geq 0. \tag{49}$$

Proof. For the total cross-sectional entropy given by

$$\omega = \sum_{i=1}^{N} \rho_i\alpha_i s_i, \tag{50}$$

we obtain the evolution equation

$$\frac{\partial \omega}{\partial t} + \frac{\partial}{\partial x}(\omega v) = \sum_{i=1}^{N} \sum_{j \neq i} H_{ij} \frac{T_j - T_i}{T_i} \tag{51}$$

from (46). Now, inside a *closed* region R the global entropy Ω is given by

$$\Omega(t) = \int_R \omega(x,t)\,\mathrm{d}x. \tag{52}$$

Hence the second law

$$\frac{\mathrm{d}\Omega}{\mathrm{d}t} \geq 0 \tag{53}$$

imposes

$$\sum_{i=1}^{N} \sum_{j \neq i} H_{ij} \frac{T_j - T_i}{T_i} \geq 0. \tag{54}$$

Now

$$\begin{aligned} \sum_{i=1}^{N} \sum_{j \neq i} H_{ij} \frac{T_j - T_i}{T_i} &= \sum_{i,j>i} \left(\frac{H_{ij}}{T_i} - \frac{H_{ji}}{T_j} \right) (T_j - T_i) \\ &= \sum_{i,j>i} H_{ij} \frac{(T_j - T_i)^2}{T_i T_j} + \sum_{i,j>i} (H_{ij} - H_{ji}) \frac{T_j - T_i}{T_j}, \end{aligned} \tag{55}$$

which remains unconditionally nonnegative only if

$$H_{ij} \geq 0, \qquad H_{ij} - H_{ji} = 0 \qquad \forall i, j. \tag{56}$$

∎

PROPOSITION 2. *The entropy evolution equations* (46) *with the condition* (49) *respect conservation of total energy.*

Proof. From (46) and the fundamental differential (48), we obtain

$$\rho_i \alpha_i \left(\frac{\partial e_i}{\partial t} + v \frac{\partial e_i}{\partial x} \right) - \frac{p \alpha_i}{\rho_i} \left(\frac{\partial \rho_i}{\partial t} + v \frac{\partial \rho_i}{\partial x} \right) = \sum_{j \neq i} H_{ij} (T_j - T_i), \tag{57}$$

where e_i is the specific internal energy of component i. Using (27), we can rewrite this as

$$\frac{\partial}{\partial t}(\rho_i \alpha_i e_i) + \frac{\partial}{\partial x}(\rho_i \alpha_i e_i v) + p \left(\frac{\partial \alpha_i}{\partial t} + \frac{\partial}{\partial x}(\alpha_i v) \right) = \sum_{j \neq i} H_{ij} (T_j - T_i). \tag{58}$$

Summing over all i and using (30) we obtain

$$\frac{\partial}{\partial t} \left(\sum_{i=1}^{N} \rho_i \alpha_i e_i \right) + \frac{\partial}{\partial x} \left(v \sum_{i=1}^{N} \rho_i \alpha_i e_i \right) + p \frac{\partial v}{\partial x} = \sum_{i=1}^{N} \sum_{j \neq i} H_{ij} (T_j - T_i), \tag{59}$$

which by (49) may be simplified to

$$\frac{\partial}{\partial t}\left(\sum_{i=1}^{N}\rho_i\alpha_i e_i\right)+\frac{\partial}{\partial x}\left(v\sum_{i=1}^{N}\rho_i\alpha_i e_i\right)+p\frac{\partial v}{\partial x}=0. \tag{60}$$

We now define the total energy E as

$$E=\sum_{i=1}^{N}\rho_i\alpha_i\left(e_i+\frac{1}{2}v^2\right). \tag{61}$$

Summing (44) over all i and adding (60), we obtain an evolution equation for E in conservative form:

$$\frac{\partial E}{\partial t}+\frac{\partial}{\partial x}\left(v(E+p)\right)=0. \tag{62}$$ ∎

2.1.1. Energy evolution equations. In this section, we aim to transform (46) into evolution equations for the energy E_i of each component:

$$E_i=\rho_i\alpha_i\left(\frac{1}{2}v^2+e_i\right). \tag{63}$$

We start by deriving some preliminary results.

LEMMA 4. *The pressure evolution equation can be written as*

$$\frac{\partial p}{\partial t}+v\frac{\partial p}{\partial x}+\rho c^2\frac{\partial v}{\partial x}=\rho c^2\sum_{i,j>i}\left(H_{ij}\left(\frac{\Gamma_i}{\rho_i c_i^2}-\frac{\Gamma_j}{\rho_j c_j^2}\right)(T_j-T_i)\right), \tag{64}$$

where

$$c^2=\left(\rho\sum_{i=1}^{N}\frac{\alpha_i}{\rho_i c_i^2}\right)^{-1}. \tag{65}$$

Here

$$c_i^2=\left(\frac{\partial p}{\partial \rho_i}\right)_{s_i} \tag{66}$$

represents the single-component velocity of sound, and Γ_i *is the Grüneisen coefficient*

$$\Gamma_i=\frac{1}{\rho_i}\left(\frac{\partial p}{\partial e_i}\right)_{\rho_i}. \tag{67}$$

Proof. The differential (48) may be rewritten as

$$\mathrm{d}p=c_i^2\,\mathrm{d}\rho_i+\Gamma_i\rho_i T_i\,\mathrm{d}s_i. \tag{68}$$

From (68) and (46) we obtain

$$\frac{\partial p}{\partial t}+v\frac{\partial p}{\partial x}=c_i^2\left(\frac{\partial \rho_i}{\partial t}+v\frac{\partial \rho_i}{\partial x}\right)+\frac{\Gamma_i}{\alpha_i}\sum_{j\neq i}H_{ij}(T_j-T_i), \tag{69}$$

which by (27) may be rewritten as

$$\frac{\alpha_i}{\rho_i c_i^2}\left(\frac{\partial p}{\partial t}+v\frac{\partial p}{\partial x}\right)+\frac{\partial \alpha_i}{\partial t}+\frac{\partial}{\partial x}\left(\alpha_i v\right)=\frac{\Gamma_i}{\rho_i c_i^2}\sum_{j\neq i}H_{ij}(T_j-T_i). \tag{70}$$

Lemma 4 follows from summing over all i. ∎

LEMMA 5. *The internal energy evolution equation for component i can be written as*

$$\begin{aligned}\frac{\partial}{\partial t}\left(\rho_i\alpha_i e_i\right)+\frac{\partial}{\partial x}\left(\rho_i\alpha_i e_i v\right)+\alpha_i p\frac{\rho c^2}{\rho_i c_i^2}\frac{\partial v}{\partial x}\\ =\theta_i\sum_{j\neq i}H_{ij}(T_j-T_i)+\frac{\rho c^2}{\rho_i c_i^2}\alpha_i\sum_{k,j>k}\left(H_{kj}(\theta_j-\theta_k)(T_j-T_k)\right),\end{aligned} \tag{71}$$

where

$$\theta_i=1-\frac{\Gamma_i p}{\rho_i c_i^2}\equiv\frac{1}{T_i}\left(\frac{\partial e_i}{\partial s_i}\right)_p. \tag{72}$$

Proof. Substitute (70) into (58) to obtain

$$\frac{\partial}{\partial t}\left(\rho_i\alpha_i e_i\right)+\frac{\partial}{\partial x}\left(\rho_i\alpha_i e_i v\right)-\frac{\alpha_i p}{\rho_i c_i^2}\left(\frac{\partial p}{\partial t}+v\frac{\partial p}{\partial x}\right)=\left(1-\frac{\Gamma_i p}{\rho_i c_i^2}\right)\sum_{j\neq i}H_{ij}(T_j-T_i). \tag{73}$$

Now (71) follows by substituting (64) into (73). ∎

PROPOSITION 3. *The evolution equation for the total energy of component i can be written as*

$$\begin{aligned}\frac{\partial E_i}{\partial t}+\frac{\partial}{\partial x}\left(E_i v\right)+\frac{\rho_i\alpha_i v}{\rho}\frac{\partial p}{\partial x}+\alpha_i p\frac{\rho c^2}{\rho_i c_i^2}\frac{\partial v}{\partial x}\\ =\theta_i\sum_{j\neq i}H_{ij}(T_j-T_i)+\frac{\rho c^2}{\rho_i c_i^2}\alpha_i\sum_{k,j>k}\left(H_{kj}(\theta_j-\theta_k)(T_j-T_k)\right),\end{aligned} \tag{74}$$

or equivalently

$$\begin{aligned}\frac{\partial E_i}{\partial t}+\frac{\partial}{\partial x}\left(E_i v\right)+\frac{\rho_i\alpha_i}{\rho}\frac{\partial}{\partial x}\left(pv\right)+\alpha_i p\left(\frac{\rho^2c^2-\rho_i^2c_i^2}{\rho\rho_i c_i^2}\right)\frac{\partial v}{\partial x}\\ =\theta_i\sum_{j\neq i}H_{ij}(T_j-T_i)+\frac{\rho c^2}{\rho_i c_i^2}\alpha_i\sum_{k,j>k}\left(H_{kj}(\theta_j-\theta_k)(T_j-T_k)\right).\end{aligned} \tag{75}$$

Proof. Add (44) and (71) to obtain (74). ∎

2.1.2. Canonical relaxation form. In this section, we explicitly express the above model in the form (1). We emphasize that since the system is partially non-conservative, there is no obvious preferred choice of variables in which to express the balance equations; however, conservation of total energy must be respected.

For the $(N = 2)$-model previously investigated, the authors [9, 12, 16, 21, 22] commonly choose to express the equations in terms of total energy and volume fraction, as stated by (20)–(24). This formulation naturally follows from performing the relaxation procedure on the model (12)–(18).

However, to preserve the symmetry in the equations, we here choose to express our model in terms of the energy evolution equations for each component. Summing these equations then automatically yields conservation of total energy, as stated by Proposition 2. In the context of (1), we obtain

$$\boldsymbol{U} = \begin{bmatrix} \rho_1\alpha_1 \\ \vdots \\ \rho_N\alpha_N \\ \rho v \\ E_1 \\ \vdots \\ E_N \end{bmatrix}, \qquad \boldsymbol{F}(\boldsymbol{U}) = \begin{bmatrix} \rho_1\alpha_1 v \\ \vdots \\ \rho_N\alpha_N v \\ \rho v^2 + p \\ E_1 v \\ \vdots \\ E_N v \end{bmatrix}, \qquad \boldsymbol{W}(\boldsymbol{U}) = \begin{bmatrix} pv \\ v \end{bmatrix}. \tag{76}$$

Furthermore, the $(2N+1) \times 2$ matrix $\boldsymbol{A}$ is given by

$$\boldsymbol{A}(\boldsymbol{U}) = \frac{1}{\rho} \begin{bmatrix} 0 & 0 \\ \vdots & \vdots \\ 0 & 0 \\ 0 & 0 \\ \rho_1\alpha_1 & \alpha_1 p \left(\frac{\rho^2 c^2 - \rho_1^2 c_1^2}{\rho_1 c_1^2} \right) \\ \vdots & \vdots \\ \rho_N\alpha_N & \alpha_N p \left(\frac{\rho^2 c^2 - \rho_N^2 c_N^2}{\rho_N c_N^2} \right) \end{bmatrix}. \tag{77}$$

The relaxation source term is given by

$$\boldsymbol{R}(\boldsymbol{U}) = - \begin{bmatrix} 0 \\ \vdots \\ 0 \\ 0 \\ \theta_1 \sum_{j \neq 1} h_{1j}(T_j - T_1) + \frac{\rho c^2}{\rho_1 c_1^2} \alpha_1 \sum_{k,j>k} \left(h_{kj}(\theta_j - \theta_k)(T_j - T_k) \right) \\ \vdots \\ \theta_N \sum_{j \neq N} h_{Nj}(T_j - T_N) + \frac{\rho c^2}{\rho_N c_N^2} \alpha_N \sum_{k,j>k} \left(h_{kj}(\theta_j - \theta_k)(T_j - T_k) \right) \end{bmatrix}, \tag{78}$$

where

$$h_{ij} = \epsilon H_{ij}. \tag{79}$$

2.1.3. Relation to five-equation model. In this section, we wish to illustrate that our model essentially reduces to the five-equation model [9, 12, 16, 21, 22] for the special case $N = 2$.

From our general model (76)–(78), we may derive an evolution equation for the volume fraction.

LEMMA 6. *The evolution equation for the volume fraction of component i can be written as*

$$\begin{aligned}(80)\quad &\frac{\partial \alpha_i}{\partial t} + v\frac{\partial \alpha_i}{\partial x} + \alpha_i \frac{\rho_i c_i^2 - \rho c^2}{\rho_i c_i^2}\frac{\partial v}{\partial x} \\ &\quad = \frac{\Gamma_i}{\rho_i c_i^2}\sum_{j\neq i} H_{ij}(T_j - T_i) - \alpha_i \frac{\rho c^2}{\rho_i c_i^2}\sum_{k,j>k}\left(H_{kj}\left(\frac{\Gamma_k}{\rho_k c_k^2} - \frac{\Gamma_j}{\rho_j c_j^2}\right)(T_j - T_k)\right).\end{aligned}$$

Proof. Substitute (64) into (70) and expand derivatives. ∎

Now for $N = 2$, this may be written as

$$\begin{aligned}(81)\quad &\frac{\partial \alpha_1}{\partial t} + v\frac{\partial \alpha_1}{\partial x} = \frac{\alpha_1\alpha_2(\rho_2 c_2^2 - \rho_1 c_1^2)}{\alpha_2\rho_1 c_1^2 + \alpha_1\rho_2 c_2^2}\frac{\partial v}{\partial x} \\ &\qquad + \frac{\alpha_1\alpha_2}{\alpha_2\rho_1 c_1^2 + \alpha_1\rho_2 c_2^2}\left(\frac{\Gamma_1}{\alpha_1} + \frac{\Gamma_2}{\alpha_2}\right)H_{12}(T_2 - T_1).\end{aligned}$$

Augmenting this with the mass, total momentum, and total energy equations (20)–(23), we recover the formulation of the five-equation model stated in [21, section 5.5].

2.2. Relaxed system. We now consider the system obtained by letting the relaxation coefficients H_{ij} tend to infinity; i.e., we achieve instantaneous thermal equilibrium. In addition to the mass and momentum conservation equations (27) and (28), we replace the componentwise energy evolution equations (74) with the following.

• *Equality of temperatures:*

$$(82)\qquad T_i = T_j = T \quad \forall i, j.$$

• *Conservation of total energy:*

$$(83)\qquad \frac{\partial E}{\partial t} + \frac{\partial}{\partial x}\left(v(E+p)\right) = 0.$$

In the context of section 1, the $(N+2)\times(2N+1)$ matrix $\mathcal{Q}$ is given by

$$(84)\qquad \mathcal{Q} = [Q_{ij}], \qquad Q_{ij} = \begin{cases} 1 & \text{if } i = j, \\ 1 & \text{if } j > i \text{ and } i = N+2, \\ 0 & \text{otherwise.}\end{cases}$$

We may then verify that (2) holds. Furthermore, we obtain

$$(85)\qquad \boldsymbol{V}(\boldsymbol{U}) = \begin{bmatrix}\rho_1\alpha_1 \\ \vdots \\ \rho_N\alpha_N \\ \rho v \\ E\end{bmatrix}, \qquad \boldsymbol{G}(\boldsymbol{U}) = \begin{bmatrix}0 \\ \vdots \\ 0 \\ 0 \\ pv\end{bmatrix}, \qquad \mathcal{Q}\boldsymbol{F}(\boldsymbol{U}) = \begin{bmatrix}\rho_1\alpha_1 v \\ \vdots \\ \rho_N\alpha_N v \\ \rho v^2 + p \\ Ev\end{bmatrix},$$

and the local equilibrium value $\mathcal{E}(\boldsymbol{V})$ is determined by (82).

Remark 2. Note that the matrix $\mathcal{Q}$ reduces to the identity matrix for the special case $N = 1$, where the equilibrium condition is already satisfied by the relaxation system. However, in section 1, we explicitly assume that

$$(86)\qquad \operatorname{rank}(\mathcal{Q}) < M = 2N + 1.$$

Throughout this paper, we will assume that $N \geq 2$ so that (86) holds.

3. Wave structure. In this section, we derive the wave velocities associated with the relaxation and relaxed models, formally given by the eigenvalues of the coefficient matrix of the system in quasi-linear form. Our derivation will rely heavily on the similarities between our systems and the well-known Euler system for single-component gas dynamics.

3.1. Relaxation system. System (76)–(78) may be expressed in an alternative form as a composition of 3 parts:

- an "isentropic Euler part" consisting of (28) and (31);
- a mass fraction part (36);
- an entropy part (46).

From (36) and (46) we immediately see that s_i and $\boldsymbol{Y}$ are characteristic variables. Hence v is an eigenvalue of the system with multiplicity $(2N-1)$, corresponding to N entropy waves and $N-1$ mass fraction waves.

From (28) and (31) we then obtain the remaining eigenvalues:

$$\lambda = v \pm \hat{c}, \tag{87}$$

where

$$\hat{c}^2 = \left(\frac{\partial p}{\partial \rho}\right)_{\boldsymbol{Y},s_1,\ldots,s_N}. \tag{88}$$

PROPOSITION 4. *The mixture sonic velocity $\hat{c}$ is given by*

$$\hat{c}^2 = \left(\rho \sum_{i=1}^{N} \frac{\alpha_i}{\rho_i c_i^2}\right)^{-1}. \tag{89}$$

Proof. Consider the differential

$$\sum_{i=1}^{N} \frac{\mathrm{d}(\rho_i \alpha_i)}{\rho_i} = \sum_{i=1}^{N} \mathrm{d}\alpha_i + \sum_{i=1}^{N} \left(\frac{\alpha_i}{\rho_i}\,\mathrm{d}\rho_i\right) = \sum_{i=1}^{N} \left(\frac{\alpha_i}{\rho_i c_i^2}\,\mathrm{d}p + \mathcal{O}(\mathrm{d}s_i)\right), \tag{90}$$

which can also be written as

$$\sum_{i=1}^{N} \frac{\mathrm{d}(\rho_i \alpha_i)}{\rho_i} = \sum_{i=1}^{N} \frac{\mathrm{d}(\rho Y_i)}{\rho_i} = \rho \sum_{i=1}^{N} \frac{\mathrm{d}Y_i}{\rho_i} + \sum_{i=1}^{N} \left(\frac{Y_i}{\rho_i}\right) \mathrm{d}\rho. \tag{91}$$

We then have

$$\hat{c}^2 = \left(\frac{\partial p}{\partial \rho}\right)_{\boldsymbol{Y},s_1,\ldots,s_N} = \frac{\sum_{i=1}^{N} \frac{Y_i}{\rho_i}}{\sum_{i=1}^{N} \frac{\alpha_i}{\rho_i c_i^2}}, \tag{92}$$

and (89) follows. ∎

Remark 3. Note that when $N = 2$, (89) reduces to a classical expression for the two-phase sonic velocity, sometimes referred to as the "Wood speed of sound" [21]. This expression is also derived in [17] by considering one phase as an elastic wall for the other.

3.2. Relaxed system. The relaxed system (85) may also be expressed in a convenient alternative form as

- a mass fraction part (36);
- a "mixture Euler" part consisting of

$$\frac{\partial \rho}{\partial t} + \frac{\partial}{\partial x}(\rho v) = 0, \tag{93}$$

$$\frac{\partial}{\partial t}(\rho v) + \frac{\partial}{\partial x}(\rho v^2 + p) = 0, \tag{94}$$

$$\frac{\partial E}{\partial t} + \frac{\partial}{\partial x}\left((E+p)v\right). \tag{95}$$

From (36) we see that there are $N-1$ characteristics with velocity v corresponding to mass fraction waves. The remaining 3 eigenvalues may now be found from the Euler system (93)–(95) by means of the following result.

PROPOSITION 5. *The mixture entropy given by*

$$s = \sum_{i=1}^{N} Y_i s_i \tag{96}$$

satisfies the characteristic equation

$$\frac{\partial s}{\partial t} + v\frac{\partial s}{\partial x} = 0. \tag{97}$$

Proof. The assumption of immiscibility implies that the differential (48) holds individually for each component. Substituting (48) into (95) and using (61), we recover (97) by textbook simplifications made possible by (93) and (94). ∎

Hence, in addition to the $N-1$ mass fraction waves and the mixture entropy wave (97), we obtain two sonic waves with velocities $v \pm \tilde{c}$, calculated in a standard way from the reduced Euler system (93)–(94). Herein, the sonic velocity $\tilde{c}$ is given by

$$\tilde{c} = \left(\frac{\partial p}{\partial \rho}\right)_{\boldsymbol{Y},s}. \tag{98}$$

3.2.1. Some thermodynamic derivatives. In order to obtain an explicit expression for $\tilde{c}$, we will first need some intermediate results. In particular, the following parameter will prove useful:

$$\zeta_i = \left(\frac{\partial T}{\partial p}\right)_{s_i} = -\frac{1}{\rho_i^2}\left(\frac{\partial \rho_i}{\partial s_i}\right)_p. \tag{99}$$

LEMMA 7. *The following thermodynamic derivatives may be expressed in terms of ζ:*

$$\left(\frac{\partial s_i}{\partial p}\right)_T = \frac{1}{\rho_i^2}\left(\frac{\partial \rho_i}{\partial T}\right)_p = -\frac{\zeta_i c_{p,i}}{T}, \tag{100}$$

$$\left(\frac{\partial \rho_i}{\partial p}\right)_T = \frac{1}{c_i^2} + \frac{\rho_i^2 \zeta_i^2 c_{p,i}}{T}, \tag{101}$$

$$\left(\frac{\partial e_i}{\partial T}\right)_p = c_{p,i}\left(1 - \zeta_i \frac{p}{T}\right), \tag{102}$$

$$\left(\frac{\partial e_i}{\partial p}\right)_T = \frac{p}{(\rho_i c_i)^2} - \zeta_i c_{p,i}\left(1 - \zeta_i \frac{p}{T}\right), \tag{103}$$

where the specific heat capacity $c_{p,i}$ is given by

$$c_{p,i} = T\left(\frac{\partial s_i}{\partial T}\right)_p. \tag{104}$$

Proof. From (99) and (104) we directly obtain (100). Furthermore, we obtain (101) from (66), (99), (104), and the relation

$$\left(\frac{\partial \rho_i}{\partial p}\right)_T = \left(\frac{\partial \rho_i}{\partial p}\right)_{s_i} + \left(\frac{\partial \rho_i}{\partial s_i}\right)_p \left(\frac{\partial s_i}{\partial p}\right)_T. \tag{105}$$

The result (102) follows from

$$\left(\frac{\partial e_i}{\partial T}\right)_p = T\left(\frac{\partial s_i}{\partial T}\right)_p + \frac{p}{\rho_i^2}\left(\frac{\partial \rho_i}{\partial T}\right)_p \tag{106}$$

and (100). Finally, (103) follows from

$$\left(\frac{\partial e_i}{\partial p}\right)_T = T\left(\frac{\partial s_i}{\partial p}\right)_T + \frac{p}{\rho_i^2}\left(\frac{\partial \rho_i}{\partial p}\right)_T \tag{107}$$

as well as (100) and (101). ∎

As we will see in the following section, expressing the relaxed sound velocity $\tilde{c}$ in terms of the parameter ζ will lead to significant simplifications.

3.2.2. The relaxed sound velocity $\tilde{c}$. Armed with these results, we are now able to obtain an explicit expression for $\tilde{c}$ as given by (98). To this end, we first state the following lemma.

LEMMA 8. *The differential* (90) *can be written as*

$$\begin{aligned}\sum_{i=1}^N \frac{\mathrm{d}(\rho_i\alpha_i)}{\rho_i} &= \sum_{i=1}^N \left(\frac{\alpha_i}{\rho_i c_i^2}\right)\mathrm{d}p - \rho\frac{\sum_{i=1}^N \zeta_i C_{p,i}}{\sum_{i=1}^N C_{p,i}}\,\mathrm{d}s \\ &\quad + \left(T\sum_{i=1}^N C_{p,i}\right)^{-1}\left(\sum_{i=1}^N \zeta_i^2 C_{p,i}\cdot\sum_{i=1}^N C_{p,i} - \left(\sum_{i=1}^N \zeta_i C_{p,i}\right)^2\right)\mathrm{d}p + \mathcal{O}(\mathrm{d}\boldsymbol{Y}),\end{aligned} \tag{108}$$

where the extensive heat capacity $C_{p,i}$ is given by

$$C_{p,i} = \rho_i\alpha_i c_{p,i}. \tag{109}$$

Proof. Use (100) and (101) to obtain

$$\sum_{i=1}^N \frac{\mathrm{d}(\rho_i\alpha_i)}{\rho_i} = \sum_{i=1}^N \left(\frac{\alpha_i}{\rho_i}\,\mathrm{d}\rho_i\right) = \sum_{i=1}^N \left(\frac{\alpha_i}{\rho_i c_i^2} + \zeta_i^2\frac{C_{p,i}}{T}\right)\mathrm{d}p - \sum_{i=1}^N \left(\zeta_i\frac{C_{p,i}}{T}\right)\mathrm{d}T. \tag{110}$$

Furthermore, use (100) and (104) when differentiating (96) to obtain

$$\mathrm{d}s = \sum_{i=1}^N \left(Y_i\frac{c_{p,i}}{T}\right)\mathrm{d}T - \sum_{i=1}^N \left(Y_i\zeta_i\frac{c_{p,i}}{T}\right)\mathrm{d}p + \mathcal{O}(\mathrm{d}\boldsymbol{Y}). \tag{111}$$

Substitute (111) for $\mathrm{d}T$ in (110), and (108) follows. ∎

To achieve further simplification, we will find use for a general summation lemma.

LEMMA 9.

$$\sum_i (x_i^2 y_i) \cdot \sum_i y_i - \left(\sum_i (x_i y_i) \right)^2 = \sum_{j>i} y_i y_j (x_j - x_i)^2. \tag{112}$$

Proof.

$$\begin{aligned}
&\sum_i (x_i^2 y_i) \cdot \sum_i y_i - \left(\sum_i (x_i y_i) \right)^2 \\
&= \sum_i (x_i^2 y_i^2) + \sum_{i \neq j} x_i^2 y_i y_j - \sum_i (x_i^2 y_i^2) - \sum_{i \neq j} x_i x_j y_i y_j \\
&= \sum_{i \neq j} \left(x_i^2 y_i y_j - x_i x_j y_i y_j \right) = \sum_{j>i} \left((x_i^2 + x_j^2) y_i y_j - 2 x_i x_j y_i y_j \right) \\
&= \sum_{j>i} y_i y_j (x_j - x_i)^2. \qquad \square
\end{aligned} \tag{113}$$

PROPOSITION 6. *The relaxed mixture sonic velocity* (98) *may be written as*

$$\tilde{c}^{-2} = \hat{c}^{-2} + \rho \left(T \sum_{i=1}^N C_{p,i} \right)^{-1} \sum_{j>i} C_{p,i} C_{p,j} (\zeta_j - \zeta_i)^2, \tag{114}$$

where $\hat{c}$*, given by* (89)*, is the mixture sonic velocity of the relaxation system of section* 2.1.

Proof. Lemma 9 allows us to write (108) as

$$\begin{aligned}
\sum_{i=1}^N \frac{\mathrm{d}(\rho_i \alpha_i)}{\rho_i} = &\left(\sum_{i=1}^N \frac{\alpha_i}{\rho_i c_i^2} + \left(T \sum_{i=1}^N C_{p,i} \right)^{-1} \sum_{j>i} C_{p,i} C_{p,j} (\zeta_j - \zeta_i)^2 \right) \mathrm{d}p \\
&- \rho \frac{\sum_{i=1}^N \zeta_i C_{p,i}}{\sum_{i=1}^N C_{p,j}} \, \mathrm{d}s + \mathcal{O}(\mathrm{d}\boldsymbol{Y}).
\end{aligned} \tag{115}$$

Using (91), we may then express the mixture sound velocity as

$$\tilde{c}^{-2} = \left(\frac{\partial \rho}{\partial p} \right)_{\boldsymbol{Y},s} = \left(\sum_{i=1}^N \frac{Y_i}{\rho_i} \right)^{-1} \left(\sum_{i=1}^N \frac{\alpha_i}{\rho_i c_i^2} + \left(T \sum_{i=1}^N C_{p,i} \right)^{-1} \sum_{j>i} C_{p,i} C_{p,j} (\zeta_j - \zeta_i)^2 \right), \tag{116}$$

and (114) follows. $\square$

3.2.3. Alternative formulations. Several equivalent formulations of the equilibrium mixture sound velocity $\tilde{c}$ are known from the literature. For equilibrium flow of two immiscible components, Städtke [23] obtained the following result:

$$\tilde{c}^{-2} = \rho \left(\alpha_1 \gamma_1 + \alpha_2 \gamma_2 - \frac{T}{C_{p,1} + C_{p,2}} (\alpha_1 \beta_1 + \alpha_2 \beta_2)^2 \right), \tag{117}$$

where

$$\beta_i = -\frac{1}{\rho_i}\left(\frac{\partial \rho_i}{\partial T}\right)_p, \tag{118}$$

$$\gamma_i = \frac{1}{\rho_i}\left(\frac{\partial \rho_i}{\partial p}\right)_T. \tag{119}$$

PROPOSITION 7. *The expression* (114) *is equivalent to* (117) *when* $N = 2$.

Proof. Using (100) and (101) to substitute for β_i and γ_i in (117), we recover

$$\tilde{c}^{-2} = \hat{c}^{-2} + \frac{\rho}{T}\frac{C_{p,1}C_{p,2}(\zeta_2 - \zeta_1)^2}{C_{p,1} + C_{p,2}}, \tag{120}$$

which corresponds to (114) for $N = 2$. ∎

Furthermore, Abgrall [1] derived the general result

$$\tilde{c}^2 = \sum_{i=1}^{N} Y_i \mathcal{P}_i + \frac{\rho e + p}{\rho}\mathcal{P}_\epsilon, \tag{121}$$

where the parameters $\mathcal{P}$ are defined through

$$\mathrm{d}p = \sum_{i=1}^{N} \mathcal{P}_i \,\mathrm{d}(\rho_i \alpha_i) + \mathcal{P}_\epsilon \,\mathrm{d}(\rho e) \tag{122}$$

with

$$e = \sum_{i=1}^{N} Y_i e_i. \tag{123}$$

In section 3.3, we will show that the expression (114) can be written in the form (121) for our model.

3.2.4. The subcharacteristic condition. Although related formulations of the mixture sound velocity $\tilde{c}$ already exist in the literature, the particular formulation (114) we have obtained in this paper will now prove useful. In particular, it straightforwardly leads to the following result.

PROPOSITION 8. *Assume that the relaxation sonic velocity* $\hat{c}$ *given by* (89) *is real and nonzero, i.e.,* $\hat{c}^2 > 0$. *Then the relaxed system of section* 2.2 *satisfies the subcharacteristic condition given by Definition* 1*, with respect to the relaxation system of section* 2.1*, subject only to the condition*

$$C_{p,i} > 0 \qquad \forall i, \tag{124}$$

which is assured by thermodynamic stability theory.

Proof. We observe that the difference

$$\tilde{c}^{-2} - \hat{c}^{-2} = \rho\left(T\sum_{i=1}^{N} C_{p,i}\right)^{-1} \sum_{j>i} C_{p,i}C_{p,j}(\zeta_j - \zeta_i)^2 \tag{125}$$

is strictly nonnegative under the condition (124). Hence

$$\tilde{c} \le \hat{c}, \tag{126}$$

and the equality holds only if all ζ_i are equal. Furthermore, in the context of Definition 1, we have that $M = 2N + 1$ and $m = N + 2$, and we assume that $N \geq 2$ as stated in Remark 2. The eigenvalues are given by

$$\lambda_1 = v - \hat{c}, \tag{127}$$

$$\lambda_2, \ldots, \lambda_{2N} = v, \tag{128}$$

$$\lambda_{2N+1} = v + \hat{c} \tag{129}$$

and

$$\tilde{\lambda}_1 = v - \tilde{c}, \tag{130}$$

$$\tilde{\lambda}_2, \ldots, \tilde{\lambda}_{N+1} = v, \tag{131}$$

$$\tilde{\lambda}_{N+2} = v + \tilde{c}. \tag{132}$$

The interlacing condition of Definition 1 becomes

$$\tilde{\lambda}_j \in [\lambda_j, \lambda_{j+N-1}] \quad \forall j, \tag{133}$$

which by inspection of (127)–(132) yields the conditions

$$v - \tilde{c} \in [v - \hat{c}, v], \tag{134}$$

$$v \in [v, v], \tag{135}$$

$$v + \tilde{c} \in [v, v + \hat{c}], \tag{136}$$

which by (126) are all satisfied. □

3.3. Quasi-linear formulation. In this section, we derive an explicit quasi-linear formulation of the relaxed system described in section 2.2. More precisely, we express the system in the form

$$\frac{\partial \boldsymbol{V}}{\partial t} + \mathcal{A}(\boldsymbol{V}) \frac{\partial \boldsymbol{V}}{\partial x} = 0, \tag{137}$$

where

$$\mathcal{A}(\boldsymbol{V}) = \frac{\partial \mathcal{F}(\boldsymbol{V})}{\partial \boldsymbol{V}}. \tag{138}$$

In addition to facilitating further analysis, such a formulation provides advantages when devising numerical methods for the model. An application of this has already been presented in [14].

3.3.1. Some intermediate results. We will start by deriving some intermediate differentials that will prove useful for our further analysis.

LEMMA 10. *The internal-energy differentials satisfy*

$$\begin{aligned} \sum_{i=1}^{N} V_i \, \mathrm{d}e_i = & \left(p - T \frac{\sum_{i=1}^{N} C_{p,i}}{\sum_{i=1}^{N} \zeta_i C_{p,i}} \right) \sum_{i=1}^{N} \frac{\mathrm{d}V_i}{\rho_i} \\ & + \left(\frac{T}{\rho \hat{c}^2} \frac{\sum_{i=1}^{N} C_{p,i}}{\sum_{i=1}^{N} \zeta_i C_{p,i}} + \frac{\sum_{j>i} C_{p,i} C_{p,j} (\zeta_j - \zeta_i)^2}{\sum_{i=1}^{N} \zeta_i C_{p,i}} \right) \mathrm{d}p. \end{aligned} \tag{139}$$

Proof. Use (102) and (103), as well as the definition (89), to obtain

$$\sum_{i=1}^{N} V_i \,\mathrm{d}e_i = \sum_{i=1}^{N} \left(C_{p,i} \left(1 - \zeta_i \frac{p}{T} \right) \right) \mathrm{d}T + \left(\frac{p}{\rho \tilde{c}^2} - \sum_{i=1}^{N} \zeta_i C_{p,i} \left(1 - \zeta_i \frac{p}{T} \right) \right) \mathrm{d}p. \tag{140}$$

Use (110) to eliminate $\mathrm{d}T$ from (140), and simplify by use of Lemma 9. ∎

LEMMA 11. *The total specific internal-energy differential may be expressed as*

$$\mathrm{d}(\rho e) = \sum_{i=1}^{N} \left(e_i + \frac{p}{\rho_i} \right) \mathrm{d}V_i - T \frac{\sum_{i=1}^{N} C_{p,i}}{\sum_{i=1}^{N} \zeta_i C_{p,i}} \sum_{i=1}^{N} \frac{\mathrm{d}V_i}{\rho_i} + \frac{T}{\rho \tilde{c}^2} \frac{\sum_{i=1}^{N} C_{p,i}}{\sum_{i=1}^{N} \zeta_i C_{p,i}} \mathrm{d}p. \tag{141}$$

Proof. Use

$$\sum_{i=1}^{N} V_i \,\mathrm{d}e_i = \mathrm{d}(\rho e) - \sum_{i=1}^{N} e_i \,\mathrm{d}V_i \tag{142}$$

in (139) and simplify using (114). ∎

LEMMA 12. *The pressure differential may be expressed as*

$$\mathrm{d}p = \rho \tilde{c}^2 \sum_{i=1}^{N} \frac{\mathrm{d}V_i}{\rho_i} - \frac{\rho \tilde{c}^2}{T} \frac{\sum_{i=1}^{N} \zeta_i C_{p,i}}{\sum_{i=1}^{N} C_{p,i}} \left(\sum_{i=1}^{N} \left(e_i + \frac{p}{\rho_i} - \frac{1}{2} v^2 \right) \mathrm{d}V_i + v \,\mathrm{d}V_{N+1} - \mathrm{d}V_{N+2} \right). \tag{143}$$

Proof. Use

$$\mathrm{d}(\rho e) = \frac{1}{2} v^2 \sum_{i=1}^{N} \mathrm{d}V_i - v \,\mathrm{d}V_{N+1} + \mathrm{d}V_{N+2} \tag{144}$$

in (141) and solve for $\mathrm{d}p$. ∎

LEMMA 13. *The pressure-transport differential may be expressed as*

$$\begin{aligned} \mathrm{d}(pv) = {} & v \rho \tilde{c}^2 \sum_{i=1}^{N} \frac{\mathrm{d}V_i}{\rho_i} - v \frac{\rho \tilde{c}^2}{T} \frac{\sum_{i=1}^{N} \zeta_i C_{p,i}}{\sum_{i=1}^{N} C_{p,i}} \sum_{i=1}^{N} \left(e_i + \frac{p}{\rho_i} - \frac{1}{2} v^2 \right) \mathrm{d}V_i - \frac{pv}{\rho} \sum_{i=1}^{N} \mathrm{d}V_i \\ & \left(\frac{p}{\rho} - v^2 \frac{\rho \tilde{c}^2}{T} \frac{\sum_{i=1}^{N} \zeta_i C_{p,i}}{\sum_{i=1}^{N} C_{p,i}} \right) \mathrm{d}V_{N+1} + v \frac{\rho \tilde{c}^2}{T} \frac{\sum_{i=1}^{N} \zeta_i C_{p,i}}{\sum_{i=1}^{N} C_{p,i}} \,\mathrm{d}V_{N+2}. \end{aligned} \tag{145}$$

Proof. Use

$$\mathrm{d}(pv) = v \,\mathrm{d}p + p \,\mathrm{d}v \tag{146}$$

together with (29) and (40) in (143). ∎

3.3.2. The Jacobi matrix. We will find it convenient to split the flux vector into convective and pressure terms as follows:

$$\mathcal{F}(\boldsymbol{V}) = \mathcal{F}_{\mathrm{c}}(\boldsymbol{V}) + \mathcal{F}_{p}(\boldsymbol{V}), \tag{147}$$

where

$$\mathcal{F}_{\mathrm{c}}(\boldsymbol{V}) = v \boldsymbol{V} \tag{148}$$

and

$$\mathcal{F}_p(\boldsymbol{V}) = \begin{bmatrix} 0 \\ 0 \\ \vdots \\ 0 \\ p \\ pv \end{bmatrix}, \qquad \boldsymbol{V} = \begin{bmatrix} V_1 \\ V_2 \\ \vdots \\ V_N \\ V_{N+1} \\ V_{N+2} \end{bmatrix} = \begin{bmatrix} \rho_1\alpha_1 \\ \rho_2\alpha_2 \\ \vdots \\ \rho_N\alpha_N \\ \rho v \\ \rho e + \frac{1}{2}\rho v^2 \end{bmatrix}. \tag{149}$$

Then we may write

$$\mathcal{A}(\boldsymbol{V}) = \mathcal{A}_{\mathrm{c}}(\boldsymbol{V}) + \mathcal{A}_p(\boldsymbol{V}), \tag{150}$$

where

$$\mathcal{A}_{\mathrm{c}}(\boldsymbol{V}) = \frac{\partial \mathcal{F}_{\mathrm{c}}(\boldsymbol{V})}{\partial \boldsymbol{V}} \qquad \text{and} \qquad \mathcal{A}_p(\boldsymbol{V}) = \frac{\partial \mathcal{F}_p(\boldsymbol{V})}{\partial \boldsymbol{V}}. \tag{151}$$

PROPOSITION 9. *The convective Jacobian matrix $\mathcal{A}_{\mathrm{c}}$ can be written as*

$$\mathcal{A}_{\mathrm{c}}(\boldsymbol{V}) = \begin{bmatrix} (1-Y_1)v & -Y_1 v & \dots & -Y_1 v & Y_1 & 0 \\ -Y_2 v & (1-Y_2)v & \dots & -Y_2 v & Y_2 & 0 \\ \vdots & \ddots & \ddots & \vdots & \vdots & \vdots \\ -Y_N v & -Y_N v & \dots & (1-Y_N)v & Y_N & 0 \\ -v^2 & -v^2 & \dots & -v^2 & 2v & 0 \\ -\left(e+\frac{1}{2}v^2\right)v & -\left(e+\frac{1}{2}v^2\right)v & \dots & -\left(e+\frac{1}{2}v^2\right)v & e+\frac{1}{2}v^2 & v \end{bmatrix}, \tag{152}$$

where

$$e = \sum_{i=1}^{N} Y_i e_i. \tag{153}$$

Proof. From (148) we obtain

$$\mathrm{d}\mathcal{F}_{\mathrm{c}} = v\,\mathrm{d}\boldsymbol{V} + \boldsymbol{V}\,\mathrm{d}v, \tag{154}$$

which together with (29) and (40) yields the result. ∎

PROPOSITION 10. *The pressure Jacobian $\mathcal{A}_p$ can be written as*

$$\mathcal{A}_p = \mathcal{A}_1 + \frac{\rho\tilde{c}^2}{T}\frac{\sum_{i=1}^{N}\zeta_i C_{p,i}}{\sum_{i=1}^{N} C_{p,i}}\mathcal{A}_2, \tag{155}$$

where

$$\mathcal{A}_1(\boldsymbol{V}) = \begin{bmatrix} 0 & 0 & \dots & 0 & 0 & 0 \\ 0 & 0 & \dots & 0 & 0 & 0 \\ \vdots & \ddots & \ddots & \vdots & \vdots & \vdots \\ 0 & 0 & \dots & 0 & 0 & 0 \\ \frac{\rho\tilde{c}^2}{\rho_1} & \frac{\rho\tilde{c}^2}{\rho_2} & \dots & \frac{\rho\tilde{c}^2}{\rho_N} & 0 & 0 \\ v\left(\frac{\rho\tilde{c}^2}{\rho_1}-\frac{p}{\rho}\right) & v\left(\frac{\rho\tilde{c}^2}{\rho_2}-\frac{p}{\rho}\right) & \dots & v\left(\frac{\rho\tilde{c}^2}{\rho_N}-\frac{p}{\rho}\right) & \frac{p}{\rho} & 0 \end{bmatrix} \tag{156}$$

and

$$\mathcal{A}_2(\boldsymbol{V}) = \begin{bmatrix} 0 & 0 & \dots & 0 & 0 & 0 \\ 0 & 0 & \dots & 0 & 0 & 0 \\ \vdots & \ddots & \ddots & \vdots & \vdots & \vdots \\ 0 & 0 & \dots & 0 & 0 & 0 \\ \frac{1}{2}v^2 - e_1 - \frac{p}{\rho_1} & \frac{1}{2}v^2 - e_2 - \frac{p}{\rho_2} & \dots & \frac{1}{2}v^2 - e_N - \frac{p}{\rho_N} & -v & 1 \\ v\left(\frac{1}{2}v^2 - e_1 - \frac{p}{\rho_1}\right) & v\left(\frac{1}{2}v^2 - e_2 - \frac{p}{\rho_2}\right) & \dots & v\left(\frac{1}{2}v^2 - e_N - \frac{p}{\rho_N}\right) & -v^2 & v \end{bmatrix}. \tag{157}$$

Proof. The result follows directly from Lemmas 12 and 13 applied to (149). ∎

By the above calculations, it follows that the relaxed system of section 2.2 can be written in the form (137), with

$$\mathcal{A} = \mathcal{A}_c + \mathcal{A}_1 + \frac{\rho\tilde{c}^2}{T}\frac{\sum_{i=1}^N \zeta_i C_{p,i}}{\sum_{i=1}^N C_{p,i}}\mathcal{A}_2, \tag{158}$$

where $\mathcal{A}_c$, $\mathcal{A}_1$, and $\mathcal{A}_2$ are given by (152), (156), and (157).

We are now in position to prove the following.

PROPOSITION 11. *The mixture sound velocity $\tilde{c}$, given by* (114)*, satisfies Abgrall's formula* (121).

Proof. From Lemma 12 it follows that

$$\mathcal{P}_i = \frac{\rho\tilde{c}^2}{\rho_i} - \frac{\rho\tilde{c}^2}{T}\frac{\sum_{i=1}^N \zeta_i C_{p,i}}{\sum_{i=1}^N C_{p,i}}\left(e_i + \frac{p}{\rho_i}\right) \tag{159}$$

and

$$\mathcal{P}_\epsilon = \frac{\rho\tilde{c}^2}{T}\frac{\sum_{i=1}^N \zeta_i C_{p,i}}{\sum_{i=1}^N C_{p,i}} \tag{160}$$

in the context of (122). By this, (121) simplifies to the trivial identity

$$\tilde{c}^2 = \sum_{i=1}^N Y_i\frac{\rho\tilde{c}^2}{\rho_i} = \sum_{i=1}^N \alpha_i\tilde{c}^2 = \tilde{c}^2. \tag{161}$$

∎

4. Summary. We have studied a *relaxation system* modeling the flow of an arbitrary number of immiscible fluids. The fluids are assumed to flow with the same velocities and to be in mechanical equilibrium, i.e., to have the same pressure. Thermal equilibrium is not assumed; instead heat transfer has been modeled by a relaxation procedure. The relaxation procedure has been carefully chosen to respect the first and second laws of thermodynamics. In this respect, we have extended upon previous works [12, 21], which considered the special case of two separate fluids.

Furthermore, we have studied the *relaxed* limit where thermal equilibrium is instantaneously imposed. This relaxed limit is sometimes referred to as the *homogeneous equilibrium model*. We have derived a formulation of the mixture sound velocity of this relaxed model, from which it is straightforward to see that the relaxed system unconditionally satisfies the *subcharacteristic condition*. The physical interpretation of this result is that the instantaneous equilibrium condition imposes a slower mixture sound velocity compared to the nonequilibrium case. Although this result may be obtained by other means, the proof presented in this paper seems original and provides insights into the effects of relevant thermodynamic parameters on sonic propagation.

Acknowledgment. We thank the anonymous reviewers for carefully reading the manuscript and making several useful remarks.

REFERENCES

[1] R. Abgrall, *An extension of Roe's upwind scheme to algebraic equilibrium real gas models*, Comput. Fluids, 19 (1991), pp. 171–182.
[2] R. Abgrall and R. Saurel, *Discrete equations for physical and numerical compressible multiphase mixtures*, J. Comput. Phys., 186 (2003), pp. 361–396.
[3] M. R. Baer and J. W. Nunziato, *A two-phase mixture theory for the deflagration-to-detonation transition (DDT) in reactive granular materials*, Int. J. Multiphase Flow, 12 (1986), pp. 861–889.
[4] M. Baudin, C. Berthon, F. Coquel, R. Masson, and Q.-H. Tran, *A relaxation method for two-phase flow models with hydrodynamic closure law*, Numer. Math., 99 (2005), pp. 411–440.
[5] M. Baudin, F. Coquel, and Q.-H. Tran, *A semi-implicit relaxation scheme for modeling two-phase flow in a pipeline*, SIAM J. Sci. Comput., 27 (2005), pp. 914–936.
[6] S. Bianchini and A. Bressan, *Vanishing viscosity solutions of nonlinear hyperbolic systems*, Ann. of Math. (2), 161 (2005), pp. 223–342.
[7] G.-Q. Chen, C. D. Levermore, and T.-P. Liu, *Hyperbolic conservation laws with stiff relaxation terms and entropy*, Comm. Pure Appl. Math., 47 (1994), pp. 787–830.
[8] G. Dal Maso, P. G. LeFloch, and F. Murat, *Definition and weak stability of nonconservative products*, J. Math. Pures Appl., 74 (1995), pp. 483–548.
[9] V. Deledicque and M. V. Papalexandris, *A conservative approximation to compressible two-phase flow models in the stiff mechanical relaxation limit*, J. Comput. Phys., 227 (2008), pp. 9241–9270.
[10] S. Evje and K. K. Fjelde, *Relaxation schemes for the calculation of two-phase flow in pipes*, Math. Comput. Modelling, 36 (2002), pp. 535–567.
[11] S. Jin and Z. Xin, *The relaxation schemes for systems of conservation laws in arbitrary space dimensions*, Comm. Pure Appl. Math., 48 (1995), pp. 235–276.
[12] A. K. Kapila, R. Menikoff, J. B. Bdzil, S. F. Son, and D. S. Stewart, *Two-phase modeling of deflagration-to-detonation transition in granular materials: Reduced equations*, Phys. Fluids, 13 (2001), pp. 3002–3024.
[13] T.-P. Liu, *Hyperbolic conservation laws with relaxation*, Commun. Math. Phys., 108 (1987), pp. 153–175.
[14] A. Morin, P. K. Aursand, T. Flåtten, and S. T. Munkejord, *Numerical resolution of CO_2 transport dynamics*, in SIAM Conference on Mathematics for Industry: Challenges and Frontiers (MI09), SIAM, Philadelphia, 2009, pp. 108–119; available online from http://www.siam.org/proceedings/industry/2009/mi09_013_morina.pdf.
[15] S. T. Munkejord, *Comparison of Roe-type methods for solving the two-fluid model with and without pressure relaxation*, Comput. Fluids, 36 (2007), pp. 1061–1080.
[16] A. Murrone and H. Guillard, *A five equation reduced model for compressible two phase flow problems*, J. Comput. Phys., 202 (2005), pp. 664–698.
[17] D. L. Nguyen, E. R. F. Winter, and M. Greiner, *Sonic velocity in two-phase systems*, Int. J. Multiphase Flow, 7 (1981), pp. 311–320.
[18] S. Qamar and G. Warnecke, *Simulation of multicomponent flows using high order central schemes*, Appl. Numer. Math., 50 (2004), pp. 183–201.
[19] V. H. Ransom and D. L. Hicks, *Hyperbolic two-pressure models for two-phase flow*, J. Comput. Phys., 53 (1984), pp. 124–151.
[20] R. Saurel and R. Abgrall, *A multiphase Godunov method for compressible multifluid and multiphase flows*, J. Comput. Phys., 150 (1999), pp. 425–467.
[21] R. Saurel, F. Petitpas, and R. Abgrall, *Modelling phase transition in metastable liquids: Application to cavitating and flashing flows*, J. Fluid Mech., 607 (2008), pp. 313–350.
[22] R. Saurel, F. Petitpas, and R. A. Berry, *Simple and efficient relaxation methods for interfaces separating compressible fluids, cavitating flows and shocks in multiphase mixtures*, J. Comput. Phys., 228 (2009), pp. 1678–1712.
[23] H. Städtke, *Gasdynamic Aspects of Two-Phase Flow*, Wiley-VCH Verlag GmbH & CO. KGaA, Weinheim, Germany, 2006.
[24] H. B. Stewart and B. Wendroff, *Two-phase flow: Models and methods*, J. Comput. Phys., 56 (1984), pp. 363–409.

D Towards a formally path-consistent Roe scheme for the six-equation two-fluid model

Alexandre Morin, Tore Flåtten and Svend T. Munkejord.
AIP Conference Proceedings, Volume 1281, No. 1, pp. 71–74, 2010.

Towards a formally path-consistent Roe scheme for the six-equation two-fluid model

Alexandre Morin*, Tore Flåtten† and Svend T. Munkejord†

*Dept. of Energy and Process Engineering, Norwegian University of Science and Technology (NTNU), NO-7491 Trondheim, Norway.
†SINTEF Energy Research, NO-7465 Trondheim, Norway.

Abstract. We start from the most common formulation of the six-equation two-fluid model, from which we remove the non-conservative temporal term using an equivalent formulation derived in the literature. We derive a partially analytical, formally path-consistent Roe scheme, using the flux-splitting method.

We first expose the model in detail, and split the flux into a convective part, a pressure part, and a non-conservative part. Then we derive an analytical Jacobian matrix of the fluxes, which allows the model to be written in quasilinear form. Finally, we explain the approach used to express formulas for the Roe-averaging of the variables. Only a simplified Roe-condition on the pressure remains. It can be fulfilled numerically, given any equation of state.

In the present article, we do not show the full results, but rather explain the approach. The full results will be explained at the conference.

Keywords: Two-phase flow, Compressible flow, Finite volume method, Numerical methods, Roe scheme
PACS: 47.11.Df, 47.40.Dc, 47.55.Ca, 47.60.Dx, 47.85.Dh

INTRODUCTION: THE MODEL

The six-equation two-fluid model [1, 3] is a well-studied two-phase flow model. In its most common formulation, it takes the general form

$$\frac{\partial \mathbf{U}}{\partial t} + \frac{\partial \mathbf{F}(\mathbf{U})}{\partial x} + \tilde{\mathbf{A}}(\mathbf{U})\frac{\partial \tilde{\mathbf{V}}(\mathbf{U})}{\partial t} + \tilde{\mathbf{B}}(\mathbf{U})\frac{\partial \tilde{\mathbf{W}}(\mathbf{U})}{\partial x} = \mathbf{S}(\mathbf{U}). \tag{1}$$

As described in [1], the non-conservative temporal term $\partial_t \tilde{\mathbf{V}}$ presents mathematical and numerical difficulties in deriving fully upwind schemes, as well as schemes that are *formally path-consistent* with respect to the definitions of the non-conservative products of the system.

In this work, we address this difficulty by taking advantage of a mathematically equivalent formulation, derived in [1], that eliminates the non-conservative temporal term. The system of equations is written as

$$\frac{\partial \mathbf{U}}{\partial t} + \frac{\partial \mathbf{F}(\mathbf{U})}{\partial x} + \mathbf{B}'(\mathbf{U})\frac{\partial \mathbf{W}(\mathbf{U})}{\partial x} = \mathbf{S}(\mathbf{U}), \tag{2}$$

where the variables vector consists of the conserved quantities for each of the two phases (mass, momentum and total energy):

$$\mathbf{U} = \begin{bmatrix} u_1 \\ u_2 \\ u_3 \\ u_4 \\ u_5 \\ u_6 \end{bmatrix} = \begin{bmatrix} \rho_\mathrm{g}\alpha_g \\ \rho_\ell\alpha_l \\ \rho_\mathrm{g}\alpha_g v_g \\ \rho_\ell\alpha_l v_l \\ \rho_\mathrm{g}\alpha_g \left(e_\mathrm{g} + \frac{1}{2}v_g^2\right) \\ \rho_\ell\alpha_l \left(e_\ell + \frac{1}{2}v_l^2\right) \end{bmatrix}. \tag{3}$$

Further, the conservative flux $\mathbf{F}(\mathbf{U})$ is split into a convective part and a pressure part, such that

$$\mathbf{F} = \mathbf{F}_\mathrm{c} + \mathbf{F}_\mathrm{p} \qquad \text{with} \qquad \mathbf{F}_\mathrm{c}(\mathbf{U}) = \begin{bmatrix} \rho_\mathrm{g}\alpha_g v_g \\ \rho_\ell \alpha_l v_l \\ \rho_\mathrm{g}\alpha_g v_g^2 \\ \rho_\ell \alpha_l v_l^2 \\ \rho_\mathrm{g}\alpha_g v_g \left(e_\mathrm{g} + \frac{1}{2}v_g^2\right) \\ \rho_\ell \alpha_l v_l \left(e_\ell + \frac{1}{2}v_l^2\right) \end{bmatrix} \quad \text{and} \quad \mathbf{F}_p(\mathbf{U}) = \begin{bmatrix} 0 \\ 0 \\ 0 \\ 0 \\ \alpha_g v_g p \\ \alpha_l v_l p \end{bmatrix}. \tag{4}$$

The term $\mathbf{B}'(\mathbf{U})\frac{\partial \mathbf{W}(\mathbf{U})}{\partial x}$ in (2) originally contains the non-conservative contributions of the fluxes, to allow using the formally path-consistent approach of Parés [5]. However, to simplify the analysis, $\mathbf{B}'(\mathbf{U})$ is modified to also contain the pressure part of the flux $\mathbf{F}_p(\mathbf{U})$, to give the system analysed in the present paper:

$$\frac{\partial \mathbf{U}}{\partial t} + \frac{\partial \mathbf{F}_c(\mathbf{U})}{\partial x} + \mathbf{B}(\mathbf{U})\frac{\partial \mathbf{W}(\mathbf{U})}{\partial x} = \mathbf{S}(\mathbf{U}), \tag{5}$$

where

$$\mathbf{B}(\mathbf{U}) = \begin{bmatrix} 0 & 0 \\ 0 & 0 \\ \alpha_g & 0 \\ \alpha_l & 0 \\ \alpha_g v_g - \eta\,\alpha_g\alpha_l\,(v_g - v_l) & \eta\,\rho_\ell\alpha_g c_\ell^2 \\ \alpha_l v_l + \eta\,\alpha_g\alpha_l\,(v_g - v_l) & \eta\,\rho_\mathrm{g}\alpha_l c_\mathrm{g}^2 \end{bmatrix} \quad \text{and} \quad \mathbf{W}(\mathbf{U}) = \begin{bmatrix} p \\ \alpha_g v_g + \alpha_l v_l \end{bmatrix}. \tag{6}$$

η is defined by

$$\eta = \frac{p}{\rho_\mathrm{g}\alpha_l c_\mathrm{g}^2 + \rho_\ell \alpha_g c_\ell^2}. \tag{7}$$

Finally, the source term $\mathbf{S}(\mathbf{U})$ can represent gravity or phase interactions. Note that this formulation does not include regularising terms making the model hyperbolic, for which a number of possibilities exists in the literature. The numerical framework we present here may be extended to include such terms, following for instance the approach in [7, 9].

QUASILINEAR FORM

In order to derive a Roe scheme [2], we first write the model in a quasilinear form:

$$\frac{\partial \mathbf{U}}{\partial t} + \mathbf{A}(\mathbf{U})\frac{\partial \mathbf{U}}{\partial x} = \mathbf{S}(\mathbf{U}), \tag{8}$$

where

$$\mathbf{A}(\mathbf{U}) = \frac{\partial \mathbf{F}_c}{\partial \mathbf{U}} + \mathbf{B}(\mathbf{U})\frac{\partial \mathbf{W}}{\partial \mathbf{U}}. \tag{9}$$

To achieve this, we first derive the analytical Jacobian matrix of the flux. A natural decomposition of the problem is to treat the convective part $\mathbf{F}_c$ separately from the rest of the flux, mainly involving the pressure, $\mathbf{B}(\mathbf{U})\frac{\partial \mathbf{W}(\mathbf{U})}{\partial x}$. The resulting Jacobian matrices will be called $\mathbf{A}_c$ and $\mathbf{A}_p$, respectively.

The matrix $\mathbf{A}_c$ is given by

$$\mathbf{A}_c = \frac{\partial \mathbf{F}_c}{\partial \mathbf{U}} = \begin{bmatrix} 0 & 0 & 1 & 0 & 0 & 0 \\ 0 & 0 & 0 & 1 & 0 & 0 \\ -v_g^2 & 0 & 2v_g & 0 & 0 & 0 \\ 0 & -v_l^2 & 0 & 2v_l & 0 & 0 \\ -v_g E_g & 0 & E_g & 0 & v_g & 0 \\ 0 & -v_l E_l & 0 & E_l & 0 & v_l \end{bmatrix} \qquad \text{where} \qquad E_\varphi = e_\varphi + \frac{1}{2}v_\varphi^2. \tag{10}$$

In order to derive the Jacobian $\mathbf{A}_p$ of the pressure flux, we need the derivative of the non-conservative flux variables, $\mathbf{W}$, with respect to the conservative variables, $\mathbf{U}$:

$$\mathbf{M} = \frac{\partial \mathbf{W}(\mathbf{U})}{\partial \mathbf{U}} = \mathscr{R}^{-1} \begin{bmatrix} \zeta_l \beta_g & (v_g - v_l)\,\alpha_l \beta_g - \mathscr{R} v_g/\rho_g \\ \zeta_g \beta_l & (v_l - v_g)\,\alpha_g \beta_l - \mathscr{R} v_l/\rho_l \\ -\zeta_l \Gamma_g v_g & \mathscr{R}/\rho_g - (v_g - v_l)\,\alpha_l \Gamma_g v_g \\ -\zeta_g \Gamma_l v_l & \mathscr{R}/\rho_l - (v_l - v_g)\,\alpha_g \Gamma_l v_l \\ \zeta_l \Gamma_g & (v_g - v_l)\,\alpha_l \Gamma_g \\ \zeta_g \Gamma_l & (v_l - v_g)\,\alpha_g \Gamma_l \end{bmatrix}^T, \tag{11}$$

where

$$\begin{aligned} \beta_g &= c_g^2 - \Gamma_g \left(e_g + \tfrac{p}{\rho_g} \right) + \tfrac{1}{2} \Gamma_g v_g^2, \quad \zeta_g = \rho_g c_g^2 - \Gamma_g p, \quad \mathscr{R} = \alpha_g \zeta_l + \alpha_l \zeta_g, \\ \beta_l &= c_l^2 - \Gamma_l \left(e_l + \tfrac{p}{\rho_l} \right) + \tfrac{1}{2} \Gamma_l v_l^2, \quad \zeta_l = \rho_l c_l^2 - \Gamma_l p. \end{aligned}$$

We define

$$\mathbf{A}_p = \mathscr{R} \mathbf{B}(\mathbf{U}) \frac{\partial \mathbf{W}(\mathbf{U})}{\partial \mathbf{U}} = \mathscr{R} \mathbf{B} \mathbf{M}, \qquad \text{hence} \qquad \mathbf{A} = \mathbf{A}_c + \mathscr{R}^{-1} \mathbf{A}_p. \tag{12}$$

DERIVATION OF THE ROE SCHEME

The Roe scheme requires the construction of a matrix at each cell interface. It is the Jacobian matrix $\mathbf{A}$ evaluated at a particular average of the variables in the neighbouring cells. This is called Roe averaging and denoted by $\hat{\mathbf{A}}$ in the following. It has to satisfy some conditions [2, 6, 7, 8], amongst which one is problematic:

$$\text{R1: } \hat{\mathbf{A}} \left(\mathbf{U}^\mathrm{L}, \mathbf{U}^\mathrm{R} \right) \left(\mathbf{U}^\mathrm{R} - \mathbf{U}^\mathrm{L} \right) = \mathbf{F}_c(\mathbf{U}^\mathrm{R}) - \mathbf{F}_c(\mathbf{U}^\mathrm{L}) + \overline{\mathbf{B}} \left(\mathbf{U}^\mathrm{L}, \mathbf{U}^\mathrm{R} \right) \left(\mathbf{W}(\mathbf{U}^\mathrm{R}) - \mathbf{W}(\mathbf{U}^\mathrm{L}) \right).$$

The matrix $\overline{\mathbf{B}}$ is a property of the mathematical solution rather than the numerical method [1], and it is assumed that it is known in the present work.

Similarly to what was done in the derivation of the Jacobian matrix, we can split the problem into a convective part and a pressure part, such that $\hat{\mathbf{A}} = \hat{\mathbf{A}}_c + \hat{\mathscr{R}}^{-1} \hat{\mathbf{A}}_p$.

The Roe condition R1 can subsequently be split in two:

$$\hat{\mathbf{A}}_c \left(\mathbf{U}^\mathrm{L}, \mathbf{U}^\mathrm{R} \right) \left(\mathbf{U}^\mathrm{R} - \mathbf{U}^\mathrm{L} \right) = \mathbf{F}_c(\mathbf{U}^\mathrm{R}) - \mathbf{F}_c(\mathbf{U}^\mathrm{L}), \tag{13}$$

$$\hat{\mathscr{R}}^{-1} \hat{\mathbf{A}}_p \left(\mathbf{U}^\mathrm{L}, \mathbf{U}^\mathrm{R} \right) \left(\mathbf{U}^\mathrm{R} - \mathbf{U}^\mathrm{L} \right) = \overline{\mathbf{B}} \left(\mathbf{U}^\mathrm{L}, \mathbf{U}^\mathrm{R} \right) \left(\mathbf{W}(\mathbf{U}^\mathrm{R}) - \mathbf{W}(\mathbf{U}^\mathrm{L}) \right). \tag{14}$$

The derivation of the Roe matrix for the convective part $\hat{\mathbf{A}}_c$ is already well known, using the parameter-vector approach of Roe [2]. Specifically, Toumi [3] gives the parameter vector for this case. On the other hand, this method is impractical for the pressure part. Instead, we follow a similar strategy as in [4]. It consists in reducing the partial Roe condition (14) on $\hat{\mathbf{A}}_p$ to two simpler ones. One will concern the pressure average, and the other the mixture-velocity average. This gives the possibility to construct a partially analytical Roe matrix for any equation of state.

From the averaging of (12) comes $\hat{\mathbf{A}}_p = \hat{\mathscr{R}} \overline{\mathbf{B}} \hat{\mathbf{M}}$. Here we recall that $\overline{\mathbf{B}}$ is known a priori, and does therefore not need Roe averaging. Inserting $\hat{\mathbf{A}}_p$ into (14) gives

$$\hat{\mathbf{M}} \left(\mathbf{U}^\mathrm{L}, \mathbf{U}^\mathrm{R} \right) \left(\mathbf{U}^\mathrm{R} - \mathbf{U}^\mathrm{L} \right) = \mathbf{W}(\mathbf{U}^\mathrm{R}) - \mathbf{W}(\mathbf{U}^\mathrm{L}), \tag{15}$$

which results in a system of two equations. The matrix $\hat{\mathbf{M}}$ is the matrix $\mathbf{M}$ evaluated for specific weighted averages of the variables in the neighbouring cells, which we will call Roe-average and denote $\hat{x}$. For example, $\hat{v_l}$ is an average of v_l^L and v_l^R. We will use the system (15) to define the Roe-averages of all the needed variables.

First, we show that the first line of the system (15) is fulfilled if we use a Roe-average of the pressure differential

$$\mathscr{R}\, \mathrm{d}p = \zeta_l \left(\frac{\zeta_g}{\rho_g} - \Gamma_g e_g \right) \mathrm{d}u_1 + \zeta_g \left(\frac{\zeta_l}{\rho_l} - \Gamma_l e_l \right) \mathrm{d}u_2 + \zeta_l \Gamma_g\, \mathrm{d}(u_1 e_g) + \zeta_g \Gamma_l\, \mathrm{d}(u_2 e_l), \tag{16}$$

as well as

$$u_5 = u_1 e_g + \frac{1}{2} u_1 v_g^2 \qquad \text{and} \qquad u_6 = u_2 e_l + \frac{1}{2} u_2 v_l^2, \tag{17}$$

and if we suppose that the velocities follow the usual Roe-averaging, weighted by $\left(\sqrt{\rho_\varphi \alpha_\varphi}\right)^{\mathrm{L,R}}$.

The condition expressed by the first line of (15) is then reduced to the condition found by Roe-averaging (16):

$$\hat{\mathscr{R}}(p^{\mathrm{R}}-p^{\mathrm{L}}) = \hat{\xi}_l\left(\widehat{\frac{\zeta_g}{\rho_g}}-\hat{\Gamma}_g\hat{e}_g\right)\left((\rho_g\alpha_g)^{\mathrm{R}}-(\rho_g\alpha_g)^{\mathrm{L}}\right)+\hat{\xi}_g\left(\widehat{\frac{\zeta_l}{\rho_l}}-\hat{\Gamma}_l\hat{e}_l\right)\left((\rho_l\alpha_l)^{\mathrm{R}}-(\rho_l\alpha_l)^{\mathrm{L}}\right) + \hat{\xi}_l\hat{\Gamma}_g\left((\rho_g\alpha_g e_g)^{\mathrm{R}}-(\rho_g\alpha_g e_g)^{\mathrm{L}}\right)+\hat{\xi}_g\hat{\Gamma}_l\left((\rho_l\alpha_l e_l)^{\mathrm{R}}-(\rho_l\alpha_l e_l)^{\mathrm{L}}\right). \tag{18}$$

Second, the same process is applied to the second line of the system (15). It is more involved, therefore we only show the results. We keep assumptions on the Roe-averaging of v_φ and we make further assumptions on the shape of the Roe-averages of α_φ and ρ_φ. Further, we define some other averaging formulas for $\breve{\alpha}$ and $\breve{\rho}$ which will be made explicit at the conference. Then we show that this second line will be reduced to the condition

$$\breve{\alpha}_g\hat{\alpha}_l\left(\widehat{\frac{\zeta_g}{\rho_g}}\right)\left((\rho_g)^{\mathrm{R}}-(\rho_g)^{\mathrm{L}}\right)-\breve{\alpha}_l\hat{\alpha}_g\left(\widehat{\frac{\zeta_\ell}{\rho_l}}\right)\left((\rho_l)^{\mathrm{R}}-(\rho_l)^{\mathrm{L}}\right) + \breve{\rho}_g\breve{\alpha}_g\hat{\alpha}_l\hat{\Gamma}_g\left((e_{\mathrm{g}})^{\mathrm{R}}-(e_{\mathrm{g}})^{\mathrm{L}}\right)-\breve{\rho}_l\breve{\alpha}_l\hat{\alpha}_g\hat{\Gamma}_l\left((e_\ell)^{\mathrm{R}}-(e_\ell)^{\mathrm{L}}\right)=0. \tag{19}$$

Further, (18) and (19) reduce to the same condition by using the appropriate expression for $\widehat{\frac{\zeta_\varphi}{\rho_\varphi}}$

$$p^{\mathrm{R}}-p^{\mathrm{L}}=\frac{\hat{\xi}_g}{\hat{\rho}_g}\left(\rho_g^{\mathrm{R}}-\rho_g^{\mathrm{L}}\right)+\breve{\rho}_g\hat{\Gamma}_g\left(e_g^{\mathrm{R}}-e_g^{\mathrm{L}}\right)=\frac{\hat{\xi}_l}{\hat{\rho}_l}\left(\rho_l^{\mathrm{R}}-\rho_l^{\mathrm{L}}\right)+\breve{\rho}_l\hat{\Gamma}_l\left(e_l^{\mathrm{R}}-e_l^{\mathrm{L}}\right). \tag{20}$$

This last condition cannot be fulfilled analytically for a general equation of state. In case of non-analytical equation of state, or if its expression is too complicated, (20) will be the only condition that will be solved numerically. The approach presented in [4] can be used for example.

ACKNOWLEDGMENT

The first author has received a PhD grant from the BIGCCS Centre. The second and the third authors were financed through the CO_2 Dynamics project. The authors acknowledge the support from the Research Council of Norway (189978, 193816), Aker Solutions, ConocoPhilips Skandinavia AS, Det Norske Veritas AS, Gassco AS, Hydro Aluminium AS, Shell Technology AS, Statkraft Development AS, Statoil Petroleum AS, TOTAL E&P Norge AS and Vattenfall AB.

REFERENCES

1. S. T. Munkejord, S. Evje and T. Flåtten, *A MUSTA scheme for a nonconservative two-fluid model*, SIAM J. Sci. Comput., 31 (2009), pp. 2587–2622.
2. P. L. Roe, *Approximate Riemann solvers, parameter vectors, and difference schemes*, J. Comput. Phys., 43 (1981), pp. 357–372.
3. I. Toumi, *An Upwind Numerical Method for Two-Fluid Two-Phase Flow Models*, Nuclear Science and Engineering, 123 (1996), pp. 147–168
4. A. Morin, P. K. Aursand, T. Flåtten and S. T. Munkejord, *Numerical Resolution of CO_2 Transport Dynamics*, SIAM Conference on Mathematics for Industry: Challenges and Frontiers (MI09), San Francisco, CA, USA, October 9–10, (2009)
5. C. Parés, *Numerical Methods for Non-Conservative Hyperbolic Systems: A Theoretical Framework*, SIAM J. Numer. Anal., 44 (2006), pp. 300–321
6. I. Toumi, *A Weak Formulation of Roe's Approximate Riemann Solver*, J. Comput. Phys., Vol. 102, Issue 2, October 1992, pp. 360–373
7. S. Evje, T. Flåtten, *Hybrid Flux-Splitting Schemes for a Common Two-Fluid Model*, J. Comput. Phys., Vol. 192, Issue 1, 2003, pp.175–210
8. M. L. Munoz-Ruiz, C. Parés, *Godunov Method for Nonconservative Hypebolic Systems*, Modélisation mathématique et analyse numérique, ISSN 0764-583X, Vol. 41, no. 1, 2007, pp. 169–185
9. D. Bestion, *The physical closure laws in the CATHARE code*, Nuclear Engineering and Design, Vol. 124, no. 3, 1990, pp. 229–245

E A Roe Scheme for a Compressible Six-Equation Two-Fluid Model

Alexandre Morin, Tore Flåtten and Svend T. Munkejord.
Submitted to the International Journal for Numerical Methods in Fluids, 2012.

INTERNATIONAL JOURNAL FOR NUMERICAL METHODS IN FLUIDS
Int. J. Numer. Meth. Fluids 0000; **00**:1–28
Published online in Wiley InterScience (www.interscience.wiley.com). DOI: 10.1002/fld

A Roe Scheme for a Compressible Six-Equation Two-Fluid Model

Alexandre Morin[1*], Tore Flåtten[2] and Svend Tollak Munkejord[2]

[1] *Department of Energy and Process Engineering, Norwegian University of Science and Technology (NTNU), Kolbjørn Hejes vei 1B, NO-7491 Trondheim, Norway.*

[2] *SINTEF Energy Research, P.O. Box 4761 Sluppen, NO-7465 Trondheim, Norway*

SUMMARY

We derive a partially analytical Roe scheme with wave limiters for the compressible six-equation two-fluid model. Specifically, we derive the Roe averages for the relevant variables. First, the fluxes are split into a convective and a pressure part. Then, independent Roe conditions are stated for these two parts. These conditions are successively reduced while defining acceptable Roe averages. For the convective part, all the averages are analytical. For the pressure part, most of the averages are analytical, while the remaining averages are dependent on the thermodynamic equation of state. This gives a large flexibility to the scheme with respect to the choice of equation of state. Furthermore, this model contains non-conservative terms. They are a challenge to handle right, and it is not the object of this paper to discuss this issue. However, the Roe averages presented in this paper are fully independent from how those terms are handled, which makes this framework compatible with any treatment of non-conservative terms. Finally, we point out that the eigenspace of this model may collapse, making the Roe scheme inapplicable. This is called resonance. We propose a fix to handle this particular case. Numerical tests show that the scheme performs well.
Copyright © 0000 John Wiley & Sons, Ltd.

Received . . .

KEY WORDS: Two-fluid model; Roe scheme; Resonance

1. INTRODUCTION

The two-fluid model is an option to simulate one-dimensional two-phase flows in pipelines [1, 2, 3, 4]. It is extensively used, particularly in the petroleum and nuclear industries [5, 6, 7, 8]. This model is derived from conservation laws for each phase for mass, momentum and energy. The phases interact through interfacial terms, some of which are not conservative. These non-conservative terms pose problems for the numerical solution of the model, since numerical schemes for conservation laws take advantage of the conservative nature of the equations. One approach is treating these terms as source terms [4, 9]. The conservative part of the model is then advanced one time step alternatively with the source terms. The latter are solved using ordinary differential equation solvers. The main drawback is that the wave propagation velocities should be affected by the non-conservative terms, which is not properly caught in this approach. The consequence is that the discontinuities that can occur with non-linear models may be smeared. Therefore, many authors have tried to include

*Correspondence to: Department of Energy and Process Engineering, Norwegian University of Science and Technology (NTNU), Kolbjørn Hejes vei 1B, NO-7491 Trondheim, Norway. Email: alexandre.morin [a] sintef.no

Copyright © 0000 John Wiley & Sons, Ltd.

them in the framework of the numerical schemes for conservation laws [10, 11, 12, 13]. In the present article, we continue the work presented in [14], making a step in the direction of properly including the non-conservative terms in the numerical scheme for the six-equation two-fluid model by a formulation suitable for the *formally path-consistent* framework of Parés [10]. Castro *et al.* [15] and Abgrall and Karni [16] showed that this approach may produce waves which violate the Rankine-Hugoniot condition. Therefore, in the present work, the propagation of each of the waves has been analysed separately. Though it tends to indicate that the effect shown in [15] and [16] occurs with our scheme, it is marginal. The advantages of being able to treat all terms in a fully upwind manner still make this scheme a better option than solving the non-conservative terms as source terms.

The MUSTA scheme is an option to solve systems of conservation laws [17, 18]. It has been applied to the six-equation two-fluid model [2], and it was shown that it performed well. However, the linearised upwind Roe scheme [19] is generally more accurate. Toumi [3] presented a Roe scheme for the same model, but he made the assumption of incompressible liquid flow. In the present article, we extend the Roe scheme for the six-equation two-fluid model to compressible flows. We show that the Roe averages can be defined independently of the choice of integration path for the non-conservative terms. Therefore we do not concentrate on finding a physically-right path. Further, the derivation of the Roe averages for the variables is mostly analytical and independent of the thermodynamics. Only two remaining scalar relations are dependent on the equation of state. There exist numerical methods to solve those two relations, therefore the scheme can also be used with "black box" thermodynamical routines.

Before we can derive the Roe scheme, we first need to eliminate the non-conservative terms containing time derivatives. This has been achieved by Munkejord *et al.* [2] by transforming the time derivatives into space derivatives. In the present article, we take advantage of this transformation to be able to write the system in quasi-linear form.

In Section 2, we first expose the six-equation two-fluid model. Then in Section 3, we derive the quasilinear expression of the model. In Section 4, the Roe condition is formulated and average formulas that satisfy it are proposed. Next, in Section 5, we explain how we deal with the non-conservative terms. Section 6 points out the resonance which can happen with the present model, and how it is solved. In Section 7, we discuss how to make the scheme second order with the wave limiters. Finally, the numerical scheme is tested on three test cases in Section 8. Section 9 summarises the results of the paper. The main symbols used are listed in Table I. The other ones are introduced in the text.

Table I. Main symbols.

Symbol	Signification
α	Volume fraction
ρ	Density
v	Velocity
e	Internal energy
p	Pressure
Γ	First Grüneisen coefficient
c	Speed of sound
E	Total energy
u_i	Components of the vector $\boldsymbol{U}$
$\boldsymbol{U}$	Vector of the conserved variables
$\boldsymbol{F}$	Vector of the fluxes
$\boldsymbol{W}$	Vector of the non-conservative variables
$\boldsymbol{B}$	Coefficient matrix in the non-conservative terms
$\boldsymbol{S}$	Vector of the algebraic source term
g	Gas phase (Subscript)
ℓ	Liquid phase (Subscript)

Copyright © 0000 John Wiley & Sons, Ltd.
Prepared using fldauth.cls

DOI: 10.1002/fld

2. THE MODEL

The most common formulation of the six-equation two-fluid model takes the general form [1, 2]

$$\frac{\partial \boldsymbol{U}}{\partial t} + \frac{\partial \boldsymbol{F}(\boldsymbol{U})}{\partial x} + \tilde{\boldsymbol{A}}(\boldsymbol{U})\frac{\partial \tilde{\boldsymbol{V}}(\boldsymbol{U})}{\partial t} + \tilde{\boldsymbol{B}}(\boldsymbol{U})\frac{\partial \tilde{\boldsymbol{W}}(\boldsymbol{U})}{\partial x} = \tilde{\boldsymbol{S}}(\boldsymbol{U}). \tag{1}$$

where the terms $\tilde{\boldsymbol{A}}\partial_t\tilde{\boldsymbol{V}}$ and $\tilde{\boldsymbol{B}}\partial_x\tilde{\boldsymbol{V}}$ are respectively the non-conservative temporal and spatial terms.

The non-conservative temporal term $\tilde{\boldsymbol{A}}\partial_t\tilde{\boldsymbol{V}}$ presents mathematical and numerical difficulties in deriving fully upwind schemes. In this work, we address this difficulty by taking advantage of a mathematically equivalent formulation, derived in [2], that eliminates the non-conservative temporal terms. The system of equations is written as

$$\frac{\partial \boldsymbol{U}}{\partial t} + \frac{\partial \boldsymbol{F}(\boldsymbol{U})}{\partial x} + \boldsymbol{B}'(\boldsymbol{U})\frac{\partial \boldsymbol{W}(\boldsymbol{U})}{\partial x} = \boldsymbol{S}(\boldsymbol{U}), \tag{2}$$

where the variables vector consists of the conserved quantities for each of the two phases (mass, momentum and total energy):

$$\boldsymbol{U} = \begin{bmatrix} u_1 \\ u_2 \\ u_3 \\ u_4 \\ u_5 \\ u_6 \end{bmatrix} = \begin{bmatrix} \alpha_{\mathrm{g}}\rho_{\mathrm{g}} \\ \alpha_\ell\rho_\ell \\ \alpha_{\mathrm{g}}\rho_{\mathrm{g}}v_{\mathrm{g}} \\ \alpha_\ell\rho_\ell v_\ell \\ \alpha_{\mathrm{g}}\rho_{\mathrm{g}}\left(e_{\mathrm{g}} + \frac{1}{2}v_{\mathrm{g}}^2\right) \\ \alpha_\ell\rho_\ell\left(e_\ell + \frac{1}{2}v_\ell^2\right) \end{bmatrix}. \tag{3}$$

Further, the conservative flux $\boldsymbol{F}(\boldsymbol{U})$ was in [2] originally split into a convective part and a pressure part, such that

$$\boldsymbol{F} = \boldsymbol{F}_{\mathrm{c}} + \boldsymbol{F}_{\mathrm{p}} \tag{4}$$

with

$$\boldsymbol{F}_{\mathrm{c}}(\boldsymbol{U}) = \begin{bmatrix} \alpha_{\mathrm{g}}\rho_{\mathrm{g}}v_{\mathrm{g}} \\ \alpha_\ell\rho_\ell v_\ell \\ \alpha_{\mathrm{g}}\rho_{\mathrm{g}}v_{\mathrm{g}}^2 \\ \alpha_\ell\rho_\ell v_\ell^2 \\ \alpha_{\mathrm{g}}\rho_{\mathrm{g}}v_{\mathrm{g}}\left(e_{\mathrm{g}} + \frac{1}{2}v_{\mathrm{g}}^2\right) \\ \alpha_\ell\rho_\ell v_\ell\left(e_\ell + \frac{1}{2}v_\ell^2\right) \end{bmatrix} \quad \text{and} \quad \boldsymbol{F}_p(\boldsymbol{U}) = \begin{bmatrix} 0 \\ 0 \\ 0 \\ 0 \\ \alpha_{\mathrm{g}}v_{\mathrm{g}}p \\ \alpha_\ell v_\ell p \end{bmatrix}. \tag{5}$$

However, in the present work, we obtain a simpler non-conservative system by modifying $\boldsymbol{B}'(\boldsymbol{U})$ to also incorporate the pressure part of the flux $\boldsymbol{F}_p(\boldsymbol{U})$. By this, we obtain the equivalent formulation of the system presented in [2]:

$$\frac{\partial \boldsymbol{U}}{\partial t} + \frac{\partial \boldsymbol{F}_c(\boldsymbol{U})}{\partial x} + \boldsymbol{B}(\boldsymbol{U})\frac{\partial \boldsymbol{W}(\boldsymbol{U})}{\partial x} = \boldsymbol{S}(\boldsymbol{U}), \tag{6}$$

where

$$\boldsymbol{B}(\boldsymbol{U}) = \begin{bmatrix} 0 & 0 & 0 \\ 0 & 0 & 0 \\ \alpha_{\mathrm{g}} & 0 & \Delta p \\ \alpha_\ell & 0 & -\Delta p \\ \alpha_{\mathrm{g}}v_{\mathrm{g}} - \eta\alpha_{\mathrm{g}}\alpha_\ell\left(v_{\mathrm{g}} - v_\ell\right) & \eta\rho_\ell\alpha_{\mathrm{g}}c_\ell^2 & v_\tau\Delta p \\ \alpha_\ell v_\ell + \eta\alpha_{\mathrm{g}}\alpha_\ell\left(v_{\mathrm{g}} - v_\ell\right) & \eta\rho_{\mathrm{g}}\alpha_\ell c_{\mathrm{g}}^2 & -v_\tau\Delta p \end{bmatrix} \tag{7}$$

and

$$\boldsymbol{W}(\boldsymbol{U}) = \begin{bmatrix} p \\ \alpha_{\mathrm{g}}v_{\mathrm{g}} + \alpha_\ell v_\ell \\ \alpha_{\mathrm{g}} \end{bmatrix}. \tag{8}$$

Copyright © 0000 John Wiley & Sons, Ltd.

Prepared using fldauth.cls
DOI: 10.1002/fld

where η is defined by

$$\eta = \frac{p}{\rho_\mathrm{g}\alpha_\ell c_\mathrm{g}^2 + \rho_\ell \alpha_\mathrm{g} c_\ell^2}. \tag{9}$$

It is well known that the basic equal-pressure two-fluid model is not hyperbolic [1, 20]. Therefore, our present model includes the regularisation terms Δp and v_τ that make it hyperbolic, often used for numerical testing [3, 4, 6, 9, 21, 22]. They can for example represent surface tension or hydrostatics. In this work, we focused on the numerical scheme, and therefore did not emphasise the physical relevance of the model closure relations. The discussions in the present article remain nevertheless relevant for any other choice of interfacial pressure regularisation term. We chose a widely used term [2, 4, 22, 23, 24] derived from mathematical considerations [25, 26]

$$\Delta p = \delta \frac{\alpha_\mathrm{g}\alpha_\ell\rho_\mathrm{g}\rho_\ell(v_\mathrm{g} - v_\ell)^2}{\alpha_\ell\rho_\mathrm{g} + \alpha_\mathrm{g}\rho_\ell}. \tag{10}$$

When the parameter δ is equal to one, this is the minimum pressure difference between the phases necessary to make the model hyperbolic at the first order of $(v_\mathrm{g} - v_\ell)$. It has been shown for some particular cases of the two-fluid six-equation model [25, 26], and for the two-fluid four-equation model without energy equations [22]. It can be shown with a perturbation method that it is also true for the general two-fluid six-equation model. With δ larger than one, the model is hyperbolic in an interval $|v_\mathrm{g} - v_\ell| < \Omega$, where Ω is some constant dependent on δ. The other term is defined by

$$v_\tau = \frac{\alpha_\ell\Gamma_\mathrm{g}v_\mathrm{g} + \alpha_\mathrm{g}\Gamma_\ell v_\ell}{\alpha_\ell\Gamma_\mathrm{g} + \alpha_\mathrm{g}\Gamma_\ell}. \tag{11}$$

Finally, the source term $\boldsymbol{S}(\boldsymbol{U})$ can represent gravity or phase interactions.

3. QUASILINEAR FORM

In order to derive a Roe scheme [19], we first write the model in a quasilinear form:

$$\frac{\partial \boldsymbol{U}}{\partial t} + \boldsymbol{A}(\boldsymbol{U})\frac{\partial \boldsymbol{U}}{\partial x} = \boldsymbol{S}(\boldsymbol{U}), \tag{12}$$

where

$$\boldsymbol{A}(\boldsymbol{U}) = \frac{\partial \boldsymbol{F}_c}{\partial \boldsymbol{U}} + \boldsymbol{B}(\boldsymbol{U})\frac{\partial \boldsymbol{W}}{\partial \boldsymbol{U}}. \tag{13}$$

To achieve this, we first derive the analytical Jacobian matrix of the flux. A natural decomposition of the problem is to treat the convective part $\boldsymbol{F}_c$ separately from the rest of the flux, mainly involving the pressure, $\boldsymbol{B}(\boldsymbol{U})\frac{\partial \boldsymbol{W}(\boldsymbol{U})}{\partial x}$. The resulting Jacobian matrices will be called $\boldsymbol{A}_c$ and $\boldsymbol{A}_p$, respectively.

3.1. Convective part

We can write the following differentials

$$\alpha_\mathrm{g}\rho_\mathrm{g}\,\mathrm{d}v_\mathrm{g} = \mathrm{d}u_3 - v_\mathrm{g}\,\mathrm{d}u_1 \tag{14}$$

$$\alpha_\ell\rho_\ell\,\mathrm{d}v_\ell = \mathrm{d}u_4 - v_\ell\,\mathrm{d}u_2 \tag{15}$$

and the matrix $\boldsymbol{A}_c$ follows

$$\boldsymbol{A}_c = \frac{\partial \boldsymbol{F}_c}{\partial \boldsymbol{U}} = \begin{bmatrix} 0 & 0 & 1 & 0 & 0 & 0 \\ 0 & 0 & 0 & 1 & 0 & 0 \\ -v_\mathrm{g}^2 & 0 & 2v_\mathrm{g} & 0 & 0 & 0 \\ 0 & -v_\ell^2 & 0 & 2v_\ell & 0 & 0 \\ -v_\mathrm{g}E_\mathrm{g} & 0 & E_\mathrm{g} & 0 & v_\mathrm{g} & 0 \\ 0 & -v_\ell E_\ell & 0 & E_\ell & 0 & v_\ell \end{bmatrix} \tag{16}$$

Copyright © 0000 John Wiley & Sons, Ltd.
Prepared using fldauth.cls

DOI: 10.1002/fld

where $E_\varphi = e_\varphi + \frac{1}{2}v_\varphi^2$.

3.2. A pressure differential

In order to derive the Jacobian $\boldsymbol{A}_p$ of the pressure flux, we need the derivative of the non-conservative flux variables, $\boldsymbol{W}$, with respect to the conservative variables, $\boldsymbol{U}$. First, some useful differentials are derived. We know from [2] that the differential of the pressure can be written

$$\mathrm{d}p = \left(c_k^2 - \Gamma_k \frac{p}{\rho_k}\right)\mathrm{d}\rho_k + \Gamma_k \rho_k \,\mathrm{d}e_k, \tag{17}$$

or equivalently:

$$\mathrm{d}p = \left(c_k^2 - \Gamma_k \left(e_k + \frac{p}{\rho_k}\right)\right)\mathrm{d}\rho_k + \Gamma_k \,\mathrm{d}(\rho_k e_k) \tag{18}$$

for $\mathrm{k} \in \mathrm{g}, \ell$. Furthermore,

$$\mathrm{d}\alpha_k = \frac{1}{\rho_k}\left(\mathrm{d}(\alpha_k\rho_k) - \alpha_k \,\mathrm{d}\rho_k\right) \tag{19}$$

$$= \frac{1}{\rho_k e_k}\left(\mathrm{d}(\alpha_k\rho_k e_k) - \alpha_k \,\mathrm{d}(\rho_k e_k)\right), \tag{20}$$

and similarly

$$\mathrm{d}\rho_k = \frac{1}{\alpha_k}\left(\mathrm{d}(\alpha_k\rho_k) - \rho_k \,\mathrm{d}\alpha_k\right), \tag{21}$$

$$\mathrm{d}(\rho_k e_k) = \frac{1}{\alpha_k}\left(\mathrm{d}(\alpha_k\rho_k e_k) - \rho_k e_k \,\mathrm{d}\alpha_k\right). \tag{22}$$

Hence we can write the differential (18) as

$$\alpha_k \,\mathrm{d}p = \left(c_k^2 - \Gamma_k \left(e_k + \frac{p}{\rho_k}\right)\right)\left(\mathrm{d}(\alpha_k\rho_k) - \rho_k \,\mathrm{d}\alpha_k\right) + \Gamma_k \left(\mathrm{d}(\alpha_k\rho_k e_k) - \rho_k e_k \,\mathrm{d}\alpha_k\right) \tag{23}$$

which simplifies to

$$\alpha_k \,\mathrm{d}p = \left(c_k^2 - \Gamma_k \left(e_k + \frac{p}{\rho_k}\right)\right)\mathrm{d}(\alpha_k\rho_k) + \Gamma_k \,\mathrm{d}(\alpha_k\rho_k e_k) - \zeta_k \,\mathrm{d}\alpha_k. \tag{24}$$

Now we express (24) for $\mathrm{k} = \mathrm{g}$ and $\mathrm{k} = \ell$, multiply them respectively by ζ_ℓ and ζ_g and add them to eliminate $\mathrm{d}\alpha_\mathrm{g}$

$$\mathcal{R}\,\mathrm{d}p = \zeta_\ell\left(\frac{\zeta_\mathrm{g}}{\rho_\mathrm{g}} - \Gamma_\mathrm{g} e_\mathrm{g}\right)\mathrm{d}u_1 + \zeta_\ell\Gamma_\mathrm{g}\,\mathrm{d}(u_1 e_\mathrm{g}) + \zeta_\mathrm{g}\left(\frac{\zeta_\ell}{\rho_\ell} - \Gamma_\ell e_\ell\right)\mathrm{d}u_2 + \zeta_\mathrm{g}\Gamma_\ell\,\mathrm{d}(u_2 e_\ell), \tag{25}$$

and in terms of the elements of the state vector $\boldsymbol{U}$, the pressure differential is

$$\mathcal{R}\,\mathrm{d}p = \zeta_\ell\beta_\mathrm{g}\,\mathrm{d}u_1 + \zeta_\mathrm{g}\beta_\ell\,\mathrm{d}u_2 - \zeta_\ell\Gamma_\mathrm{g}v_\mathrm{g}\,\mathrm{d}u_3 - \zeta_\mathrm{g}\Gamma_\ell v_\ell\,\mathrm{d}u_4 + \zeta_\ell\Gamma_\mathrm{g}\,\mathrm{d}u_5 + \zeta_\mathrm{g}\Gamma_\ell\,\mathrm{d}u_6, \tag{26}$$

where

$$\zeta_k = \rho_k c_k^2 - \Gamma_k p, \tag{27}$$

$$\beta_k = c_k^2 - \Gamma_k\left(e_k + \frac{p}{\rho_k}\right) + \frac{1}{2}\Gamma_k v_k^2, \tag{28}$$

$$\mathcal{R} = \alpha_\mathrm{g}\zeta_\ell + \alpha_\ell\zeta_\mathrm{g}. \tag{29}$$

Copyright © 0000 John Wiley & Sons, Ltd.
Prepared using fldauth.cls

DOI: 10.1002/fld

3.3. A volume-fraction differential

Now, we derive a volume-fraction differential. We start from

$$\mathrm{d}u_1 = \rho_\mathrm{g}\,\mathrm{d}\alpha_\mathrm{g} + \alpha_\mathrm{g}\,\mathrm{d}\rho_\mathrm{g}, \tag{30}$$

in which we substitute the density differential extracted from (17)

$$\mathrm{d}u_1 = \rho_\mathrm{g}\,\mathrm{d}\alpha_\mathrm{g} + \frac{\alpha_\mathrm{g}\rho_\mathrm{g}}{\rho_\mathrm{g}c_\mathrm{g}^2 - p\Gamma_\mathrm{g}}\left(\mathrm{d}p - \Gamma_\mathrm{g}\rho_\mathrm{g}\,\mathrm{d}e_\mathrm{g}\right). \tag{31}$$

Now, through the expression of the pressure differential (25) and $\mathrm{d}(u_1e_\mathrm{g}) = u_1\,\mathrm{d}e_\mathrm{g} + e_\mathrm{g}\,\mathrm{d}u_1$, we obtain

$$\mathcal{R}\,\mathrm{d}\alpha_\mathrm{g} = \alpha_\ell\left(\frac{\zeta_\mathrm{g}}{\rho_\mathrm{g}} - \Gamma_\mathrm{g}e_\mathrm{g}\right)\mathrm{d}u_1 - \alpha_\mathrm{g}\left(\frac{\zeta_\ell}{\rho_\ell} - \Gamma_\ell e_\ell\right)\mathrm{d}u_2 + \alpha_\ell\Gamma_\mathrm{g}\,\mathrm{d}(u_1e_\mathrm{g}) - \alpha_\mathrm{g}\Gamma_\ell\,\mathrm{d}(u_2e_\ell), \tag{32}$$

and in terms of the elements of the state vector $\boldsymbol{U}$, the volume-fraction differential is

$$\mathcal{R}\,\mathrm{d}\alpha_\mathrm{g} = \alpha_\ell\beta_\mathrm{g}\,\mathrm{d}u_1 - \alpha_\mathrm{g}\beta_\ell\,\mathrm{d}u_2 - \alpha_\ell\Gamma_\mathrm{g}v_\mathrm{g}\,\mathrm{d}u_3 - \alpha_\mathrm{g}\Gamma_\ell v_\ell\,\mathrm{d}u_4 + \alpha_\ell\Gamma_\mathrm{g}\,\mathrm{d}u_5 - \alpha_\mathrm{g}\Gamma_\ell\,\mathrm{d}u_6. \tag{33}$$

3.4. Velocity differentials

Finally, through the volume-fraction differential (33) and

$$\mathrm{d}v_\mathrm{g} = \frac{1}{\alpha_\mathrm{g}\rho_\mathrm{g}}\left(\mathrm{d}u_3 - v_\mathrm{g}\,\mathrm{d}u_1\right), \tag{34}$$

$$\mathrm{d}v_\ell = \frac{1}{\alpha_\ell\rho_\ell}\left(\mathrm{d}u_4 - v_\ell\,\mathrm{d}u_2\right), \tag{35}$$

we obtain the following differentials

$$\begin{aligned}\mathcal{R}\,\mathrm{d}(\alpha_\mathrm{g}v_\mathrm{g}) = {} & v_\mathrm{g}\left(\alpha_\ell\beta_\mathrm{g} - \frac{\mathcal{R}}{\rho_\mathrm{g}}\right)\mathrm{d}u_1 - \alpha_\mathrm{g}\beta_\ell v_\mathrm{g}\,\mathrm{d}u_2 \\ & + \left(\frac{\mathcal{R}}{\rho_\mathrm{g}} - \alpha_\ell\Gamma_\mathrm{g}v_\mathrm{g}^2\right)\mathrm{d}u_3 + \alpha_\mathrm{g}\Gamma_\ell v_\mathrm{g}v_\ell\,\mathrm{d}u_4 + \alpha_\ell\Gamma_\mathrm{g}v_\mathrm{g}\,\mathrm{d}u_5 - \alpha_\mathrm{g}\Gamma_\ell v_\mathrm{g}\,\mathrm{d}u_6,\end{aligned} \tag{36}$$

$$\begin{aligned}\mathcal{R}\,\mathrm{d}(\alpha_\ell v_\ell) = {} & -\alpha_\ell\beta_\mathrm{g}v_\ell\,\mathrm{d}u_1 + v_\ell\left(\alpha_\mathrm{g}\beta_\ell - \frac{\mathcal{R}}{\rho_\ell}\right)\mathrm{d}u_2 \\ & + \alpha_\ell\Gamma_\mathrm{g}v_\mathrm{g}v_\ell\,\mathrm{d}u_3 + \left(\frac{\mathcal{R}}{\rho_\ell} - \alpha_\mathrm{g}\Gamma_\ell v_\ell^2\right)\mathrm{d}u_4 - \alpha_\ell\Gamma_\mathrm{g}v_\ell\,\mathrm{d}u_5 + \alpha_\mathrm{g}\Gamma_\ell v_\ell\,\mathrm{d}u_6.\end{aligned} \tag{37}$$

3.5. Pressure part

With the help of the differentials (26), (33), (36) and (37), we can write the Jacobian matrix of $\boldsymbol{W}$ defined in (7)

$$\boldsymbol{M} = \frac{\partial \boldsymbol{W}\left(\boldsymbol{U}\right)}{\partial \boldsymbol{U}} = \mathcal{R}^{-1}\begin{bmatrix} \zeta_\ell\beta_\mathrm{g} & \left(v_\mathrm{g} - v_\ell\right)\alpha_\ell\beta_\mathrm{g} - \mathcal{R}v_\mathrm{g}/\rho_\mathrm{g} & \alpha_\ell\beta_\mathrm{g} \\ \zeta_\mathrm{g}\beta_\ell & \left(v_\ell - v_\mathrm{g}\right)\alpha_\mathrm{g}\beta_\ell - \mathcal{R}v_\ell/\rho_\ell & -\alpha_\mathrm{g}\beta_\ell \\ -\zeta_\ell\Gamma_\mathrm{g}v_\mathrm{g} & \mathcal{R}/\rho_\mathrm{g} - \left(v_\mathrm{g} - v_\ell\right)\alpha_\ell\Gamma_\mathrm{g}v_\mathrm{g} & -\alpha_\ell\Gamma_\mathrm{g}v_\mathrm{g} \\ -\zeta_\mathrm{g}\Gamma_\ell v_\ell & \mathcal{R}/\rho_\ell - \left(v_\ell - v_\mathrm{g}\right)\alpha_\mathrm{g}\Gamma_\ell v_\ell & \alpha_\mathrm{g}\Gamma_\ell v_\ell \\ \zeta_\ell\Gamma_\mathrm{g} & \left(v_\mathrm{g} - v_\ell\right)\alpha_\ell\Gamma_\mathrm{g} & \alpha_\ell\Gamma_\mathrm{g} \\ \zeta_\mathrm{g}\Gamma_\ell & \left(v_\ell - v_\mathrm{g}\right)\alpha_\mathrm{g}\Gamma_\ell & -\alpha_\mathrm{g}\Gamma_\ell \end{bmatrix}^T, \tag{38}$$

The matrix $\boldsymbol{A}_p$ is defined as

$$\boldsymbol{A}_p = \mathcal{R}\boldsymbol{B}(\boldsymbol{U})\frac{\partial \boldsymbol{W}(\boldsymbol{U})}{\partial \boldsymbol{U}} = \mathcal{R}\boldsymbol{B}\boldsymbol{M}, \tag{39}$$

such that the Jacobian matrix $\boldsymbol{A}$ is

$$\boldsymbol{A} = \boldsymbol{A}_c + \mathcal{R}^{-1}\boldsymbol{A}_p. \tag{40}$$

Copyright © 0000 John Wiley & Sons, Ltd.
Prepared using fldauth.cls

DOI: 10.1002/fld

4. THE ROE SCHEME

The Roe scheme requires the construction of a matrix at each cell interface. One seeks here the Jacobian matrix $\boldsymbol{A}$ evaluated at a particular average of the variables in the neighbouring cells. This is called Roe averaging and denoted by $\hat{\boldsymbol{A}}$ in the following. It has to satisfy some conditions [19, 22, 27, 28],

- R1: $\hat{\boldsymbol{A}}\left(\boldsymbol{U}^{\mathrm{L}},\boldsymbol{U}^{\mathrm{R}}\right)$ is diagonalisable with real eigenvalues,
- R2: $\hat{\boldsymbol{A}}\left(\boldsymbol{U}^{\mathrm{L}},\boldsymbol{U}^{\mathrm{R}}\right)\rightarrow\boldsymbol{A}\left(\bar{\boldsymbol{U}}\right)$ smoothly as $\boldsymbol{U}^{\mathrm{L}},\boldsymbol{U}^{\mathrm{R}}\rightarrow\bar{\boldsymbol{U}}$,
- R3: $\hat{\boldsymbol{A}}\left(\boldsymbol{U}^{\mathrm{L}},\boldsymbol{U}^{\mathrm{R}}\right)\left(\boldsymbol{U}^{\mathrm{R}}-\boldsymbol{U}^{\mathrm{L}}\right)=$

$$\boldsymbol{F}_c(\boldsymbol{U}^{\mathrm{R}})-\boldsymbol{F}_c(\boldsymbol{U}^{\mathrm{L}})+\overline{\boldsymbol{B}}\left(\boldsymbol{U}^{\mathrm{L}},\boldsymbol{U}^{\mathrm{R}}\right)\left(\boldsymbol{W}(\boldsymbol{U}^{\mathrm{R}})-\boldsymbol{W}(\boldsymbol{U}^{\mathrm{L}})\right).$$

The condition R3 is found by using the definition of $\overline{\boldsymbol{B}}$ in [2] in the Roe condition in [27]. The condition R1 will be fulfilled as long as the matrix $\hat{\boldsymbol{A}}(\boldsymbol{U}^{\mathrm{L}},\boldsymbol{U}^{\mathrm{R}})$ is defined as the matrix $\boldsymbol{A}(\hat{\boldsymbol{U}})$ evaluated for some Roe-average state $\hat{\boldsymbol{U}}$ of the left and right states $\boldsymbol{U}^{\mathrm{L}}$ and $\boldsymbol{U}^{\mathrm{R}}$, and that $\hat{\boldsymbol{U}}$ is within the hyperbolic domain of the model. R2 will in this case also be trivially fulfilled. However, the condition R3 is problematic. Note that the matrix $\overline{\boldsymbol{B}}$ is a property of the path chosen to evaluate the non-conservative products, and is independent of the numerical method [2]. Specifically, it will be shown in Section 4.2 that $\overline{\boldsymbol{B}}$ disappears from condition R3, so that the Roe averages can be defined independently of $\overline{\boldsymbol{B}}$. In this section, it is assumed that it is known. It will be discussed in Section 5.

Similarly to what was done in the derivation of the Jacobian matrix, we can split the problem into a convective part and a pressure part, such that $\hat{\boldsymbol{A}}=\hat{\boldsymbol{A}}_c+\hat{\mathcal{R}}^{-1}\hat{\boldsymbol{A}}_p$. Then we can remark that if the subconditions

$$\hat{\boldsymbol{A}}_c\left(\boldsymbol{U}^{\mathrm{L}},\boldsymbol{U}^{\mathrm{R}}\right)\left(\boldsymbol{U}^{\mathrm{R}}-\boldsymbol{U}^{\mathrm{L}}\right)=\boldsymbol{F}_c(\boldsymbol{U}^{\mathrm{R}})-\boldsymbol{F}_c(\boldsymbol{U}^{\mathrm{L}}), \tag{41}$$

$$\hat{\mathcal{R}}^{-1}\hat{\boldsymbol{A}}_p\left(\boldsymbol{U}^{\mathrm{L}},\boldsymbol{U}^{\mathrm{R}}\right)\left(\boldsymbol{U}^{\mathrm{R}}-\boldsymbol{U}^{\mathrm{L}}\right)=\overline{\boldsymbol{B}}\left(\boldsymbol{U}^{\mathrm{L}},\boldsymbol{U}^{\mathrm{R}}\right)\left(\boldsymbol{W}(\boldsymbol{U}^{\mathrm{R}})-\boldsymbol{W}(\boldsymbol{U}^{\mathrm{L}})\right) \tag{42}$$

are fulfilled, then the Roe condition R3 will be fulfilled. Therefore, we choose to split R3 in two, (41) and (42), and to build the partial matrices $\hat{\boldsymbol{A}}_c$ and $\hat{\boldsymbol{A}}_p$ that satisfy each its own condition, so that $\hat{\boldsymbol{A}}$ will satisfy R3.

4.1. Convective part

The derivation of the Roe matrix for the convective part $\hat{\boldsymbol{A}}_c$ is already well known, using the parameter-vector approach of Roe [19]. Specifically, Toumi [3] gives the parameter vector for this case. The condition (41) is fulfilled for a matrix $\hat{\boldsymbol{A}}_c$ defined as the matrix $\boldsymbol{A}_c$ (16) evaluated for the following Roe-averages of the velocity and the internal energy

$$\hat{v}_k=\frac{\left(\sqrt{\alpha_k\rho_k}v_k\right)^{\mathrm{L}}+\left(\sqrt{\alpha_k\rho_k}v_k\right)^{\mathrm{R}}}{\left(\sqrt{\alpha_k\rho_k}\right)^{\mathrm{L}}+\left(\sqrt{\alpha_k\rho_k}\right)^{\mathrm{R}}}, \tag{43}$$

$$\hat{e}_k=\tilde{e}_k+\frac{1}{2}\frac{\sqrt{(\alpha_k\rho_k)^{\mathrm{L}}(\alpha_k\rho_k)^{\mathrm{R}}}\left(v_k^{\mathrm{R}}-v_k^{\mathrm{L}}\right)^2}{\left(\left(\sqrt{\alpha_k\rho_k}\right)^{\mathrm{L}}+\left(\sqrt{\alpha_k\rho_k}\right)^{\mathrm{R}}\right)^2} \tag{44}$$

where

$$\tilde{e}_k=\frac{\left(\sqrt{\alpha_k\rho_k}e_k\right)^{\mathrm{L}}+\left(\sqrt{\alpha_k\rho_k}e_k\right)^{\mathrm{R}}}{\left(\sqrt{\alpha_k\rho_k}\right)^{\mathrm{L}}+\left(\sqrt{\alpha_k\rho_k}\right)^{\mathrm{R}}}. \tag{45}$$

Copyright © 0000 John Wiley & Sons, Ltd.
Prepared using fldauth.cls

DOI: 10.1002/fld

4.2. Relation for the pressure part

On the other hand, the parameter-vector approach is impractical for the pressure part. Instead, we follow a strategy similar to that in [29]. It consists in reducing the partial Roe condition (42) on $\hat{\boldsymbol{A}}_p$ to two scalar ones. One will concern the pressure average, and the other the mixture-velocity average. This approach will give analytical averaging formulas for all the variables but the pressure, for which we will have a relation to satisfy. This relation will be dependent on the equation of state and will generally have to be solved numerically. Thus we can construct a partially analytical Roe matrix for any equation of state.

By analogy with the the definition of $\boldsymbol{A}_p$ in (39), we look for $\hat{\boldsymbol{A}}_p$ in the form $\hat{\boldsymbol{A}}_p = \hat{\mathcal{R}}\overline{\boldsymbol{B}}\hat{\boldsymbol{M}}$. Inserting this into (42) gives

$$\hat{\boldsymbol{M}}\left(\boldsymbol{U}^{\mathrm{L}}, \boldsymbol{U}^{\mathrm{R}}\right)\left(\boldsymbol{U}^{\mathrm{R}} - \boldsymbol{U}^{\mathrm{L}}\right) = \boldsymbol{W}(\boldsymbol{U}^{\mathrm{R}}) - \boldsymbol{W}(\boldsymbol{U}^{\mathrm{L}}), \tag{46}$$

which results in a system of three equations. The matrix $\overline{\boldsymbol{B}}$ disappears from this system, therefore the Roe condition R3 can be satisfied without making any assumption on how $\boldsymbol{B}$ is averaged. Thus the Roe scheme can be derived independently of the choice of the non-conservative term averaging.

4.3. Velocity average for the pressure part

The first line of the system (46) reads

$$\begin{aligned}\hat{\mathcal{R}}\left(p^{\mathrm{R}} - p^{\mathrm{L}}\right) = {}& \hat{\zeta}_\ell\hat{\beta}_{\mathrm{g}}\left(u_1^{\mathrm{R}} - u_1^{\mathrm{L}}\right) + \hat{\zeta}_{\mathrm{g}}\hat{\beta}_\ell\left(u_2^{\mathrm{R}} - u_2^{\mathrm{L}}\right) - \hat{\zeta}_\ell\hat{\Gamma}_{\mathrm{g}}\hat{v}_{\mathrm{g}}\left(u_3^{\mathrm{R}} - u_3^{\mathrm{L}}\right) \\ & - \hat{\zeta}_{\mathrm{g}}\hat{\Gamma}_\ell\hat{v}_\ell\left(u_4^{\mathrm{R}} - u_4^{\mathrm{L}}\right) + \hat{\zeta}_\ell\hat{\Gamma}_{\mathrm{g}}\left(u_5^{\mathrm{R}} - u_5^{\mathrm{L}}\right) + \hat{\zeta}_{\mathrm{g}}\hat{\Gamma}_\ell\left(u_6^{\mathrm{R}} - u_6^{\mathrm{L}}\right).\end{aligned} \tag{47}$$

When the velocities are averaged following the formula (43), and if we choose

$$\hat{\beta}_k = \frac{\hat{\zeta}_k}{\hat{\rho}_k} - \hat{\Gamma}_k\left(\tilde{e}_k - \frac{1}{2}\hat{v}_k^2\right), \tag{48}$$

this expression is equivalent to the "Roe-average" of the pressure differential (25)

$$\begin{aligned}&\hat{\mathcal{R}}\left(p^{\mathrm{R}} - p^{\mathrm{L}}\right) = \\ &\quad\hat{\zeta}_\ell\left(\widehat{\left(\frac{\zeta_{\mathrm{g}}}{\rho_{\mathrm{g}}}\right)} - \hat{\Gamma}_{\mathrm{g}}\tilde{e}_{\mathrm{g}}\right)\left((\alpha_{\mathrm{g}}\rho_{\mathrm{g}})^{\mathrm{R}} - (\alpha_{\mathrm{g}}\rho_{\mathrm{g}})^{\mathrm{L}}\right) + \hat{\zeta}_{\mathrm{g}}\left(\widehat{\left(\frac{\zeta_\ell}{\rho_\ell}\right)} - \hat{\Gamma}_\ell\tilde{e}_\ell\right)\left((\alpha_\ell\rho_\ell)^{\mathrm{R}} - (\alpha_\ell\rho_\ell)^{\mathrm{L}}\right) \\ &\qquad + \hat{\zeta}_\ell\hat{\Gamma}_{\mathrm{g}}\left((\alpha_{\mathrm{g}}\rho_{\mathrm{g}}e_{\mathrm{g}})^{\mathrm{R}} - (\alpha_{\mathrm{g}}\rho_{\mathrm{g}}e_{\mathrm{g}})^{\mathrm{L}}\right) + \hat{\zeta}_{\mathrm{g}}\hat{\Gamma}_\ell\left((\alpha_\ell\rho_\ell e_\ell)^{\mathrm{R}} - (\alpha_\ell\rho_\ell e_\ell)^{\mathrm{L}}\right)\end{aligned} \tag{49}$$

Proof
Equating the right-hand sides of (47) and (49), as well as using (48) and

$$u_5 = u_1 e_{\mathrm{g}} + \frac{1}{2}u_1 v_{\mathrm{g}}^2, \tag{50}$$

$$u_6 = u_2 e_\ell + \frac{1}{2}u_2 v_\ell^2, \tag{51}$$

we obtain

$$\begin{aligned}&\frac{1}{2}\hat{\zeta}_\ell\hat{\Gamma}_{\mathrm{g}}\hat{v}_{\mathrm{g}}^2\left((\alpha_{\mathrm{g}}\rho_{\mathrm{g}})^{\mathrm{R}} - (\alpha_{\mathrm{g}}\rho_{\mathrm{g}})^{\mathrm{L}}\right) + \frac{1}{2}\hat{\zeta}_{\mathrm{g}}\hat{\Gamma}_\ell\hat{v}_\ell^2\left((\alpha_\ell\rho_\ell)^{\mathrm{R}} - (\alpha_\ell\rho_\ell)^{\mathrm{L}}\right) \\ &\qquad - \hat{\zeta}_\ell\hat{\Gamma}_{\mathrm{g}}\hat{v}_{\mathrm{g}}\left((\alpha_{\mathrm{g}}\rho_{\mathrm{g}}v_{\mathrm{g}})^{\mathrm{R}} - (\alpha_{\mathrm{g}}\rho_{\mathrm{g}}v_{\mathrm{g}})^{\mathrm{L}}\right) - \hat{\zeta}_{\mathrm{g}}\hat{\Gamma}_\ell\hat{v}_\ell\left((\alpha_\ell\rho_\ell v_\ell)^{\mathrm{R}} - (\alpha_\ell\rho_\ell v_\ell)^{\mathrm{L}}\right) \\ &\qquad + \frac{1}{2}\hat{\zeta}_\ell\hat{\Gamma}_{\mathrm{g}}\left((\alpha_{\mathrm{g}}\rho_{\mathrm{g}}v_{\mathrm{g}}^2)^{\mathrm{R}} - (\alpha_{\mathrm{g}}\rho_{\mathrm{g}}v_{\mathrm{g}}^2)^{\mathrm{L}}\right) + \frac{1}{2}\hat{\zeta}_{\mathrm{g}}\hat{\Gamma}_\ell\left((\alpha_\ell\rho_\ell v_\ell^2)^{\mathrm{R}} - (\alpha_\ell\rho_\ell v_\ell^2)^{\mathrm{L}}\right) = 0.\end{aligned} \tag{52}$$

Copyright © 0000 John Wiley & Sons, Ltd.
Prepared using fldauth.cls

DOI: 10.1002/fld

which is satisfied if

$$\frac{1}{2}\hat{\zeta}_\ell\hat{\Gamma}_{\rm g}\hat{v}_{\rm g}^2\left((\alpha_{\rm g}\rho_{\rm g})^{\rm R}-(\alpha_{\rm g}\rho_{\rm g})^{\rm L}\right)-\hat{\zeta}_\ell\hat{\Gamma}_{\rm g}\hat{v}_{\rm g}\left((\alpha_{\rm g}\rho_{\rm g}v_{\rm g})^{\rm R}-(\alpha_{\rm g}\rho_{\rm g}v_{\rm g})^{\rm L}\right)+\frac{1}{2}\hat{\zeta}_\ell\hat{\Gamma}_{\rm g}\left((\alpha_{\rm g}\rho_{\rm g}v_{\rm g}^2)^{\rm R}-(\alpha_{\rm g}\rho_{\rm g}v_{\rm g}^2)^{\rm L}\right)=0 \quad (53)$$

and

$$\frac{1}{2}\hat{\zeta}_{\rm g}\hat{\Gamma}_\ell\hat{v}_\ell^2\left((\alpha_\ell\rho_\ell)^{\rm R}-(\alpha_\ell\rho_\ell)^{\rm L}\right)-\hat{\zeta}_{\rm g}\hat{\Gamma}_\ell\hat{v}_\ell\left((\alpha_\ell\rho_\ell v_\ell)^{\rm R}-(\alpha_\ell\rho_\ell v_\ell)^{\rm L}\right)+\frac{1}{2}\hat{\zeta}_{\rm g}\hat{\Gamma}_\ell\left((\alpha_\ell\rho_\ell v_\ell^2)^{\rm R}-(\alpha_\ell\rho_\ell v_\ell^2)^{\rm L}\right)=0 \quad (54)$$

hold independently. They simplify to

$$\hat{v}_{\rm g}^2\left((\alpha_{\rm g}\rho_{\rm g})^{\rm R}-(\alpha_{\rm g}\rho_{\rm g})^{\rm L}\right)-2\left((\alpha_{\rm g}\rho_{\rm g}v_{\rm g})^{\rm R}-(\alpha_{\rm g}\rho_{\rm g}v_{\rm g})^{\rm L}\right)+\left((\alpha_{\rm g}\rho_{\rm g}v_{\rm g}^2)^{\rm R}-(\alpha_{\rm g}\rho_{\rm g}v_{\rm g}^2)^{\rm L}\right)=0 \quad (55)$$

and

$$\hat{v}_\ell^2\left((\alpha_\ell\rho_\ell)^{\rm R}-(\alpha_\ell\rho_\ell)^{\rm L}\right)-2\left((\alpha_\ell\rho_\ell v_\ell)^{\rm R}-(\alpha_\ell\rho_\ell v_\ell)^{\rm L}\right)+\left((\alpha_\ell\rho_\ell v_\ell^2)^{\rm R}-(\alpha_\ell\rho_\ell v_\ell^2)^{\rm L}\right)=0 \quad (56)$$

which in turn are satisfied if the velocity follows the averaging formula (43). □

4.4. Further simplification of the first line of the system (46)

Let us assume that the averages are such that the following equalities hold

$$(\alpha_k\rho_k)^{\rm R}-(\alpha_k\rho_k)^{\rm L}=\hat{\alpha_k}\left(\rho_k^{\rm R}-\rho_k^{\rm L}\right)+\hat{\rho}_k\left(\alpha_k^{\rm R}-\alpha_k^{\rm L}\right), \quad (57)$$

$$(\alpha_k\rho_k e_k)^{\rm R}-(\alpha_k\rho_k e_k)^{\rm L}=\hat{\alpha}_k\left((\rho_k e_k)^{\rm R}-(\rho_k e_k)^{\rm L}\right)+\hat{\rho}_k\tilde{e}_k\left(\alpha_k^{\rm R}-\alpha_k^{\rm L}\right). \quad (58)$$

$$(59)$$

We also observe that

$$(\rho_k e_k)^{\rm R}-(\rho_k e_k)^{\rm L}=\breve{\rho}_k\left(e_k^{\rm R}-e_k^{\rm L}\right)+\tilde{e}_k\left(\rho_k^{\rm R}-\rho_k^{\rm L}\right), \quad (60)$$

where $\tilde{e}_k$ is given by (45) and

$$\breve{\rho}_k=\frac{\rho_k^{\rm L}\rho_k^{\rm R}}{\hat{\rho}_k}. \quad (61)$$

Now, through the definition

$$\widehat{\left(\frac{\zeta_k}{\rho_k}\right)}=\frac{\hat{\zeta}_k}{\hat{\rho}_k}, \quad (62)$$

(49) can be further simplified. The condition deriving from the first line of the system finally reads

$$\hat{\mathcal{R}}\left(p^{\rm R}-p^{\rm L}\right)=\hat{\alpha}_{\rm g}\hat{\zeta}_\ell\frac{\hat{\zeta}_{\rm g}}{\hat{\rho}_{\rm g}}\left(\rho_{\rm g}^{\rm R}-\rho_{\rm g}^{\rm L}\right)+\hat{\alpha}_\ell\hat{\zeta}_{\rm g}\frac{\hat{\zeta}_\ell}{\hat{\rho}_\ell}\left(\rho_\ell^{\rm R}-\rho_\ell^{\rm L}\right)+\breve{\rho}_{\rm g}\hat{\alpha}_{\rm g}\hat{\zeta}_\ell\hat{\Gamma}_{\rm g}\left(e_{\rm g}^{\rm R}-e_{\rm g}^{\rm L}\right)+\breve{\rho}_\ell\hat{\alpha}_\ell\hat{\zeta}_{\rm g}\hat{\Gamma}_\ell\left(e_\ell^{\rm R}-e_\ell^{\rm L}\right). \quad (63)$$

Copyright © 0000 John Wiley & Sons, Ltd.
Prepared using fldauth.cls

DOI: 10.1002/fld

4.5. Simplification of the second line of the system (46)

The second line of the system (46) reads

$$\begin{aligned}\hat{\mathcal{R}}\left((\alpha_{\mathrm{g}}v_{\mathrm{g}}+\alpha_\ell v_\ell)^{\mathrm{R}}-(\alpha_{\mathrm{g}}v_{\mathrm{g}}+\alpha_\ell v_\ell)^{\mathrm{L}}\right)=&\\ \left((\hat{v}_{\mathrm{g}}-\hat{v}_\ell)\hat{\alpha}_\ell\hat{\beta}_{\mathrm{g}}-\frac{\hat{\mathcal{R}}\hat{v}_{\mathrm{g}}}{\hat{\rho}_{\mathrm{g}}}\right)\left(u_1^{\mathrm{R}}-u_1^{\mathrm{L}}\right)-\left((\hat{v}_{\mathrm{g}}-\hat{v}_\ell)\hat{\alpha}_{\mathrm{g}}\hat{\beta}_\ell-\frac{\hat{\mathcal{R}}\hat{v}_\ell}{\hat{\rho}_\ell}\right)\left(u_2^{\mathrm{R}}-u_2^{\mathrm{L}}\right)&\\ +\left(\frac{\hat{\mathcal{R}}}{\hat{\rho}_{\mathrm{g}}}-(\hat{v}_{\mathrm{g}}-\hat{v}_\ell)\hat{\alpha}_\ell\hat{\Gamma}_{\mathrm{g}}\hat{v}_{\mathrm{g}}\right)\left(u_3^{\mathrm{R}}-u_3^{\mathrm{L}}\right)+\left(\frac{\hat{\mathcal{R}}}{\hat{\rho}_\ell}+(\hat{v}_{\mathrm{g}}-\hat{v}_\ell)\hat{\alpha}_{\mathrm{g}}\hat{\Gamma}_\ell\hat{v}_\ell\right)\left(u_4^{\mathrm{R}}-u_4^{\mathrm{L}}\right)&\\ +(\hat{v}_{\mathrm{g}}-\hat{v}_\ell)\hat{\alpha}_\ell\hat{\Gamma}_{\mathrm{g}}\left(u_5^{\mathrm{R}}-u_5^{\mathrm{L}}\right)-(\hat{v}_{\mathrm{g}}-\hat{v}_\ell)\hat{\alpha}_{\mathrm{g}}\hat{\Gamma}_\ell\left(u_6^{\mathrm{R}}-u_6^{\mathrm{L}}\right).\quad(64)\end{aligned}$$

This expression will be successively simplified by assuming averaging formulas for the different variables. We first list them. The velocities will follow the same averaging as for the convective part, given by (43). Then, the density Roe-averaging takes the form

$$\hat{\rho}_k=\sqrt{\rho_k^{\mathrm{L}}\rho_k^{\mathrm{R}}}\frac{\sqrt{(\alpha_k\rho_k)^{\mathrm{L}}}+\sqrt{(\alpha_k\rho_k)^{\mathrm{R}}}}{\sqrt{\alpha_k^{\mathrm{L}}\rho_k^{\mathrm{R}}}+\sqrt{\alpha_k^{\mathrm{R}}\rho_k^{\mathrm{L}}}},\tag{65}$$

the volume fraction will be averaged as

$$\hat{\alpha}_k=\frac{\sqrt{\alpha_k^{\mathrm{R}}\rho_k^{\mathrm{L}}}\alpha_k^{\mathrm{L}}+\sqrt{\alpha_k^{\mathrm{L}}\rho_k^{\mathrm{R}}}\alpha_k^{\mathrm{R}}}{\sqrt{\alpha_k^{\mathrm{L}}\rho_k^{\mathrm{R}}}+\sqrt{\alpha_k^{\mathrm{R}}\rho_k^{\mathrm{L}}}},\tag{66}$$

while the internal energy has to have a different form than in the convective part. Its Roe average will be $\tilde{e}$ as defined in (45). Note that the averages (65) and (66) satisfy the relations (57) and (58).

If we assume the velocity Roe-average (43), (64) simplifies to

$$\begin{aligned}\hat{\mathcal{R}}\left((\alpha_{\mathrm{g}}v_{\mathrm{g}})^{\mathrm{R}}-(\alpha_{\mathrm{g}}v_{\mathrm{g}})^{\mathrm{L}}\right)=\hat{v}_{\mathrm{g}}\left(\hat{\alpha}_\ell\left(\widehat{\left(\frac{\zeta_{\mathrm{g}}}{\rho_{\mathrm{g}}}\right)}-\hat{\Gamma}_{\mathrm{g}}\tilde{e}_{\mathrm{g}}\right)-\frac{\hat{\mathcal{R}}}{\hat{\rho}_{\mathrm{g}}}\right)\left(u_1^{\mathrm{R}}-u_1^{\mathrm{L}}\right)&\\ -\hat{\alpha}_{\mathrm{g}}\hat{v}_{\mathrm{g}}\left(\widehat{\left(\frac{\zeta_\ell}{\rho_\ell}\right)}-\hat{\Gamma}_\ell\tilde{e}_\ell\right)\left(u_2^{\mathrm{R}}-u_2^{\mathrm{L}}\right)+\frac{\hat{\mathcal{R}}}{\hat{\rho}_{\mathrm{g}}}\left(u_3^{\mathrm{R}}-u_3^{\mathrm{L}}\right)&\\ +\hat{\alpha}_\ell\hat{\Gamma}_{\mathrm{g}}\hat{v}_{\mathrm{g}}\left((\alpha_{\mathrm{g}}\rho_{\mathrm{g}}e_{\mathrm{g}})^{\mathrm{R}}-(\alpha_{\mathrm{g}}\rho_{\mathrm{g}}e_{\mathrm{g}})^{\mathrm{L}}\right)-\hat{\alpha}_{\mathrm{g}}\hat{\Gamma}_\ell\hat{v}_{\mathrm{g}}\left((\alpha_\ell\rho_\ell e_\ell)^{\mathrm{R}}-(\alpha_\ell\rho_\ell e_\ell)^{\mathrm{L}}\right)\quad(67)\end{aligned}$$

and

$$\begin{aligned}\hat{\mathcal{R}}\left((\alpha_\ell v_\ell)^{\mathrm{R}}-(\alpha_\ell v_\ell)^{\mathrm{L}}\right)=-\hat{\alpha}_\ell\hat{v}_\ell\left(\widehat{\left(\frac{\zeta_{\mathrm{g}}}{\rho_{\mathrm{g}}}\right)}-\hat{\Gamma}_{\mathrm{g}}\tilde{e}_{\mathrm{g}}\right)\left(u_1^{\mathrm{R}}-u_1^{\mathrm{L}}\right)&\\ +\hat{v}_\ell\left(\hat{\alpha}_{\mathrm{g}}\left(\widehat{\left(\frac{\zeta_\ell}{\rho_\ell}\right)}-\hat{\Gamma}_\ell\tilde{e}_\ell\right)-\frac{\hat{\mathcal{R}}}{\hat{\rho}_\ell}\right)\left(u_2^{\mathrm{R}}-u_2^{\mathrm{L}}\right)+\frac{\hat{\mathcal{R}}}{\hat{\rho}_\ell}\left(u_4^{\mathrm{R}}-u_4^{\mathrm{L}}\right)&\\ -\hat{\alpha}_\ell\hat{\Gamma}_{\mathrm{g}}\hat{v}_\ell\left((\alpha_{\mathrm{g}}\rho_{\mathrm{g}}e_{\mathrm{g}})^{\mathrm{R}}-(\alpha_{\mathrm{g}}\rho_{\mathrm{g}}e_{\mathrm{g}})^{\mathrm{L}}\right)+\hat{\alpha}_{\mathrm{g}}\hat{\Gamma}_\ell\hat{v}_\ell\left((\alpha_\ell\rho_\ell e_\ell)^{\mathrm{R}}-(\alpha_\ell\rho_\ell e_\ell)^{\mathrm{L}}\right).\quad(68)\end{aligned}$$

Proof

The above conditions (67)–(68) are summed, and the right-hand side of the resulting expression is equated to that of the condition (64). This results in the two conditions already found for the convective part (55)–(56), and they are satisfied for the velocity averaging formula (43). □

Copyright © 0000 John Wiley & Sons, Ltd.
Prepared using fldauth.cls

DOI: 10.1002/fld

4.6. Density average

Then, if we assume a density average of the form (65), the conditions (67)–(68) reduce to

$$\hat{\mathcal{R}}\left((\alpha_{\mathrm{g}})^{\mathrm{R}}-(\alpha_{\mathrm{g}})^{\mathrm{L}}\right)=\hat{\alpha}_{\ell}\left(\widehat{\left(\frac{\zeta_{\mathrm{g}}}{\rho_{\mathrm{g}}}\right)}-\hat{\Gamma}_{\mathrm{g}}\tilde{e}_{\mathrm{g}}\right)\left(u_1^{\mathrm{R}}-u_1^{\mathrm{L}}\right)-\hat{\alpha}_{\mathrm{g}}\left(\widehat{\left(\frac{\zeta_{\ell}}{\rho_{\ell}}\right)}-\hat{\Gamma}_{\ell}\tilde{e}_{\ell}\right)\left(u_2^{\mathrm{R}}-u_2^{\mathrm{L}}\right)$$
$$+\hat{\alpha}_{\ell}\hat{\Gamma}_{\mathrm{g}}\left((\alpha_{\mathrm{g}}\rho_{\mathrm{g}}e_{\mathrm{g}})^{\mathrm{R}}-(\alpha_{\mathrm{g}}\rho_{\mathrm{g}}e_{\mathrm{g}})^{\mathrm{L}}\right)-\hat{\alpha}_{\mathrm{g}}\hat{\Gamma}_{\ell}\left((\alpha_{\ell}\rho_{\ell}e_{\ell})^{\mathrm{R}}-(\alpha_{\ell}\rho_{\ell}e_{\ell})^{\mathrm{L}}\right). \quad (69)$$

Proof
First, observe that

$$(\alpha_k v_k)^{\mathrm{R}}-(\alpha_k v_k)^{\mathrm{L}}=\check{\alpha}_k\left(v_k^{\mathrm{R}}-v_k^{\mathrm{L}}\right)+\hat{v}_k\left(\alpha_k^{\mathrm{R}}-\alpha_k^{\mathrm{L}}\right) \quad (70)$$

where $\hat{v}_k$ is given by (43), $\hat{\rho}_k$ by (65) and

$$\check{\alpha}_k=\frac{\sqrt{(\alpha_k\rho_k)^{\mathrm{R}}}\alpha_k^{\mathrm{L}}+\sqrt{(\alpha_k\rho_k)^{\mathrm{L}}}\alpha_k^{\mathrm{R}}}{\sqrt{(\alpha_k\rho_k)^{\mathrm{L}}}+\sqrt{(\alpha_k\rho_k)^{\mathrm{R}}}}. \quad (71)$$

These averaging formulas also satisfy

$$\check{\alpha}_{\mathrm{g}}\left(v_{\mathrm{g}}^{\mathrm{R}}-v_{\mathrm{g}}^{\mathrm{L}}\right)=-\frac{\hat{v}_{\mathrm{g}}}{\hat{\rho}_{\mathrm{g}}}\left(u_1^{\mathrm{R}}-u_1^{\mathrm{L}}\right)+\frac{1}{\hat{\rho}_{\mathrm{g}}}\left(u_3^{\mathrm{R}}-u_3^{\mathrm{L}}\right) \quad (72)$$

$$\check{\alpha}_{\ell}\left(v_{\ell}^{\mathrm{R}}-v_{\ell}^{\mathrm{L}}\right)=-\frac{\hat{v}_{\ell}}{\hat{\rho}_{\ell}}\left(u_2^{\mathrm{R}}-u_2^{\mathrm{L}}\right)+\frac{1}{\hat{\rho}_{\ell}}\left(u_4^{\mathrm{R}}-u_4^{\mathrm{L}}\right). \quad (73)$$

Now, write (70) for phases g and ℓ, substitute into them respectively (72) and (73), and substitute them in turn respectively into (67) and (68). Since $\alpha_{\mathrm{g}}+\alpha_{\ell}=1$, both expression reduce to (69). □

4.7. Internal energy average for the pressure part

Finally, if we assume that the volume fraction average follows (66) and the internal energy average follows the form of $\tilde{e}$ in (45), the condition (69) can be written as

$$\widehat{\left(\frac{\zeta_{\mathrm{g}}}{\rho_{\mathrm{g}}}\right)}\left(\rho_{\mathrm{g}}^{\mathrm{R}}-\rho_{\mathrm{g}}^{\mathrm{L}}\right)-\widehat{\left(\frac{\zeta_{\ell}}{\rho_{\ell}}\right)}\left(\rho_{\ell}^{\mathrm{R}}-\rho_{\ell}^{\mathrm{L}}\right)+\check{\rho}_{\mathrm{g}}\hat{\Gamma}_{\mathrm{g}}\left(e_{\mathrm{g}}^{\mathrm{R}}-e_{\mathrm{g}}^{\mathrm{L}}\right)-\check{\rho}_{\ell}\hat{\Gamma}_{\ell}\left(e_{\ell}^{\mathrm{R}}-e_{\ell}^{\mathrm{L}}\right)=0, \quad (74)$$

where we have used the shorthand (61).

Proof
Recall the expressions (57), (58) and (60). Substituting them into (69), using (66) and (45) as averaging formulas, as well as defining

$$\hat{\mathcal{R}}=\hat{\alpha}_{\mathrm{g}}\hat{\zeta}_{\ell}+\hat{\alpha}_{\ell}\hat{\zeta}_{\mathrm{g}} \quad (75)$$

yields the result after cancelling the equal terms. □

4.8. A relation for the pressure average

We have now reduced the two first lines of the system resulting from the pressure part of the Roe condition to the expressions (63) and (74). With the definitions of the averages (43), (45), (65) and (66) as well as the definitions (62) and (75), they can be recombined as

$$p^{\mathrm{R}}-p^{\mathrm{L}}=\frac{\hat{\zeta}_{\mathrm{g}}}{\hat{\rho}_{\mathrm{g}}}\left(\rho_{\mathrm{g}}^{\mathrm{R}}-\rho_{\mathrm{g}}^{\mathrm{L}}\right)+\check{\rho}_{\mathrm{g}}\hat{\Gamma}_{\mathrm{g}}\left(e_{\mathrm{g}}^{\mathrm{R}}-e_{\mathrm{g}}^{\mathrm{L}}\right) \quad (76)$$

$$=\frac{\hat{\zeta}_{\ell}}{\hat{\rho}_{\ell}}\left(\rho_{\ell}^{\mathrm{R}}-\rho_{\ell}^{\mathrm{L}}\right)+\check{\rho}_{\ell}\hat{\Gamma}_{\ell}\left(e_{\ell}^{\mathrm{R}}-e_{\ell}^{\mathrm{L}}\right). \quad (77)$$

This resembles a Roe average of the differential (17).

Copyright © 0000 John Wiley & Sons, Ltd.
Prepared using fldauth.cls

DOI: 10.1002/fld

4.9. Simplification of the third line of the system (46)

The third line of the system (46) reads

$$\begin{aligned}\hat{\mathcal{R}}\left(\alpha_{\mathrm{g}}^{\mathrm{R}}-\alpha_{\mathrm{g}}^{\mathrm{L}}\right)&=\hat{\alpha}_{\ell}\hat{\beta}_{\mathrm{g}}\left(u_1^{\mathrm{R}}-u_1^{\mathrm{L}}\right)-\hat{\alpha}_{\mathrm{g}}\hat{\beta}_{\ell}\left(u_2^{\mathrm{R}}-u_2^{\mathrm{L}}\right)\\&-\hat{\alpha}_{\ell}\hat{\Gamma}_{\mathrm{g}}\hat{v}_{\mathrm{g}}\left(u_3^{\mathrm{R}}-u_3^{\mathrm{L}}\right)+\hat{\alpha}_{\mathrm{g}}\hat{\Gamma}_{\ell}\hat{v}_{\ell}\left(u_4^{\mathrm{R}}-u_4^{\mathrm{L}}\right)+\hat{\alpha}_{\ell}\hat{\Gamma}_{\mathrm{g}}\left(u_5^{\mathrm{R}}-u_5^{\mathrm{L}}\right)-\hat{\alpha}_{\mathrm{g}}\hat{\Gamma}_{\ell}\left(u_6^{\mathrm{R}}-u_6^{\mathrm{L}}\right),\end{aligned}\tag{78}$$

where $\hat{\beta}_k$ is given by (48) and $\hat{\mathcal{R}}$ is as defined in (75).

Now, if the velocities are averaged following the formula (43), the condition (78) reduces to

$$\begin{aligned}&\hat{\mathcal{R}}\left(\alpha_{\mathrm{g}}^{\mathrm{R}}-\alpha_{\mathrm{g}}^{\mathrm{L}}\right)=\\&\hat{\alpha}_{\ell}\left(\frac{\hat{\zeta}_{\mathrm{g}}}{\hat{\rho}_{\mathrm{g}}}-\hat{\Gamma}_{\mathrm{g}}\tilde{e}_{\mathrm{g}}\right)\left((\alpha_{\mathrm{g}}\rho_{\mathrm{g}})^{\mathrm{R}}-(\alpha_{\mathrm{g}}\rho_{\mathrm{g}})^{\mathrm{L}}\right)-\hat{\alpha}_{\mathrm{g}}\left(\frac{\hat{\zeta}_{\ell}}{\hat{\rho}_{\ell}}-\hat{\Gamma}_{\ell}\tilde{e}_{\ell}\right)\left((\alpha_{\ell}\rho_{\ell})^{\mathrm{R}}-(\alpha_{\ell}\rho_{\ell})^{\mathrm{L}}\right)\\&+\hat{\alpha}_{\ell}\hat{\Gamma}_{\mathrm{g}}\left((\alpha_{\mathrm{g}}\rho_{\mathrm{g}}e_{\mathrm{g}})^{\mathrm{R}}-(\alpha_{\mathrm{g}}\rho_{\mathrm{g}}e_{\mathrm{g}})^{\mathrm{L}}\right)-\hat{\alpha}_{\mathrm{g}}\hat{\Gamma}_{\ell}\left((\alpha_{\ell}\rho_{\ell}e_{\ell})^{\mathrm{R}}-(\alpha_{\ell}\rho_{\ell}e_{\ell})^{\mathrm{L}}\right),\end{aligned}\tag{79}$$

Proof

Equating the right-hand sides of the expression (78) and (79) yields

$$\begin{aligned}&\frac{1}{2}\hat{\alpha}_{\ell}\hat{\Gamma}_{\mathrm{g}}\hat{v}_{\mathrm{g}}^2\left((\alpha_{\mathrm{g}}\rho_{\mathrm{g}})^{\mathrm{R}}-(\alpha_{\mathrm{g}}\rho_{\mathrm{g}})^{\mathrm{L}}\right)-\frac{1}{2}\hat{\alpha}_{\mathrm{g}}\hat{\Gamma}_{\ell}\hat{v}_{\ell}\left((\alpha_{\ell}\rho_{\ell})^{\mathrm{R}}-(\alpha_{\ell}\rho_{\ell})^{\mathrm{L}}\right)\\&-\hat{\alpha}_{\ell}\hat{\Gamma}_{\mathrm{g}}\hat{v}_{\mathrm{g}}\left((\alpha_{\mathrm{g}}\rho_{\mathrm{g}}v_{\mathrm{g}})^{\mathrm{R}}-(\alpha_{\mathrm{g}}\rho_{\mathrm{g}}v_{\mathrm{g}})^{\mathrm{L}}\right)+\hat{\alpha}_{\mathrm{g}}\hat{\Gamma}_{\ell}\hat{v}_{\ell}\left((\alpha_{\ell}\rho_{\ell}v_{\ell})^{\mathrm{R}}-(\alpha_{\ell}\rho_{\ell}v_{\ell})^{\mathrm{L}}\right)\\&+\frac{1}{2}\hat{\alpha}_{\ell}\hat{\Gamma}_{\mathrm{g}}\left((\alpha_{\mathrm{g}}\rho_{\mathrm{g}}v_{\mathrm{g}}^2)^{\mathrm{R}}-(\alpha_{\mathrm{g}}\rho_{\mathrm{g}}v_{\mathrm{g}}^2)^{\mathrm{L}}\right)-\frac{1}{2}\hat{\alpha}_{\mathrm{g}}\hat{\Gamma}_{\ell}\left((\alpha_{\ell}\rho_{\ell}v_{\ell}^2)^{\mathrm{R}}-(\alpha_{\ell}\rho_{\ell}v_{\ell}^2)^{\mathrm{L}}\right)=0,\end{aligned}\tag{80}$$

which is satisfied by the averaging formula (43). □

Finally, if we assume that the averaging formulas for the volume fraction $\hat{\alpha}$ (66), the density $\hat{\rho}$ (65) and the internal energy $\tilde{e}$ (45) hold, the condition (79) simplifies to

$$\frac{\hat{\zeta}_{\mathrm{g}}}{\hat{\rho}_{\mathrm{g}}}\left(\rho_{\mathrm{g}}^{\mathrm{R}}-\rho_{\mathrm{g}}^{\mathrm{L}}\right)-\frac{\hat{\zeta}_{\ell}}{\hat{\rho}_{\ell}}\left(\rho_{\ell}^{\mathrm{R}}-\rho_{\ell}^{\mathrm{L}}\right)+\breve{\rho}_{\mathrm{g}}\hat{\Gamma}_{\mathrm{g}}\left(e_{\mathrm{g}}^{\mathrm{R}}-e_{\mathrm{g}}^{\mathrm{L}}\right)-\breve{\rho}_{\ell}\hat{\Gamma}_{\ell}\left(e_{\ell}^{\mathrm{R}}-e_{\ell}^{\mathrm{L}}\right)=0.\tag{81}$$

Proof

Using the relations (57) and (58), the expression (79) can be written as

$$\begin{aligned}&\left(\frac{\hat{\zeta}_{\mathrm{g}}}{\hat{\rho}_{\mathrm{g}}}-\hat{\Gamma}_{\mathrm{g}}\tilde{e}_{\mathrm{g}}\right)\left(\rho_{\mathrm{g}}^{\mathrm{R}}-\rho_{\mathrm{g}}^{\mathrm{L}}\right)-\left(\frac{\hat{\zeta}_{\ell}}{\hat{\rho}_{\ell}}-\hat{\Gamma}_{\ell}\tilde{e}_{\ell}\right)\left(\rho_{\ell}^{\mathrm{R}}-\rho_{\ell}^{\mathrm{L}}\right)\\&+\hat{\Gamma}_{\mathrm{g}}\left((\rho_{\mathrm{g}}e_{\mathrm{g}})^{\mathrm{R}}-(\rho_{\mathrm{g}}e_{\mathrm{g}})^{\mathrm{L}}\right)-\hat{\Gamma}_{\ell}\left((\rho_{\ell}e_{\ell})^{\mathrm{R}}-(\rho_{\ell}e_{\ell})^{\mathrm{L}}\right)=0.\end{aligned}\tag{82}$$

The expression (81) follows from using the relation (60). □

The relation (81) is satisfied whenever the relations resulting from the two first lines (76) and (77) are satisfied.

4.10. Remaining variables

The last variables in the conditions (76) and (77) for which we did not define a Roe average are ζ_k and Γ_k. Recall the definition $\zeta_k=\rho_k c_k^2-\Gamma_k p$. It is dependent on the equation of state because the speed of sound c and Γ are thermodynamical parameters. Therefore the remaining averaging formulas cannot be deduced analytically from these conditions without specifying the equation of state. On the other hand, there exist approaches to construct the required averages numerically, when the equation of state is in the form of a "black box"

Copyright © 0000 John Wiley & Sons, Ltd.
Prepared using fldauth.cls

DOI: 10.1002/fld

(see for example the approach presented in [29]). This is an advantage when using tabulated equations of state.

Note that the internal energy averages for the convective part (44) and the pressure part (45) are different from each other. Hence the full matrix cannot in general be written in the form

$$\hat{\boldsymbol{A}}(\boldsymbol{U}^{\mathrm{L}},\boldsymbol{U}^{\mathrm{R}}) = \boldsymbol{A}(\hat{\boldsymbol{U}}(\boldsymbol{U}^{\mathrm{L}},\boldsymbol{U}^{\mathrm{R}})). \tag{83}$$

In addition, in general

$$\hat{\alpha}_{\mathrm{g}} + \hat{\alpha}_{\ell} \neq 1. \tag{84}$$

However, this is just a feature of the formulation of the averaging and does not in any way affect the numerical consistency of the scheme. In particular, the conditions R2 and R3 are unconditionally satisfied. The condition R1 holds only conditionally for the model itself, and is discussed in more detail in Section 6.

4.11. Application to stiffened gas

The derivation above was independent of the choice of equation of state. For the purpose of numerical testing in the present work, we have used the stiffened gas equation of state. This equation of state is based on the ideal gas law, to which a factor is added to reduce the compressibility. It can then represent liquid-like fluids in addition to gases. It is expressed by

$$p(\rho,T) = \frac{\gamma-1}{\gamma}\rho C_p T - p_\infty \tag{85}$$

$$e(\rho,T) = \frac{C_p}{\gamma}T + \frac{p_\infty}{\rho}. \tag{86}$$

where γ, p_∞ and C_p are constants.

To represent a two-phase flow of a liquid and a gas at mechanical equilibrium, we then define two fluids following the equation of state (85)–(86), sharing the same pressure and whose volume fractions sum to one. To evaluate the state of the two fluids from the vector of conserved variables, we use in the present work the algorithm described in [30].

With the choice of an equation of state, we are now able to define Roe averages for ζ_k and Γ_k. First, we can write

$$p = \Gamma_k \rho_k e_k - \gamma_k p_\infty, \tag{87}$$

where Γ is the first Grüneisen coefficient, which for the stiffened gas equation of state is $\Gamma = \gamma - 1$. This gives

$$\mathrm{d}p = \Gamma_k \,\mathrm{d}(\rho_k e_k) = \Gamma_k e_k \,\mathrm{d}\rho_k + \Gamma_k \rho_k \,\mathrm{d}e_k. \tag{88}$$

By comparison with the differential (17), we deduce

$$\zeta_k = \Gamma_k e_k \rho_k. \tag{89}$$

We choose to define the averages as

$$\hat{\Gamma}_k = \Gamma_k, \tag{90}$$

and

$$\hat{\zeta}_k = \Gamma_k \breve{e}_k \hat{\rho}_k. \tag{91}$$

We now need to define the average $\breve{e}_k$ in order to satisfy the Roe condition (42). From (76)–(77) and (87), we obtain

$$p^{\mathrm{R}} - p^{\mathrm{L}} = \Gamma_k(\rho_k^{\mathrm{R}} e_k^{\mathrm{R}} - \rho_k^{\mathrm{L}} e_k^{\mathrm{L}}) = \frac{\Gamma_k \breve{e}_k \hat{\rho}_k}{\hat{\rho}_k}(\rho_k^{\mathrm{R}} - \rho_k^{\mathrm{L}}) + \breve{\rho}_k \Gamma_k (e_k^{\mathrm{R}} - e_k^{\mathrm{L}}) \tag{92}$$

Copyright © 0000 John Wiley & Sons, Ltd.
Prepared using fldauth.cls

DOI: 10.1002/fld

which simplifies to

$$\rho_k^{\mathrm{R}} e_k^{\mathrm{R}} - \rho_k^{\mathrm{L}} e_k^{\mathrm{L}} = \frac{\breve{e}_k \hat{\rho}_k}{\hat{\rho}_k}(\rho_k^{\mathrm{R}} - \rho_k^{\mathrm{L}}) + \breve{\rho}_k(e_k^{\mathrm{R}} - e_k^{\mathrm{L}}) \tag{93}$$

which is verified by the definition (61) and the internal energy average (45)

$$\breve{e}_k = \frac{\sqrt{\alpha_k^{\mathrm{L}}\rho_k^{\mathrm{L}}}e_k^{\mathrm{L}} + \sqrt{\alpha_k^{\mathrm{R}}\rho_k^{\mathrm{R}}}e_k^{\mathrm{R}}}{\sqrt{\alpha_k^{\mathrm{L}}\rho_k^{\mathrm{L}}} + \sqrt{\alpha_k^{\mathrm{R}}\rho_k^{\mathrm{R}}}} = \tilde{e}_k. \tag{94}$$

Note that with the stiffened gas equation of state, the Roe average of the pressure is not used.

5. NON-CONSERVATIVE TERMS

In the *formally path-conservative* framework [10], the non-conservative terms are integrated between the left and right states along a given path, giving the averaging formulas for the non-conservative factors gathered in the matrix $\boldsymbol{B}$. Some previous works pointed out that this approach may converge to a weak solution with the wrong shock speeds [15, 16]. Other approaches to handle non-conservative terms consist in flux splitting, see for example [4]. In these approaches, the solution is advanced one time step with the conservative fluxes, before the non-conservative terms are applied as source terms. Therefore the whole wave structure is not captured during the conservative time step. This results in smearing of the discontinuities. By letting the non-conservative terms affect the wave structure of the model, this smearing is avoided. The *formally path-conservative* framework allows that, since all the differential terms are solved at the same time. Further, this is an advantage for the purpose of analysis since we have access, at least numerically, to the real velocity of the waves.

Choosing the right integration path for the matrix $\boldsymbol{B}$ is not the object of this article. As shown with (46), the matrix $\boldsymbol{B}$ disappears from the Roe condition. Therefore the choice of the path does not interact with the derivation of the Roe averages, and the Roe scheme here presented is independent of the choice of path. However, it has been observed that if the $\boldsymbol{B}$-averages are too different from the Roe averages, the resulting matrix $\boldsymbol{A}$ may have complex eigenvalues. Now, in [2], it was shown that the averaging method for the matrix $\boldsymbol{B}$ has limited effect on the results for Toumi's shock tube with the six-equation system. Therefore, we found it convenient to choose the Roe averages for evaluating the matrix $\boldsymbol{B}$. The pressure can have a particular treatment. Since we have used the stiffened gas equation of state, the Roe average of the pressure is not used (cf. Section 4.11). This average generally has to be found numerically using the relations (76)–(77). We have here simply used the arithmetic average for the pressure in the matrix $\boldsymbol{B}$.

Note that our scheme can only be said to be implicitly path-consistent, as the existence of a definite path corresponding to these averages is here an a priori assumption. In this respect, we follow the approach of [2]. Nevertheless, our method will be *formally path-consistent* for any path giving the $\boldsymbol{B}$-averaging employed in this paper.

6. RESONANCE OF THE SYSTEM

When the velocities are equal to each other, the Jacobian matrix $\boldsymbol{A}$ (40) is not diagonalisable. The system is then said to be resonant. Since the Roe scheme is based on diagonalising this matrix, this seriously impairs the robustness of the method.

Copyright © 0000 John Wiley & Sons, Ltd.

Prepared using fldauth.cls
DOI: 10.1002/fld

6.1. Collapse of the eigenspace

The two-fluid model has six eigenvalues. Two of them correspond to the speed of the pressure waves in both directions, two others correspond to the speed of the interfacial waves – also called volume-fraction waves – in both directions. The last two correspond to the convection speed of the entropy in each phase. Only the last two are known analytically: v_g and v_ℓ. Otherwise, the eigenstructure of the two-fluid model is in general not known. However, when $v_\mathrm{g} = v_\ell$, we are able to obtain general analytical eigenvalues and eigenvectors for the entropy and volume-fraction waves. If we substitute v_m for v_g and v_ℓ in the matrix $\boldsymbol{A}$ (40), v_m is an eigenvalue with multiplicity four. The corresponding eigenvector can be shown to be

$$\boldsymbol{X}_{v_\mathrm{m}} = \begin{bmatrix} \omega_1 \\ \omega_2 \\ v_\mathrm{m}\omega_1 \\ v_\mathrm{m}\omega_2 \\ \frac{1}{2}v_\mathrm{m}^2\omega_1 - e_\mathrm{g}\rho_\mathrm{g}\omega_3 \\ \frac{1}{2}v_\mathrm{m}^2\omega_2 + e_\ell\rho_\ell\omega_3 \end{bmatrix}. \tag{95}$$

This vector only contains three degrees of freedom $(\omega_1, \omega_2, \omega_3)$, which is less than the multiplicity of the eigenvalue. This shows that the matrix is not diagonalisable. When $v_\mathrm{g} \neq v_\ell$, however, the eigenvalues become generally distinct, and so do the eigenvectors. In particular, the eigenvectors corresponding to the eigenvalues v_g and v_ℓ are respectively

$$\boldsymbol{X}_{v_\mathrm{g}} = \begin{bmatrix} 1 \\ 0 \\ v_\mathrm{g} \\ 0 \\ \frac{1}{2}v_\mathrm{g}^2 \\ 0 \end{bmatrix} \qquad \text{and} \qquad \boldsymbol{X}_{v_\ell} = \begin{bmatrix} 0 \\ 1 \\ 0 \\ v_\ell \\ 0 \\ \frac{1}{2}v_\ell^2 \end{bmatrix}. \tag{96}$$

These vectors describe the entropy waves, propagating at the velocity of the phases. We can remark that when $(v_\mathrm{g}, v_\ell) \to (v_\mathrm{m}, v_\mathrm{m})$

$$\boldsymbol{X}_{v_\mathrm{m}} = \omega_1 \boldsymbol{X}_{v_\mathrm{g}}(v_\mathrm{g} = v_\mathrm{m}) + \omega_2 \boldsymbol{X}_{v_\ell}(v_\ell = v_\mathrm{m}) + \omega_3 \begin{bmatrix} 0 \\ 0 \\ 0 \\ 0 \\ -e_\mathrm{g}\rho_\mathrm{g} \\ e_\ell\rho_\ell \end{bmatrix}. \tag{97}$$

Both eigenvectors describing the entropy waves are independent and present in $\boldsymbol{X}_{v_\mathrm{m}}$, while only one dimension remains for the vectors describing the volume-fraction waves. We deduce that the eigenspace collapsing is the one associated with the volume-fraction waves. Those waves do indeed become identical when they propagate at identical velocities, therefore their corresponding eigenvectors cross each other at $v_\mathrm{g} = v_\ell$. Note that this is a purely mathematical phenomenon, not a physical one. The eigenspace collapses because the waves become identical, such that their eigenvectors become equal. Physically, both waves are still present, but superimposed. This is why resonance is not a problem for the MUSTA method [2], which does not use the eigenstructure of the model.

6.2. Correction of the numerical scheme

This results in the Roe scheme being inapplicable when $|v_\mathrm{g} - v_\ell| < \varepsilon$ (ε being a small quantity depending on the machine precision) because the vectors will be indistinct at machine precision. To overcome this difficulty, we will take advantage of the continuity of the eigenvectors with respect to $v_\mathrm{g} - v_\ell$.

Copyright © 0000 John Wiley & Sons, Ltd.

Prepared using fldauth.cls
DOI: 10.1002/fld

For some small ε, for each interface where the averaged state is such that $|v_g - v_\ell| < \varepsilon$, we apply the following procedure. For an interface between the cell i and $i+1$, the velocities are modified as follows

$$v_g^i \to v_g^i + \varepsilon \qquad v_g^{i+1} \to v_g^{i+1} + \varepsilon \tag{98}$$

$$v_\ell^i \to v_\ell^i - \varepsilon \qquad v_\ell^{i+1} \to v_\ell^{i+1} - \varepsilon, \tag{99}$$

before the Roe fluctuations (cf. [31], p. 80) are evaluated at the interface for these states. Then the velocities are again modified as

$$v_g^i \to v_g^i - \varepsilon \qquad v_g^{i+1} \to v_g^{i+1} - \varepsilon \tag{100}$$

$$v_\ell^i \to v_\ell^i + \varepsilon \qquad v_\ell^{i+1} \to v_\ell^{i+1} + \varepsilon. \tag{101}$$

The Roe fluctuations are also evaluated for these states. Then the approximate fluctuations with the original velocities are obtained by taking the arithmetic average.

6.3. Effect of the regularisation of the model

The regularisation term Δp used in this work vanishes when $v_g = v_\ell$, and resonance occurs. Now, theoretically, if the pressure difference between the phases is not zero when $v_g = v_\ell$, resonance should be avoided. This is because the eigenvalues associated with volume fraction waves then are slightly different from each other. However, physically sensible regularisation terms will generally give small pressure differences compared to the phase pressures. To investigate whether this is enough to avoid the resonance problems, we added to our regularisation term Δp a term in the form proposed by Soo [32] (pp. 319–321), $C \cdot p$, where p is the pressure, and C is a constant. These investigations showed a strong loss of numerical accuracy in the proximity of the state $v_g = v_\ell$, even when the system would theoretically not be resonant for the volume-fraction waves. This is due to the eigenvectors matrix being badly conditioned. A constant C of the order of unity – thus Δp of the order of the fluid pressure – was necessary in order to be able to run the scheme without the resonance fix exposed in the previous section. This is not physical, therefore the fix is also necessary with any physically meaningful pressure difference Δp between the phases.

7. SECOND ORDER SCHEME WITH WAVE LIMITERS

The Roe scheme presented so far is first order. It can be made second order by using the MUSCL [33] reconstruction of the data, along with e.g. a second-order Runge-Kutta solver for the time integration. However, a specific second-order extension of the Roe scheme exists, that does not require several stages in the time integration, thus saving computational time. It is the wave-limiter approach described in the book of LeVeque [31] (pp. 181–183). This method consists in comparing the waves at an interface with the corresponding upwind waves. The wave $\boldsymbol{\omega}^p_{i-1/2}$, of family p and at the interface where the flux is to be evaluated $(i-1/2)$, is defined by

$$\boldsymbol{\omega}^p_{i-1/2} = \left(\ell^p_{i-1/2} \Delta \boldsymbol{U}_{i-1/2}\right) r^p_{i-1/2}, \tag{102}$$

where $\ell^p_{i-1/2}$ and $r^p_{i-1/2}$ are the respectively left and right eigenvectors corresponding to the p^{th} eigenvalue of the Riemann problem at interface $i-1/2$. $\Delta \boldsymbol{U}_{i-1/2}$ is the jump at interface $i-1/2$. At the upwind interface, the wave is defined by

$$\boldsymbol{\omega}^p_{I-1/2} = \left(\ell^p_{I-1/2} \Delta \boldsymbol{U}_{I-1/2}\right) r^p_{I-1/2}, \tag{103}$$

where $I \in [i-1, i+1]$ selects the adjacent interface in the upwind direction. Whether the upwind interface is the left or the right one depends on the sign of the p^{th} eigenvalue. Then

Copyright © 0000 John Wiley & Sons, Ltd.

Prepared using fldauth.cls
DOI: 10.1002/fld

a smoothness measure is evaluated, similar to the slope ratio in the MUSCL approach, in order to construct a wave correction. The smoothness measure for wave p is defined by

$$\theta^p_{i-1/2} = \frac{\boldsymbol{\omega}^p_{I-1/2} \cdot \boldsymbol{\omega}^p_{i-1/2}}{\boldsymbol{\omega}^p_{i-1/2} \cdot \boldsymbol{\omega}^p_{i-1/2}}. \tag{104}$$

The drawback of this method is that it is dependent on the ordering of the eigenvalues, because the definition of the upwind wave $\boldsymbol{\omega}^p_{I-1/2}$ uses the eigenstructure of the Riemann problem at the upwind interface $I-1/2$. To employ (104), one needs to know which wave the index p actually represents. For the two-fluid model, the eigenvalues must be calculated numerically, and we have in general no method of determining which eigenvalue belongs to which family of waves. Hence the above method is not directly applicable, for it will fail each time the eigenvalues change order from an interface to the next. Instead, Lax and Liu [34] defined a new smoothness measure, where the information coming from adjacent cells only comes from the jump $\Delta \boldsymbol{U}_{I-1/2}$, which is independent of the wave ordering. The upwind wave is now defined as

$$\widehat{\boldsymbol{\omega}}^p_{I-1/2} = \left(\ell^p_{i-1/2} \Delta \boldsymbol{U}_{I-1/2}\right) r^p_{i-1/2}. \tag{105}$$

Remark that only the eigenvectors at interface $i-1/2$ are used. The smoothness measure is now defined as

$$\theta^p_{i-1/2} = \frac{\widehat{\boldsymbol{\omega}}^p_{I-1/2} \cdot \boldsymbol{\omega}^p_{i-1/2}}{\boldsymbol{\omega}^p_{i-1/2} \cdot \boldsymbol{\omega}^p_{i-1/2}}. \tag{106}$$

This smoothness measure is however a less precise measure of the variation in the wave, since it decomposes the jump $\Delta \boldsymbol{U}_{I-1/2}$ at the upwind interface using the eigenvectors of the Riemann problem at interface $i-1/2$. This can in some cases produce an oscillation in the solution, as will be discussed in the numerical results.

A limited version of the wave is then defined as [31, p. 182]

$$\tilde{\boldsymbol{\omega}}^p_{i-1/2} = \phi(\theta^p_{i-1/2}) \widehat{\boldsymbol{\omega}}^p_{i-1/2}, \tag{107}$$

where $\phi(\theta)$ is the limiter function, which is used to evaluate the limited flux

$$\tilde{\boldsymbol{F}}_{i-1/2} = \frac{1}{2} \sum_{p=1}^{m} |s^p_{i-1/2}| \left(1 - \frac{\Delta t}{\Delta x} |s^p_{i-1/2}|\right) \tilde{\boldsymbol{\omega}}^p_{i-1/2}. \tag{108}$$

The scheme with the second-order extension then reads

$$\boldsymbol{U}^{n+1}_i = \boldsymbol{U}^n_i - \frac{\Delta t}{\Delta x} \left(\mathcal{A}^- \Delta \boldsymbol{U}_{i+1/2} + \mathcal{A}^+ \Delta \boldsymbol{U}_{i-1/2}\right) - \frac{\Delta t}{\Delta x} \left(\tilde{\boldsymbol{F}}_{i+1/2} - \tilde{\boldsymbol{F}}_{i-1/2}\right), \tag{109}$$

where the fluctuations $\mathcal{A}^{\pm} \Delta \boldsymbol{U}_{i-1/2}$ and the wave velocities $s^p_{i-1/2}$ are those of the classical Roe scheme, defined in [31, p. 120].

8. NUMERICAL RESULTS

Some tests have been run on the six-equation two-fluid model using the presently described Roe scheme. Since some of the waves can have a zero velocity, an entropy fix is needed. Harten's entropy fix [31] (p. 324) with $\delta_{\text{Hart}} = 20$ is therefore active on all the test cases. Note that the MUSTA method does not require an entropy fix. The thermodynamical parameters used in the stiffened gas equation of state (85)–(86) are listed in Table II.

Copyright © 0000 John Wiley & Sons, Ltd.

Prepared using fldauth.cls
DOI: 10.1002/fld

Table II. Thermodynamical parameters for the stiffened gas equation of state.

	Gas (g)	Liquid (ℓ)
$\gamma\,(-)$	1.4	2.8
$p_\infty\,(\mathrm{Pa})$	0.0	8.5×10^8
$C_p\,(\mathrm{J/(kg.K)})$	1008.7	4186.0

8.1. Isolated waves

Castro *et al.* [15] and Abgrall and Karni [16] write that formally path-consistent schemes may feature slightly wrong wave velocities, compared to the wave velocities predicted by the Rankine-Hugoniot system for a given averaging of $\overline{\boldsymbol{B}}$. In the present section, we test the Rankine-Hugoniot system on each of the six waves occurring in the two-fluid six-equation model. All the tests start with the same left state, given in Table X in Appendix A. The six right states were produced by numerically browsing the Rankine-Hugoniot system

$$\sigma\left(\boldsymbol{U}^R-\boldsymbol{U}^L\right)=\hat{\boldsymbol{A}}\left(\boldsymbol{U}^L,\boldsymbol{U}^R\right)\left(\boldsymbol{U}^R-\boldsymbol{U}^L\right). \tag{110}$$

When relevant, a shock has been chosen rather than a rarefaction. The right states can be found from $\Delta\boldsymbol{U}$ listed in Table XI in Appendix A through

$$\boldsymbol{U}_R=\boldsymbol{U}_L+\Delta\boldsymbol{U}. \tag{111}$$

The waves are numbered by increasing order of velocity. Waves 1 and 6 are the pressure waves, waves 2 and 4 are the volume fraction waves and waves 3 and 5 are the entropy waves.

The waves propagate in a domain of 10,000 cells, and are located at $t=0\,\mathrm{s}$ either at cell 100 for the right-going waves, or at cell 900 for the left-going waves. The simulation time is determined so that the wave travels to the other end of the tube. The minmod wave limiter is used and the CFL number is 0.5. $\delta=2$ was used in the regularisation term (10). To evaluate the propagation velocity, the location of the waves is estimated to be at the inflexion point of $u_1=\alpha_\mathrm{g}\rho_\mathrm{g}$ (or $u_2=\alpha_\ell\rho_\ell$ when $u_1=\alpha_\mathrm{g}\rho_\mathrm{g}$ is constant).

The Rankine-Hugoniot condition is tested by evaluating the two sides of the Rankine-Hugoniot system (110): $\sigma\Delta\boldsymbol{U}$ and $\hat{\boldsymbol{A}}\cdot\Delta\boldsymbol{U}$. The measured wave velocity σ and the relative error of the two sides of the system for each wave type is reported in Table III. When one of the sides was a zero, the relative error has been replaced by an absolute error, denoted by (abs.) in the result table.

We can see that the relative error is most of the time on the order of 10^{-5} or lower, and that it is very similar for all variables. This indicates that this small error comes from the wave velocity σ, but that the jump satisfies the Rankine-Hugoniot system rather strictly. The error in the wave velocity σ may be explained either by the uncertainty in locating the waves, or by a slightly wrong propagation velocity. The exception is wave 2. The relative error goes up to 10^{-3} for the momentum components, and is not homogeneous for all the variables. This indicates that the jump in itself slightly violates the Rankine-Hugoniot condition. This phenomenon seems similar to what was observed in [16], though here in a much smaller scale.

This test shows that the wave velocities and jumps satisfy the Rankine-Hugoniot condition reasonably well in the conditions presented here. However, the error may be larger for increasing shock amplitudes.

8.2. Shock tube

The next test case is the shock tube introduced by Toumi [3], and also studied in [2, 4, 24]. This shock tube activates the resonance fix described in Section 6, since $v_\mathrm{g}=0$ and $v_\ell=0$ at $t=0\,\mathrm{s}$. The parameter in this fix is taken to be $\varepsilon=10^{-3}\,\mathrm{m/s}$. The initial states are given

Copyright © 0000 John Wiley & Sons, Ltd.

Prepared using fldauth.cls
DOI: 10.1002/fld

Table III. Relative error in Rankine-Hugoniot conditions for the isolated wave test

Wave 1		Wave 2		Wave 3	
$\sigma = -366.83$		$\sigma = -4.9214$		$\sigma = 10.000068$	
u_1	4.5857×10^{-5}	u_1	1.7004×10^{-5}	u_1	0.0
u_2	4.5305×10^{-5}	u_2	2.1544×10^{-5}	u_2	6.7568×10^{-5}
u_3	4.5612×10^{-5}	u_3	1.1157×10^{-3}	u_3	2.8099×10^{-5}(abs.)
u_4	4.5356×10^{-5}	u_4	-4.3392×10^{-4}	u_4	6.6350×10^{-5}
u_5	4.5855×10^{-5}	u_5	1.6157×10^{-5}	u_5	1.7770×10^{-4}(abs.)
u_6	4.5168×10^{-5}	u_6	2.0390×10^{-5}	u_6	6.4933×10^{-5}
Wave 4		Wave 5		Wave 6	
$\sigma = 76.579$		$\sigma = 100.033$		$\sigma = 514.69$	
u_1	4.2484×10^{-4}	u_1	3.3333×10^{-5}	u_1	8.1034×10^{-5}
u_2	4.2487×10^{-4}	u_2	0.0	u_2	8.0726×10^{-5}
u_3	4.2675×10^{-4}	u_3	3.3307×10^{-5}	u_3	8.1191×10^{-5}
u_4	4.2411×10^{-4}	u_4	-5.8668×10^{-4}(abs.)	u_4	8.1009×10^{-5}
u_5	4.2477×10^{-4}	u_5	3.3282×10^{-5}	u_5	8.1091×10^{-5}
u_6	4.2505×10^{-4}	u_6	-6.0766×10^{-3}(abs.)	u_6	8.0694×10^{-5}

in Table IV. In the regularisation term (10), $\delta = 2$ was used. The results at $t = 0.06\,\mathrm{s}$ for different grid resolutions are presented in Figure 1. The result from the MUSCL-MUSTA scheme with 2 substeps and the minmod slope limiter, presented in [2], is used for the reference curves on a grid of 10,000 cells. The curve for the Roe scheme presented in this article, on the same grid, match the reference curves to plotting accuracy. For the lower resolutions, the plateau between the slow waves is not well resolved. A similar behaviour is observed with the MUSCL-MUSTA method, but it is more pronounced with the Roe method, especially for the liquid velocity. To understand where this overshoot comes from, we use the similarity property of the solution. The shock tube is run on a fine grid of 10,000 cells, with the minmod limiter. The liquid-velocity profiles at different time steps are plotted against the similarity parameter x/t on Figure 2. We can see that an oscillation appears for the wave at $x/t \approx 100\,\mathrm{m/s}$, but that the wave after all converges to the expected wave. This is due to the limiter with the Lax and Liu smoothness-measure definition (cf. Section 7) being more imprecise the larger the jump is. Using the original definition of the smoothness measure by LeVeque, the original oscillation is present but much smaller. Note, however, that the latter requires that the waves be ordered the same way in adjacent computational cells, and therefore cannot generally be used with the present system. It is a particular case that it works on this test case, where the velocities keep the same ordering during the simulation. The oscillation does not appear at all without wave limiter, as shown on Figure 3.

Table IV. Initial states for Toumi's shock tube

	Symbol (unit)	Left	Right
Gas vol. frac.	α_g (−)	0.25	0.10
Pressure	p (MPa)	20	10
Gas velocity	v_g (m/s)	0	0
Liq. velocity	v_ℓ (m/s)	0	0
Temperatures	T_g, T_ℓ (K)	308.15	308.15

8.3. Moving Gauss curve

The Roe schemes without and with flux limiters are expected to be first and second order, respectively, for smooth solutions. This test case consists in a smooth volume-fraction profile

Copyright © 0000 John Wiley & Sons, Ltd.
Prepared using fldauth.cls

DOI: 10.1002/fld

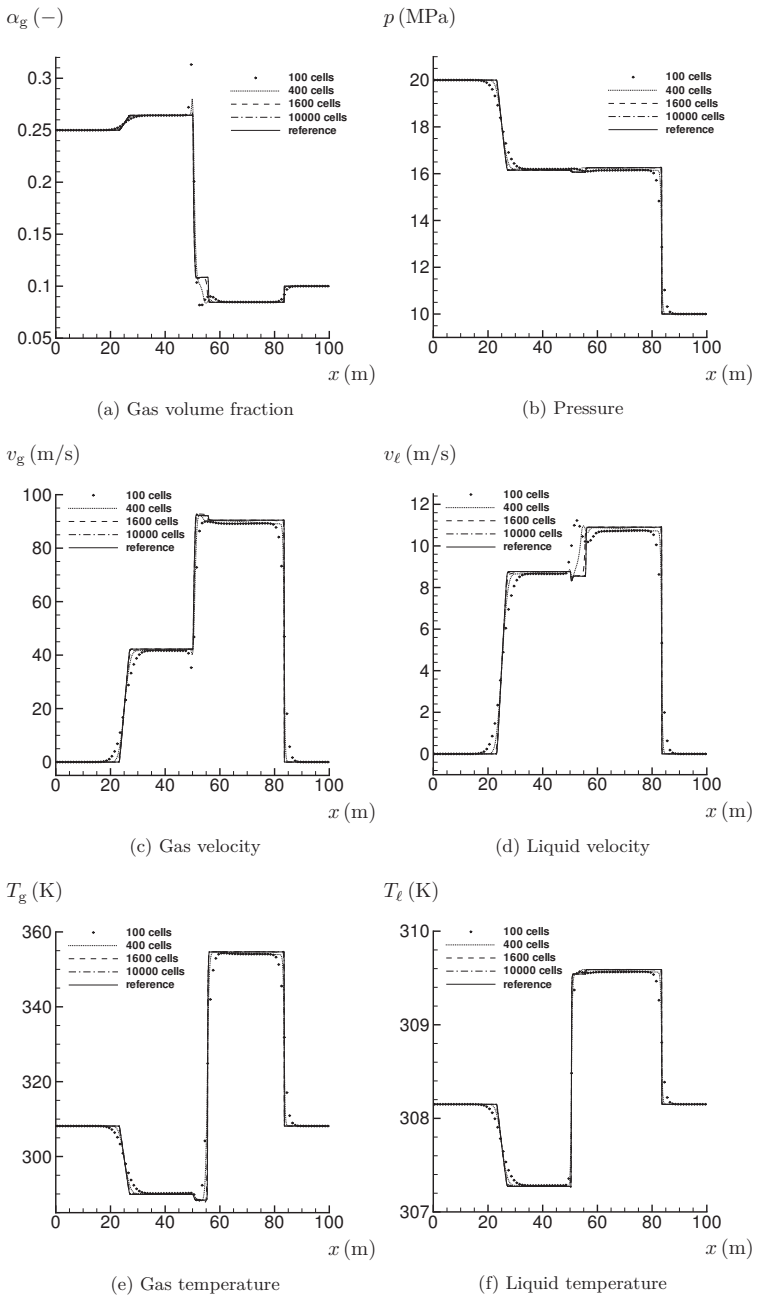

(a) Gas volume fraction (b) Pressure

(c) Gas velocity (d) Liquid velocity

(e) Gas temperature (f) Liquid temperature

Figure 1. Convergence of the scheme with minmod limiter on Toumi's shock tube at $t = 0.06s$. CFL=0.5. The reference curves are produced with the MUSCL-MUSTA scheme, with the minmod slope limiter on a grid of 10,000 cells, CFL=0.5.

Copyright © 0000 John Wiley & Sons, Ltd.
Prepared using fldauth.cls

DOI: 10.1002/fld

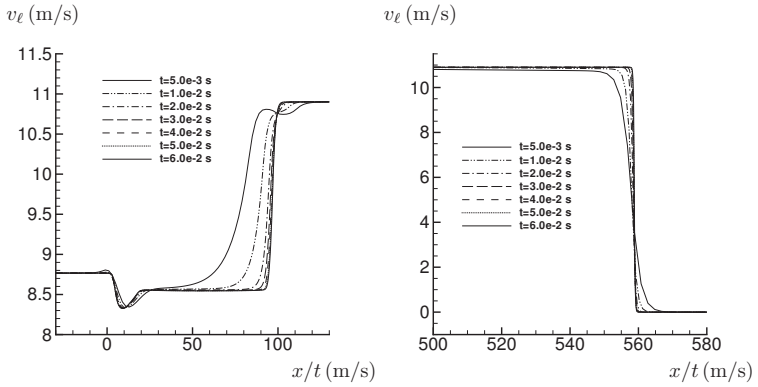

(a) Slow waves (b) Fast wave

Figure 2. Solution of Toumi's shock tube at different times plotted against the similarity parameter x/t. 10,000 cells, minmod limiter, CFL=0.5.

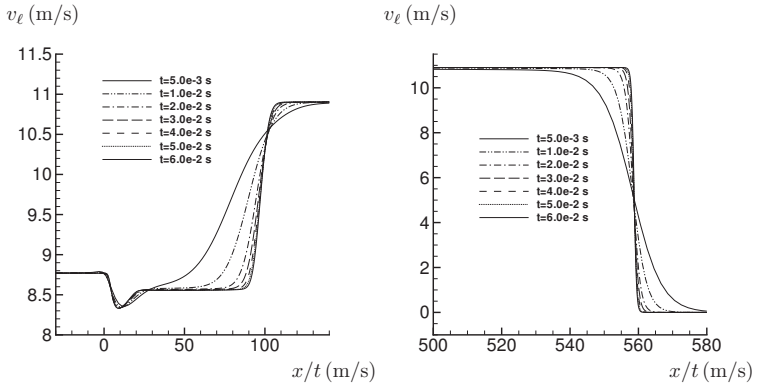

(a) Slow waves (b) Fast wave

Figure 3. Solution of Toumi's shock tube at different times plotted against the similarity parameter x/t. 10,000 cells, no limiter, CFL=0.5.

(a Gauss curve) being advected with the flow. The two phases having the same velocity, the profile should not be distorted. We use this case to evaluate the convergence order of the scheme.

The case is initialised with all the quantities being uniform, apart from the gas volume fraction which follows a scaled Gauss curve

$$\alpha_{\mathrm{g},0} = 0.1 + 0.8 \exp\left(-\frac{(x-\mu)^2}{2\sigma^2}\right) \tag{112}$$

where $\sigma = 0.42$ and $\mu = 6\,\mathrm{m}$. The other quantities are given in Table V.

The solution is compared to the analytical solution at $t = 0.03\,\mathrm{s}$. The Gauss curved is advected at the velocity 100 m/s, therefore the analytical solution is given by the equation (112) where σ is unchanged and $\mu = 9\,\mathrm{m}$. The error and the convergence order are listed in Table VI for the Roe scheme without wave limiter, and the Roe scheme with the minmod

Copyright © 0000 John Wiley & Sons, Ltd.
Prepared using fldauth.cls

DOI: 10.1002/fld

Table V. Initial state for the moving Gauss curve case

	Symbol (unit)	Initial value
Pressure	p (MPa)	0.1
Gas velocity	v_{g} (m/s)	100
Liq. velocity	v_{ℓ} (m/s)	100
Temperatures	$T_{\mathrm{g},\ell}$ (K)	315.9

wave limiter. The parameter in the resonance fix is $\varepsilon = 10^{-3}\,\mathrm{m/s}$. $\delta = 2$ was used in the regularisation term (10). Figure 4 gives an illustration of the convergence. We can see that for the scheme with wave limiter, the second order convergence is observed already from 200 cells. For the scheme without limiter, which is first order, the expected convergence order is attained for a finer grid than for the second order scheme.

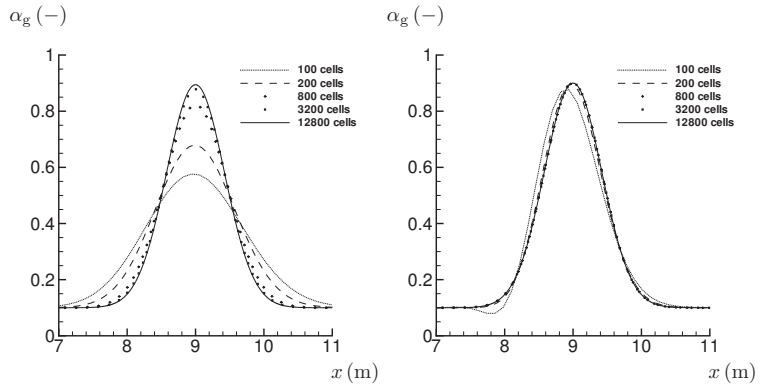

(a) No limiter (b) Minmod Limiter

Figure 4. Convergence for the moving Gauss curve, Roe with and without limiter. $t = 0.03s$.

Table VI. Moving Gauss curve: convergence order of the Roe scheme without wave limiter, and with the minmod wave limiter, both with a resonance fix parameter $\varepsilon = 10^{-3}\,\mathrm{m/s}$

	Roe		MC-Roe	
Cells	$\|\mathcal{E}(\alpha_{\mathrm{g}})\|_1$	n	$\|\mathcal{E}(\alpha_{\mathrm{g}})\|_1$	n
100	4.122×10^{-1}	–	1.192×10^{-1}	–
200	2.615×10^{-1}	0.66	3.028×10^{-2}	1.98
400	1.523×10^{-1}	0.78	7.625×10^{-3}	1.99
800	8.341×10^{-2}	0.87	1.908×10^{-3}	2.00
1600	4.386×10^{-2}	0.93	4.770×10^{-4}	2.00
3200	2.252×10^{-2}	0.96	1.193×10^{-4}	2.00
6400	1.142×10^{-2}	0.98	2.982×10^{-5}	2.00
12800	5.749×10^{-3}	0.99	7.455×10^{-6}	2.00

This test is also used to check the sensitivity of the solution to the parameter ε in the resonance fix. The velocities should remain uniform and equal to their initial value, but they are slightly deformed. Table VII shows the maximum error in the velocities as a function of ε. Recall that the ε parameter determines how close the gas and liquid velocities can be. We can see that the error is very dependent on it. In this test, it was not possible to decrease ε

Copyright © 0000 John Wiley & Sons, Ltd.
Prepared using fldauth.cls

DOI: 10.1002/fld

further. Otherwise, the code crashes due to the diagonalisation routine returning conjugate complex eigenvalues, though with negligible imaginary part. This is caused by a strong loss of numerical accuracy, since two eigenvectors become almost parallel. The matrix should in theory be diagonalisable with real eigenvalues. The ε parameter should be set so that the diagonalisation routine always returns real eigenvalues. A value of $\varepsilon = 10^{-3}$ m/s worked well for this case.

Table VII. Moving Gauss curve: Maximum error in the gas and liquid velocities depending on the ε parameter in the resonance fix.

ε	$\|v_\mathrm{g} - 100\|_\mathrm{max}$	$\|v_\ell - 100\|_\mathrm{max}$
10^{-0}	8.35×10^{-2}	1.34×10^{-1}
10^{-1}	8.34×10^{-4}	1.30×10^{-3}
10^{-2}	8.34×10^{-6}	1.30×10^{-5}
10^{-3}	8.00×10^{-8}	1.30×10^{-7}

8.4. Water faucet

The last test is the water-faucet test case. It was introduced by Ransom [35] and is a standard test case for one-dimensional two-fluid models and numerical methods to solve them. In particular, it exposes the ability of the scheme to accurately capture the slow-moving mass waves, which is of interest e.g. in pipe-transport applications. This case has been studied for example in [2, 4, 9, 22, 24, 28, 36]. It consists in a vertical tube initially filled with a mixture of uniform gas fraction $\alpha_\mathrm{g} = 0.2$. The tube is closed for the gas at the top. The liquid flows downwards, and is injected from the top at a liquid fraction of $\alpha_\ell = 0.8$. At time $t = 0$, the gravity is turned on. The liquid already present in the tube accelerates downwards, while a thinning jet forms from the top of the tube. Some gas is sucked in in counter-current to fill the space freed by the thinning jet. Table VIII presents the parameters used in this work. $\delta = 1.2$ was used in the regularisation term (10).

Table VIII. Parameter values for the water-faucet test case

	Symbol (unit)	Value
Gas vol. frac.	α_g $(-)$	0.20
Pressure	p (MPa)	0.1
Gas velocity	v_g (m/s)	0.0
Liq. velocity	v_ℓ (m/s)	10.0
Temperatures	T_g, T_ℓ (K)	315.9
Gravity	g (m/s^2)	9.81

The upper boundary condition should impose a zero velocity on the gas phase, while allowing one characteristic to leave the domain, since the flow is subsonic and entering the tube. The four other characteristics are entering the domain. Therefore, five variables have to be set, while one is extrapolated. At the bottom, the liquid flows out at subsonic velocity, while the gas may flow in or out, at subsonic velocity. Depending on the gas velocity, three or four variables have to be extrapolated, while three or two respectively have to be set. Table IX shows the variables chosen (the same as in [2]), if they are extrapolated or set, and in the latter case, their value.

The entropy is evaluated according to the expression

$$s = C_p \ln \left(\frac{\gamma (p + p_\infty)^{\frac{1}{\gamma}} (p^0 + p_\infty)^{1-\frac{1}{\gamma}}}{\rho(\gamma - 1) C_p T^0} \right) \tag{113}$$

where T^0 and p^0 are some reference parameters at which $s = 0\,\mathrm{J/K}$. s_ℓ^in is once and for all evaluated with (113) at the initial pressure and temperature of the water jet (and using the

Copyright © 0000 John Wiley & Sons, Ltd.

Prepared using fldauth.cls
DOI: 10.1002/fld

Table IX. Variables for the boundary conditions for the water faucet case.

		Top		Bottom	
Variable	Unit		Value		Value
Volume fraction	$\alpha_{\mathrm{g}}\,(-)$	Set	0.2	Extrapolated	–
Pressure	$p\,(\mathrm{MPa})$	Extrapolated	–	Set	0.1
Momentum	$m_{\mathrm{g}}\,(\mathrm{kg}/(\mathrm{m}^2\cdot\mathrm{s}))$	Set	0	Extrapolated	–
Momentum	$m_\ell\,(\mathrm{kg}/(\mathrm{m}^2\cdot\mathrm{s}))$	Set	m_ℓ^{in}	Extrapolated	–
Entropy	$s_{\mathrm{g}}\,(\mathrm{J/K})$	Extrapolated	–	Set or Extr.	$s_{\mathrm{g}}^{\mathrm{atm}}$
Entropy	$s_\ell\,(\mathrm{J/K})$	Set	s_ℓ^{in}	Extrapolated	–

equation of state to evaluate the density), and remains the same over time. The momentum m_ℓ^{in} also remains constant over time, and is equal to the initial momentum of the water jet $m_\ell^{0,\mathrm{in}} = \rho_\ell^{0,\mathrm{in}} v_\ell^{0,\mathrm{in}}$ evaluated at the state given in Table VIII. Finally, in the case where the gas entropy has to be set at the bottom, $s_{\mathrm{g}}^{\mathrm{atm}}$ is equal to its initial value, evaluated using (113) and the values in Table VIII.

The results of a mesh sensitivity study are plotted at $t = 0.6s$ in Figure 5. They are compared to the results from the MUSCL-MUSTA scheme from [2], with the minmod slope limiter. This shows that the two schemes converge to the same solution, to plotting accuracy.

Finally, we assessed the computational efficiency of the Roe scheme compared to the MUSTA scheme. We compared the CPU time used to solve the water faucet case on grids from 50 to 800 cells, with the second order extension. Remark that the flux limiter approach for the Roe scheme requires a first-order forward Euler time step, while the MUSCL-MUSTA approach requires a second-order Runge-Kutta time step. The results are presented in Figure 6. In this case, the Roe and the MUSCL-MUSTA methods perform similarly in terms of convergence error compared to CPU time. However, the profiling of the code gives useful information. In the case of the Roe scheme, 60% of the CPU time is used on diagonalising the Jacobian, while only 3% is used on evaluating the primary variables, which means solving the equation of state. In the case of the MUSCL-MUSTA method with two substeps, 30% of the CPU time is used on solving the equation of state. Here, the stiffened gas equation of state is used, which is a simple one to solve. More accurate equations of state may take considerably more time to solve, thus impairing the efficiency of the MUSTA method.

9. CONCLUSION

A partially analytical Roe scheme for the six-equation two-fluid model has been derived and implemented. For most of the variables, an analytical Roe average is given. The average of the few remaining variables must generally be found numerically and is dependent on the equation of state. This makes the scheme flexible with respect to the choice of equation of state.

The central idea of this work was to include the non-conservative terms in the quasilinear form, so that the wave structure of the system reflects the effects of all the terms in the model. However, the numerical solution is dependent on the choice of an integration path for the non-conservative terms, which can present problems. One advantage of the present derivation is that the definition of the Roe averages can be made independent from the integration path. Only the averages of the non-conservative factors will be affected by a change of family of path.

We have seen that the six-equation two-fluid model with the regularisation used in this work is prone to resonance when the liquid and gas velocity are equal. The Jacobian matrix becomes non-diagonalisable. A fix has been devised by taking advantage of the continuity of the eigenvalues and eigenvectors.

Copyright © 0000 John Wiley & Sons, Ltd.
Prepared using fldauth.cls

DOI: 10.1002/fld

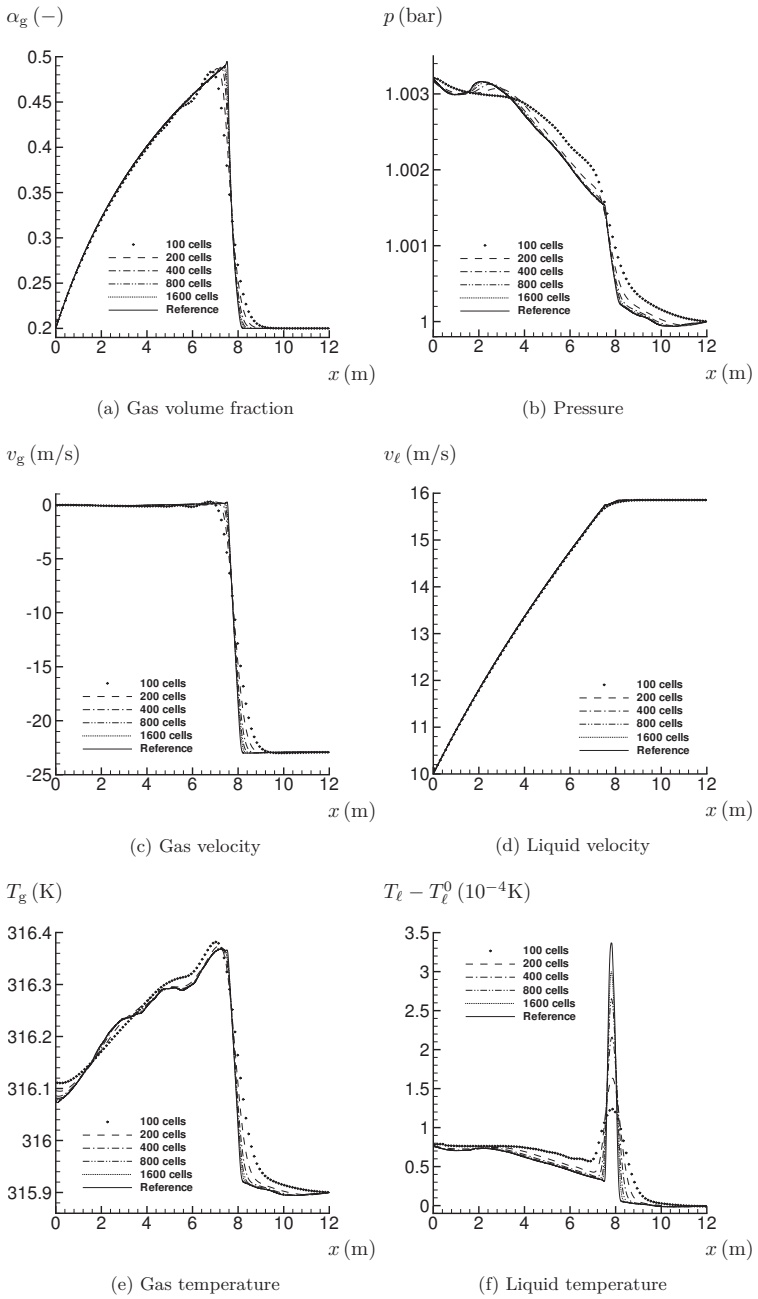

(a) Gas volume fraction

(b) Pressure

(c) Gas velocity

(d) Liquid velocity

(e) Gas temperature

(f) Liquid temperature

Figure 5. Convergence of the scheme on the water faucet test case at $t = 0.6s$ with the minmod wave limiter. CFL=0.5. The reference curves are produced with the MUSCL-MUSTA scheme, with the minmod slope limiter on a grid of 10,000 cells, CFL=0.5.

Copyright © 0000 John Wiley & Sons, Ltd.

Prepared using fldauth.cls
DOI: 10.1002/fld

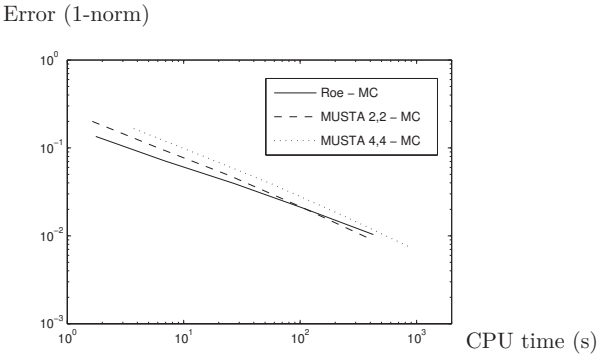

Figure 6. CPU time versus 1-norm of the error on α_g of the numerical solution compared to the reference (Roe scheme, MC limiter, 10000 cells). 50 to 800 cells, Roe and MUSCL-MUSTA with MC limiter, t=0.6s, CFL=0.5. Fortran 90 on an Intel® Xeon® CPU X5570 at 2.93GHz.

Finally, four test cases show that the scheme performs well. Even though some previous work showed that the *formally path-consistent* approach can feature a wrong wave structure, the test cases show that this problem is limited here.

A. ISOLATED WAVES

The common left state for the isolated wave test is given in Table X. The right states are found from $\Delta \boldsymbol{U}$ listed in Table XI through

$$\boldsymbol{U}_R = \boldsymbol{U}_L + \Delta \boldsymbol{U}. \tag{114}$$

Table X. Left state for the isolated wave test

	Symbol	Value
Gas vol. frac.	$\alpha_g\,(-)$	0.2
Pressure	$p\,(\mathrm{Pa})$	1×10^7
Gas density	$\rho_g\,(\mathrm{kg/m^3})$	100
Liq. density	$\rho_\ell\,(\mathrm{kg/m^3})$	1000
Gas. velocity	$v_g\,(\mathrm{m/s})$	100
Liq. velocity	$v_\ell\,(\mathrm{m/s})$	10

ACKNOWLEDGEMENT

A.M. and S.T.M. were financed through the BIGCCS Centre. T.F. was financed through the CO_2 Dynamics project. The authors acknowledge the support from the Research Council of Norway (189978, 193816), Aker Solutions, ConocoPhilips, Det Norske Veritas, Gassco, GDF SUEZ, Hydro, Shell, Statoil, TOTAL and Vattenfall.

References

1. Stewart HB, Wendroff B. Two-phase flow: Models and methods. *J. Comput. Phys.* 1984; **56** : 363–409.
2. Munkejord ST, Evje S, Flåtten T. A MUSTA scheme for a nonconservative two-fluid model. *SIAM J. Sci. Comput.* 2009; **31** : 2587–2622.

Copyright © 0000 John Wiley & Sons, Ltd.
Prepared using fldauth.cls

DOI: 10.1002/fld

Table XI. $\Delta \boldsymbol{U}$ for the isolated wave test

Wave 1		Wave 2		Wave 3	
α_{g}	-7.0948×10^{-5}	α_{g}	-7.5304×10^{-5}	α_{g}	0.0
p	1.3294×10^{4}	p	-6.6182×10	p	0.0
ρ_{g}	9.5032×10^{-2}	ρ_{g}	-2.0232×10^{-5}	ρ_{g}	0.0
ρ_{ℓ}	5.5275×10^{-3}	ρ_{ℓ}	1.5760×10^{-4}	ρ_{ℓ}	-1.3006
v_{g}	-2.7770×10^{-1}	v_{g}	3.9541×10^{-2}	v_{g}	0.0
v_{ℓ}	-3.5498×10^{-2}	v_{ℓ}	-1.4068×10^{-3}	v_{ℓ}	0.0
Wave 4		**Wave 5**		**Wave 6**	
α_{g}	7.5127×10^{-5}	α_{g}	0.0	α_{g}	6.6758×10^{-5}
p	-3.2942×10^{2}	p	0.0	p	-2.3681×10^{4}
ρ_{g}	-4.3715×10^{-3}	ρ_{g}	2.8360×10^{-1}	ρ_{g}	-1.6911×10^{-1}
ρ_{ℓ}	-9.5450×10^{-5}	ρ_{ℓ}	0.0	ρ_{ℓ}	-9.8297×10^{-3}
v_{g}	-7.7818×10^{-3}	v_{g}	0.0	v_{g}	-5.6380×10^{-1}
v_{ℓ}	-6.2563×10^{-3}	v_{ℓ}	0.0	v_{ℓ}	-4.7076×10^{-2}

3. Toumi I. An Upwind Numerical Method for Two-Fluid Two-Phase Flow Models. *Nuclear Science and Engineering* 1996; **123** : 147–168.
4. Paillère H, Corre C, García Cascales JR. On the extension of the AUSM^{+} scheme to compressible two-fluid models. *Comput. & Fluids* 2003; **32** : 891–916.
5. Bendiksen KH, Malnes D, Moe R, Nuland S. The dynamic two-fluid model OLGA: Theory and application. *SPE Prod. Eng.* 1991; **6** : 171–180.
6. Bestion D. The physical closure laws in the CATHARE code. *Nuclear Engineering and Design* 1990; **124** : 229–245.
7. Larsen M, Hustvedt E, Hedne P, Straume T. Petra: A novel computer code for simulation of slug flow. Proc. of *SPE Annual Technical Conference and Exhibition, SPE 38841* 1997; 1–12.
8. *WAHA3 Code Manual*, JSI Report IJS-DP-8841, Jožef Stefan Insitute, Ljubljana, Slovenia, 2004.
9. Coquel F, El Amine K, Godlewski E. A numerical method using upwind schemes for the resolution of two-phase flows. *J. Comput. Phys.* 1997; **136** : 272–288.
10. Parés C. Numerical Methods for Non-Conservative Hyperbolic Systems: A Theoretical Framework. *SIAM J. Numer. Anal.* 2006; **44** : 300–321.
11. Toro EF. Riemann solvers with evolved initial conditions. *Internat. J. Numer. Methods Fluids* 2006; **52** : 433–453.
12. Castro CE, Toro EF. A Riemann solver and upwind methods for a two-phase flow model in non-conservative form. *Internat. J. Numer. Methods Fluids* 2006; **50** : 275–307.
13. Martínez Ferrer PJ, Flåtten T, Munkejord ST. On the effect of temperature and velocity relaxation in two-phase flow models. *ESAIM: M2AN* 2012; **46** : 411–442.
14. Morin A, Flåtten T and Munkejord ST. Towards a formally path-consistent Roe scheme for the six-equation two-fluid model. *AIP Conference Proceedings* 2010; **1281** : 71–74.
15. Castro MJ, LeFloch PG, Muñoz-Ruiz ML, Parés C. Why many theories of shock waves are necessary: Convergence error in formally path-consistent schemes. *J. Comput. Phys.* 2008; **227** : 8107–8129.
16. Abgrall R, Karni S. A comment on the computation of non-conservative products. *J. Comput. Phys.* 2010; **229** : 2759–2763.
17. Toro EF. MUSTA: A multi-stage numerical flux. *Appl. Numer. Math* 2006; **56** : 1464–1479.
18. Toro EF, Titarev VA. MUSTA fluxes for systems of conservation laws. *J. Comput. Phys.* 2006; **216** : 403–429.
19. Roe PL. Approximate Riemann solvers, parameter vectors, and difference schemes. *J. Comput. Phys.* 1981; **43** : 357–372.
20. Lax PD. On the notion of hyperbolicity. *Comm. Pure Appl. Math.* 1980; **33** : 395–397.
21. Cortes J, Debussche A, Toumi I. A density perturbation method to study the eigenstructure of two-phase flow equation systems. *J. Comput. Phys.* 1998; **147** : 463–484.
22. Evje S, Flåtten T. Hybrid Flux-Splitting Schemes for a Common Two-Fluid Model. *J. Comput. Phys.* 2003; **192** : 175–210.
23. Chang CH, Liou MS. A robust and accurate approach to computing compressible multiphase flow: Stratified flow model and AUSM^{+}-up scheme. *J. Comput. Phys.* 2007; **225** : 850–873.
24. Munkejord ST. Comparison of Roe-type methods for solving the two-fluid model with and without pressure relaxation. *Comput. & Fluids* 2007; **36** : 1061–1080.
25. Stuhmiller JH. The influence of interfacial pressure forces on the character of two-phase flow model equations. *Int. J. Multiphas. Flow* 1977; **3** : 551–560.
26. Toumi I, Kumbaro A. An Approximate Linearized Riemann Solver for a Two-Fluid Model. *J. Comput. Phys* 1996; **124** : 286–300.
27. Toumi I. A Weak Formulation of Roe's Approximate Riemann Solver. *J. Comput. Phys.* 1992; **102** : 360–373.

Copyright © 0000 John Wiley & Sons, Ltd.
Prepared using fldauth.cls

DOI: 10.1002/fld

28. Muñoz-Ruiz ML, Parés C. Godunov Method for Nonconservative Hypebolic Systems. *ESAIM: M2AN* 2007; **41** : 169–185.
29. Morin A, Aursand PK, Flåtten T, Munkejord ST. Numerical Resolution of CO_2 Transport Dynamics. Proc. of *SIAM Conference on Mathematics for Industry: Challenges and Frontiers (MI09)*, San Francisco, CA, USA, October 9–10, 2009.
30. Flåtten T, Morin A, Munkejord ST. On solutions to equilibrium problems for systems of stiffened gases. *SIAM Journal on Applied Mathematics* 2011; **71** : 41–67.
31. LeVeque RJ. *Finite Volume Methods for Hyperbolic Problems*, Cambridge University Press 2002, ISBN 0-521-00924-3.
32. Soo SL. *Multiphase fluid dynamics*. Science Press, Beijing 1990, ISBN 0–291–39781–6.
33. van Leer B. Towards the ultimate conservative difference scheme V. A second order sequel to Godunov's method. *J. Comput. Phys.* 1979; **32** : 101–136.
34. Lax PD, Liu XD. Solution of two dimensional Riemann problem of gas dynamics by positive schemes. *SIAM J. Sci. Comput.* 1998; **19** : 319–340.
35. Ransom VH. Faucet flow. *Numerical Benchmark Tests, Multiphase Science and Technology, Vol. 3*, G. F. Hewitt, J. M. Delhaye and N. Zuber eds. Hemisphere/Springer, Washington DC, 1987, 465–467.
36. Trapp JA, Riemke RA. A nearly-implicit hydrodynamic numerical scheme for two-phase flows. *J. Comput. Phys.* 1986; **66** : 62–82.

Copyright © 0000 John Wiley & Sons, Ltd.
Prepared using fldauth.cls

DOI: 10.1002/fld

F On interface transfer terms in two-fluid models

Alexandre Morin and Tore Flåtten
International Journal of Multiphase Flow, Volume 45, pp. 24-29, 2012.

International Journal of Multiphase Flow 45 (2012) 24–29

Contents lists available at SciVerse ScienceDirect

International Journal of Multiphase Flow

journal homepage: www.elsevier.com/locate/ijmulflow

On interface transfer terms in two-fluid models

Tore Flåtten [a,*], Alexandre Morin [b]

[a] SINTEF Energy Research, P.O. Box 4761 Sluppen, NO-7465 Trondheim, Norway
[b] Department of Energy and Process Engineering, Norwegian University of Science and Technology (NTNU), Kolbjørn Hejes vei 1B, NO-7491 Trondheim, Norway

ARTICLE INFO

Article history:
Received 21 December 2011
Received in revised form 8 March 2012
Accepted 10 May 2012
Available online 17 May 2012

Keywords:
Two-fluid model
Heat transfer
Hyperbolic

ABSTRACT

In this note we consider two-fluid models based on the usual formulations for conservation of mass, total momentum and total energy. We present some potentially useful general relationships between the interface exchange terms and the evolution of the mechanical variables. In particular, we discuss the possibility of obtaining in this framework a model that is both thermodynamically reversible and possesses real eigenvalues. We formally prove that such a model must include terms associated with the virtual mass force.

We then address a technical issue regarding the modelling of interface transfer terms in the energy equations. In particular, we demonstrate how the formulation of the non-conservative products in these equations determine whether the interface exchange terms represent heat or energy transfer.

© 2012 Elsevier Ltd. All rights reserved.

1. Introduction

We are interested in the classical compressible model for two-phase flow assuming mechanical equilibrium between the phases, and a separate velocity field for each phase (Bendiksen et al., 1991; Bestion, 1990; Stewart and Wendroff, 1984). With the standard closure assumptions, this model possesses complex eigenvalues (Stewart and Wendroff, 1984; Toumi, 1996; Toumi and Kumbaro, 1996). The mathematical and physical implications of this fact have been extensively discussed during the past decades (Keyfitz et al., 2003, 2004; Lax, 1957, 1980; Sever, 2005, 2008; Stewart and Wendroff, 1984).

In particular, this model is generally *ill-posed* in the sense that smooth solutions are expected to be absolutely unstable under perturbations (Sever, 2005). Obviously, this calls into question the usefulness of these equations for modelling and simulation. A common practice is to introduce regularizing terms to render the eigenvalues real. These terms typically take the form of interface momentum exchange terms, and may be classified in two main categories:

- *interface pressure corrections* (Bestion, 1990; Munkejord and Papin, 2007; Stuhmiller, 1977), involving spatial derivatives in the volume fraction;
- *virtual mass force terms* (Bestion, 1990; Lahey, 1991; Städtke, 2006; Toumi, 1996), involving spatial derivatives in the velocities.

A very general analysis including both these effects was performed by Jones and Prosperetti (1985). Considering the incompressible limit, the authors here showed that hyperbolicity is a necessary condition for stability of steady uniform flows, even in the presence of algebraic momentum source terms.

It is known (Saurel et al., 2003), but not widely discussed in the literature, that such differential regularizing terms tend to introduce a fundamental problem on the physical level; the model ceases to satisfy the second law of thermodynamics. In fact, several issues regarding the modelling of interface transfer terms seem to be only implicitly discussed in the recent literature. The aim of this paper is to clarify some of these issues. In this respect, we provide what seems to us some explicit original calculations, although the topics we address are highly classical and our conclusions should not be surprising.

In particular, we aim to shed light on the following two modelling issues:

1. The apparent incompatibility between thermodynamic reversibility and well-posedness for our two-fluid models. Assuming thermal equilibrium, we here provide a general explicit condition on the interface momentum exchange term that is necessary and sufficient for global entropy to be conserved for smooth solutions. This condition is rather strict and excludes a large class of models from being simultaneously well-posed and reversible.
2. The interpretation of the interface transfer terms in the energy balance equations. We argue that in the standard formulation, these terms should be interpreted as heat transfer terms rather than energy transfer terms, and we make this interpretation mathematically precise.

* Corresponding author.
E-mail addresses: Tore.Flatten@sintef.no (T. Flåtten), alexandre.morin@ntnu.no (A. Morin).

0301-9322/$ - see front matter © 2012 Elsevier Ltd. All rights reserved.
http://dx.doi.org/10.1016/j.ijmultiphaseflow.2012.05.002

Our paper is organized as follows. In Section 2, we describe the general framework for the two-fluid models we will consider. In Section 3, we derive a relationship between interphasic heat transfer and the evolution of the pressure and volume fraction. In Section 4, we present a similar result for the momentum exchange term. A main result of our paper is the Eq. (24), which gives a simple general relationship between heat and momentum transfer in our two-fluid models.

In Section 5, we apply these results by considering the special case of thermal equilibrium between the phases. In particular, we are able to derive the general, and rather restrictive, explicit condition (36) that must be satisfied by the momentum exchange term in order for the model to be thermodynamically reversible. This result allows us to prove that such a model can be well-posed with real eigenvalues only if this term includes spatial derivatives in the velocities. The purpose of this analysis is not to advocate the use of such a model; rather, the main insight gained is that models in our framework that *do not* satisfy this condition are unquestionably fundamentally unphysical.

In Section 6, we discuss the interpretation of the interface transfer terms in the standard formulation of the energy equations. In particular, we provide two mathematically equivalent formulations of the energy equations; in one formulation, the right-hand side terms will represent *heat transfer*; in the alternative formulation, these terms will represent *internal energy* transfer. The relationship between these two kinds of source terms is made explicit, and gives us an expression for the amount of heat transferred that will be converted to mechanical work.

Finally, in Section 7, the results of this paper are summarized.

2. The two-fluid model

We consider here the highly classical two-fluid model presented for instance by Stewart and Wendroff (1984), based on fundamental conservation principles. For simplicity, we will limit our discussion to the formulation in one space dimension.

Physically, it is commonly recognized that such a formulation is most sensibly interpreted as an *averaging* of a local description of separate flow fields (Ishii, 1975; Stewart and Wendroff, 1984). In Ishii (1975) the focus is on time averaging, but spatial and ensemble averaging are alternative viable approaches (Drew and Passman, 1999; Stewart and Wendroff, 1984). In this framework, we focus on the model derived from the following basic assumptions of conservation of masses, momentum and total energy:

A1: Mass is conserved for each phase:

$$\frac{\partial}{\partial t}(\rho_g \alpha_g) + \frac{\partial}{\partial x}(\rho_g \alpha_g v_g) = 0, \tag{1}$$

$$\frac{\partial}{\partial t}(\rho_\ell \alpha_\ell) + \frac{\partial}{\partial x}(\rho_\ell \alpha_\ell v_\ell) = 0. \tag{2}$$

A2: Total momentum is conserved in the form:

$$\frac{\partial}{\partial t}(\rho_g \alpha_g v_g + \rho_\ell \alpha_\ell v_\ell) + \frac{\partial}{\partial x}\left(\rho_g \alpha_g v_g^2 + \rho_\ell \alpha_\ell v_\ell^2 + p\right) = 0. \tag{3}$$

A3: Total energy is conserved in the form:

$$\frac{\partial}{\partial t}(E_g + E_\ell) + \frac{\partial}{\partial x}((E_g + \alpha_g p) v_g + (E_\ell + \alpha_\ell p) v_\ell) = 0. \tag{4}$$

Herein, external and dissipative forces have been neglected, and we have assumed the following notation for the phase $k \in \{g,\ell\}$:

ρ_k	density
v_k	velocity
α_k	volume fraction
E_k	energy
p	pressure common to both phases

Here the volume fractions satisfy

$$\alpha_g + \alpha_\ell = 1, \tag{5}$$

and the phasic energies are given by

$$E_k = \rho_k \alpha_k \left(e_k + \frac{1}{2} v_k^2\right), \tag{6}$$

where e_k is the specific internal energy.

Within the context of averaging, (1) and (2) can be taken as the definition of the velocities v_k. That these velocities appear in unmodified form also for the momentum and energy Eqs. (3) and (4) is here an assumption, although common, that is mainly based on the desire to avoid excessive complexities in the model (Stewart and Wendroff, 1984). In this respect, we remark that alternative formulations of (3) and (4) may, and perhaps should, be considered (Song and Ishii, 2001; Stewart and Wendroff, 1984).

For the thermodynamic closure, we assume that each phase may be equipped with a free energy $G_k(p, T_k)$, and that the fundamental thermodynamic differential

$$\mathrm{d}e_k = T_k \mathrm{d}s_k + \frac{p}{\rho_k^2}\mathrm{d}\rho_k \tag{7}$$

is valid. Herein, T_k and s_k are the temperatures and specific entropies of the phases. It should be noted that (7) is in itself a rather strong assumption; given that the entropies, energies and densities are to be interpreted in an *averaged* sense, relating them through a unique equation of state is a simplification motivated mainly by convenience (Stewart and Wendroff, 1984).

2.1. Well-posedness and reversibility

In addition to these basic conservation principles, we want our model to satisfy the second law of thermodynamics. In particular, we here insist that the model should be purely fluid-mechanical, i.e. thermodynamically *reversible* for smooth solutions.

In particular, we assume that some model is given that is locally fully defined, including a complete set of constitutive relations. Then reversibility should hold whenever this model is applied to a physical region with no exchange of mass, energy or heat with the surroundings. Mathematically, we represent such a region as a closed loop in space (periodic boundary conditions), and we exclude any terms representing interactions with the environment.

Given these considerations, we impose the following requirement:

A4: Global entropy is conserved for smooth solutions:

$$\frac{\mathrm{d}}{\mathrm{d}t}\oint_R (\rho_g \alpha_g s_g + \rho_\ell \alpha_\ell s_\ell)\mathrm{d}x = 0, \tag{8}$$

where the integral is taken over any *closed* region R, i.e. we have

$$R = [x_1, x_2),$$

with periodic boundary conditions.

We also want our model to be globally linearizable, and the velocity of information propagation should be finite:

A5: The model can be written in quasilinear form

$$\frac{\partial \boldsymbol{U}}{\partial t} + \boldsymbol{A}(\boldsymbol{U})\frac{\partial \boldsymbol{U}}{\partial x} = 0, \tag{9}$$

where $\boldsymbol{U}$ is the vector of evolved variables and $\boldsymbol{A}(\boldsymbol{U})$ is a smooth function.
Finally, the initial value problem should be well posed:

A6: All eigenvalues of $\boldsymbol{A}(\boldsymbol{U})$ are real for all $\boldsymbol{U}$ in some physically relevant domain $\mathcal{D}$.

Additional relations are needed to close the model. Although a multitude of such closures have so far been proposed in the literature, we are not aware of any full model that satisfies all conditions A1–A6 in any general sense.

In this paper, we will derive a potentially useful condition that such a model must satisfy. We first derive some basic mathematical relationships.

3. Entropy exchange terms

With no loss of generality, we may write entropy evolution equations for each phase in the form

$$\frac{\partial}{\partial t}(\rho_k\alpha_k s_k)+\frac{\partial}{\partial x}(\rho_k\alpha_k s_k v_k)=\sigma_k, \tag{10}$$

where the local entropy modification term σ_k is so far unknown. However, we may state the following general result.

Proposition 1. *If the mass conservation assumption A1 holds, then in the context of (10) we have*

$$T_k\sigma_k=\frac{\alpha_k}{\Gamma_k}\left(\frac{\partial p}{\partial t}+v_k\frac{\partial p}{\partial x}\right)+\frac{\rho_k c_k^2}{\Gamma_k}\left(\frac{\partial\alpha_k}{\partial t}+\frac{\partial}{\partial x}(\alpha_k v_k)\right), \tag{11}$$

where

$$c_k^2=\left(\frac{\partial p}{\partial\rho_k}\right)_{s_k} \tag{12}$$

represents the phasic sound velocity and

$$\Gamma_k=\frac{1}{\rho_k T_k}\left(\frac{\partial p}{\partial s_k}\right)_{\rho_k} \tag{13}$$

is the Grüneisen coefficient.

Proof. By assumption A1 we obtain

$$\sigma_k=\rho_k\alpha_k\left(\frac{\partial s_k}{\partial t}+v_k\frac{\partial s_k}{\partial x}\right) \tag{14}$$

and

$$\alpha_k\left(\frac{\partial\rho_k}{\partial t}+v_k\frac{\partial\rho_k}{\partial x}\right)=-\rho_k\left(\frac{\partial\alpha_k}{\partial t}+\frac{\partial}{\partial x}(\alpha_k v_k)\right). \tag{15}$$

The result then follows from the differential

$$T_k\mathrm{d}s_k=\frac{1}{\Gamma_k\rho_k}(\mathrm{d}p-c_k^2\mathrm{d}\rho_k). \quad \square \tag{16}$$

3.1. Relation to internal energy

Through the fundamental differential (7), this can be recast in terms of internal energy evolution as follows:

$$\begin{aligned}\frac{\partial}{\partial t}(\rho_k\alpha_k e_k)+\frac{\partial}{\partial x}(\rho_k\alpha_k e_k v_k)=&\frac{\alpha_k}{\Gamma_k}\left(\frac{\partial p}{\partial t}+v_k\frac{\partial p}{\partial x}\right)\\&+\left(\frac{\rho_k c_k^2}{\Gamma_k}-p\right)\left(\frac{\partial\alpha_k}{\partial t}+\frac{\partial}{\partial x}(\alpha_k v_k)\right),\end{aligned} \tag{17}$$

where we have used A1:

$$\frac{\partial}{\partial t}(\rho_k\alpha_k e_k)\frac{\partial}{\partial x}(\rho_k\alpha_k e_k v_k)=\rho_k\alpha_k\left(\frac{\partial e_k}{\partial t}+v_k\frac{\partial e_k}{\partial x}\right). \tag{18}$$

4. Momentum exchange terms

With no loss of generality, the momentum conservation assumption A2 can be rewritten as

$$\frac{\partial}{\partial t}(\rho_g\alpha_g v_g)+\frac{\partial}{\partial x}\left(\rho_g\alpha_g v_g^2\right)+\alpha_g\frac{\partial p}{\partial x}+\mathcal{M}=0, \tag{19}$$

$$\frac{\partial}{\partial t}(\rho_\ell\alpha_\ell v_\ell)+\frac{\partial}{\partial x}(\rho_\ell\alpha_\ell v_\ell^2)+\alpha_\ell\frac{\partial p}{\partial x}-\mathcal{M}=0, \tag{20}$$

where the interface momentum exchange term $\mathcal{M}$ is determined from the closure relations. Using assumption A1, we can then derive kinetic energy evolution equations:

$$\frac{\partial}{\partial t}\left(\frac{1}{2}\rho_g\alpha_g v_g^2\right)+\frac{\partial}{\partial x}\left(\frac{1}{2}\rho_g\alpha_g v_g^3\right)=-v_g\left(\mathcal{M}+\alpha_g\frac{\partial p}{\partial x}\right), \tag{21}$$

$$\frac{\partial}{\partial t}\left(\frac{1}{2}\rho_\ell\alpha_\ell v_\ell^2\right)+\frac{\partial}{\partial x}\left(\frac{1}{2}\rho_\ell\alpha_\ell v_\ell^3\right)=v_\ell\left(\mathcal{M}-\alpha_\ell\frac{\partial p}{\partial x}\right). \tag{22}$$

We then obtain the following potentially useful proposition.

Proposition 2. *If the assumptions A1–A3 and the differential (7) hold, the momentum exchange term $\mathcal{M}$ satisfies*

$$\begin{aligned}(v_g-v_\ell)\mathcal{M}=&\left(\frac{\rho_g c_g^2}{\Gamma_g}-\frac{\rho_\ell c_\ell^2}{\Gamma_\ell}\right)\frac{\partial\alpha_g}{\partial t}+\frac{\rho_g c_g^2}{\Gamma_g}\frac{\partial}{\partial x}(\alpha_g v_g)+\frac{\rho_\ell c_\ell^2}{\Gamma_\ell}\frac{\partial}{\partial x}(\alpha_\ell v_\ell)\\&+\left(\frac{\alpha_g}{\Gamma_g}+\frac{\alpha_\ell}{\Gamma_\ell}\right)\frac{\partial p}{\partial t}+\left(\frac{\alpha_g v_g}{\Gamma_g}+\frac{\alpha_\ell v_\ell}{\Gamma_\ell}\right)\frac{\partial p}{\partial x}.\end{aligned} \tag{23}$$

Proof. Add (21) and (22) to (17) and compare with (4). $\square$

Note the general validity of (23), which at first sight may look like a *definition* of $\mathcal{M}$. However, on the contrary, this equation merely provides us with information about how the interface momentum term affects the evolution of the pressure and volume fraction.

In particular, we have the following simple relation:

$$T_g\sigma_g+T_\ell\sigma_\ell=(v_g-v_\ell)\mathcal{M}, \tag{24}$$

which follows from (11) and (23). From this we immediately see that if entropy is conserved along the flow in each phase, i.e.

$$\sigma_k\equiv 0, \tag{25}$$

then our only choice of $\mathcal{M}$ that conserves total energy is

$$\mathcal{M}\equiv 0, \tag{26}$$

which is the standard non-hyperbolic model (Stewart and Wendroff, 1984) for which real-valued eigenvalues occur only for $v_g = v_\ell$. This indicates a fundamental incompatibility between well-posedness and reversibility for models satisfying the assumptions A1–A3. We will now investigate this issue further by relaxing the requirement that $\sigma_k = 0$.

5. Thermal equilibrium

For simplicity, we now limit ourselves to the special case that the phases are in thermal equilibrium, i.e.

$$T=T_g=T_\ell. \tag{27}$$

This simplification is justified by the fact that any valid *general* model must also be valid for the equilibrium states (27). Further-

more, the equilibrium condition (27) may also be imposed as a closure relation for the model, as was done for instance by Martínez Ferrer et al. (2012).

We now introduce the local total entropy variation $\mathcal{S}$:

$$\mathcal{S} = \sigma_g + \sigma_\ell, \tag{28}$$

so that the relation (24) simplifies to

$$T\mathcal{S} = (v_g - v_\ell)\mathcal{M}. \tag{29}$$

We may then write the reversibility condition A4 as:

$$\frac{\mathrm{d}}{\mathrm{d}t}\oint_R(\rho_g\alpha_g s_g + \rho_\ell\alpha_\ell s_\ell)\mathrm{d}x = \oint_R\left(\mathcal{S} - \frac{\partial}{\partial x}(\rho_g\alpha_g s_g v_g + \rho_\ell\alpha_\ell s_\ell v_\ell)\right)\mathrm{d}x = \oint_R \mathcal{S}\mathrm{d}x = 0, \tag{30}$$

for any distribution $\boldsymbol{U}(x)$ on the closed region R. Hence if $\mathcal{S}$ is a function of $\boldsymbol{U}$, it becomes an algebraic entropy source term, and (30) can only be generally satisfied if

$$\mathcal{S}(\boldsymbol{U}) \equiv 0. \tag{31}$$

However, our condition A5 allows $\mathcal{S}$ to be a function of the spatial derivative of $\boldsymbol{U}$:

$$\mathcal{S} = \mathcal{S}(\partial_x\boldsymbol{U}) = \sum_i B_i(\boldsymbol{U})\frac{\partial U_i}{\partial x}, \tag{32}$$

and the condition (30) may still be non-trivially satisfied. Now, the classical *gradient theorem* states that a line integral over an arbitrary closed path in a vector field is identically zero if and only if the integrand is a gradient of some potential function. We now recall that the condition A4 states that reversibility must hold for *all* smooth solutions; hence the entropy integral (30) must be zero for *any* spatial distribution $\boldsymbol{U}(x)$.

We may consequently apply the gradient theorem to the space of physically admissible states $\mathcal{D}$ to which $\boldsymbol{U}$ belongs, i.e. we consider arbitrary curves in $\mathcal{D}$ parametrized by the variable $x \in [x_1,\ x_2) = R$, representing the possible initial conditions $\boldsymbol{U}(x)$. By this, the condition that (30) must hold for *any* distribution $\boldsymbol{U}(x)$ implies the existence of a potential function $Z(\boldsymbol{U})$ such that

$$\oint_R \mathcal{S}\mathrm{d}x = \oint_R \nabla_{\boldsymbol{U}} Z(\boldsymbol{U})\cdot\frac{\partial \boldsymbol{U}}{\partial x}\mathrm{d}x = 0. \tag{33}$$

Hence $\mathcal{S}\mathrm{d}x$ must be an *exact* differential, i.e. we have

$$B_i = \frac{\partial Z}{\partial U_i}, \tag{34}$$

and in particular

$$\mathcal{S} = \frac{\partial}{\partial x}Z(\boldsymbol{U}). \tag{35}$$

In other words, $\mathcal{S}$ can be interpreted as an *entropy flux*. This gives us a main result of this paper.

Proposition 3. *Consider a subdomain $\mathcal{D}$ of the admissible thermal equilibrium states. Consider a two-fluid model satisfying the assumptions A1–A3, A5 and the fundamental differential (7) for all $\boldsymbol{U} \in \mathcal{D}$. Then, for all $\boldsymbol{U} \in \mathcal{D}$, the reversibility condition A4 is satisfied if and only if there exists a function $W(U)$ such that the interface momentum exchange term can be written as*

$$\mathcal{M} = T(v_g - v_\ell)\frac{\partial W}{\partial x} + 2WT\frac{\partial}{\partial x}(v_g - v_\ell) \tag{36}$$

for all $\boldsymbol{U} \in \mathcal{D}$.

Proof. With no loss of generality, we may write Z as

$$Z(\boldsymbol{U}) = W(\boldsymbol{U})(v_g - v_\ell)^2, \tag{37}$$

where $W(U)$ is some function. Now substituting (37) in (29) and cancelling terms, we obtain (36). □

This result opens for the possibility that some appropriate $\boldsymbol{W}(\boldsymbol{U})$ may be found, making the reversible model at least conditionally hyperbolic. This question will not be pursued in the current paper.

However, we may use (36) as a convenient tool for testing the thermodynamic consistency of various established models. In particular, we have the following proposition.

Proposition 4. *Any model satisfying the assumptions A1–A5 with $\mathcal{M} \neq 0$ must involve terms of the form $\partial_x v_k$ in $\mathcal{M}$.*

Proof. If this does not hold, it follows from (36) that $W(U)$ would have to satisfy

$$v_s\frac{\partial W}{\partial v_s} + 2W = 0, \tag{38}$$

where

$$v_s = v_g - v_\ell. \tag{39}$$

Now (38) can be integrated to yield

$$W(\boldsymbol{U}) = C v_s^{-2}, \tag{40}$$

where C is independent of v_s. By substituting this result into (37), it follows that $Z(U)$, and hence $\mathcal{S}$, must be independent of v_s. However, it follows from (29) and the smoothness of $\mathcal{M}$ that $\mathcal{S}$ must disappear when $v_s = 0$. Hence we must have $\mathcal{S} \equiv 0$, giving $\mathcal{M} \equiv 0$. □

We remark that $\mathcal{M} = 0$ corresponds to the standard non-hyperbolic formulation of the model, violating the condition A6 for all $v_s \neq 0$. Hence Proposition 4 may be restated as follows:

Any model satisfying the assumptions A1–A6 in any general sense must involve spatial derivatives of the velocities in the momentum exchange term. Physically, such velocity derivatives are most naturally interpreted as being associated with the *virtual mass force* (Jones and Prosperetti, 1985; Lahey, 1991).

In particular, this result immediately rules out all models based solely on interface pressure corrections in the framework A1–A3 (Bestion, 1990; Martínez Ferrer et al., 2012; Stuhmiller, 1977). We remark that hydrostatic pressure corrections, used to simulate surface waves and regime transitions (De Henau and Raithby, 1995; Holmås et al., 2008), typically operate with separate pressures in each phase and hence do not fit into our framework A2.

We emphasize that the converse of Proposition 4 does not necessarily hold. The standard formulations of the virtual mass force terms do not in general satisfy (36) – and hence the resulting model is not thermodynamically reversible.

It should also be noted that the standard formulations of the virtual mass force (Jones and Prosperetti, 1985; Lahey, 1991) involve not only spatial, but also temporal, derivatives of the velocities. However, our current framework applies also in this case; the temporal derivatives can always be equivalently reformulated in terms of spatial derivatives through a mathematical transformation. This point will be demonstrated in the next section, where such a transformation is performed on the energy equations.

6. Energy transfer terms

We now turn our attention to the modelling of interface energy exchange terms. With no loss of generality, we may write the assumption A3 in the standard form (Martínez Ferrer et al., 2012; Munkejord et al., 2009; Paillère et al., 2003; Stewart and Wendroff, 1984):

$$\frac{\partial E_g}{\partial t}+\frac{\partial}{\partial x}(v_g(E_g+\alpha_g p))+p\frac{\partial \alpha_g}{\partial t}+Q=0, \tag{41}$$

$$\frac{\partial E_\ell}{\partial t}+\frac{\partial}{\partial x}(v_\ell(E_\ell+\alpha_\ell p))+p\frac{\partial \alpha_\ell}{\partial t}-Q=0. \tag{42}$$

Herein, the interpretation of the interface exchange term Q deserves some attention. Given that (41) and (42) balances total energy, one may be tempted to interpret Q as representing the amount of *energy* being transferred between the phases. However, the presence of the term $p\partial_t\alpha$ complicates this picture somewhat. In fact, in the form (41) and (42), the equations are not evolution equations for the energies; strictly speaking, they are evolution equations for the differential $d\,J_k$ given by

$$dJ_k = \mathrm{d}E_k + p\mathrm{d}\alpha_k. \tag{43}$$

In other words, the source term Q will modify the volume fractions as well as the energies of each phase. This means, in the context of (41) and (42), it makes more sense to interpret Q as *heat and kinetic energy* transfer terms rather than *energy transfer* terms. In the following, we will make this notion more precise, and present an alternative formulation of the energy balance equations where the source terms are truly energy transfer terms.

This may be considered an advantage from a purely heuristic point of view, although the resulting formulation is more involved than (41) and (42). Nevertheless, this alternative formulation has previously proven fruitful in devising numerical schemes (Martínez Ferrer et al., 2012; Munkejord et al., 2009).

In this respect, the main purpose of this section is to make the following point: *the modelling of the interface energy exchange terms is sensitive to the choice of formulation of the non-conservative terms representing mechanical work exchanged between the phases.*

6.1. Internal and kinetic energy

Using assumption A1 and the fundamental differential (7), we may rewrite the entropy Eq. (10) as follows:

$$\frac{\partial}{\partial t}(\rho_k\alpha_k e_k)+\frac{\partial}{\partial x}(\rho_k\alpha_k e_k v_k)+p\left(\frac{\partial \alpha_k}{\partial t}+\frac{\partial}{\partial x}(\alpha_k v_k)\right)=T_k\sigma_k. \tag{44}$$

Now adding (21) and (22) to (44) and comparing to (41) and (42), we obtain

$$Q=\mathcal{M}v_g-T_g\sigma_g=\mathcal{M}v_\ell+T_\ell\sigma_\ell. \tag{45}$$

In other words, Q represents the sum of the interface heat transfer and kinetic energy transfer terms, as may be expected; the mechanical work the phases perform on each other is encoded in the term $p\partial_t\alpha_k$.

6.2. Energy evolution equations

As was done in (Martínez Ferrer et al., 2012; Munkejord et al., 2009), we now aim to reformulate (41) and (42) to replace the $p\partial_t\alpha$-term with spatial derivatives. We may rewrite (11) as an evolution equation for the volume fraction:

$$\beta\frac{\partial \alpha_g}{\partial t}+\rho_g\alpha_\ell c_g^2\frac{\partial}{\partial x}(\alpha_g v_g)-\rho_\ell\alpha_g c_\ell^2\frac{\partial}{\partial x}(\alpha_\ell v_\ell)+\alpha_g\alpha_\ell(v_g-v_\ell)\frac{\partial p}{\partial x} = \alpha_\ell\Gamma_g T_g\sigma_g-\alpha_g\Gamma_\ell T_\ell\sigma_\ell, \tag{46}$$

where

$$\beta=\rho_g\alpha_\ell c_g^2+\rho_\ell\alpha_g c_\ell^2. \tag{47}$$

Substituting (46) into (41) and (42) we obtain

$$\frac{\partial E_g}{\partial t}+\frac{\partial}{\partial x}(E_g v_g)+(\alpha_g v_g-\eta\alpha_g\alpha_\ell(v_g-v_\ell))\frac{\partial p}{\partial x} +\eta\rho_\ell\alpha_g c_\ell^2\frac{\partial}{\partial x}(\alpha_g v_g+\alpha_\ell v_\ell)=\eta(\alpha_g\Gamma_\ell T_\ell\sigma_\ell-\alpha_\ell\Gamma_g T_g\sigma_g)-Q, \tag{48}$$

$$\frac{\partial E_\ell}{\partial t}+\frac{\partial}{\partial x}(E_\ell v_\ell)+(\alpha_\ell v_\ell+\eta\alpha_g\alpha_\ell(v_g-v_\ell))\frac{\partial p}{\partial x} +\eta\rho_g\alpha_\ell c_g^2\frac{\partial}{\partial x}(\alpha_g v_g+\alpha_\ell v_\ell)=Q-\eta(\alpha_g\Gamma_\ell T_\ell\sigma_\ell-\alpha_\ell\Gamma_g T_g\sigma_g), \tag{49}$$

where

$$\eta=\frac{p}{\beta}. \tag{50}$$

6.2.1. Interpretation of source terms

To recapitulate, we may now write the energy equations in the two equivalent forms:

- Standard formulation:

$$\frac{\partial E_g}{\partial t}+\frac{\partial}{\partial x}(v_g(E_g+\alpha_g p))+p\frac{\partial \alpha_g}{\partial t}=\mathcal{H}_g-\mathcal{M}v_g, \tag{51}$$

$$\frac{\partial E_\ell}{\partial t}+\frac{\partial}{\partial x}(v_\ell(E_\ell+\alpha_\ell p))+p\frac{\partial \alpha_\ell}{\partial t}=\mathcal{H}_\ell+\mathcal{M}v_\ell. \tag{52}$$

- Formulation with spatial derivatives:

$$\frac{\partial E_g}{\partial t}+\frac{\partial}{\partial x}(E_g v_g)+(\alpha_g v_g-\eta\alpha_g\alpha_\ell(v_g-v_\ell))\frac{\partial p}{\partial x} +\eta\rho_\ell\alpha_g c_\ell^2\frac{\partial}{\partial x}(\alpha_g v_g+\alpha_\ell v_\ell)=\mathcal{E}_g-\mathcal{M}v_g, \tag{53}$$

$$\frac{\partial E_\ell}{\partial t}+\frac{\partial}{\partial x}(E_\ell v_\ell)+(\alpha_\ell v_\ell+\eta\alpha_g\alpha_\ell(v_g-v_\ell))\frac{\partial p}{\partial x} +\eta\rho_g\alpha_\ell c_g^2\frac{\partial}{\partial x}(\alpha_g v_g+\alpha_\ell v_\ell)=\mathcal{E}_\ell+\mathcal{M}v_\ell. \tag{54}$$

Herein:

- $\mathcal{M}v_k$ are *kinetic energy* transfer terms;
- $\mathcal{H}_k=T_k\sigma_k$ are *heat* transfer terms;
- $\mathcal{E}_k$ are *internal energy* transfer terms.

We observe that the following relations hold between the heat and energy transfer terms:

$$\mathcal{E}_g=\mathcal{H}_g+\eta(\alpha_g\Gamma_\ell\mathcal{H}_\ell-\alpha_\ell\Gamma_g\mathcal{H}_g), \tag{55}$$

$$\mathcal{E}_\ell=\mathcal{H}_\ell-\eta(\alpha_g\Gamma_\ell\mathcal{H}_\ell-\alpha_\ell\Gamma_g\mathcal{H}_g). \tag{56}$$

In particular, the term

$$\mathcal{W}=\eta(\alpha_g\Gamma_\ell\mathcal{H}_\ell-\alpha_\ell\Gamma_g\mathcal{H}_g) \tag{57}$$

represents the mechanical work the phases perform on each other as a result of energy being transferred.

7. Summary

We have addressed some technical issues regarding the modelling of interface transfer terms in a class of two-fluid models commonly studied in the literature. In particular, we have discussed the compatibility between thermodynamic reversibility and well-posedness in two-fluid models based on simple formulations for conservation of masses, energy and momentum. We have derived an explicit condition on the interface momentum exchange term for these models to be reversible. In particular, this condition states that any such well-posed, reversible model must include virtual mass force terms; more precisely, the momentum exchange term must include spatial derivatives in the velocities.

Furthermore, we have showed that in the standard formulation of the energy balance equations, interface exchange terms play the role of heat transfer terms. We have discussed an alternative formulation where the interface terms transfer energy. We have also provided an explicit relationship between the amount of heat transferred and the mechanical work exchanged between the phases.

Acknowledgments

The first author was financed through the CO_2 Dynamics Project. The second author has received a PhD grant from the BIGCCS Centre. The authors acknowledge the support from the Research Council of Norway (189978, 193816), Aker Solutions, ConocoPhilips, Det Norske Veritas, Gassco, GDF SUEZ, Hydro, Shell, Statkraft, Statoil, TOTAL and Vattenfall.

We are grateful to our colleagues Xiaoju Du, Steinar Evje and Svend Tollak Munkejord for fruitful discussions. We also thank the anonymous reviewer for several helpful remarks.

References

Bendiksen, K.H., Malnes, D., Moe, R., Nuland, S., 1991. The dynamic two-fluid model OLGA: theory and application. SPE Prod. Eng. 6, 171–180.
Bestion, D., 1990. The physical closure laws in the CATHARE code. Nucl. Eng. Des. 124, 229–245.
De Henau, V., Raithby, G.D., 1995. A transient two-fluid model for the simulation of slug flow in pipelines–I. Theory. Int. J. Multiphase Flow 21, 335–349.
Drew, D.A., Passman, S.L., 1999. Theory of multicomponent fluids. Applied Mathematical Sciences, vol. 135. Springer-Verlag, New York.
Holmås, H., Sira, T., Langtangen, H.P., 2008. Analysis of a 1D incompressible two-fluid model including artificial diffusion. IMA J. Appl. Math. 73, 651–667.
Ishii, M., 1975. Thermo-Fluid Dynamic Theory of Two-Phase Flow. Eyrolles, Paris.
Jones, A.V., Prosperetti, A., 1985. On the suitability of first-order differential models for two-phase flow prediction. Int. J. Multiphase Flow 11, 133–148.
Keyfitz, B.L., Sanders, R., Sever, M., 2003. Lack of hyperbolicity in the two-fluid model for two-phase incompressible flow. Discrete Cont. Dyn. – B 3, 541–563.
Keyfitz, B.L., Sever, M., Zhang, F., 2004. Viscous singular shock structure for a nonhyperbolic two-fluid model. Nonlinearity 17, 1731–1747.
Lahey, R.T., 1991. Void wave propagation phenomena in two-phase flow (Kern Award Lecture). AIChE J. 37, 123–135.
Lax, P.D., 1957. Asymptotic solutions of oscillatory initial value problems. Duke Math. J. 24, 627–646.
Lax, P.D., 1980. On the notion of hyperbolicity. Commun. Pure Appl. Math. 33, 395–397.
Martínez Ferrer, P.J., Flåtten, T., Munkejord, S.T., 2012. On the effect of temperature and velocity relaxation in two-phase flow models. ESAIM-Math. Model. Num. 46, 411–442.
Munkejord, S.T., Evje, S., Flåtten, T., 2009. A MUSTA scheme for a nonconservative two-fluid model. SIAM J. Sci. Comput. 31, 2587–2622.
Munkejord, S.T., Papin, M., 2007. The effect of interfacial pressure in the discrete-equation multiphase model. Comput. Fluids 36, 742–757.
Paillère, H., Corre, C., Carcía Gascales, J.R., 2003. On the extension of the AUSM+ scheme to compressible two-fluid models. Comput. Fluids 32, 891–916.
Saurel, S., Gavrilyuk, S., Renaud, F., 2003. A multiphase model with internal degrees of freedom: application to shock-bubble interaction. J. Fluid Mech. 495, 283–321.
Sever, M., 2005. Solutions of a nonhyperbolic pair of balance laws. ESAIM: M2AN Math. Model. Numer. Anal. 39, 37–58.
Sever, M., 2008. A model of discontinuous, incompressible two-phase flow. J. Math. Fluid Mech. 10, 203–223.
Song, J., Ishii, M., 2001. The one-dimensional two-fluid model with momentum flux parameters. Nucl. Eng. Des. 205, 145–158.
Städtke, H., 2006. Gasdynamic Aspects of Two-Phase Flow. Wiley-VCH Verlag GmbH & Co. KGaA, Weinheim, Germany.
Stewart, H.B., Wendroff, B., 1984. Review article; two-phase flow: models and methods. J. Comput. Phys. 56, 363–409.
Stuhmiller, J.H., 1977. The influence of interfacial pressure forces on the character of two-phase flow model equations. Int. J. Multiphase Flow 3, 551–560.
Toumi, I., 1996. An upwind numerical method for two-fluid two-phase flow models. Nucl. Sci. Eng. 123, 147–168.
Toumi, I., Kumbaro, A., 1996. An approximate linearized riemann solver for a two-fluid model. J. Comput. Phys. 124, 286–300.

G A Two-Fluid Four-Equation Model with Instantaneous Thermodynamical Equilibrium

Alexandre Morin and Tore Flåtten
Submitted to the SIAM Journal on Applied Mathematics, 2012.

A TWO-FLUID FOUR-EQUATION MODEL WITH INSTANTANEOUS THERMODYNAMICAL EQUILIBRIUM

ALEXANDRE MORIN[†] AND TORE FLÅTTEN[‡]

Abstract.
We derive a four-equation version of a common two-fluid model for pipe flow, containing one mixture mass equation and one mixture energy equation. The motivation is to obtain a fluid-dynamical model where the mixture is in thermodynamical equilibrium at all time. We start from a five-equation model with instantaneous thermal equilibrium, to which we add phase relaxation terms. An interfacial velocity appears, for which we give an expression based on the second law of thermodynamics. We then derive the limit of this model when the relaxation becomes instantaneous. The time derivatives appearing in this process are subsequently transformed into spatial derivatives to be able to use numerical methods for conservation laws. The Jacobian matrix of the fluxes can then be evaluated, and the system be put into quasilinear form. From the Jacobian matrix, we are able to extract the sound speed intrinsic to the model. By comparison to the sound speed in other two-phase flow models, we extend some previous results showing that the effect of relaxation on sound speed is independent of the order in which the variables are relaxed. We also check the subcharacteristic condition and place the model in a hierarchy of two-phase flow models. Finally, this model requires a regularisation term to be hyperbolic. We postulate that this term takes the form of an interfacial pressure difference. With the help of a perturbation method, we find an expression for the pressure difference that makes the model hyperbolic.

Key words. Two-phase flows, relaxation, two-fluid model, subcharacteristic condition

AMS subject classifications. 76T10,76N15,35L60,80M35

1. Introduction. One-dimensional two-phase flows in pipelines may be modelled using the two-fluid model [20, 23, 28, 31]. The two-fluid model is characterised by the fact that it has two momentum equations. Therefore, the phase velocities are independent from each other, as opposed to the drift-flux model [11, 21, 26] where there is only one momentum equation for the mixture. The six-equation version of the two-fluid model is used for example in the nuclear industry [4, 33]. In this version, the phases are in mechanical equilibrium – they are at the same pressure at all time – but not in chemical and thermal equilibrium. A five-equation version has been chosen for pipeline flow simulation [3], in which the phases are assumed to be in mechanical and thermal equilibrium. A seven-equation version, where the phases are allowed to be totally out of equilibrium – both have their own pressure, temperature and chemical potential – has also been derived [2, 25]. The aim was to avoid the non-hyperbolicity [13, 29] of the six-equation model.

Relaxation source terms may be added to the model to bring it towards equilibrium at a finite rate. This has been studied for example in [10, 12, 15, 22, 24, 25, 32]. An equilibrium system may also be approached by a relaxation system with very stiff source terms [1]. For instance, the six-equation model with a stiff temperature relaxation will behave similarly to the five-equation model with one mixture energy equation. However, numerical methods for hyperbolic systems do not naturally handle algebraic source terms. With a splitting approach, the fluxes are advanced one time step alternately with the source terms. The latter are solved using ordinary differential equation solvers. However, when the relaxation is instantaneous, it should directly

[†]Department of Energy and Process Engineering, Norwegian University of Science and Technology (NTNU), Kolbjørn Hejes vei 1B, NO-7491 Trondheim, Norway. alexandre.morin [a] sintef.no

[‡]SINTEF Energy Research, P.O. Box 4761 Sluppen, NO-7465 Trondheim, Norway

affect the propagation speed of the waves. This time splitting may cause smearing of the discontinuities in this case. Thus it is preferable to use the equilibrium system.

For the simulation of the two-phase flow of a mixture with phase change, the equation of state plays an important role. For example, the Span-Wagner equation of state is accurate for two-phase mixtures of CO_2 [27]. However it is an equilibrium equation of state, which means that the fluid-dynamical model must handle a mixture that is at equilibrium at all time. Therefore, a four-equation version of the two-fluid model has to be derived in order to use such equilibrium-based equations of state. In the present paper, we derive this model from the two-fluid five-equation model presented in [10], where we replace the individual phase mass-equations by a mixture mass equation and an instantaneous chemical equilibrium assumption. As mentioned in the previous paragraph, this will modify the wave structure of the model compared to the initial five-equation model. In fact, this phenomenon has been studied, and a stability condition has been derived, called the subcharacteristic condition [6, 10, 12, 16, 22]. It says that for a relaxation system and its corresponding equilibrium system, the speed of the waves of corresponding families will be lower in the equilibrium system than in the relaxation system. In [10], the authors began to establish a hierarchy of two-phase flow models with respect to the subcharacteristic condition, where they concentrated on velocity and thermal relaxation. In addition, they showed that the sound speed is reduced by the same factor regardless of the order in which the relaxation processes are performed.

The four-equation model thus derived is expected to be non-hyperbolic when the gas and liquid velocities are different from each other. Therefore, we add to the derivation a regularising term. We choose to use an interfacial pressure term of the sort often used with the six-equation two-fluid model [4, 7, 8, 9, 23, 31]. We then obtain an explicit expression for the pressure difference involved in this term. We do this with the help of a perturbation method [30, 31], which gives a well known form for this term [5, 9, 19, 20, 23, 29].

The structure of the paper is as follows. In Section 2, we present the five-equation model, to which we add relaxation source terms for phase change. These involve an interfacial momentum velocity, for which we give an expression with the help of entropy considerations. In Section 3, the four-equation model is derived. The phase change relaxation source term is expressed by means of derivatives, so that no algebraic terms remain in the system. Also, the problematic time derivatives are transformed into spatial derivatives. Then, in Section 4, the system is written in quasilinear form, which involves finding the Jacobian of the fluxes. In Section 5, the speed of sound of the model is evaluated, and the subcharacteristic condition with respect to other two-phase flow models verified. In Section 6, we show how a perturbation method gives an expression for the interfacial pressure difference that makes the model hyperbolic. Finally, in Section 7, we discuss the phenomenon of resonance which is known to occur in the kind of two-fluid models we consider [14, 17, 18]. Section 8 summarises the results of the paper. The main symbols used are listed in Table 1.1. The other ones are introduced in the text.

2. The five equation model with phase relaxation. The two-fluid five-equation model studied by Martinez *et. al.* [10] describes a one-dimensional two-phase flow where the pressure and the temperature are kept equal in both phases at all times. This follows from the assumption of instantaneous mechanical and thermal equilibrium. However, the two phases will in general not be in chemical equilibrium. Algebraic relaxation terms representing phase change should then act to attract the

TABLE 1.1
Main symbols.

Symbol	Signification
c	Speed of sound
C_p	Specific heat capacity at constant pressure
e	Internal energy
E	Phasic total energy ($E = \alpha\rho(e + 1/2v^2)$)
f_i	Components of the vector $\boldsymbol{F}$
p	Pressure
T	Temperature
u_i	Components of the vector $\boldsymbol{U}$
v	Velocity
w_i	Components of the vector $\boldsymbol{W}$
α	Volume fraction
Γ	First Grüneisen coefficient
ε	Perturbation parameter
μ	Chemical potential
ρ	Density
$\boldsymbol{A}$	Jacobian
$\boldsymbol{B}$	Coefficient matrix in the non-conservative terms
$\boldsymbol{F}$	Vector of the fluxes
$\boldsymbol{U}$	Vector of the conserved variables
$\boldsymbol{W}$	Vector of the non-conservative variables
g	Gas phase (Subscript)
ℓ	Liquid phase (Subscript)

phases towards equilibrium. The model with phase relaxation is

$$\frac{\partial \alpha_{\mathrm{g}}\rho_{\mathrm{g}}}{\partial t} + \frac{\partial \alpha_{\mathrm{g}}\rho_{\mathrm{g}}v_{\mathrm{g}}}{\partial x} = \mathcal{K}(\mu_\ell - \mu_{\mathrm{g}}), \tag{2.1}$$

$$\frac{\partial \alpha_\ell\rho_\ell}{\partial t} + \frac{\partial \alpha_\ell\rho_\ell v_\ell}{\partial x} = \mathcal{K}(\mu_{\mathrm{g}} - \mu_\ell), \tag{2.2}$$

$$\frac{\partial \alpha_{\mathrm{g}}\rho_{\mathrm{g}}v_{\mathrm{g}}}{\partial t} + \frac{\partial \alpha_{\mathrm{g}}\rho_{\mathrm{g}}v_{\mathrm{g}}^2}{\partial x} + \alpha_{\mathrm{g}}\frac{\partial p}{\partial x} = v_{\mathrm{i}}\mathcal{K}(\mu_\ell - \mu_{\mathrm{g}}), \tag{2.3}$$

$$\frac{\partial \alpha_\ell\rho_\ell v_\ell}{\partial t} + \frac{\partial \alpha_\ell\rho_\ell v_\ell^2}{\partial x} + \alpha_\ell\frac{\partial p}{\partial x} = v_{\mathrm{i}}\mathcal{K}(\mu_{\mathrm{g}} - \mu_\ell), \tag{2.4}$$

$$\frac{\partial (E_{\mathrm{g}} + E_\ell)}{\partial t} + \frac{\partial}{\partial x}((E_{\mathrm{g}} + \alpha_{\mathrm{g}}p)v_{\mathrm{g}} + (E_\ell + \alpha_\ell p)v_\ell) = 0, \tag{2.5}$$

where

$$E = \alpha\rho\left(e + \frac{1}{2}v^2\right), \tag{2.6}$$

$\mathcal{K}$ is a positive relaxation constant, μ is the chemical potential, and v_{i} is some interface velocity. Assuming that the phases are composed of only one component, we may express the chemical potential as

$$\mu = e + \frac{p}{\rho} - Ts. \tag{2.7}$$

2.1. Interfacial momentum velocity. Through entropy considerations, we are able to give an expression for the interface velocity v_i. We will derive the mixture entropy evolution equation and show that the second law of thermodynamics naturally suggests the expression

$$v_\mathrm{i} = \frac{1}{2}(v_\mathrm{g} + v_\ell). \tag{2.8}$$

We first derive the kinetic energy evolution equations, by multiplying the momentum equations (2.3) and (2.4) by v_g and v_ℓ respectively. For the gas phase, after expansion of the derivatives, we obtain

$$v_\mathrm{g}^2\frac{\partial \alpha_\mathrm{g}\rho_\mathrm{g}}{\partial t} + \alpha_\mathrm{g}\rho_\mathrm{g}v_\mathrm{g}\frac{\partial v_\mathrm{g}}{\partial t} + v_\mathrm{g}^2\frac{\partial \alpha_\mathrm{g}\rho_\mathrm{g}v_\mathrm{g}}{\partial x} + \alpha_\mathrm{g}\rho_\mathrm{g}v_\mathrm{g}^2\frac{\partial v_\mathrm{g}}{\partial x} + \alpha_\mathrm{g}v_\mathrm{g}\frac{\partial p}{\partial x} = v_\mathrm{g}v_\mathrm{i}\mathcal{K}(\mu_\ell - \mu_\mathrm{g}). \tag{2.9}$$

The same applies to the liquid phase. After the use of the mass equation and reorganisation, the equations read

$$\frac{\partial}{\partial t}\left(\frac{1}{2}\alpha_\mathrm{g}\rho_\mathrm{g}v_\mathrm{g}^2\right) + \frac{\partial}{\partial x}\left(\frac{1}{2}\alpha_\mathrm{g}\rho_\mathrm{g}v_\mathrm{g}^3\right) + \alpha_\mathrm{g}v_\mathrm{g}\frac{\partial p}{\partial x} = v_\mathrm{g}\left(v_\mathrm{i} - \frac{1}{2}v_\mathrm{g}\right)\mathcal{K}(\mu_\ell - \mu_\mathrm{g}), \tag{2.10}$$

$$\frac{\partial}{\partial t}\left(\frac{1}{2}\alpha_\ell\rho_\ell v_\ell^2\right) + \frac{\partial}{\partial x}\left(\frac{1}{2}\alpha_\ell\rho_\ell v_\ell^3\right) + \alpha_\ell v_\ell\frac{\partial p}{\partial x} = v_\ell\left(v_\mathrm{i} - \frac{1}{2}v_\ell\right)\mathcal{K}(\mu_\mathrm{g} - \mu_\ell). \tag{2.11}$$

Using the latter equations, we can now cancel the kinetic energy contribution in the mixture total energy equation (2.5), which gives

$$\begin{aligned}\frac{\partial}{\partial t}\left(\alpha_\mathrm{g}\rho_\mathrm{g}e_\mathrm{g} + \alpha_\ell\rho_\ell e_\ell\right) + \frac{\partial}{\partial x}\left(\alpha_\mathrm{g}\rho_\mathrm{g}e_\mathrm{g}v_\mathrm{g} + \alpha_\ell\rho_\ell e_\ell v_\ell\right)\\ + p\frac{\partial \alpha_\mathrm{g}v_\mathrm{g}}{\partial x} + p\frac{\partial \alpha_\ell v_\ell}{\partial x} = (v_\mathrm{g} - v_\ell)\left(v_\mathrm{i} - \frac{1}{2}(v_\mathrm{g} + v_\ell)\right)\mathcal{K}(\mu_\mathrm{g} - \mu_\ell).\end{aligned} \tag{2.12}$$

By the mass equation, we obtain an evolution equation for the material derivatives of the phasic internal energy

$$\begin{aligned}\alpha_\mathrm{g}\rho_\mathrm{g}\frac{D_\mathrm{g}e_\mathrm{g}}{Dt} + \alpha_\ell\rho_\ell\frac{D_\ell e_\ell}{Dt} + p\frac{\partial \alpha_\mathrm{g}v_\mathrm{g}}{\partial x} + p\frac{\partial \alpha_\ell v_\ell}{\partial x}\\ = \left((v_\mathrm{g} - v_\ell)\left(v_\mathrm{i} - \frac{1}{2}(v_\mathrm{g} + v_\ell)\right) + e_\mathrm{g} - e_\ell\right)\mathcal{K}(\mu_\mathrm{g} - \mu_\ell),\end{aligned} \tag{2.13}$$

where we have introduced the phase specific material derivative $\frac{D_\mathrm{k}}{Dt} = \frac{\partial}{\partial t} + v_\mathrm{k}\frac{\partial}{\partial x}$.

Using the fundamental thermodynamic relation

$$\mathrm{d}e = \frac{p}{\rho^2}\,\mathrm{d}\rho + T\,\mathrm{d}s, \tag{2.14}$$

we can transform the previous equation into an entropy equation. First, (2.14) is expressed in terms of material derivatives and substituted in the internal energy equation (2.13)

$$\begin{aligned}\alpha_\mathrm{g}\rho_\mathrm{g}\left(T\frac{D_\mathrm{g}s_\mathrm{g}}{Dt} + \frac{p}{\rho_\mathrm{g}^2}\frac{D_\mathrm{g}\rho_\mathrm{g}}{Dt}\right) + \alpha_\ell\rho_\ell\left(T\frac{D_\ell s_\ell}{Dt} + \frac{p}{\rho_\ell^2}\frac{D_\ell\rho_\ell}{Dt}\right) + p\frac{\partial \alpha_\mathrm{g}v_\mathrm{g}}{\partial x} + p\frac{\partial \alpha_\ell v_\ell}{\partial x}\\ = \left((v_\mathrm{g} - v_\ell)\left(v_\mathrm{i} - \frac{1}{2}(v_\mathrm{g} + v_\ell)\right) + e_\mathrm{g} - e_\ell\right)\mathcal{K}(\mu_\mathrm{g} - \mu_\ell).\end{aligned} \tag{2.15}$$

By the mass equations (2.1)–(2.2), it can be simplified to

$$\alpha_{\mathrm{g}}\rho_{\mathrm{g}}T\frac{D_{\mathrm{g}}s_{\mathrm{g}}}{\partial t}+\alpha_{\ell}\rho_{\ell}T\frac{D_{\ell}s_{\ell}}{\partial t} = \left((v_{\mathrm{g}}-v_{\ell})\left(v_{\mathrm{i}}-\frac{1}{2}(v_{\mathrm{g}}+v_{\ell})\right)+e_{\mathrm{g}}+\frac{p}{\rho_{\mathrm{g}}}-e_{\ell}-\frac{p}{\rho_{\ell}}\right)\mathcal{K}(\mu_{\mathrm{g}}-\mu_{\ell}), \quad (2.16)$$

and using again the mass equations, we obtain the evolution equation for the mixture entropy

$$T\left(\frac{\partial\alpha_{\mathrm{g}}\rho_{\mathrm{g}}s_{\mathrm{g}}}{\partial t}+\frac{\partial\alpha_{\ell}\rho_{\ell}s_{\ell}}{\partial t}+\frac{\partial\alpha_{\mathrm{g}}\rho_{\mathrm{g}}s_{\mathrm{g}}v_{\mathrm{g}}}{\partial x}+\frac{\partial\alpha_{\ell}\rho_{\ell}s_{\ell}v_{\ell}}{\partial x}\right) = \left((v_{\mathrm{g}}-v_{\ell})\left(v_{\mathrm{i}}-\frac{1}{2}(v_{\mathrm{g}}+v_{\ell})\right)+\mu_{\mathrm{g}}-\mu_{\ell}\right)\mathcal{K}(\mu_{\mathrm{g}}-\mu_{\ell}) \quad (2.17)$$

since the chemical potential can be expressed as in (2.7).

Now, the second law of thermodynamics imposes that the right-hand side of (2.17) should be greater than zero

$$\left((v_{\mathrm{g}}-v_{\ell})\left(v_{\mathrm{i}}-\frac{1}{2}(v_{\mathrm{g}}+v_{\ell})\right)+\mu_{\mathrm{g}}-\mu_{\ell}\right)\mathcal{K}(\mu_{\mathrm{g}}-\mu_{\ell})\geq 0. \quad (2.18)$$

We have that

$$\mathcal{K}(\mu_{\mathrm{g}}-\mu_{\ell})^2\geq 0, \quad (2.19)$$

so that, if

$$(v_{\mathrm{g}}-v_{\ell})\left(v_{\mathrm{i}}-\frac{1}{2}(v_{\mathrm{g}}+v_{\ell})\right)\mathcal{K}(\mu_{\mathrm{g}}-\mu_{\ell})\geq 0, \quad (2.20)$$

the condition is always verified. It is natural to assume that the interfacial velocity should be independent of the chemical potentials. In this case, the condition can only be verified for

$$v_{\mathrm{i}}=\frac{1}{2}(v_{\mathrm{g}}+v_{\ell}). \quad (2.21)$$

This is the same expression as proposed in [28], though it was not physically motivated.

3. The four-equation model. We wish to derive a four-equation model from the above five-equation model, where we assume the phase change to be instantaneous. The two phases will then at all times be in equilibrium. This is achieved by letting $\mathcal{K}\to\infty$ in the model (2.1)–(2.5). Since the repartition of the mass in the phases now is entirely governed by thermodynamics, we only need one mixture mass evolution equation, instead of one for each phase as in (2.1)–(2.2). We therefore sum (2.1) and (2.2) to give the mixture mass evolution equation of the four-equation model

$$\frac{\partial(\alpha_{\mathrm{g}}\rho_{\mathrm{g}}+\alpha_{\ell}\rho_{\ell})}{\partial t}+\frac{\partial(\alpha_{\mathrm{g}}\rho_{\mathrm{g}}v_{\mathrm{g}}+\alpha_{\ell}\rho_{\ell}v_{\ell})}{\partial x}=0, \quad (3.1)$$

and specify $\mu_{\mathrm{g}}=\mu_{\ell}$. The remaining three other evolution equations of the four-equation model are the same as in the five-equation model (2.3)–(2.5). However, since

$\mathcal{K} \to \infty$ and $\mu_\mathrm{g} = \mu_\ell$, $\mathcal{K}(\mu_\mathrm{g} - \mu_\ell)$ is an undefined limit. It needs to be substituted using the phase mass equations (2.1) and (2.2). This gives the model

$$\frac{\partial(\alpha_\mathrm{g}\rho_\mathrm{g} + \alpha_\ell\rho_\ell)}{\partial t} + \frac{\partial(\alpha_\mathrm{g}\rho_\mathrm{g}v_\mathrm{g} + \alpha_\ell\rho_\ell v_\ell)}{\partial x} = 0, \tag{3.2}$$

$$\frac{\partial \alpha_\mathrm{g}\rho_\mathrm{g}v_\mathrm{g}}{\partial t} + \frac{\partial \alpha_\mathrm{g}\rho_\mathrm{g}v_\mathrm{g}^2}{\partial x} + \alpha_\mathrm{g}\frac{\partial p}{\partial x} = \frac{v_\mathrm{g} + v_\ell}{2}\left(\frac{\partial \alpha_\mathrm{g}\rho_\mathrm{g}}{\partial t} + \frac{\partial \alpha_\mathrm{g}\rho_\mathrm{g}v_\mathrm{g}}{\partial x}\right), \tag{3.3}$$

$$\frac{\partial \alpha_\ell\rho_\ell v_\ell}{\partial t} + \frac{\partial \alpha_\ell\rho_\ell v_\ell^2}{\partial x} + \alpha_\ell\frac{\partial p}{\partial x} = \frac{v_\mathrm{g} + v_\ell}{2}\left(\frac{\partial \alpha_\ell\rho_\ell}{\partial t} + \frac{\partial \alpha_\ell\rho_\ell v_\ell}{\partial x}\right), \tag{3.4}$$

$$\frac{\partial(E_\mathrm{g} + E_\ell)}{\partial t} + \frac{\partial}{\partial x}((E_\mathrm{g} + \alpha_\mathrm{g}p)v_\mathrm{g} + (E_\ell + \alpha_\ell p)v_\ell) = 0. \tag{3.5}$$

Further, the internal energy equation becomes

$$\frac{\partial}{\partial t}\left(\alpha_\mathrm{g}\rho_\mathrm{g}e_\mathrm{g} + \alpha_\ell\rho_\ell e_\ell\right) + \frac{\partial}{\partial x}\left(\alpha_\mathrm{g}\rho_\mathrm{g}e_\mathrm{g}v_\mathrm{g} + \alpha_\ell\rho_\ell e_\ell v_\ell\right) + p\frac{\partial \alpha_\mathrm{g}v_\mathrm{g}}{\partial x} + p\frac{\partial \alpha_\ell v_\ell}{\partial x} = 0. \tag{3.6}$$

In the entropy equation (2.17), since $\mathcal{K}(\mu_\mathrm{g} - \mu_\ell)$ is finite, we have that $\mathcal{K}(\mu_\mathrm{g} - \mu_\ell)^2 \to 0$. The entropy equation becomes

$$\frac{\partial \alpha_\mathrm{g}\rho_\mathrm{g}s_\mathrm{g}}{\partial t} + \frac{\partial \alpha_\ell\rho_\ell s_\ell}{\partial t} + \frac{\partial \alpha_\mathrm{g}\rho_\mathrm{g}s_\mathrm{g}v_\mathrm{g}}{\partial x} + \frac{\partial \alpha_\ell\rho_\ell s_\ell v_\ell}{\partial x} = 0. \tag{3.7}$$

Now, to be able to have the model in quasilinear form, we first need to express the time derivatives $\partial_t\alpha_\mathrm{g}\rho_\mathrm{g}$ and $\partial_t\alpha_\ell\rho_\ell$ in terms of spatial derivatives.

3.1. Some differentials. Some useful differentials can be derived from the assumptions of equilibrium. From the expression of the thermodynamic potential (2.7) and the fundamental thermodynamic relation (2.14), we obtain

$$\mathrm{d}\mu = \frac{1}{\rho}\,\mathrm{d}p - s\,\mathrm{d}T. \tag{3.8}$$

Since $\mu_\mathrm{g} = \mu_\ell$, we can write

$$\left(\frac{1}{\rho_\mathrm{g}} - \frac{1}{\rho_\ell}\right)\mathrm{d}p = (s_\mathrm{g} - s_\ell)\,\mathrm{d}T. \tag{3.9}$$

Remark that, with the Clapeyron equation, we can write

$$s_\mathrm{g} - s_\ell = \frac{L}{T}, \tag{3.10}$$

where

$$L = e_\mathrm{g} + \frac{p}{\rho_\mathrm{g}} - e_\ell - \frac{p}{\rho_\ell} \tag{3.11}$$

is the *latent heat*. Thus the differential becomes

$$\left(\frac{1}{\rho_\mathrm{g}} - \frac{1}{\rho_\ell}\right)\mathrm{d}p = \frac{L}{T}\,\mathrm{d}T. \tag{3.12}$$

Then, we obtain an entropy differential from [12] for the gas phase

$$\mathrm{d}s_\mathrm{g} = -\frac{\Gamma_\mathrm{g}C_{p,\mathrm{g}}}{\rho_\mathrm{g}c_\mathrm{g}^2}\,\mathrm{d}p + \frac{C_{p,\mathrm{g}}}{T}\,\mathrm{d}T, \tag{3.13}$$

which with the help of (3.12) becomes

$$\mathrm{d}s_\mathrm{g} = -C_{p,\mathrm{g}} \left(\frac{\Gamma_\mathrm{g}}{\rho_\mathrm{g} c_\mathrm{g}^2} + \frac{\rho_\mathrm{g} - \rho_\ell}{\rho_\mathrm{g} \rho_\ell L} \right) \mathrm{d}p. \tag{3.14}$$

We also obtain an internal energy differential from [11] for the gas phase

$$\begin{aligned} \mathrm{d}e_\mathrm{g} &= \left(\frac{\partial e_\mathrm{g}}{\partial T} \right)_p \mathrm{d}T + \left(\frac{\partial e_\mathrm{g}}{\partial p} \right)_T \mathrm{d}p \\ &= C_{p,\mathrm{g}} \left(1 - \frac{\Gamma_\mathrm{g} p}{\rho_\mathrm{g} c_\mathrm{g}^2} \right) \mathrm{d}T + \left(\frac{p}{\rho_\mathrm{g}^2 c_\mathrm{g}^2} - \frac{\Gamma_\mathrm{g} T}{\rho_\mathrm{g} c_\mathrm{g}^2} C_{p,\mathrm{g}} \left(1 - \frac{\Gamma_\mathrm{g} p}{\rho_\mathrm{g} c_\mathrm{g}^2} \right) \right) \mathrm{d}p, \end{aligned} \tag{3.15}$$

which can be written through (3.12) as

$$\mathrm{d}e_\mathrm{g} = \frac{1}{\rho_\mathrm{g} c_\mathrm{g}^2} \left(\frac{p}{\rho_\mathrm{g}} - T C_{p,\mathrm{g}} (\rho_\mathrm{g} c_\mathrm{g}^2 - \Gamma_\mathrm{g} p) \left(\frac{\rho_\mathrm{g} - \rho_\ell}{\rho_\mathrm{g} \rho_\ell L} + \frac{\Gamma_\mathrm{g}}{\rho_\mathrm{g} c_\mathrm{g}^2} \right) \right) \mathrm{d}p. \tag{3.16}$$

We obtain the counterpart for the liquid phase of these differentials by symmetry of the phases.

To simplify the expressions, we rewrite the two last expressions using shorthands for variable groups which will repetitively appear in the present article. We first define

$$\chi_\mathrm{g} = \frac{\Gamma_\mathrm{g}}{\rho_\mathrm{g} c_\mathrm{g}^2} + \frac{\rho_\mathrm{g} - \rho_\ell}{\rho_\mathrm{g} \rho_\ell L}, \tag{3.17}$$

$$\chi_\ell = \frac{\Gamma_\ell}{\rho_\ell c_\ell^2} + \frac{\rho_\mathrm{g} - \rho_\ell}{\rho_\mathrm{g} \rho_\ell L}, \tag{3.18}$$

and then

$$\Psi_\mathrm{g} = 1 + \rho_\mathrm{g} T C_{p,\mathrm{g}} \Gamma_\mathrm{g} \chi_\mathrm{g}, \tag{3.19}$$

$$\Psi_\ell = 1 + \rho_\ell T C_{p,\ell} \Gamma_\ell \chi_\ell. \tag{3.20}$$

This gives

$$\mathrm{d}s_\mathrm{g} = -C_{p,\mathrm{g}} \chi_\mathrm{g} \, \mathrm{d}p. \tag{3.21}$$

and

$$\mathrm{d}e_\mathrm{g} = \left(\frac{p}{\rho_\mathrm{g}^2 c_\mathrm{g}^2} \Psi_\mathrm{g} - T C_{p,\mathrm{g}} \chi_\mathrm{g} \right) \mathrm{d}p. \tag{3.22}$$

where we recognise an expression similar to the fundamental thermodynamic relation (2.14)

$$\mathrm{d}e_\mathrm{g} = \frac{p}{\rho_\mathrm{g}^2 c_\mathrm{g}^2} \Psi_\mathrm{g} \, \mathrm{d}p + T \, \mathrm{d}s_\mathrm{g}. \tag{3.23}$$

3.2. Treatment of the time derivatives. From the differentials (3.21) and (3.22) as well as the mixture mass equation (3.2), internal energy equation (3.6) and entropy equation (3.7), we are able to find three relations between $\partial_t p$, $\partial_t \alpha_\mathrm{g} \rho_\mathrm{g}$ and $\partial_t \alpha_\ell \rho_\ell$ and spatial derivatives. Therefore we can find an expression for each of the time derivatives.

The first relation is the mass equation (3.2)

$$\frac{\partial(\alpha_{\mathrm{g}}\rho_{\mathrm{g}}+\alpha_\ell\rho_\ell)}{\partial t}+\frac{\partial(\alpha_{\mathrm{g}}\rho_{\mathrm{g}}v_{\mathrm{g}}+\alpha_\ell\rho_\ell v_\ell)}{\partial x}=0. \tag{3.24}$$

Then, the derivatives are expanded in the entropy equation (3.7). The derivatives $\partial_t s_{\mathrm{k}}$ and $\partial_x s_{\mathrm{k}}$ are subsequently substituted using the entropy differential (3.21) to obtain a second relation

$$\begin{aligned}-(\alpha_{\mathrm{g}}\rho_{\mathrm{g}}C_{p,\mathrm{g}}\chi_{\mathrm{g}}+\alpha_\ell\rho_\ell C_{p,\ell}\chi_\ell)\frac{\partial p}{\partial t}-(\alpha_{\mathrm{g}}\rho_{\mathrm{g}}C_{p,\mathrm{g}}\chi_{\mathrm{g}}v_{\mathrm{g}}+\alpha_\ell\rho_\ell C_{p,\ell}\chi_\ell v_\ell)\frac{\partial p}{\partial x}\\ +s_{\mathrm{g}}\frac{\partial\alpha_{\mathrm{g}}\rho_{\mathrm{g}}}{\partial t}+s_\ell\frac{\partial\alpha_\ell\rho_\ell}{\partial t}+s_{\mathrm{g}}\frac{\partial\alpha_{\mathrm{g}}\rho_{\mathrm{g}}v_{\mathrm{g}}}{\partial x}+s_\ell\frac{\partial\alpha_\ell\rho_\ell v_\ell}{\partial x}=0.\end{aligned} \tag{3.25}$$

Finally, the same treatment is applied to the internal energy equation (3.6) with the differential (3.22), which gives a third relation

$$\begin{aligned}&\left(\alpha_{\mathrm{g}}\rho_{\mathrm{g}}\left(\frac{p}{\rho_{\mathrm{g}}^2c_{\mathrm{g}}^2}\Psi_{\mathrm{g}}-TC_{p,\mathrm{g}}\chi_{\mathrm{g}}\right)+\alpha_\ell\rho_\ell\left(\frac{p}{\rho_\ell^2c_\ell^2}\Psi_\ell-TC_{p,\ell}\chi_\ell\right)\right)\frac{\partial p}{\partial t}\\ &\quad+\left(\alpha_{\mathrm{g}}\rho_{\mathrm{g}}\left(\frac{p}{\rho_{\mathrm{g}}^2c_{\mathrm{g}}^2}\Psi_{\mathrm{g}}-TC_{p,\mathrm{g}}\chi_{\mathrm{g}}\right)v_{\mathrm{g}}+\alpha_\ell\rho_\ell\left(\frac{p}{\rho_\ell^2c_\ell^2}\Psi_\ell-TC_{p,\ell}\chi_\ell\right)v_\ell\right)\frac{\partial p}{\partial x}\\ &+e_{\mathrm{g}}\frac{\partial\alpha_{\mathrm{g}}\rho_{\mathrm{g}}}{\partial t}+e_\ell\frac{\partial\alpha_\ell\rho_\ell}{\partial t}+e_{\mathrm{g}}\frac{\partial\alpha_{\mathrm{g}}\rho_{\mathrm{g}}v_{\mathrm{g}}}{\partial x}+e_\ell\frac{\partial\alpha_\ell\rho_\ell v_\ell}{\partial x}+p\frac{\partial\alpha_{\mathrm{g}}v_{\mathrm{g}}}{\partial x}+p\frac{\partial\alpha_\ell v_\ell}{\partial x}=0.\end{aligned} \tag{3.26}$$

Solving these three relations, we obtain an expression which takes the form of the gas-phase mass equation on the left hand side, which can be substituted in the momentum equation for the gas phase (3.3)

$$\frac{\partial\alpha_{\mathrm{g}}\rho_{\mathrm{g}}}{\partial t}+\frac{\partial\alpha_{\mathrm{g}}\rho_{\mathrm{g}}v_{\mathrm{g}}}{\partial x}=-\mathcal{P}\frac{\partial p}{\partial x}-\mathcal{V}\left(\frac{\partial\alpha_{\mathrm{g}}v_{\mathrm{g}}}{\partial x}+\frac{\partial\alpha_\ell v_\ell}{\partial x}\right), \tag{3.27}$$

where

$$\mathcal{V}=\frac{T(\alpha_{\mathrm{g}}\rho_{\mathrm{g}}C_{p,\mathrm{g}}\chi_{\mathrm{g}}+\alpha_\ell\rho_\ell C_{p,\ell}\chi_\ell)}{L\left(\frac{\alpha_{\mathrm{g}}}{\rho_{\mathrm{g}}c_{\mathrm{g}}^2}\Psi_{\mathrm{g}}+\frac{\alpha_\ell}{\rho_\ell c_\ell^2}\Psi_\ell\right)+T(\alpha_{\mathrm{g}}\rho_{\mathrm{g}}C_{p,\mathrm{g}}\chi_{\mathrm{g}}+\alpha_\ell\rho_\ell C_{p,\ell}\chi_\ell)\frac{\rho_{\mathrm{g}}-\rho_\ell}{\rho_{\mathrm{g}}\rho_\ell}}, \tag{3.28}$$

$$\mathcal{P}=\frac{\alpha_{\mathrm{g}}\alpha_\ell T(v_{\mathrm{g}}-v_\ell)\left(\rho_\ell C_{p,\ell}\chi_\ell\frac{\Psi_{\mathrm{g}}}{\rho_{\mathrm{g}}c_{\mathrm{g}}^2}-\rho_{\mathrm{g}}C_{p,\mathrm{g}}\chi_{\mathrm{g}}\frac{\Psi_\ell}{\rho_\ell c_\ell^2}\right)}{L\left(\frac{\alpha_{\mathrm{g}}}{\rho_{\mathrm{g}}c_{\mathrm{g}}^2}\Psi_{\mathrm{g}}+\frac{\alpha_\ell}{\rho_\ell c_\ell^2}\Psi_\ell\right)+T(\alpha_{\mathrm{g}}\rho_{\mathrm{g}}C_{p,\mathrm{g}}\chi_{\mathrm{g}}+\alpha_\ell\rho_\ell C_{p,\ell}\chi_\ell)\frac{\rho_{\mathrm{g}}-\rho_\ell}{\rho_{\mathrm{g}}\rho_\ell}}. \tag{3.29}$$

For the liquid phase, we remark that the mass equation gives

$$\frac{\partial\alpha_\ell\rho_\ell}{\partial t}+\frac{\partial\alpha_\ell\rho_\ell v_\ell}{\partial x}=-\frac{\partial\alpha_{\mathrm{g}}\rho_{\mathrm{g}}}{\partial t}-\frac{\partial\alpha_{\mathrm{g}}\rho_{\mathrm{g}}v_{\mathrm{g}}}{\partial x}, \tag{3.30}$$

so that we have

$$\frac{\partial\alpha_\ell\rho_\ell}{\partial t}+\frac{\partial\alpha_\ell\rho_\ell v_\ell}{\partial x}=\mathcal{P}\frac{\partial p}{\partial x}+\mathcal{V}\left(\frac{\partial\alpha_{\mathrm{g}}v_{\mathrm{g}}}{\partial x}+\frac{\partial\alpha_\ell v_\ell}{\partial x}\right). \tag{3.31}$$

3.3. Regularising term. As with the six- and five-equation two-fluid models, we expect the present four-equation model not to be hyperbolic when the gas and liquid velocities are different from each other [13, 29]. The eigenvalues associated with the volume-fraction waves are expected to be complex. We choose to include a regularising term similar to the interfacial-pressure regularising term for the six-equation two-fluid model [4, 7, 8, 9, 23, 31]. It consists in applying a pressure difference Δp between the two phases. The momentum equations are transformed into

$$\frac{\partial \alpha_\mathrm{g}\rho_\mathrm{g}v_\mathrm{g}}{\partial t} + \frac{\partial \alpha_\mathrm{g}\rho_\mathrm{g}v_\mathrm{g}^2}{\partial x} + \alpha_\mathrm{g}\frac{\partial p}{\partial x} + \Delta p\frac{\partial \alpha_\mathrm{g}}{\partial x} = \frac{v_\mathrm{g}+v_\ell}{2}\left(\frac{\partial \alpha_\mathrm{g}\rho_\mathrm{g}}{\partial t} + \frac{\partial \alpha_\mathrm{g}\rho_\mathrm{g}v_\mathrm{g}}{\partial x}\right), \tag{3.32}$$

and

$$\frac{\partial \alpha_\ell\rho_\ell v_\ell}{\partial t} + \frac{\partial \alpha_\ell\rho_\ell v_\ell^2}{\partial x} + \alpha_\ell\frac{\partial p}{\partial x} + \Delta p\frac{\partial \alpha_\ell}{\partial x} = \frac{v_\mathrm{g}+v_\ell}{2}\left(\frac{\partial \alpha_\ell\rho_\ell}{\partial t} + \frac{\partial \alpha_\ell\rho_\ell v_\ell}{\partial x}\right), \tag{3.33}$$

while the mass and energy equations are not modified.

3.4. Expression of the model. As a result of the present section, the four-equation model (3.2)–(3.5) can be written, using (3.27), (3.31), (3.32) and (3.33), in the following form

$$\frac{\partial(\alpha_\mathrm{g}\rho_\mathrm{g} + \alpha_\ell\rho_\ell)}{\partial t} + \frac{\partial(\alpha_\mathrm{g}\rho_\mathrm{g}v_\mathrm{g} + \alpha_\ell\rho_\ell v_\ell)}{\partial x} = 0, \tag{3.34}$$

$$\begin{aligned}\frac{\partial \alpha_\mathrm{g}\rho_\mathrm{g}v_\mathrm{g}}{\partial t} + \frac{\partial \alpha_\mathrm{g}\rho_\mathrm{g}v_\mathrm{g}^2}{\partial x} + \left(\alpha_\mathrm{g} + \frac{v_\mathrm{g}+v_\ell}{2}\mathcal{P}\right)\frac{\partial p}{\partial x} \\ + \frac{v_\mathrm{g}+v_\ell}{2}\mathcal{V}\frac{\partial(\alpha_\mathrm{g}v_\mathrm{g} + \alpha_\ell v_\ell)}{\partial x} + \Delta p\frac{\partial \alpha_\mathrm{g}}{\partial x} = 0,\end{aligned} \tag{3.35}$$

$$\begin{aligned}\frac{\partial \alpha_\ell\rho_\ell v_\ell}{\partial t} + \frac{\partial \alpha_\ell\rho_\ell v_\ell^2}{\partial x} + \left(\alpha_\ell - \frac{v_\mathrm{g}+v_\ell}{2}\mathcal{P}\right)\frac{\partial p}{\partial x} \\ - \frac{v_\mathrm{g}+v_\ell}{2}\mathcal{V}\frac{\partial(\alpha_\mathrm{g}v_\mathrm{g} + \alpha_\ell v_\ell)}{\partial x} + \Delta p\frac{\partial \alpha_\ell}{\partial x} = 0,\end{aligned} \tag{3.36}$$

$$\frac{\partial(E_\mathrm{g} + E_\ell)}{\partial t} + \frac{\partial}{\partial x}((E_\mathrm{g} + \alpha_\mathrm{g}p)v_\mathrm{g} + (E_\ell + \alpha_\ell p)v_\ell) = 0. \tag{3.37}$$

4. Quasilinear form. We wish to write the model in quasilinear form

$$\frac{\partial \boldsymbol{U}}{\partial t} + \boldsymbol{A}(\boldsymbol{U})\frac{\partial \boldsymbol{U}}{\partial x} = 0, \tag{4.1}$$

where the vector of variables $\boldsymbol{U}$ is defined as

$$\boldsymbol{U} = \begin{pmatrix} \alpha_\mathrm{g}\rho_\mathrm{g} + \alpha_\ell\rho_\ell \\ \alpha_\mathrm{g}\rho_\mathrm{g}v_\mathrm{g} \\ \alpha_\ell\rho_\ell v_\ell \\ E_\mathrm{g} + E_\ell \end{pmatrix}. \tag{4.2}$$

The matrix $\boldsymbol{A}(\boldsymbol{U})$ is the Jacobian of the flux. The flux is split into a conservative and a non-conservative part, such that the system can be written as

$$\frac{\partial \boldsymbol{U}}{\partial t} + \frac{\partial \boldsymbol{F}_c(\boldsymbol{U})}{\partial x} + \boldsymbol{B}(\boldsymbol{U})\frac{\partial \boldsymbol{W}(\boldsymbol{U})}{\partial x} = 0, \tag{4.3}$$

where the conservative flux is

$$\boldsymbol{F}_c(\boldsymbol{U}) = \begin{pmatrix} \alpha_\mathrm{g}\rho_\mathrm{g}v_\mathrm{g} + \alpha_\ell\rho_\ell v_\ell \\ \alpha_\mathrm{g}\rho_\mathrm{g}v_\mathrm{g}^2 \\ \alpha_\ell\rho_\ell v_\ell^2 \\ (E_\mathrm{g} + \alpha_\mathrm{g}p)v_\mathrm{g} + (E_\ell + \alpha_\ell p)v_\ell \end{pmatrix}, \tag{4.4}$$

while the non-conservative contributions are

$$\boldsymbol{B}(\boldsymbol{U}) = \begin{pmatrix} 0 & 0 & 0 \\ \alpha_\mathrm{g} + \frac{v_\mathrm{g}+v_\ell}{2}\mathcal{P} & \frac{v_\mathrm{g}+v_\ell}{2}\mathcal{V} & \Delta p \\ \alpha_\ell - \frac{v_\mathrm{g}+v_\ell}{2}\mathcal{P} & -\frac{v_\mathrm{g}+v_\ell}{2}\mathcal{V} & -\Delta p \\ 0 & 0 & 0 \end{pmatrix} \quad \text{and} \quad \boldsymbol{W} = \begin{pmatrix} p \\ \alpha_\mathrm{g}v_\mathrm{g} + \alpha_\ell v_\ell \\ \alpha_\mathrm{g} \end{pmatrix}. \tag{4.5}$$

4.1. Some differentials. In order to write the Jacobian of the fluxes, we need to express the differentials of some variables in terms of the differential of the components of the variable vector $\boldsymbol{U}$. We will find them with the help of the fundamental relation of thermodynamics (2.14) as well as the differentials of the components of the vector $\boldsymbol{U}$. First, we will express all the differentials in terms of the differential of the gas density. Then, the other differentials will follow.

We recall from the previous section the differential (3.23)

$$\mathrm{d}e_\mathrm{g} = \frac{p}{\rho_\mathrm{g}^2 c_\mathrm{g}^2}\Psi_\mathrm{g}\,\mathrm{d}p + T\,\mathrm{d}s_\mathrm{g}. \tag{4.6}$$

By identification with the fundamental thermodynamic relation (2.14), we can deduce

$$\Psi_\mathrm{g}\,\mathrm{d}p = c_\mathrm{g}^2\,\mathrm{d}\rho_\mathrm{g}, \tag{4.7}$$

and using the relation between pressure and temperature differentials (3.12), we obtain

$$-\Psi_\mathrm{g}\frac{\rho_\mathrm{g}\rho_\ell L}{T(\rho_\mathrm{g} - \rho_\ell)}\,\mathrm{d}T = c_\mathrm{g}^2\,\mathrm{d}\rho_\mathrm{g}. \tag{4.8}$$

Now, we write the differential of the thermodynamic potentials for both phases in terms of their respective density differentials, using (4.7) and (4.8)

$$\mathrm{d}\mu_\mathrm{g} = \frac{1}{\rho_\mathrm{g}}\,\mathrm{d}p - s_\mathrm{g}\,\mathrm{d}T = \frac{1}{\rho_\mathrm{g}}\frac{c_\mathrm{g}^2}{\Psi_\mathrm{g}}\,\mathrm{d}\rho_\mathrm{g} + s_\mathrm{g}\frac{c_\mathrm{g}^2}{\Psi_\mathrm{g}}\frac{T(\rho_\mathrm{g} - \rho_\ell)}{\rho_\mathrm{g}\rho_\ell L}\,\mathrm{d}\rho_\mathrm{g} \tag{4.9}$$

$$\mathrm{d}\mu_\ell = \frac{1}{\rho_\ell}\,\mathrm{d}p - s_\ell\,\mathrm{d}T = \frac{1}{\rho_\ell}\frac{c_\ell^2}{\Psi_\ell}\,\mathrm{d}\rho_\ell + s_\ell\frac{c_\ell^2}{\Psi_\ell}\frac{T(\rho_\mathrm{g} - \rho_\ell)}{\rho_\mathrm{g}\rho_\ell L}\,\mathrm{d}\rho_\ell \tag{4.10}$$

and equate them, using the assumption of chemical equilibrium. Implicitly, we also use the mechanical and thermal equilibrium assumptions, since we have expressed the pressure and temperature differentials in terms of the gas as well as of the liquid phase variables. This gives a relation between the density differentials:

$$\frac{c_\mathrm{g}^2}{\Psi_\mathrm{g}}\,\mathrm{d}\rho_\mathrm{g} = \frac{c_\ell^2}{\Psi_\ell}\,\mathrm{d}\rho_\ell. \tag{4.11}$$

Next, we need a relation for the energy differentials. For the gas phase, we find it using the differential of $p(\rho_\mathrm{g}, e_\mathrm{g})$

$$\mathrm{d}p = \left(c_\mathrm{g}^2 - \Gamma_\mathrm{g}\frac{p}{\rho_\mathrm{g}}\right)\mathrm{d}\rho_\mathrm{g} + \Gamma_\mathrm{g}\rho_\mathrm{g}\,\mathrm{d}e_\mathrm{g}, \tag{4.12}$$

where $\mathrm{d}p$ is replaced using (3.22). After simplification, we obtain

$$\frac{\Psi_\mathrm{g}}{\left(\frac{p}{\rho_\mathrm{g}^2 c_\mathrm{g}^2}\Psi_\mathrm{g} - TC_{p,\mathrm{g}}\chi_\mathrm{g}\right)}\,\mathrm{d}e_\mathrm{g} = c_\mathrm{g}^2\,\mathrm{d}\rho_\mathrm{g}. \tag{4.13}$$

For the liquid phase, we first use the phase symmetry to obtain

$$\frac{\Psi_\ell}{\left(\frac{p}{\rho_\ell^2 c_\ell^2}\Psi_\ell - TC_{p,\ell}\chi_\ell\right)}\,\mathrm{d}e_\ell = c_\ell^2\,\mathrm{d}\rho_\ell, \tag{4.14}$$

and then replace the liquid density differential using (4.11)

$$\frac{1}{\left(\frac{p}{\rho_\ell^2 c_\ell^2}\Psi_\ell - TC_{p,\ell}\chi_\ell\right)}\,\mathrm{d}e_\ell = \frac{c_\mathrm{g}^2}{\Psi_\mathrm{g}}\,\mathrm{d}\rho_\mathrm{g}. \tag{4.15}$$

Further, we seek an expression for the differential of the volume fraction. From the differential of the first component of the vector $\boldsymbol{U}$, we have

$$\mathrm{d}u_1 = \alpha_\mathrm{g}\,\mathrm{d}\rho_\mathrm{g} + \alpha_\ell\,\mathrm{d}\rho_\ell + (\rho_\mathrm{g} - \rho_\ell)\,\mathrm{d}\alpha_\mathrm{g}, \tag{4.16}$$

where ρ_ℓ is eliminated using the differential (4.11)

$$(\rho_\mathrm{g} - \rho_\ell)\,\mathrm{d}\alpha_\mathrm{g} = \mathrm{d}u_1 - \left(\alpha_\mathrm{g} + \alpha_\ell\frac{c_\mathrm{g}^2\Psi_\ell}{c_\ell^2\Psi_\mathrm{g}}\right)\mathrm{d}\rho_\mathrm{g}. \tag{4.17}$$

Finally, we would like to find an expression for the velocity differentials. For the gas phase, we start from the differential of the second component of the vector $\boldsymbol{U}$

$$\mathrm{d}u_2 = \mathrm{d}(\alpha_\mathrm{g}\rho_\mathrm{g}v_\mathrm{g}) = \alpha_\mathrm{g}\rho_\mathrm{g}\,\mathrm{d}v_\mathrm{g} + \alpha_\mathrm{g}v_\mathrm{g}\,\mathrm{d}\rho_\mathrm{g} + \rho_\mathrm{g}v_\mathrm{g}\,\mathrm{d}\alpha_\mathrm{g}, \tag{4.18}$$

where $\mathrm{d}\alpha_\mathrm{g}$ is replaced using (4.17) to obtain

$$\alpha_\mathrm{g}\rho_\mathrm{g}\,\mathrm{d}v_\mathrm{g} = -\frac{\rho_\mathrm{g}v_\mathrm{g}}{\rho_\mathrm{g} - \rho_\ell}\,\mathrm{d}u_1 + \mathrm{d}u_2 + \frac{v_\mathrm{g}}{\rho_\mathrm{g} - \rho_\ell}\left(\alpha_\mathrm{g}\rho_\ell + \alpha_\ell\rho_\mathrm{g}\frac{c_\mathrm{g}^2\Psi_\ell}{c_\ell^2\Psi_\mathrm{g}}\right)\mathrm{d}\rho_\mathrm{g}. \tag{4.19}$$

By phase symmetry, we deduce that

$$\alpha_\ell\rho_\ell\,\mathrm{d}v_\ell = \frac{\rho_\ell v_\ell}{\rho_\mathrm{g} - \rho_\ell}\,\mathrm{d}u_1 + \mathrm{d}u_3 - \frac{v_\ell}{\rho_\mathrm{g} - \rho_\ell}\left(\alpha_\ell\rho_\mathrm{g} + \alpha_\mathrm{g}\rho_\ell\frac{c_\ell^2\Psi_\mathrm{g}}{c_\mathrm{g}^2\Psi_\ell}\right)\mathrm{d}\rho_\ell. \tag{4.20}$$

In order to express it in terms of the differential for the gas density, we use (4.11) to obtain

$$\alpha_\ell\rho_\ell\,\mathrm{d}v_\ell = \frac{\rho_\ell v_\ell}{\rho_\mathrm{g} - \rho_\ell}\,\mathrm{d}u_1 + \mathrm{d}u_3 - \frac{v_\ell}{\rho_\mathrm{g} - \rho_\ell}\left(\alpha_\mathrm{g}\rho_\ell + \alpha_\ell\rho_\mathrm{g}\frac{c_\mathrm{g}^2\Psi_\ell}{c_\ell^2\Psi_\mathrm{g}}\right)\mathrm{d}\rho_\mathrm{g}. \tag{4.21}$$

Now, using the differential of the mixture internal energy, we are able to deduce a differential for the gas density $\mathrm{d}\rho_\mathrm{g}$. We have that

$$\mathrm{d}(\alpha_\mathrm{g}\rho_\mathrm{g}e_\mathrm{g}) + \mathrm{d}(\alpha_\ell\rho_\ell e_\ell) = \mathrm{d}u_4 - \frac{v_\mathrm{g}}{2}\,\mathrm{d}u_2 - \frac{v_\ell}{2}\,\mathrm{d}u_3 - \frac{1}{2}\alpha_\mathrm{g}\rho_\mathrm{g}v_\mathrm{g}\,\mathrm{d}v_\mathrm{g} - \frac{1}{2}\alpha_\ell\rho_\ell v_\ell\,\mathrm{d}v_\ell. \tag{4.22}$$

After having replaced all the differentials using the expressions (4.11), (4.13), (4.15), (4.17), (4.19) and (4.21) previously derived, we obtain the density differential

$$\mathrm{d}\rho_\mathrm{g} = \frac{1}{\Phi}\frac{\Psi_\mathrm{g}}{c_\mathrm{g}^2}\left(\frac{\mathcal{E}}{\rho_\mathrm{g}-\rho_\ell}\,\mathrm{d}u_1 - v_\mathrm{g}\,\mathrm{d}u_2 - v_\ell\,\mathrm{d}u_3 + \mathrm{d}u_4\right) \tag{4.23}$$

where we have used the following shorthands to simplify the expressions

$$\begin{aligned}\Phi = \alpha_\mathrm{g}\frac{p}{\rho_\mathrm{g}c_\mathrm{g}^2}\Psi_\mathrm{g} + \alpha_\ell\frac{p}{\rho_\ell c_\ell^2}\Psi_\ell - (\alpha_\mathrm{g}\rho_\mathrm{g}TC_{p,\mathrm{g}}\chi_\mathrm{g} + \alpha_\ell\rho_\ell TC_{p,\ell}\chi_\ell)\\ + \frac{1}{\rho_\mathrm{g}-\rho_\ell}\left(-e_\mathrm{g} + \frac{1}{2}v_\mathrm{g}^2 + e_\ell - \frac{1}{2}v_\ell^2\right)\left(\alpha_\mathrm{g}\rho_\ell\frac{\Psi_\mathrm{g}}{c_\mathrm{g}^2} + \alpha_\ell\rho_\mathrm{g}\frac{\Psi_\ell}{c_\ell^2}\right)\end{aligned} \tag{4.24}$$

and

$$\mathcal{E} = -\rho_\mathrm{g}\left(e_\mathrm{g} - \frac{1}{2}v_\mathrm{g}^2\right) + \rho_\ell\left(e_\ell - \frac{1}{2}v_\ell^2\right). \tag{4.25}$$

All the other differentials now follow. The differential of the volume fraction follows from (4.17) in which $\mathrm{d}\rho_\mathrm{g}$ is replaced using (4.23)

$$\begin{aligned}\mathrm{d}\alpha_\mathrm{g} = \frac{1}{\rho_\mathrm{g}-\rho_\ell}\,\mathrm{d}u_1\\ - \frac{1}{\rho_\mathrm{g}-\rho_\ell}\frac{1}{\Phi}\left(\alpha_\mathrm{g}\frac{\Psi_\mathrm{g}}{c_\mathrm{g}^2} + \alpha_\ell\frac{\Psi_\ell}{c_\ell^2}\right)\left(\frac{\mathcal{E}}{\rho_\mathrm{g}-\rho_\ell}\,\mathrm{d}u_1 - v_\mathrm{g}\,\mathrm{d}u_2 - v_\ell\,\mathrm{d}u_3 + \mathrm{d}u_4\right).\end{aligned} \tag{4.26}$$

The differential of the pressure follows from (4.7)

$$\mathrm{d}p = \frac{1}{\Phi}\left(\frac{\mathcal{E}}{\rho_\mathrm{g}-\rho_\ell}\,\mathrm{d}u_1 - v_\mathrm{g}\,\mathrm{d}u_2 - v_\ell\,\mathrm{d}u_3 + \mathrm{d}u_4\right). \tag{4.27}$$

The differential of the liquid density follows from (4.11)

$$\mathrm{d}\rho_\ell = \frac{1}{\Phi}\frac{\Psi_\ell}{c_\ell^2}\left(\frac{\mathcal{E}}{\rho_\mathrm{g}-\rho_\ell}\,\mathrm{d}u_1 - v_\mathrm{g}\,\mathrm{d}u_2 - v_\ell\,\mathrm{d}u_3 + \mathrm{d}u_4\right). \tag{4.28}$$

The differentials of the internal energies follow from (4.13) and (4.15)

$$\mathrm{d}e_\mathrm{g} = \frac{1}{\Phi}\left(\frac{p}{\rho_\mathrm{g}^2c_\mathrm{g}^2}\Psi_\mathrm{g} - TC_{p,\mathrm{g}}\chi_\mathrm{g}\right)\left(\frac{\mathcal{E}}{\rho_\mathrm{g}-\rho_\ell}\,\mathrm{d}u_1 - v_\mathrm{g}\,\mathrm{d}u_2 - v_\ell\,\mathrm{d}u_3 + \mathrm{d}u_4\right), \tag{4.29}$$

$$\mathrm{d}e_\ell = \frac{1}{\Phi}\left(\frac{p}{\rho_\ell^2c_\ell^2}\Psi_\ell - TC_{p,\ell}\chi_\ell\right)\left(\frac{\mathcal{E}}{\rho_\mathrm{g}-\rho_\ell}\,\mathrm{d}u_1 - v_\mathrm{g}\,\mathrm{d}u_2 - v_\ell\,\mathrm{d}u_3 + \mathrm{d}u_4\right). \tag{4.30}$$

The differentials of the velocities follow from (4.19) and (4.21)

$$\begin{aligned}\alpha_\mathrm{g}\rho_\mathrm{g}\,\mathrm{d}v_\mathrm{g} = -\frac{\rho_\mathrm{g}v_\mathrm{g}}{\rho_\mathrm{g}-\rho_\ell}\,\mathrm{d}u_1 + \mathrm{d}u_2 + \frac{1}{\Phi}\frac{v_\mathrm{g}}{\rho_\mathrm{g}-\rho_\ell}\\ \cdot\left(\alpha_\mathrm{g}\rho_\ell\frac{\Psi_\mathrm{g}}{c_\mathrm{g}^2} + \alpha_\ell\rho_\mathrm{g}\frac{\Psi_\ell}{c_\ell^2}\right)\left(\frac{\mathcal{E}}{\rho_\mathrm{g}-\rho_\ell}\,\mathrm{d}u_1 - v_\mathrm{g}\,\mathrm{d}u_2 - v_\ell\,\mathrm{d}u_3 + \mathrm{d}u_4\right),\end{aligned} \tag{4.31}$$

$$\begin{aligned}\alpha_\ell\rho_\ell\,\mathrm{d}v_\ell = \frac{\rho_\ell v_\ell}{\rho_\mathrm{g}-\rho_\ell}\,\mathrm{d}u_1 + \mathrm{d}u_3 - \frac{1}{\Phi}\frac{v_\ell}{\rho_\mathrm{g}-\rho_\ell}\\ \cdot\left(\alpha_\mathrm{g}\rho_\ell\frac{\Psi_\mathrm{g}}{c_\mathrm{g}^2} + \alpha_\ell\rho_\mathrm{g}\frac{\Psi_\ell}{c_\ell^2}\right)\left(\frac{\mathcal{E}}{\rho_\mathrm{g}-\rho_\ell}\,\mathrm{d}u_1 - v_\mathrm{g}\,\mathrm{d}u_2 - v_\ell\,\mathrm{d}u_3 + \mathrm{d}u_4\right).\end{aligned} \tag{4.32}$$

4.2. Jacobian of the fluxes. We are now able to derive the Jacobian of the conservative fluxes $\boldsymbol{F}_c(\boldsymbol{U})$ (4.4) and of the vector $\boldsymbol{W}(\boldsymbol{U})$ in the non-conservative fluxes (4.5). To do so, we express the differentials of the components of the vectors $\boldsymbol{F}_c(\boldsymbol{U})$ and $\boldsymbol{W}(\boldsymbol{U})$ in terms of the differentials of the components of $\boldsymbol{U}$. First, we simply have

$$\mathrm{d}f_1 = \mathrm{d}(\alpha_\mathrm{g}\rho_\mathrm{g}v_\mathrm{g} + \alpha_\ell\rho_\ell v_\ell) = \mathrm{d}u_2 + \mathrm{d}u_3. \tag{4.33}$$

Then for the second component

$$\mathrm{d}f_2 = \mathrm{d}(\alpha_\mathrm{g}\rho_\mathrm{g}v_\mathrm{g}^2) = v_\mathrm{g}\,\mathrm{d}(\alpha_\mathrm{g}\rho_\mathrm{g}v_\mathrm{g}) + \alpha_\mathrm{g}\rho_\mathrm{g}v_\mathrm{g}\,\mathrm{d}v_\mathrm{g} = v_\mathrm{g}\,\mathrm{d}u_2 + \alpha_\mathrm{g}\rho_\mathrm{g}v_\mathrm{g}\,\mathrm{d}v_\mathrm{g}, \tag{4.34}$$

where $\mathrm{d}v_\mathrm{g}$ is substituted using (4.31)

$$\begin{aligned}\mathrm{d}f_2 = &-\frac{\rho_\mathrm{g}v_\mathrm{g}^2}{\rho_\mathrm{g}-\rho_\ell}\,\mathrm{d}u_1 + 2v_\mathrm{g}\,\mathrm{d}u_2 + \frac{1}{\Phi}\frac{v_\mathrm{g}^2}{\rho_\mathrm{g}-\rho_\ell}\\ &\cdot\left(\alpha_\mathrm{g}\rho_\ell\frac{\Psi_\mathrm{g}}{c_\mathrm{g}^2} + \alpha_\ell\rho_\mathrm{g}\frac{\Psi_\ell}{c_\ell^2}\right)\left(\frac{\mathcal{E}}{\rho_\mathrm{g}-\rho_\ell}\,\mathrm{d}u_1 - v_\mathrm{g}\,\mathrm{d}u_2 - v_\ell\,\mathrm{d}u_3 + \mathrm{d}u_4\right).\end{aligned} \tag{4.35}$$

Similarly, for the third component

$$\mathrm{d}f_3 = v_\ell\,\mathrm{d}u_3 + \alpha_\ell\rho_\ell v_\ell\,\mathrm{d}v_\ell, \tag{4.36}$$

where $\mathrm{d}v_\ell$ is substituted using (4.32)

$$\begin{aligned}\mathrm{d}f_3 = &\frac{\rho_\ell v_\ell^2}{\rho_\mathrm{g}-\rho_\ell}\,\mathrm{d}u_1 + 2v_\ell\,\mathrm{d}u_3 - \frac{1}{\Phi}\frac{v_\ell^2}{\rho_\mathrm{g}-\rho_\ell}\\ &\cdot\left(\alpha_\mathrm{g}\rho_\ell\frac{\Psi_\mathrm{g}}{c_\mathrm{g}^2} + \alpha_\ell\rho_\mathrm{g}\frac{\Psi_\ell}{c_\ell^2}\right)\left(\frac{\mathcal{E}}{\rho_\mathrm{g}-\rho_\ell}\,\mathrm{d}u_1 - v_\mathrm{g}\,\mathrm{d}u_2 - v_\ell\,\mathrm{d}u_3 + \mathrm{d}u_4\right).\end{aligned} \tag{4.37}$$

Finally, the fourth component can be written as

$$\begin{aligned}\mathrm{d}f_4 = &\frac{1}{2}v_\mathrm{g}^2\,\mathrm{d}u_2 + \frac{1}{2}v_\ell^2\,\mathrm{d}u_3 + (\rho_\mathrm{g}e_\mathrm{g}v_\mathrm{g} + v_\mathrm{g}p - \rho_\ell e_\ell v_\ell - v_\ell p)\,\mathrm{d}\alpha_\mathrm{g}\\ &+ (\alpha_\mathrm{g}v_\mathrm{g} + \alpha_\ell v_\ell)\,\mathrm{d}p + \alpha_\mathrm{g}e_\mathrm{g}v_\mathrm{g}\,\mathrm{d}\rho_\mathrm{g} + \alpha_\ell e_\ell v_\ell\,\mathrm{d}\rho_\ell + \alpha_\mathrm{g}\rho_\mathrm{g}v_\mathrm{g}\,\mathrm{d}e_\mathrm{g} + \alpha_\ell\rho_\ell v_\ell\,\mathrm{d}e_\ell\\ &+ \left(\alpha_\mathrm{g}\rho_\mathrm{g}\left(e_\mathrm{g} + v_\mathrm{g}^2\right) + \alpha_\mathrm{g}p\right)\mathrm{d}v_\mathrm{g} + \left(\alpha_\ell\rho_\ell\left(e_\ell + v_\ell^2\right) + \alpha_\ell p\right)\mathrm{d}v_\ell,\end{aligned} \tag{4.38}$$

which after replacement of the differentials and simplification becomes

$$\begin{aligned}\mathrm{d}f_4 = &\frac{-\rho_\mathrm{g}v_\mathrm{g}^3 + \rho_\ell v_\ell^3}{\rho_\mathrm{g}-\rho_\ell}\,\mathrm{d}u_1 + \left(e_\mathrm{g} + \frac{3}{2}v_\mathrm{g}^2 + \frac{p}{\rho_\mathrm{g}}\right)\mathrm{d}u_2 + \left(e_\ell + \frac{3}{2}v_\ell^2 + \frac{p}{\rho_\ell}\right)\mathrm{d}u_3\\ &+\frac{1}{\Phi}\left[\frac{v_\mathrm{g}^3 - v_\ell^3}{\rho_\mathrm{g}-\rho_\ell}\left(\alpha_\mathrm{g}\rho_\ell\frac{\Psi_\mathrm{g}}{c_\mathrm{g}^2} + \alpha_\ell\rho_\mathrm{g}\frac{\Psi_\ell}{c_\ell^2}\right) + \alpha_\mathrm{g}v_\mathrm{g} + \alpha_\ell v_\ell - T(\alpha_\mathrm{g}\rho_\mathrm{g}v_\mathrm{g}C_{p,\mathrm{g}}\chi_\mathrm{g} + \alpha_\ell\rho_\ell v_\ell C_{p,\ell}\chi_\ell)\right]\\ &\cdot\left(\frac{\mathcal{E}}{\rho_\mathrm{g}-\rho_\ell}\,\mathrm{d}u_1 - v_\mathrm{g}\,\mathrm{d}u_2 - v_\ell\,\mathrm{d}u_3 + \mathrm{d}u_4\right).\end{aligned} \tag{4.39}$$

Similarly, for the non-conservative part of the fluxes, we need to derive a Jacobian matrix for the vector $\boldsymbol{W}$. First, we can remark that

$$\mathrm{d}w_1 = \mathrm{d}p, \tag{4.40}$$

which gives after substitution of the differentials

$$\mathrm{d}w_1 = \frac{1}{\Phi}\left(\frac{\mathcal{E}}{\rho_\mathrm{g}-\rho_\ell}\,\mathrm{d}u_1 - v_\mathrm{g}\,\mathrm{d}u_2 - v_\ell\,\mathrm{d}u_3 + \mathrm{d}u_4\right). \tag{4.41}$$

For the second component, we have that

$$\mathrm{d}w_2 = \mathrm{d}(\alpha_\mathrm{g}v_\mathrm{g} + \alpha_\ell v_\ell) = \frac{1}{\rho_\mathrm{g}}(\mathrm{d}u_2 - \alpha_\mathrm{g}v_\mathrm{g}\,\mathrm{d}\rho_\mathrm{g}) + \frac{1}{\rho_\ell}(\mathrm{d}u_3 - \alpha_\ell v_\ell\,\mathrm{d}\rho_\ell), \tag{4.42}$$

which gives

$$\begin{aligned}\mathrm{d}w_2 = \frac{1}{\rho_\mathrm{g}}\,\mathrm{d}u_2 + \frac{1}{\rho_\ell}\,\mathrm{d}u_3 - \frac{1}{\Phi}&\left(\alpha_\mathrm{g}v_\mathrm{g}\frac{\Psi_\mathrm{g}}{\rho_\mathrm{g}c_\mathrm{g}^2} + \alpha_\ell v_\ell\frac{\Psi_\ell}{\rho_\ell c_\ell^2}\right)\\ &\cdot\left(\frac{\mathcal{E}}{\rho_\mathrm{g}-\rho_\ell}\,\mathrm{d}u_1 - v_\mathrm{g}\,\mathrm{d}u_2 - v_\ell\,\mathrm{d}u_3 + \mathrm{d}u_4\right).\end{aligned} \tag{4.43}$$

Finally, the third component is the volume fraction differential (4.26)

$$\mathrm{d}w_3 = \mathrm{d}\alpha_\mathrm{g}, \tag{4.44}$$

thus

$$\begin{aligned}\mathrm{d}w_3 = \frac{1}{\rho_\mathrm{g}-\rho_\ell}\,\mathrm{d}u_1 - \frac{1}{\rho_\mathrm{g}-\rho_\ell}\frac{1}{\Phi}&\left(\alpha_\mathrm{g}\frac{\Psi_\mathrm{g}}{c_\mathrm{g}^2} + \alpha_\ell\frac{\Psi_\ell}{c_\ell^2}\right)\\ &\cdot\left(\frac{\mathcal{E}}{\rho_\mathrm{g}-\rho_\ell}\,\mathrm{d}u_1 - v_\mathrm{g}\,\mathrm{d}u_2 - v_\ell\,\mathrm{d}u_3 + \mathrm{d}u_4\right).\end{aligned} \tag{4.45}$$

4.3. The matrices in the quasilinear form. We can now write the matrix $\boldsymbol{A}(\boldsymbol{U})$ appearing in the quasilinear form (4.1). According to the flux-splitting strategy, the matrix is split in a conservative part and a non-conservative part. With the help of (4.33), (4.35), (4.37) and (4.39), the conservative part is written as

$$\begin{aligned}\boldsymbol{A}_c(\boldsymbol{U}) &= \frac{\partial \boldsymbol{F}_c(\boldsymbol{U})}{\partial \boldsymbol{U}}\\ &= \begin{pmatrix} 0 & 1 & 1 & 0\\ -\frac{\rho_\mathrm{g}v_\mathrm{g}^2}{\rho_\mathrm{g}-\rho_\ell} + \frac{v_\mathrm{g}^2\mathcal{E}}{\rho_\mathrm{g}-\rho_\ell}\Sigma_\rho & 2v_\mathrm{g} - v_\mathrm{g}^3\Sigma_\rho & -v_\mathrm{g}^2v_\ell\Sigma_\rho & v_\mathrm{g}^2\Sigma_\rho\\ \frac{\rho_\ell v_\ell^2}{\rho_\mathrm{g}-\rho_\ell} - \frac{v_\ell^2\mathcal{E}}{\rho_\mathrm{g}-\rho_\ell}\Sigma_\rho & v_\mathrm{g}v_\ell^2\Sigma_\rho & 2v_\ell + v_\ell^3\Sigma_\rho & -v_\ell^2\Sigma_\rho\\ a_{41} & a_{42} & a_{43} & (v_\mathrm{g}^3 - v_\ell^3)\Sigma_\rho + \Omega \end{pmatrix}\end{aligned} \tag{4.46}$$

where

$$a_{41} = \frac{-\rho_\mathrm{g}v_\mathrm{g}^3 + \rho_\ell v_\ell^3}{\rho_\mathrm{g}-\rho_\ell} + \left((v_\mathrm{g}^3 - v_\ell^3)\Sigma_\rho + \Omega\right)\frac{\mathcal{E}}{\rho_\mathrm{g}-\rho_\ell}, \tag{4.47}$$

$$a_{42} = \left(e_\mathrm{g} + \frac{3}{2}v_\mathrm{g}^2 + \frac{p}{\rho_\mathrm{g}}\right) - \left((v_\mathrm{g}^3 - v_\ell^3)\Sigma_\rho + \Omega\right)v_\mathrm{g}, \tag{4.48}$$

$$a_{43} = \left(e_\ell + \frac{3}{2}v_\ell^2 + \frac{p}{\rho_\ell}\right) - \left((v_\mathrm{g}^3 - v_\ell^3)\Sigma_\rho + \Omega\right)v_\ell. \tag{4.49}$$

We have also introduced the shorthands

$$\Sigma_\rho = \frac{1}{\Phi}\frac{1}{(\rho_\mathrm{g}-\rho_\ell)}\left(\alpha_\mathrm{g}\rho_\ell\frac{\Psi_\mathrm{g}}{c_\mathrm{g}^2} + \alpha_\ell\rho_\mathrm{g}\frac{\Psi_\ell}{c_\ell^2}\right) \tag{4.50}$$

and

$$\Omega = \frac{1}{\Phi}\left(\alpha_{\mathrm{g}} v_{\mathrm{g}} + \alpha_\ell v_\ell - \alpha_{\mathrm{g}}\rho_{\mathrm{g}} v_{\mathrm{g}} T C_{p,\mathrm{g}} \chi_{\mathrm{g}} - \alpha_\ell \rho_\ell v_\ell T C_{p,\ell}\chi_\ell\right). \tag{4.51}$$

For the non-conservative part, we can express the Jacobian of the vector $\boldsymbol{W}(\boldsymbol{U})$ using (4.41), (4.43) and (4.45)

$$\boldsymbol{M}(\boldsymbol{U}) = \frac{\partial \boldsymbol{W}(\boldsymbol{U})}{\partial \boldsymbol{U}} = \begin{pmatrix} \frac{1}{\Phi}\frac{\mathcal{E}}{\rho_{\mathrm{g}}-\rho_\ell} & -\frac{v_{\mathrm{g}}}{\Phi} & -\frac{v_\ell}{\Phi} & \frac{1}{\Phi} \\ -\frac{\mathcal{E}}{\rho_{\mathrm{g}}-\rho_\ell}\Sigma_v & \frac{1}{\rho_{\mathrm{g}}} + v_{\mathrm{g}}\Sigma_v & \frac{1}{\rho_\ell} + v_\ell \Sigma_v & -\Sigma_v \\ \frac{1}{\rho_{\mathrm{g}}-\rho_\ell} - \frac{\mathcal{E}}{\rho_{\mathrm{g}}-\rho_\ell}\Sigma & v_{\mathrm{g}}\Sigma & v_\ell \Sigma & -\Sigma \end{pmatrix} \tag{4.52}$$

where

$$\Sigma = \frac{1}{\Phi}\frac{1}{\rho_{\mathrm{g}}-\rho_\ell}\left(\alpha_{\mathrm{g}}\frac{\Psi_{\mathrm{g}}}{c_{\mathrm{g}}^2} + \alpha_\ell \frac{\Psi_\ell}{c_\ell^2}\right), \tag{4.53}$$

$$\Sigma_v = \frac{1}{\Phi}\left(\alpha_{\mathrm{g}} v_{\mathrm{g}}\frac{\Psi_{\mathrm{g}}}{\rho_{\mathrm{g}} c_{\mathrm{g}}^2} + \alpha_\ell v_\ell \frac{\Psi_\ell}{\rho_\ell c_\ell^2}\right). \tag{4.54}$$

The Jacobian of the non-conservative fluxes then follows from

$$\boldsymbol{A}_p(\boldsymbol{U}) = \boldsymbol{B}(\boldsymbol{U}) \cdot \boldsymbol{M}(\boldsymbol{U}). \tag{4.55}$$

The Jacobian of the whole system is then

$$\boldsymbol{A}(\boldsymbol{U}) = \boldsymbol{A}_c(\boldsymbol{U}) + \boldsymbol{A}_p(\boldsymbol{U}). \tag{4.56}$$

5. Subcharacteristic condition. The subcharacteristic condition is a stability condition which states that the stiff limit of a relaxation model – called the equilibrium model – can only be stable if the wave speeds of the equilibrium system do not exceed the speeds of the corresponding waves of its relaxation system [6, 12, 16, 22]. We expect the two-fluid models mentioned in the present paper to respect this condition since the underlying physical models describe a stable reality. Figure 5.1 presents the model hierarchy, where TF and DF, respectively, denote the two-fluid and the drift-flux models, and the index, the number of conservation equations in the model. Each arrow designates the relaxation performed from one model to the next. The subcharacteristic condition has been proved for some of the relaxation processes in [10] and [12]. In the present section, we prove the subcharacteristic condition for the remaining relaxation processes $\mathrm{TF}_5 \to \mathrm{TF}_4$ and $\mathrm{TF}_4 \to \mathrm{DF}_3$.

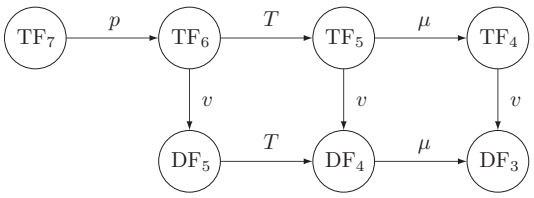

FIG. 5.1. *Hierarchy of the two-phase flow models. TF: two-phase model. DF: drift-flux model. Index: Number of conservation equations.*

5.1. Speed of sound. The eigenvalues of the Jacobian of the fluxes $\boldsymbol{A}(\boldsymbol{U})$ are the propagation velocities of the quantities defined by the eigenvectors of $\boldsymbol{A}(\boldsymbol{U})$, also called waves. In the present model, these waves are the volume-fraction waves and the pressure waves. When $v_\mathrm{g} = 0$ and $v_\ell = 0$, the matrix $\boldsymbol{A}(\boldsymbol{U})$ becomes

$$\boldsymbol{A}(\boldsymbol{U}(v_\mathrm{g}=0, v_\ell=0)) = \begin{pmatrix} 0 & 1 & 1 & 0 \\ \frac{\alpha_\mathrm{g}(\rho_\mathrm{g}e_\mathrm{g}-\rho_\ell e_\ell)c^2_{\mathrm{TF4}}}{(\alpha_\ell\rho_\mathrm{g}+\alpha_\mathrm{g}\rho_\ell)T(s_\mathrm{g}-s_\ell)} & 0 & 0 & -\frac{\alpha_\mathrm{g}(\rho_\mathrm{g}-\rho_\ell)c^2_{\mathrm{TF4}}}{(\alpha_\ell\rho_\mathrm{g}+\alpha_\mathrm{g}\rho_\ell)T(s_\mathrm{g}-s_\ell)} \\ \frac{\alpha_\ell(\rho_\mathrm{g}e_\mathrm{g}-\rho_\ell e_\ell)c^2_{\mathrm{TF4}}}{(\alpha_\ell\rho_\mathrm{g}+\alpha_\mathrm{g}\rho_\ell)T(s_\mathrm{g}-s_\ell)} & 0 & 0 & -\frac{\alpha_\ell(\rho_\mathrm{g}-\rho_\ell)c^2_{\mathrm{TF4}}}{(\alpha_\ell\rho_\mathrm{g}+\alpha_\mathrm{g}\rho_\ell)T(s_\mathrm{g}-s_\ell)} \\ 0 & e_\mathrm{g}+\frac{p}{\rho_\mathrm{g}} & e_\ell+\frac{p}{\rho_\ell} & 0 \end{pmatrix}, \quad (5.1)$$

where

$$c_{\mathrm{TF4}} = \sqrt{\frac{\alpha_\ell\rho_\mathrm{g}+\alpha_\mathrm{g}\rho_\ell}{\rho_\mathrm{g}\rho_\ell\left(\frac{\alpha_\mathrm{g}}{\rho_\mathrm{g}c^2_\mathrm{g}}\Psi_\mathrm{g}+\frac{\alpha_\ell}{\rho_\ell c^2_\ell}\Psi_\ell+T(\alpha_\mathrm{g}\rho_\mathrm{g}C_{p,\mathrm{g}}\chi_\mathrm{g}+\alpha_\ell\rho_\ell C_{p,\ell}\chi_\ell)\frac{\rho_\mathrm{g}-\rho_\ell}{\rho_\mathrm{g}\rho_\ell L}\right)}}. \quad (5.2)$$

Its eigenvalues are then $0, 0, c_{\mathrm{TF4}}$ and $-c_{\mathrm{TF4}}$. The waves with zero velocity are the volume-fraction waves, while the two other are the pressure waves. We deduce that c_{TF4} is the speed of sound of the model. This speed of sound is dependent on the thermodynamical assumptions, here that the phases are at all times at equilibrium. The expression (5.2) uses the variable blocks that are involved in the Jacobian matrices. We can also reorganise it to a more compact form

$$c_{\mathrm{TF4}} = \sqrt{\frac{\alpha_\ell\rho_\mathrm{g}+\alpha_\mathrm{g}\rho_\ell}{\rho_\mathrm{g}\rho_\ell\left(\frac{\alpha_\mathrm{g}}{\rho_\mathrm{g}c^2_\mathrm{g}}+\frac{\alpha_\ell}{\rho_\ell c^2_\ell}+T(\alpha_\mathrm{g}\rho_\mathrm{g}C_{p,\mathrm{g}}\chi^2_\mathrm{g}+\alpha_\ell\rho_\ell C_{p,\ell}\chi^2_\ell)\right)}}. \quad (5.3)$$

Note that the speed of sound can be used to simplify (3.28) and (3.29)

$$\mathcal{V} = \frac{\rho_\mathrm{g}\rho_\ell}{\alpha_\ell\rho_\mathrm{g}+\alpha_\mathrm{g}\rho_\ell}\frac{T}{L}(\alpha_\mathrm{g}\rho_\mathrm{g}C_{p,\mathrm{g}}\chi_\mathrm{g}+\alpha_\ell\rho_\ell C_{p,\ell}\chi_\ell)c^2_{\mathrm{TF4}}, \quad (5.4)$$

$$\mathcal{P} = \frac{\alpha_\mathrm{g}\alpha_\ell\rho_\mathrm{g}\rho_\ell(v_\mathrm{g}-v_\ell)}{\alpha_\ell\rho_\mathrm{g}+\alpha_\mathrm{g}\rho_\ell}\frac{T}{L}\left(\rho_\ell C_{p,\ell}\chi_\ell\frac{\Psi_\mathrm{g}}{\rho_\mathrm{g}c^2_\mathrm{g}}-\rho_\mathrm{g}C_{p,\mathrm{g}}\chi_\mathrm{g}\frac{\Psi_\ell}{\rho_\ell c^2_\ell}\right)c^2_{\mathrm{TF4}}. \quad (5.5)$$

5.2. Eigenvalues for the equal velocity limit. The eigenstructure for the general case is not accessible. However, when $v_\mathrm{g} = v_\ell$, we are able to find the eigenvalues of the system. For this, we write the characteristic polynomial of the matrix $\boldsymbol{A}(\boldsymbol{U})$ where the velocities have been substituted with $v_\mathrm{g} = v_\mathrm{m}$ and $v_\ell = v_\mathrm{m}$

$$\Pi_{A,v_\mathrm{g}=v_\ell} = \mathrm{Det}(\boldsymbol{A}(\boldsymbol{U}_{v_\mathrm{g}=v_\ell}) - \lambda\cdot\boldsymbol{I}_4), \quad (5.6)$$

where $\boldsymbol{I}_4$ is the identity matrix of rank 4. This polynomial can be simplified to

$$\Pi_{A,v_\mathrm{g}=v_\ell} = (\lambda - v_\mathrm{m})^2\cdot(\lambda-(v_\mathrm{m}+c_{\mathrm{TF4}}))\cdot(\lambda-(v_\mathrm{m}-c_{\mathrm{TF4}})). \quad (5.7)$$

Thus, the resulting eigenvalues are

$$\boldsymbol{\Lambda}_{\mathrm{TF4}} = \begin{pmatrix} v_\mathrm{m}-c_{\mathrm{TF4}} \\ v_\mathrm{m} \\ v_\mathrm{m} \\ v_\mathrm{m}+c_{\mathrm{TF4}} \end{pmatrix}. \quad (5.8)$$

5.3. Speed of sound in other models. The speed of sound of the five-equation model is given in [10]. In order to express it in terms of the parameters used in the present article, we first derive a relation. In [10], the parameter

$$\zeta = \left(\frac{\partial T}{\partial p}\right)_s = -\frac{1}{\rho^2}\left(\frac{\partial \rho}{\partial s}\right)_p \tag{5.9}$$

is used. The triple product rule gives

$$\zeta = \frac{1}{\rho^2}\left(\frac{\partial p}{\partial s}\right)_\rho \Bigg/ \left(\frac{\partial p}{\partial \rho}\right)_s, \tag{5.10}$$

where

$$\left(\frac{\partial p}{\partial \rho}\right)_s = c^2, \tag{5.11}$$

and, from [20],

$$\left(\frac{\partial p}{\partial s}\right)_\rho = \Gamma \rho T. \tag{5.12}$$

Thus

$$\zeta = \frac{\Gamma T}{\rho c^2}. \tag{5.13}$$

The speed of sound in the five-equation model, taken from [10] and simplified, is

$$c_{\mathrm{TF5}} = \sqrt{\frac{\alpha_{\mathrm{g}}\rho_\ell + \alpha_\ell \rho_{\mathrm{g}}}{\rho_{\mathrm{g}}\rho_\ell\left(\frac{\alpha_{\mathrm{g}}}{\rho_{\mathrm{g}}c_{\mathrm{g}}^2} + \frac{\alpha_\ell}{\rho_\ell c_\ell^2} + \frac{\alpha_{\mathrm{g}}\rho_{\mathrm{g}}C_{p,\mathrm{g}}\alpha_\ell\rho_\ell C_{p,\ell}T\left(\frac{\Gamma_{\mathrm{g}}}{\rho_{\mathrm{g}}c_{\mathrm{g}}^2} - \frac{\Gamma_\ell}{\rho_\ell c_\ell^2}\right)^2}{\alpha_{\mathrm{g}}\rho_{\mathrm{g}}C_{p,\mathrm{g}} + \alpha_\ell\rho_\ell C_{p,\ell}}\right)}}. \tag{5.14}$$

We also know from [12] the speed of sound in the drift-flux three-equation model. This model can be seen as the limit of the drift-flux four-equation model with instantaneous phase relaxation, or as the limit of the two-fluid four-equation model (3.34)–(3.37) with instantaneous velocity relaxation. This is obtained by summing equations (3.35) and (3.36) and assuming $v_{\mathrm{g}} = v_\ell$. After simplification, the speed of sound can be written

$$c_{\mathrm{DF3}} = \frac{1}{\sqrt{(\alpha_{\mathrm{g}}\rho_{\mathrm{g}} + \alpha_\ell\rho_\ell)\left(\frac{\alpha_{\mathrm{g}}}{\rho_{\mathrm{g}}c_{\mathrm{g}}^2} + \frac{\alpha_\ell}{\rho_\ell c_\ell^2} + T(\alpha_{\mathrm{g}}\rho_{\mathrm{g}}C_{p,\mathrm{g}}\chi_{\mathrm{g}}^2 + \alpha_\ell\rho_\ell C_{p,\ell}\chi_\ell^2)\right)}}. \tag{5.15}$$

5.4. Comparison of the speeds of sound. In [10], the authors compared the speeds of sound of four of the two-phase flow models in Figure 5.1 – the TF_6, TF_5, DF_5 and DF_4 models. They showed that the effect of the instantaneous relaxation of a given type on the mixture speed of sound is independent of the order in which relaxations are performed. For example, the effect of relaxing the velocity multiplies the speed of sound by a constant factor

$$\frac{c_{\mathrm{TF5}}}{c_{\mathrm{DF4}}} = \frac{c_{\mathrm{TF6}}}{c_{\mathrm{DF5}}} = \sqrt{(\alpha_{\mathrm{g}}\rho_{\mathrm{g}} + \alpha_\ell\rho_\ell)\left(\frac{\alpha_{\mathrm{g}}}{\rho_{\mathrm{g}}} + \frac{\alpha_\ell}{\rho_\ell}\right)}, \tag{5.16}$$

By rearranging the expression above, they also arrive at

$$\frac{c_{\mathrm{DF5}}}{c_{\mathrm{DF4}}} = \frac{c_{\mathrm{TF6}}}{c_{\mathrm{TF5}}}, \tag{5.17}$$

which shows that the same conclusion applies to the effect of thermal relaxation.

Now, in the present work, we derived TF_4 from the TF_5 model previously mentioned by performing instantaneous phase relaxation, and found its sound speed (5.3). By comparing it to the speed of sound in the DF_3 (5.15), we immediately see that we can extend the ratio relation (5.16) with

$$\frac{c_{\mathrm{TF4}}}{c_{\mathrm{DF3}}} = \frac{c_{\mathrm{TF5}}}{c_{\mathrm{DF4}}} = \frac{c_{\mathrm{TF6}}}{c_{\mathrm{DF5}}}, \tag{5.18}$$

which shows that the velocity relaxation once more has an independent effect on the speed of sound. From the above relation, we can deduce

$$\frac{c_{\mathrm{DF4}}}{c_{\mathrm{DF3}}} = \frac{c_{\mathrm{TF5}}}{c_{\mathrm{TF4}}}, \tag{5.19}$$

hence, the effect of phase relaxation on the sound speed is also independent from the order of the relaxation steps.

Using the results of [10] on the ordering of the speeds of sound, we can write from (5.18)

$$c_{\mathrm{DF3}} \leq c_{\mathrm{TF4}}. \tag{5.20}$$

Now, we take the difference between the two speeds of sound c_{TF4} and c_{TF5}, or more precisely the inverse of their squares, which gives

$$c_{\mathrm{TF4}}^{-2} - c_{\mathrm{TF5}}^{-2} = \frac{\rho_{\mathrm{g}}\rho_{\ell}}{\alpha_{\ell}\rho_{\mathrm{g}} + \alpha_{\mathrm{g}}\rho_{\ell}} \frac{T(\alpha_{\mathrm{g}}\rho_{\mathrm{g}}C_{p,\mathrm{g}}\chi_{\mathrm{g}} + \alpha_{\ell}\rho_{\ell}C_{p,\ell}\chi_{\ell})^2}{\alpha_{\mathrm{g}}\rho_{\mathrm{g}}C_{p,\mathrm{g}} + \alpha_{\ell}\rho_{\ell}C_{p,\ell}}. \tag{5.21}$$

This difference is always positive, which proves that

$$c_{\mathrm{TF4}} \leq c_{\mathrm{TF5}}. \tag{5.22}$$

Consequently, from (5.19)

$$c_{\mathrm{DF3}} \leq c_{\mathrm{DF4}}. \tag{5.23}$$

5.5. Subcharacteristic condition and model hierarchy. We can now extend the results SC1–SC4 in [10] by adding the two-fluid four-equation and the drift-flux three-equation models to the hierarchy. Following the argument in [10], as well as referring to (5.8) and to the eigenvalues of the drift-flux three-equation model in [12], we can state:

SC5: The model DF3 statisfies the subcharacteristic condition with respect to TF4.

SC6: The model DF3 statisfies the subcharacteristic condition with respect to DF4.

SC7: The model TF4 statisfies the weak subcharacteristic condition with respect to TF5.

Here we follow the definitions of the subcharacteristic and weak subcharacteristic conditions given in [10]. For the two-fluid models, due to algebraic complexity, the general eigenvalues are not known. Therefore, we only discussed the case where the gas and liquid velocities are equal, which only proves a weak subcharacteristic condition.

6. Condition for hyperbolicity. The canonical model derived above, with $\Delta p = 0$, is generally not hyperbolic. Identically to the two-fluid six-equation model, the eigenvalues related to the volume-fraction waves are complex as soon as the gas and liquid velocities are different from each other [13, 29]. The pressure difference term Δp has been added to make the model hyperbolic. In order to find an expression for Δp, we will use a perturbation method around the state where $v_\mathrm{g} = v_\ell$. Based on the experience from the two-fluid six-equation model [5, 9, 19, 20, 23, 29], we look for it in the form $\Delta p = \mathcal{C} \cdot (v_\mathrm{g} - v_\ell)^2$. We know, from the section above, the speed of sound of the model, c_{TF4}. The variable defined as

$$\varepsilon = \frac{v_\mathrm{g} - v_\ell}{2 \cdot c_{\mathrm{TF4}}} \tag{6.1}$$

is small for subsonic velocities and is therefore suitable as a perturbation parameter. We first evaluate the characteristic polynomial

$$\Pi_A = \mathrm{Det}(\boldsymbol{A}(\boldsymbol{U}) - \lambda \cdot \boldsymbol{I}_4), \tag{6.2}$$

where $\boldsymbol{I}_4$ is the identity matrix of rank 4. In this polynomial, we make a variable change through

$$\lambda = \frac{v_\mathrm{g} + v_\ell}{2} + a \cdot c_{\mathrm{TF4}}, \tag{6.3}$$

where a is the new unknown. Then, all the occurences of the velocity are eliminated by substituting

$$v_\mathrm{g} = v_\mathrm{m} + \varepsilon \cdot c_{\mathrm{TF4}}, \tag{6.4}$$

$$v_\ell = v_\mathrm{m} - \varepsilon \cdot c_{\mathrm{TF4}}, \tag{6.5}$$

where v_m is the arithmetic average of v_g and v_ℓ. This is in compliance with the definition of ε (6.1).

Now, we perform a power-series expansion of the eigenvalues in terms of the degree of ε. To do so, the variable a is substituted by

$$a = \sum_{i=0}^{N} \left(b_i \cdot \varepsilon^i \right), \tag{6.6}$$

where N must be higher than the highest degree of ε that we wish in the expansion. Then we will sequentially solve

$$\mathrm{degree}(\Pi_A, \varepsilon, i) = 0 \tag{6.7}$$

for the coefficients b_i, starting from $i = 0$, where $\mathrm{degree}(\Pi_A, \varepsilon, i)$ returns the coefficient of the i^{th} degree of ε in $\Pi_A(\varepsilon)$.

The zeroth degree gives a fourth order equation in b_0,

$$\frac{\rho_\mathrm{g}^4 \rho_\ell^4 (\alpha_\ell \rho_\mathrm{g} + \alpha_\mathrm{g} \rho_\ell)^4 L^4}{(\rho_\mathrm{g} - \rho_\ell)^8 c_{\mathrm{TF4}}^4} (b_0 - 1)(b_0 + 1) b_0^2 = 0, \tag{6.8}$$

whose four solutions are $b_0 = -1$, $b_0 = 1$, and twice $b_0 = 0$. The first two give the approximate eigenvalues

$$\lambda = \frac{v_\mathrm{g} + v_\ell}{2} \pm c_{\mathrm{TF4}} + \mathcal{O}\left(\frac{v_\mathrm{g} - v_\ell}{2 \cdot c_{\mathrm{TF4}}} \right), \tag{6.9}$$

which are clearly the eigenvalues related to the pressure waves. The double solution $b_0 = 0$ corresponds to the volume-fraction waves, which are of interest here. For this wave family, we push to the next degree of the expansion. However, the first degree of the polynomial $\Pi_A(\varepsilon)$ vanishes when $b_0 = 0$. We then go to the second degree. Fortunately, b_2 vanishes from the second degree, and we are left with a second order equation in b_1

$$((\alpha_\mathrm{g}\rho_\ell + \alpha_\ell\rho_\mathrm{g})b_1^2 + 2(\alpha_\mathrm{g}\rho_\ell - \alpha_\ell\rho_\mathrm{g})b_1 + (\alpha_\mathrm{g}\rho_\ell + \alpha_\ell\rho_\mathrm{g}) - 4\mathcal{C}) \cdot \frac{\rho_\mathrm{g}^4\rho_\ell^4 L^4(\alpha_\mathrm{g}\rho_\ell + \alpha_\ell\rho_\mathrm{g})^3}{c_{\mathrm{TF4}}^4(\rho_\mathrm{g} - \rho_\ell)^8} = 0. \quad (6.10)$$

The reduced discriminant of the equation is

$$\begin{aligned}\Delta &= (\alpha_\mathrm{g}\rho_\ell - \alpha_\ell\rho_\mathrm{g})^2 - (\alpha_\mathrm{g}\rho_\ell + \alpha_\ell\rho_\mathrm{g})(\alpha_\mathrm{g}\rho_\ell + \alpha_\ell\rho_\mathrm{g} - 4\mathcal{C}) \\ &= -4\alpha_\mathrm{g}\alpha_\ell\rho_\mathrm{g}\rho_\ell + 4(\alpha_\mathrm{g}\rho_\ell + \alpha_\ell\rho_\mathrm{g})\mathcal{C}.\end{aligned} \quad (6.11)$$

Therefore b_1 will only be real if

$$\mathcal{C} \geq \frac{\alpha_\mathrm{g}\alpha_\ell\rho_\mathrm{g}\rho_\ell}{\alpha_\mathrm{g}\rho_\ell + \alpha_\ell\rho_\mathrm{g}}, \quad (6.12)$$

which is the same constraint as the one obtained for the six-equation model [29]. The solutions are then

$$b_1 = \frac{-\alpha_\mathrm{g}\rho_\ell + \alpha_\ell\rho_\mathrm{g} \pm 2\sqrt{-\alpha_\mathrm{g}\alpha_\ell\rho_\mathrm{g}\rho_\ell + (\alpha_\mathrm{g}\rho_\ell + \alpha_\ell\rho_\mathrm{g})\mathcal{C}}}{\alpha_\mathrm{g}\rho_\ell + \alpha_\ell\rho_\mathrm{g}}. \quad (6.13)$$

This gives the approximate eigenvalues for the volume-fraction waves

$$\lambda = \frac{v_\mathrm{g} + v_\ell}{2} + \frac{-\alpha_\mathrm{g}\rho_\ell + \alpha_\ell\rho_\mathrm{g} \pm 2\sqrt{-\alpha_\mathrm{g}\alpha_\ell\rho_\mathrm{g}\rho_\ell + (\alpha_\mathrm{g}\rho_\ell + \alpha_\ell\rho_\mathrm{g})\mathcal{C}}}{\alpha_\mathrm{g}\rho_\ell + \alpha_\ell\rho_\mathrm{g}} \frac{v_\mathrm{g} - v_\ell}{2} + \mathcal{O}\left(\frac{v_\mathrm{g} - v_\ell}{2 \cdot c_{\mathrm{TF4}}}\right). \quad (6.14)$$

We deduce from the above that the model with the regularising term expressed as

$$\Delta p = \frac{\alpha_\mathrm{g}\alpha_\ell\rho_\mathrm{g}\rho_\ell}{\alpha_\mathrm{g}\rho_\ell + \alpha_\ell\rho_\mathrm{g}}(v_\mathrm{g} - v_\ell)^2 \quad (6.15)$$

is hyperbolic at first order around the state where $v_\mathrm{g} = v_\ell$. To make the model actually hyperbolic when $v_\mathrm{g} \neq v_\ell$, it is common to define the pressure difference as

$$\Delta p = \delta\frac{\alpha_\mathrm{g}\alpha_\ell\rho_\mathrm{g}\rho_\ell}{\alpha_\mathrm{g}\rho_\ell + \alpha_\ell\rho_\mathrm{g}}(v_\mathrm{g} - v_\ell)^2, \quad (6.16)$$

where $\delta > 1$ [5, 9, 20, 23].

7. Resonance. The two-fluid models are prone to resonance, which means that the eigenvector space collapses under some conditions, and the Jacobian of the fluxes becomes singular [14, 17, 18]. This is due to the eigenvectors related to the volume-fraction waves becoming parallel when the gas and liquid velocities are equal. The physical explanation is that the volume-fraction waves become identical – identical jump and propagation velocity. This is not a problem for numerical methods that do not use the eigenstructure of the system, because the two waves actually exist and are superimposed. However, this is problematic for numerical methods that use the eigenstructure, because it looks like information is lost. In this case, a fix can be used to overcome this issue, for example the one described in [18].

8. Conclusion. The aim of the article was to derive a two-fluid model for two phases reaching instantaneous equilibrium. This is required in order to be able to use equilibrium-based equations of state.

We have derived a two-fluid four-equation model as the limit of a five-equation model when the phase relaxation becomes instantaneous. The phase relaxation source terms involve an interfacial momentum velocity, for which we found an expression respecting the second law of thermodynamics. This model was then put in quasilinear form by deriving the differentials of the primary variables. Then the intrinsic speed of sound of the model has been extracted.

We have placed our model in a hierarchy of two-phase flow relaxation models. It has been proved in previous works that the subcharacteristic condition is satisfied for a part of this hierarchy. In the present work, we have proved that it is satisfied for the rest of our hierarchy.

Finally, we applied a perturbation method around the state where the gas and liquid velocities are equal. This helped deriving an expression for the pressure difference in the regularisation term which makes the model hyperbolic.

This model is ready to implement, using numerical methods for conservation laws. One should nevertheless keep in mind that the model is prone to resonance, so that methods that use the eigenstructure of the system will require a fix when the gas and liquid velocities are equal or close to each other.

Acknowledgment. This publication has been produced with support from the BIGCCS Centre, performed under the Norwegian research program Centres for Environment-friendly Energy Research (FME). The authors acknowledge the following partners for their contributions: Aker Solutions, ConocoPhillips, Det Norske Veritas, Gassco, Hydro, Shell, Statoil, TOTAL, GDF SUEZ and the Research Council of Norway (193816/S60).

We are thankful to our colleagues Peder Kristian Aursand, Morten Hammer and Svend Tollak Munkejord for useful discussions.

REFERENCES

[1] P. K. Aursand, S. Evje, T. Flåtten, K. E. T. Giljarhus and S. T. Munkejord, *An exponential time-differencing method for monotonic relaxation systems*, submitted (2011). Available online from `http://www.math.ntnu.no/conservation/2011/008.html`

[2] M. R. Baer and J. W. Nunziato, *A two-phase mixture theory for the deflagration-to-detonation transition (DDT) in reactive granular materials*, Int. J. Multiphase Flow, 12 (1986), pp. 861–889

[3] K. H. Bendiksen, D. Malnes, R. Moe and S. Nuland, *The dynamic two-fluid model OLGA: Theory and application*, SPE Prod. Eng., 6 (1991), pp. 171–180.

[4] D. Bestion, *The physical closure laws in the CATHARE code*, Nuclear Engineering and Design, 124 (1990), pp. 229–245.

[5] C.-H. Chang and M.-S. Liou, *A robust and accurate approach to computing compressible multiphase flow: Stratified flow model and AUSM$^+$-up scheme*, J. Comput. Phys., 225 (2007), pp. 850–873.

[6] G.-Q. Chen, C. D. Levermore and T.-P. Liu, *Hyperbolic conservation laws with stiff relaxation terms and entropy*, Comm. Pure Appl. Math., 47 (1994), pp. 787–830.

[7] F. Coquel, K. El Amine and E. Godlewski, *A numerical method using upwind schemes for the resolution of two-phase flows*, J. Comput. Phys., 136 (1997), pp. 272–288.

[8] J. Cortes, A. Debussche and I. Toumi, *A density perturbation method to study the eigenstructure of two-phase flow equation systems*, J. Comput. Phys., 147 (1998), pp. 463–484.

[9] S. Evje and T. Flåtten, *Hybrid Flux-Splitting Schemes for a Common Two-Fluid Model*, J. Comput. Phys., 192 (2003), pp. 175–210.

[10] P. J. Martínez Ferrer, T. Flåtten and S. T. Munkejord, *On the effect of temperature and velocity relaxation in two-phase flow models*, ESAIM-Math. Model. Num., 46 (2012), pp. 411–442.
[11] T. Flåtten, A. Morin, S. T. Munkejord, *Wave propagation in multicomponent flow models*, SIAM J. Appl. Math., 70 (2010), pp. 2861-2882.
[12] T. Flåtten, H. Lund, *Relaxation two-phase flow models and the subcharacteristic condition*, Mathematical Models and Methods in Applied Sciences, 21 (2011), pp. 2379-2407.
[13] D. Gidaspow, *Modeling of two-phase flow. Round table discussion (RT-1-2)*, Proc. 5th Int. Heat Transfer Conf. VII (1974), p. 163.
[14] E. Isaacson and B. Temple, *Nonlinear resonance in inhomogeneous systems of conservation laws*, Contemp. Math., 108 (1990), pp. 63–77.
[15] K. H. Karlsen, C. Klingenberg and N. H. Risebro, *A relaxation system for conservation laws with a discontinuous coefficient*, Math. Comput., 73 (2004), pp. 1235–1259.
[16] T.-P. Liu, *Hyperbolic conservation laws with relaxation*, Commun. Math. Phys., 108 (1987), pp. 153–175.
[17] T.-P. Liu, *Nonlinear resonance for quasilinear hyperbolic equation*, J. Math. Phys., 28 (1987), pp. 2593–2602.
[18] A. Morin, T. Flåtten and S. T. Munkejord, *A Roe scheme for a compressible six-equation two-fluid model*, submitted (2012). Available online from `http://folk.ntnu.no/morin/`
[19] S. T. Munkejord, *Comparison of Roe-type methods for solving the two-fluid model with and without pressure relaxation*. Comput. & Fluids, 36 (2007), pp. 1061–1080.
[20] S. T. Munkejord, S. Evje, T. Flåtten, *A Musta scheme for a nonconservative two-fluid model*, SIAM J. Sci. Comput., 31 (2009), pp. 2587–2622.
[21] A. Murrone and H. Guillard, *A five equation reduced model for compressible two phase flow problems*, J. Comput. Phys., 202 (2005), pp. 664–698.
[22] R. Natalini, *Recent results on hyperbolic relaxation problems. Analysis of systems of conservation laws*, Chapman & Hall/CRC Monogr. Surv. Pure Appl. Math., (1999), pp. 128–198.
[23] H. Paillère, C. Corre and J. R. García Cascales, *On the extension of the AUSM$^+$ scheme to compressible two-fluid models*, Comput. & Fluids, 32 (2003), pp. 891–916.
[24] L. Pareschi and G. Russo, *Implicit-explicit Runge-Kutta schemes and applications to hyperbolic systems with relaxation*, J. Sci. Comput., 25 (2005), pp. 129–155.
[25] R. Saurel and R. Abgrall, *A multiphase Godunov method for compressible multifluid and multiphase flows*, J. Comput. Phys., 150 (1999), pp. 425–467.
[26] R. Saurel, F. Petitpas and R. Abgrall, *Modelling phase transition in metastable liquids: application to cavitating and flashing flows*, J. Fluid Mech., 607 (2008), pp. 313–350.
[27] R. Span and W. Wagner, *A New Equation of State for Carbon Dioxide Covering the Fluid Region from the Triple-Point Temperature to 1100 K at Pressures up to 800 MPa*, J. Phys. Chem. Ref. Data, 25 (1996), pp. 1509–1596.
[28] H. B. Stewart and B. Wendroff, *Two-phase flow: Models and methods*. J. Comput. Phys., 56 (1984), pp. 363–409.
[29] J. H. Stuhmiller, *The influence of interfacial pressure forces on the character of two-phase flow model equations*. Int. J. Multiphas. Flow, 3 (1977), pp. 551–560.
[30] I. Toumi and A. Kumbaro, *An Approximate Linearized Riemann Solver for a Two-Fluid Model*, J. Comput. Phys., 124 (1996), pp. 286–300.
[31] I. Toumi, *An Upwind Numerical Method for Two-Fluid Two-Phase Flow Models*. Nuclear Science and Engineering, 123 (1996), pp. 147–168.
[32] Q. H. Tran, M. Baudin and F. Coquel, *A relaxation method via the Born-Infeld system*, Math. Mod. Meth. Appl. S., 19 (2009), pp. 1203–1240.
[33] *WAHA3 Code Manual*, JSI Report IJS-DP-8841, Jožef Stefan Insitute, Ljubljana, Slovenia, 2004

H Pipeline flow modelling with source terms due to leakage: The straw method

Alexandre Morin, Steinar Kragset and Svend T. Munkejord.
Accepted for publication in Energy Procedia, 2012.

Available online at www.sciencedirect.com

ScienceDirect

Energy Procedia 00 (2011) 000–000

Energy Procedia

www.elsevier.com/locate/procedia

TRONDHEIM CCS CONFERENCE

Pipeline flow modelling with source terms due to leakage: The straw method

Alexandre Morin[b], Steinar Kragset[a], Svend Tollak Munkejord[a,*]

[a]*SINTEF Energy Research, P.O. Box 4761, NO-7465 Trondheim, Norway*
[b]*Norwegian University of Science and Technology (NTNU), NO-7491 Trondheim, Norway*

Abstract

A numerical method for calculating the leakage flow rate through a crack in a pressurized pipeline is presented. Calculations of the flow inside, and leakage from, a pipeline with a running crack are performed. For the case of single-phase flow, the flow through the crack can also be calculated using choked-flow theory. The two methods are compared and identical results obtained. The advantage of the present method is that it does not rely on analytical expressions for the flow through the crack, and it is therefore thought to be applicable for two-phase flow, including phase transition. Hence it may be of use in the development of coupled fluid-structure models for the assessment of running ductile fracture in carbon dioxide transport pipelines.

© 2010 Published by Elsevier Ltd. Selection and/or peer-review under responsibility of [name organizer]

Keywords: CO_2 transport; flow through a crack; choked flow; fluid dynamics; thermodynamics

1. Introduction

Pipelines are a common and convenient way of transporting natural gas, and with the increasing interest in carbon capture and storage (CCS) technology, pipeline transport will also become an important link between the capture and storage sites of CO_2. As for natural gas, a rupture of a CO_2 pipeline can cause serious accidents as well as economic losses and must be avoided. In order to control and predict the risk of accidental failure, such as a running fracture initiated e.g. by damage to the pipeline by a third party, the fracture properties of the pipe materials have long been a subject of study. A semi-empirical model based on research at the Battelle memorial institute in the 1970s [1] where the fluid flow

* Corresponding author. Tel.: +47 73593897; fax: +47 73592889.
E-mail address: svend.t.munkejord@sintef.no.

and the material structure behaviour are assumed to be uncoupled processes, is traditionally used for the assessment of running ductile fractures. New pipeline materials have, however, motivated the search for improved models, and it is natural to consider a coupling of the fluid and structure processes [2]. Moreover, the thermodynamic properties of CO_2 are different from those of natural gas at the relevant conditions for pipeline transport. It is not clear how e.g. phase change and a large heat capacity will influence the fracture mechanics. Further, various impurities will be present in the transported CO_2, and even small amounts will change the properties compared to pure CO_2 [3,4]. Therefore, a flexible framework is required with respect to the employed equations of state. For hydrocarbon mixtures, the Peng–Robinson equation of state is appropriate, and was used by Oke et al. [5] in a study of a fluid model for pipeline puncture.

In Berstad et al. [6], a coupled fluid-structure model was presented and tested by comparisons to full-scale experiments of running ductile fractures in steel pipelines. In this model, the effect of the leakage of the fluid through the crack opening is included in the one-dimensional fluid equations as source terms. The emerging fluid pressure is then coupled back into the structure part of the model as a load. In order to evaluate the source terms in the fluid part, the fracture is modelled by a sequence of orifices and the leakage is assumed to be an isentropic process. By using the ideal-gas equation of state and the choked-flow theory it is possible to derive analytical expressions for them. The model agreed well with the experiments, but is still restricted to the ideal gas case and therefore premature to be applied for CO_2 at typical operating conditions. A generalization of the model to handle other equations of state may follow two paths, either an analytical approach where the source terms are derived explicitly as in [6], or a numerical approach in which the source terms are evaluated using the flow solver. It is the latter that will be studied here, and it will be referred to as “the straw method”. In this study, we assume the fracture opening to be given, so that the structure part of the model can be ignored, and the focus is on a one-dimensional fluid model inflicted by a radial leakage. Also, this study intends to prove the concept of the straw method, therefore we consider only single-phase, ideal gas, for which we have analytical results. However, this method is developed to be easily generalized to two-phase mixtures.

In the following, the governing equations of the one-dimensional (1D) fluid model will be presented in Section 2, and Section 3 then gives an introduction to the straw method. Section 4 explains the implementation of the straw method for a pipe filled with pressurized gas. Further, Section 5 presents some numerical simulations of a pipe depressurization due to a running fracture. Finally, Section 6 concludes the paper.

2. Governing equations

It was shown in Berstad et al. [6] that the leakage of the fluid in a fractured pipeline, illustrated in Fig. 1, can be incorporated into the Euler equations, as source terms written on the right-hand side:

$$\frac{\partial \rho}{\partial t} + \frac{\partial (\rho u)}{\partial x} = -\zeta_e, \tag{1}$$

$$\frac{\partial (\rho u)}{\partial t} + \frac{\partial (\rho u^2)}{\partial x} + \frac{\partial p}{\partial x} = -u\zeta_e, \tag{2}$$

$$\frac{\partial E}{\partial t} + \frac{\partial \left[(E+p)u \right]}{\partial x} = -(E_e + p_e)\frac{1}{\rho_e}\zeta_e. \tag{3}$$

Herein, p, ρ and u are the pressure, density and the x-directed velocity, respectively, and $E = \rho(e + u^2/2)$ is the total energy per unit volume, with e being the internal specific energy. The general source term ζ_e is the leakage mass flow rate and can be written

$$\zeta_e = \rho_e u_e \frac{2r_e}{A}, \tag{4}$$

where the subscript e indicates that the quantities are taken in the crack opening through which the fluid may escape. This opening is given by its width $2r_e(x)$, whereas the cross section of the main pipe is A. For simple equations of state, analytical expressions can be derived for the escape quantities [6], but in general, numerical methods must be used.

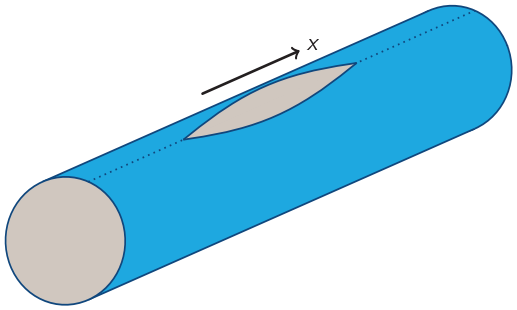

Fig. 1. A section of the pipeline with a fracture running along the x-direction.

3. The straw method

The straw method takes the fracture geometry as given. The main challenge is to evaluate the flow rate through the fracture. For a two-phase flow with a "black box" equation of state, an attempt to develop analytical expressions for choked flow may lead to intractable expressions, let alone the inclusion of phase change. An alternative idea is then to let the flow rate be evaluated by a numerical solver analogously to what happens inside the pipe. We assume here that the fracture along the pipe can be modelled by a sequence of transversal tubes, whose length is the thickness of the pipe steel. These tubes are plugged into the main pipe, and their cross-sections represent the crack opening (see Fig. 2). The fluid dynamics in the tubes, as well as in the pipe, is solved as one-dimensional conservation laws averaged over the cross-section. By inserting one tube in each of the fractured pipe cells, we obtain a discretization of the fracture along the pipe. The variation of the fracture width is represented by adjusting the tube diameters at each time step. The propagation of the fracture is accounted for by adding new tubes along the pipe.

The inlet flows in the transversal sub-tubes become mass, momentum and internal-energy source terms for the flow in the main pipe. To simplify, we assume that the flow in the pipe is quasi-stationary with regard to the flow through the fracture, therefore we let the sub-tubes reach steady-state flow between the pipe and outside pressures at all time steps. Particular attention has to be given to the boundary conditions for the sub-tubes, depending on whether the outflow is choked or not.

In the present paper, we validate the approach by applying the straw method to a single-phase pure gas. We can thus compare the results to those obtained by a method using the analytical expressions from the choked-flow theory.

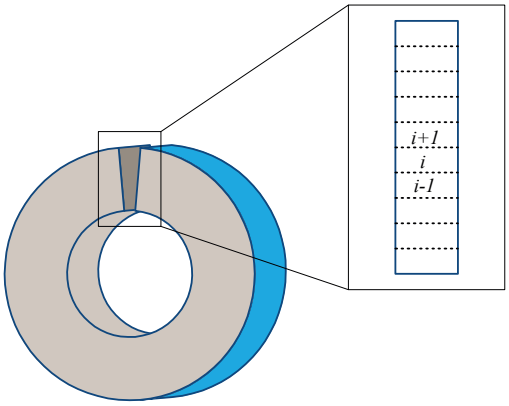

Fig. 2. A small section of the pipe where the exaggerated pipe wall is partly open due to a crack. The flow rate through the opening is evaluated separately by modelling the crack as a sequence of small tubes, or straws, transversal to the main pipe as indicated. Each tube is discretized into finite volumes, *i*.

4. Implementation of the straw method

This section begins by explaining how the flow through the crack is modelled, and how it is implemented in the numerical framework. Then the boundary conditions that apply to the straw are detailed.

4.1. Modelling choices

Fig. 3 (a) illustrates the leakage flow through a crack in a pipe, where the crack is thought of as an orifice. Ahead of the orifice, the fluid inside the pipe is accelerated, while the pressure decreases. The streamlines are contracting and all leading to the orifice. Downstream of the orifice, the fluid is expanding and decelerating, while mixing with the outside air [7]. We assume that the flow ahead of the orifice is isentropic. This supposes that heat exchange can be neglected, which is acceptable due to the high velocity of the gas. This also supposes that we can neglect the viscosity. In this situation, the flow is similar to that in a convergent nozzle leading to the orifice, see Fig. 3 (b). However, downstream of the crack, the mixing with the outside air makes the isentropic assumption invalid. We therefore decide not to model the diverging part. Instead, we let the outflow boundary condition govern the release pressure. Fig. 3 (c) shows the pressure profile along the leakage flow. Two regimes can be distinguished. In the subcritical regime, which the pressure at the orifice is equal to the atmospheric pressure. The velocity across the orifice is then subsonic. In the supercritical regime, also called choked flow, the pressure at the orifice becomes independent of the atmospheric pressure. The velocity across the orifice is then exactly equal to the sound speed in the fluid. This duality may be problematic when the pressure ratio is supercritical, because the outflow pressure at the orifice is not known *a priori*. This may cause convergence problems that the boundary conditions have to handle.

In the present work, the straw is of constant cross-section. When there is no phase change or friction, the steady state is reached when the pressure profile is flat. The flow ahead of the orifice has to be accounted for in the inlet boundary condition. Actually, in this work the straw is only present to connect the two boundary conditions, see Fig. 4.

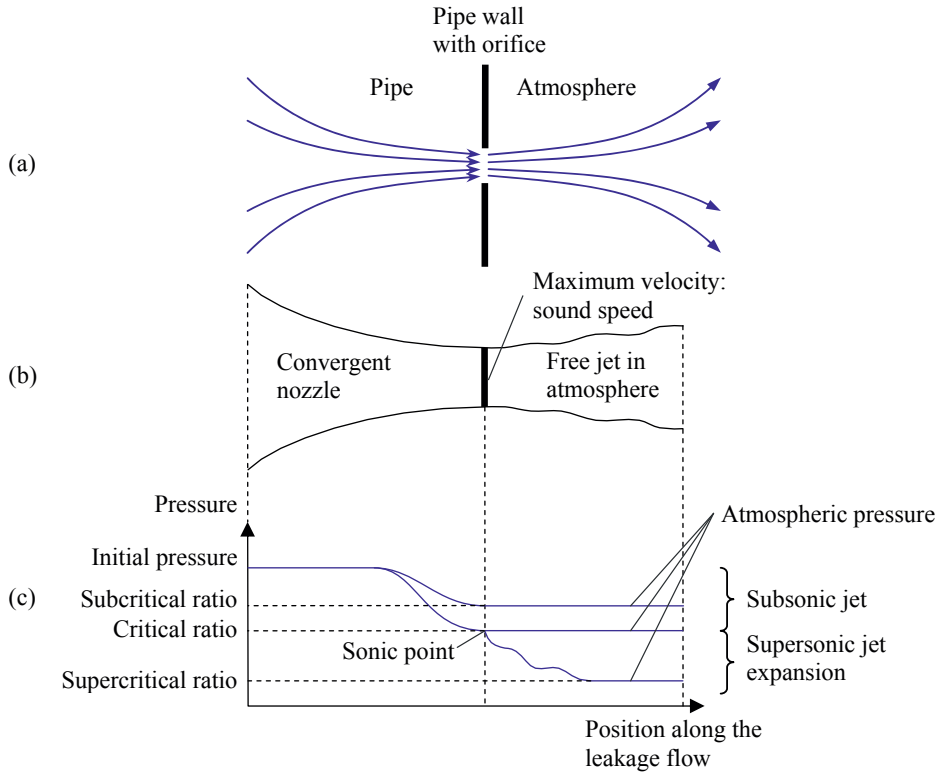

Fig. 3. (a) Real situation of a leak across an orifice in the pipe wall; (b) Model of the leakage flow using a convergent nozzle and a free jet in atmosphere; (c) Pressure profile in the adopted model, depending on the ratio of the internal pressure to the surrounding (atmospheric) pressure.

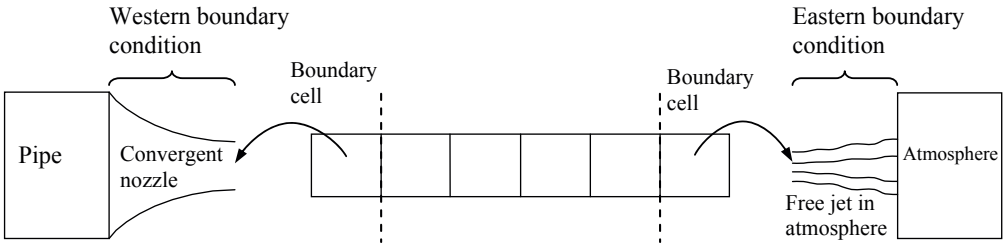

Fig. 4. Practical implementation of the straw method.

4.2. Straw inlet boundary condition

The convergent flow is accounted for by the inlet boundary condition. Since the model contains three equations, three quantities have to be taken care of to fully describe the state of the fluid at the straw boundary. Depending on the flow regime, these quantities are either specified to be equal to their values in the pipe, or extrapolated from the straw. In the straw method, before the steady state is attained, we expect either a subsonic or a supersonic outflow from the pipe, or a reversed subsonic inflow.

In an isentropic flow, the entropy s is a conserved quantity since we can write

$$\rho\frac{\partial s}{\partial t}+\rho u\frac{\partial(s)}{\partial x}=\rho\frac{Ds}{Dt}=0. \tag{5}$$

Next, we need a quantity characterizing the energy. We start from the energy equation

$$\frac{\partial E}{\partial t}+\frac{\partial\left(E+p\right)u}{\partial x}=0, \tag{6}$$

in which we add and subtract the time derivative of the pressure

$$\frac{\partial\left(E+p\right)}{\partial t}+\frac{\partial\left(E+p\right)u}{\partial x}-\frac{\partial p}{\partial t}=0. \tag{7}$$

In steady state, we recover a conservation equation

$$\rho\frac{\partial\left(h+u^2/2\right)}{\partial t}+\rho u\frac{\partial\left(h+u^2/2\right)}{\partial x}=\rho\frac{D\left(h+u^2/2\right)}{Dt}=0. \tag{8}$$

Therefore the second chosen quantity is what we can call the total enthalpy per unit volume, $H=\rho\left(h+u^2/2\right)$, where h is the specific enthalpy. The third chosen quantity is the momentum, ρu.

Table 1 shows which variables are specified or extrapolated depending on the flow regime. In the subsonic regime, the effect of this boundary condition is to convert the mechanical potential energy of the pressure into kinetic energy. The total enthalpy, which contains all the potential energy but the mechanical potential energy, is conserved along the convergent nozzle. On the other hand, the straw imposes the momentum and indirectly the kinetic energy. Together with the entropy, from the pipe or from the straw depending on the direction of the flow, we can determine the thermodynamic state of the fluid as well as its velocity.

Table 1. Straw inlet boundary conditions.

	Specified to be equal to its value in the pipe	Extrapolated from the straw
Supersonic outflow from pipe	s, H, ρu	-
Sonic/subsonic outflow from pipe	s, H	ρu
Subsonic inflow to pipe	H	s, ρu

4.3. Straw outlet boundary condition

The outlet boundary condition has to account for the discharge to the atmosphere. Most of the time, the flow leaving the straw is either exactly sonic or subsonic. Due to the fact that we do not model the jet in the atmosphere, the release pressure is not necessarily the atmospheric pressure. As shown in Fig. 3 (c), if the pressure ratio is subcritical, atmospheric pressure applies at the orifice. However, if the ratio is supercritical, the release pressure at the orifice is different from the atmospheric pressure. In calculations, this may cause the pressure to oscillate between the atmospheric pressure and the orifice pressure.

To cover all the possible situations, subsonic or supersonic outflow, and subsonic inflow, we again choose three variables to specify or extrapolate. Here we use the natural primitive variables: the density, the velocity and the pressure. Table 2 shows how the variables are either specified or extrapolated. In the supersonic regime, the pressure is extrapolated from the straw, and therefore the atmosphere does not have any effect on the flow in the straw, as expected. In the subsonic regime, the straw always decides over the discharge velocity, whereas the density comes from the side from which the fluid is flowing.

Table 2. Straw outlet boundary conditions.

	Specified to be equal to the atmospheric value	Extrapolated from the straw
Supersonic outflow from pipe	-	ρ, u, p
Sonic/subsonic outflow from pipe	p	ρ, u
Subsonic inflow to pipe	ρ, p	u

As can be seen in Table 2, the pressure is imposed or not, depending on whether the flow is sonic or supersonic. Now, when the flow is choked, the velocity at the straw end should be exactly sonic, while the pressure in the straw and in the atmosphere will be very different from each other (Fig. 3 (c)). Therefore numerically, the slightest oscillation of velocity around the sonic point will cause a large variation in pressure, thus hindering convergence. Since we are only interested in the steady state in the straw, we can speed up convergence by correcting the imposed boundary pressure, as long as the correction term vanishes in steady state. We define λ as the difference between the flow velocity and the sound speed. For a constant C that we choose equal to 0.1s/m, the outlet boundary pressure is defined as

$$p_{boun} = \begin{cases} p_{straw} & \text{if } \lambda \geq 0 \text{ (simple extrapolation)} \\ p_{straw} + \left(p_{straw} - p_{atm} \right) C\lambda & \text{if } \lambda < 0 \text{ and } \left| C\lambda \right| < 1 \\ p_{boun} = p_{atm} & \text{if } \lambda < 0 \text{ and } \left| C\lambda \right| > 1 \end{cases} \tag{9}$$

Note that the boundary pressure p_{boun} is a continuous function of λ, the atmospheric pressure p_{atm}, and the straw pressure p_{straw}. Further, in steady choked flow, λ=0, and we recover the simple extrapolation. In steady subsonic flow, p_{atm}= p_{straw}, so that the outflow pressure is the atmospheric pressure. Therefore the correction term does not have any effect in steady state.

5. Numerical results

Numerical tests have been performed for a pipe filled with methane at 122 bar, closed at both extremities. The pipe is 12m long, has a diameter of 0.261m and is divided into 400 cells. After 2ms, a crack is initiated in the middle of the pipe, propagating at a constant velocity of 100m/s in both directions. The crack is shaped like a sinus function (cf. Fig. 1) and its width at maximum opening is 0.2m. We let it evolve during 30ms.

The numerical method used is the multi-stage (MUSTA) centred method with four cells and four substeps [8,9] with forward Euler time steps. The source terms are solved with first order time splitting.

Fig. 5 shows the evolution of the pressure in the pipe at approximately 1m (x=4.995m) and 3m (x=2.985m) from where the crack is initiated. We see that the depressurization begins later for the red curve, further from the crack, than for the green curve. This is due to the depressurization wave travelling from the crack towards the extremities of the pipe. The kink in the red curve is due to the reflection wave from the closed end of the pipe. There is also a smaller kink in the green curve at t=0.0012s, due to the crack tip passing at the corresponding position. The black squares – denoted "ref" – are the results using the choked flow theory. We see that the results are practically identical, thus showing that the straw method in one dimension gives the same results as the analytical theory to reasonable accuracy.

Fig. 6 shows the pressure profile in the tube at four different times. The depressurization starts in the middle of the pipe, where the crack is initiated. Then decompression waves begin to propagate towards the extremities, faster than the crack progresses. The crack tips are located at the two kinks in the pressure profile, e.g., at about 4 and 8 m in the last graph. Further, there is a ridge in the pressure profile in the middle of the pipe. Although this ridge probably exists in reality, its size may be exaggerated in this method. The ridge is due to the fluid flowing towards the middle of the pipe and colliding with the fluid from the other side. In reality, the fluid is deflected transversally towards the crack, but in one-dimensional flow, the fluid is constrained to move longitudinally. Therefore it has to stop first, thus building up pressure, before it is accelerated again transversally in the straws. However, the total enthalpy is conserved in both cases. Further, since this always happens in a region of the pipe where there already is a crack, it does not impact the crack-propagation problem.

6. Concluding remarks

We have presented a numerical method to evaluate the leakage flow rate through a fracture in a pipe. The method has been applied to single-phase flow, where a direct comparison to choked-flow theory is possible. The two methods were compared for a case with a running fracture. The results obtained were identical to plotting accuracy; therefore it is insignificant whether the leakage flow is a sequence of orifice flows or of straw flows in the single-phase case. Hence, we deduce from the results of Berstad et al. [6] that our approach is valid.

This method was developed with the extension to two-phase flows in mind. Such an extension is future work, but is believed to be reasonably straightforward, since it does not rely on finding analytical expressions for the flow through the fracture. The only model-specific part is the adaptation of the boundary conditions of the straw, following the same principles of release in the atmosphere at the outflow, and conservation of entropy, total enthalpy and momentum at the inflow. The present method is

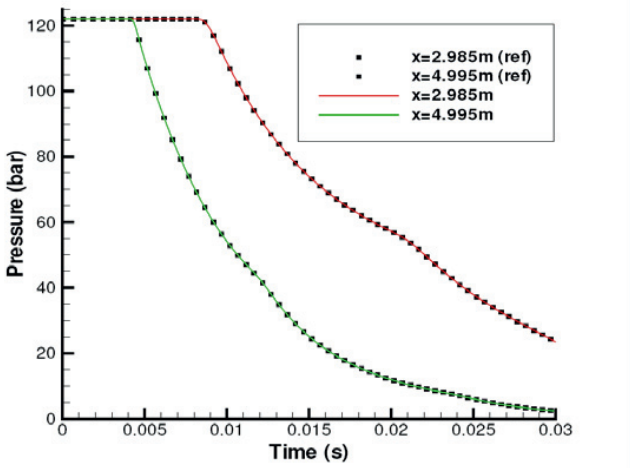

Fig. 5. Evolution of the pressure in the pipe at two positions.

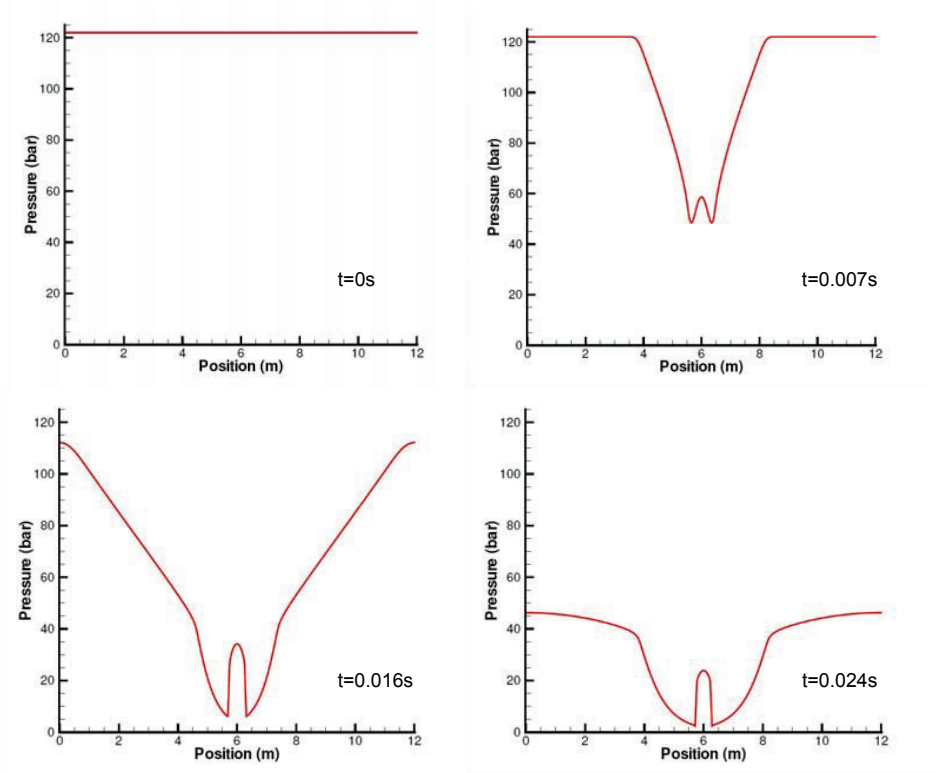

Fig. 6. Pressure profile in the pipe at four different times.

hoped to be of use in the development of coupled fluid-structure models for the assessment of running ductile fracture.

In the single-phase case, the flow in the straw itself is uniform, everything happening in the boundary conditions, which is why orifices and straws give indistinguishable results. The aim with the straw method for two-phase flow is to let the straw account for phase change due to the depressurization across the fracture. This is an important aspect, since the sound speed may change significantly when the gas volume fraction is changing. Since the flow rate is limited by the sound speed, phase change across the crack will have an effect on the flow rate. This modelling choice will have to be assessed by comparison to experimental results with two-phase flows.

Compared to previous work [5,6], the present method offers a high flexibility with respect to the flow model, for example single-phase flow or two-phase flow with or without phase change, friction or heat exchange in the pipe and across the fracture. And last but not least it can naturally handle any thermodynamical routine, either analytical or "black box".

Acknowledgements

This publication has been produced with support from the BIGCCS Centre, performed under the Norwegian research program *Centres for Environment-friendly Energy Research (FME)*. The authors acknowledge the following partners for their contributions: Aker Solutions, ConocoPhilips, Det Norske Veritas, Gassco, Hydro, Shell, Statkraft, Statoil, TOTAL, GDF SUEZ and the Research Council of Norway (193816/S60).

References

[1] Maxey, W.A. Fracture initiation, propagation and arrest. *Fifth Symposium on Line Pipe Research*. American Gas Association, Houston; 1974

[2] O'Donoghue, P. E., Green, S. T. , Kanninen, M. F., and P. K. Bowles. The development of a fluid/structure interaction model for flawed fluid containement boundaries with applications to gas transmission and distribution piping. *Computers & Structures* 1991;**38**:5/6, pp. 501–513

[3] de Visser, E., Hendriks, C., Barrio, M., Mølnvik, M. J., de Koeijer, G., Liljemark, S., and Le Gallo, Y. Dynamis CO2 quality recommendations. *International Journal of Greenhouse Gas Control* 2008;**2**:4, pp. 478–484

[4] Munkejord, S. T., Jakobsen, J. P., Austegard, A., and Mølnvik, M. J. Thermo- and fluid-dynamical modelling of two-phase multi-component carbon dioxide mixtures. *International Journal of Greenhouse Gas Control* 2010;**4**:4, pp. 589–596

[5] Oke, A., Mahgerefteh, H., Economou, I., and Rykov, Y. A transient outflow model for pipeline rupture. *Chemical engineering science* 2003;**58**, pp. 4591–4604

[6] Berstad, T., Dørum, C., Jakobsen, J.P., Kragset, S., Li, H., Lund, H., Morin, A., Munkejord, S.T., Mølnvik, M.J., Nordhagen, H.O. and Østby, E. CO_2 pipeline integrity: A new evaluation methodology. *Energy Procedia* 2011;**4**, pp. 3000–3007

[7] White, F. M. Fluid Mechanics, sixth edition, McGraw-Hill international edition; 2008, ISBN 978-0-07-128645-9

[8] Toro, E. F. MUSTA: A Multi-stage numerical flux, *Appl. Numer. Math.* 2006; **56**, pp. 1464–1479

[9] Toro, E. F., and Titarev, V. A. MUSTA fluxes for systems of conservation laws, *J. Comput. Phys.* 2006; **216**, pp. 403–429